

TECHNIQUE FOR PREDICTING GROUND-WATER
DISCHARGE TO SURFACE COAL MINES AND
RESULTING CHANGES IN HEAD

By Linda S. Weiss, Devin L. Galloway, and Audrey L. Ishii

U.S. GEOLOGICAL SURVEY

Water-Resources Investigations Report 86-4156



Urbana, Illinois

1986

UNITED STATES DEPARTMENT OF THE INTERIOR

DONALD PAUL HODEL, Secretary

GEOLOGICAL SURVEY

Dallas L. Peck, Director

For additional information
write to:

District Chief
U.S. Geological Survey
Water Resources Division
102 E. Main Street, 4th Floor
Urbana, IL 61801

Copies of this report can be
purchased from:

Books and Open-File Reports Section
Western Distribution Branch
U.S. Geological Survey
Box 25425, Federal Center
Denver, CO 80225
[Phone: (303) 236-7476]

CONTENTS

	Page
Abstract.....	1
Introduction.....	1
Purpose and scope.....	2
Acknowledgments.....	3
Previous studies.....	3
Geologic setting.....	3
Description of technique.....	4
Conceptual models.....	4
First cut.....	7
Multiple cuts.....	13
Ground-water flow system.....	16
Computer models.....	16
First cut.....	17
Multiple cuts.....	19
Limitations.....	19
Application of technique.....	22
Use of model output.....	23
First cut.....	24
Multiple cuts.....	46
Summary.....	60
References cited.....	61
Glossary of technical terms.....	64
Appendixes.....	A-1
A. Technique evaluation.....	A-1
Comparison with other techniques.....	A-1
Field test.....	A-4
Sensitivity analysis.....	A-9
Mass balance.....	A-33
References cited.....	A-35
B. Graphs showing dimensionless total-head profiles for the hypothetical aquifers.....	B-1
C. Graphs showing dimensionless seepage-flux profiles for the hypothetical aquifers.....	C-1
D. Graphs showing dimensionless total-head profiles for the hypothetical-aquifer/multiple-cut combinations.....	D-1
E. Graphs showing dimensionless seepage-flux profiles for the hypothetical-aquifer/multiple-cut combinations.....	E-1

ILLUSTRATIONS

Figures	Page
1-2. Maps showing:	
1. Generalized bedrock geology of Illinois (from Willman and others, 1975, p. 21).....	5
2. Generalized surficial geology of Illinois (from Willman and others, 1975, p. 22).....	6
3-13. Schematics showing:	
3. Summary of the age, origin, and thickness of Illinois rocks (modified from Willman and others, 1975, p. 10).....	8
4. Plan view of geometry of aquifer and first cut of surface coal mine and location of vertical section..	10
5. Vertical sections of aquifer showing ground-water drainage to first cut.....	11
6. Plan view of geometry of aquifer and multiple cuts of surface coal mine and location of vertical section.....	14
7. Vertical sections of aquifer showing ground-water drainage to multiple cuts.....	15
8. Two-dimensional, block-centered, finite-difference grid for drainage to first cut for model cross section.....	18
9. Two-dimensional, block-centered, finite-difference grids for drainage to multiple cuts for model cross sections.....	20
10. Diagram of preliminary information for Example 1-- First cut.....	27
11. Diagram of preliminary information for Example 2-- First cut.....	29
12. Diagram of preliminary information for Example 3-- First cut.....	31
13. Diagram of preliminary information for Example 4-- First cut.....	34
14-15. Flow charts showing:	
14. Interpolative steps for unconfined aquifer portion of Example 4--First cut.....	38
15. Interpolative steps for confined aquifer portion of Example 4--First cut.....	43
16-19. Schematics showing:	
16. Diagram of preliminary information for Example 1-- Multiple cuts.....	49
17. Diagram of preliminary information for Example 2-- Multiple cuts.....	51
18. Diagram of preliminary information for Example 3-- Multiple cuts.....	54
19. Diagram of preliminary information for Example 4-- Multiple cuts.....	58

ILLUSTRATIONS

	Page
Figures	
A1-A2. Graphs showing:	
A1. Head profiles for sample problem at time 90 days.....	A-2
A2. Head profiles for sample problem at time 630 days.....	A-3
A3. Map showing location of Industry Mine in McDonough County, Illinois.....	A-5
A4. Schematic showing stratigraphic column showing geologic units found in the area of Industry Mine.....	A-7
A5. Schematic showing geologic section of aquifer at Industry Mine, McDonough County.....	A-8
A6-A17. Graphs showing:	
A6. Measured and calculated heads for well 8002.....	A-10
A7. Calculated seepage fluxes into Industry Mine.....	A-11
A8. Dimensionless heads at time 10 days for thickness sensitivity.....	A-13
A9. Dimensionless heads at time 90 days for thickness sensitivity.....	A-14
A10. Dimensionless seepage fluxes for thickness sensitivity.....	A-15
A11. Dimensionless-head profiles at time 10 days for increases in geologic-material moisture characteristics for sensitivity analysis.....	A-17
A12. Dimensionless-head profiles at time 90 days for increases in geologic-material moisture characteristics for sensitivity analysis.....	A-18
A13. Dimensionless-head profiles at time 10 days for decreases in geologic-material moisture characteristics for sensitivity analysis.....	A-19
A14. Dimensionless-head profiles at time 90 days for decreases in geologic-material moisture characteristics for sensitivity analysis.....	A-20
A15. Dimensionless seepage-flux profiles for increases in geologic-material moisture characteristics for sensitivity analysis.....	A-21
A16. Dimensionless seepage-flux profiles for decreases in geologic-material moisture characteristics for sensitivity analysis.....	A-22
A17. Dimensionless seepage-flux profiles, with closure criteria of 0.1 millimeter and 0.5 millimeter.....	A-34

TABLES

	Page
Table 1. Geologic materials and hypothetical-aquifer characteristics typical of Illinois surface coal-mining regions.....	12
2. Calculations from Example 4--First cut.....	36
A1. Control-parameter values and percentage change from control values for the various geologic materials in sensitivity analysis.....	A-16
A2. Relative sensitivity of dimensionless head to selected changes in aquifer characteristics.....	A-24
A3. Relative sensitivity of dimensionless seepage flux to selected changes in aquifer characteristics.....	A-27

CONVERSION FACTORS

For use of readers who prefer to use inch-pound units, conversion factors for the metric (International System) terms used in this report are listed below:

<u>Multiply metric unit</u>	<u>By</u>	<u>To obtain inch-pound unit</u>
meter (m)	3.281	foot (ft)
square meter (m ²)	10.76	square foot (ft ²)
cubic meter (m ³)	35.31	cubic foot (ft ³)
meter per day (m/d)	3.281 1,198	foot per day (ft/d) foot per year (ft/yr)
meter squared per day (m ² /d)	10.76	foot squared per day (ft ² /d)
gram (g)	0.002205	pound, avoirdupois (lb)
meter-day squared per gram [(m-d ²)/g]	1,488	foot-day squared per pound [(ft-d ²)/lb]
gram per cubic meter (g/m ³)	6.245 x 10 ⁻⁵	pound per cubic foot (lb/ft ³)

SYMBOLS USED IN TEXT

<u>Symbol</u>	<u>Dimension</u>	<u>Description</u>
D	L	Initial saturated thickness of the aquifer in the vertical direction
GM	-	Geologic material
H	L	Total head of fluid
IH	L	Initial head of aquifer
K_{sat}	LT^{-1}	Saturated hydraulic conductivity
L	L	Length of aquifer in horizontal direction
S_y	-	Specific yield
VS2D	-	Variably-saturated, two-dimensional, ground-water flow, finite-difference, numerical model
g	LT^{-2}	Gravitational acceleration
h'	-	Dimensionless total head of fluid
h_b	L	Bubbling or air entry pressure head of fluid; Brooks and Corey coefficient
h_p	L	Pressure head of fluid
h_z	L	Elevation head of fluid
q	L^2T^{-1}	Discharge per unit length of excavation into the surface coal mine
q'	-	Dimensionless discharge, or seepage flux, into the surface coal mine
t	T	Elapsed time of drainage since excavation of the first cut
t'	-	Dimensionless time
t^*	T	Time associated with average daily rate of mine advancement (used in multiple-cut examples)
t_o	T	Multiple-cut time
w_o	L	Multiple-cut width

SYMBOLS USED IN TEXT

<u>Symbol</u>	<u>Dimension</u>	<u>Description</u>
x	L	Horizontal distance from the seepage face of the first cut from $x = 0$ to $x = L$
x'	-	Dimensionless distance
x*	L	Distance associated with average daily rate of mine advancement (used in multiple-cut examples)
z	L	Vertical distance from the impermeable bed at $z = 0$ to $z = D$
α	LT^2M^{-1}	Aquifer matrix compressibility
β	LT^2M^{-1}	Fluid compressibility
λ	-	Pore-size distribution index; Brooks and Corey coefficient
ϕ	-	Porosity, equal to the moisture content at saturation
θ_r	-	Residual moisture content at which the capillary conductivity may be considered infinitesimal; Brooks and Corey coefficient

TECHNIQUE FOR PREDICTING GROUND-WATER DISCHARGE TO
SURFACE COAL MINES AND RESULTING CHANGES IN HEAD

By Linda S. Weiss, Devin L. Galloway, and Audrey L. Ishii

ABSTRACT

Changes in seepage flux and head (ground-water level) from ground-water drainage into a surface coal mine can be predicted by a technique that considers drainage from the unsaturated zone. The user applies site-specific data to precalculated head and seepage-flux profiles.

Ground-water flow through hypothetical aquifer cross sections was simulated using the U.S. Geological Survey finite-difference model, VS2D, which considers variably-saturated, two-dimensional flow. Conceptual models considered were (1) drainage to a first cut, and (2) drainage to multiple cuts, which includes drainage effects of an area surface mine. Dimensionless head and seepage-flux profiles from 246 simulations are presented.

Step-by-step instructions and examples are presented. Users are required to know aquifer characteristics and to estimate size and timing of the mine operation at a proposed site. Calculated ground-water drainage to the mine is from one excavated face only. First cut considers confined and unconfined aquifers of a wide range of permeabilities; multiple cuts considers unconfined aquifers of higher permeabilities only.

The technique, developed for Illinois coal-mining regions that use area surface mining and evaluated with an actual field example, will be useful in assessing potential hydrologic impacts of mining. Application is limited to hydrogeologic settings and mine operations similar to those considered. Fracture flow, recharge, and leakage are not considered.

INTRODUCTION

Coal-miners in Illinois, and in other areas with flat to gently rolling terrain, typically use a method called "area surface mining" (Hamilton and Wilson, 1977, p. 28-29; National Research Council, 1981, p. 36-38). The first cut of the surface coal mine is an open trench cut through the overburden to the coal. The coal is extracted, a second parallel cut is excavated, and the overburden from this cut is placed into the previous cut as spoil. The process continues and subsequent cuts are made until either the mine boundary is reached or the coal is too deep to be mined economically. The rate at which the cuts are made depends on factors such as the size of the machinery used to do the excavating, the length of the mine parallel to the cut, weather, and economic conditions.

The State of Illinois, under the Surface Mining Control and Reclamation Act of 1977, requires coal companies to assess the probable impacts of surface coal mining on the local ground-water hydrology. Prior to excavation, mining companies are required to submit geologic and hydrologic data that identify local aquifers within the proposed mining area (Nawrocki, 1979).

Analytical and numerical solutions are available for predicting ground-water drainage to surface excavations. Most available solutions to ground-water-drainage problems consider flow only in the saturated zone. Those solutions that include the unsaturated zone are limited in scale and require complex computer modeling. A general technique that includes drainage from the unsaturated zone is needed for predicting ground-water drainage to an excavation.

Purpose and Scope

The purpose of this report is to describe a technique that can be used for predicting ground-water drainage into surface coal mines. The technique uses geologic and hydrologic data collected prior to mining. The technique includes consideration of the unsaturated zone through precalculated head and seepage-flux profiles; hence, access to a computer is not required by the user. It was developed for areas in Illinois where area surface mining is used. It is limited to hydrogeologic settings and surface-mining methods common to Illinois. Users are cautioned that the technique (1) provides estimates, (2) makes use of simplifying assumptions to approximate actual hydrogeologic conditions and mine operations, and (3) has been evaluated with only one set of field data.

The equations used to describe ground-water flow (Lappala and others, 1985) consider flow in both the unsaturated and saturated zones. The complex solution to the variably-saturated, ground-water-drainage problem is simplified through the use of computer-generated profiles that can be applied to a range of mine-drainage problems.

It was assumed that drainage to surface mines in Illinois could be represented by two simplified conceptual models: (1) Drainage to a first cut and (2) drainage to multiple cuts. Various hypothetical aquifers represent hydrogeologic conditions and mine operations. A computer model that considers flow in the saturated and unsaturated zones was used to simulate up to 2 years of flow through each aquifer.

Guidelines are given for deciding which of the two conceptual models, if either, is applicable to conditions at a proposed mine site. For the chosen conceptual model, an explanation is given of how to match hydrogeologic conditions and mine operation to one or more of the simulated aquifers. Examples are given of how to predict ground-water-level changes and seepage flux at a proposed mine by using the nondimensional output from one or more of the simulated aquifers. Limitations of the applicability of the technique are discussed.

The report is divided into two main sections. The first section includes the development and application of the technique and includes examples and limitations. The second section consists of five appendixes. Appendix A is an evaluation of the technique in terms of its comparison to other methods, use of an actual field test, and analyses of sensitivity and mass balance. Appendixes B through E are groups of illustrations that are used in the computations.

Acknowledgments

The Freeman United Coal Mining Company granted personnel of the U.S. Geological Survey access to their Industry Mine for hydrogeologic studies. Their cooperation and assistance is gratefully acknowledged.

PREVIOUS STUDIES

Traditional methods of predicting ground-water seepage into surface mines have used solutions to drainage from large, unconfined aquifers into surface reservoirs (Freeze and Cherry, 1979, p. 484). Most were developed using experimental, analytical, and numerical solutions and were limited to saturated-flow conditions. Ibrahim and Brutsaert (1965) studied unsteady, free-surface, ground-water flow into a fully-penetrating surface reservoir using a Hele-Shaw viscous-fluid-flow model. Boussinesq (1877, 1904) applied the general solution of the heat-flow equation to agricultural tile drainage and developed analytical series expansion solutions. Glover (1964) and Haushild and Kruse (1962) analyzed unsteady, ground-water flow into a surface reservoir from an unconfined aquifer. Yeh (1970) used a numerical model to simulate one-dimensional, unsteady, ground-water flow through a large unconfined aquifer to a surface reservoir. Verma and Brutsaert (1971) used a numerical model to simulate one-dimensional and two-dimensional unconfined ground-water seepage. Bair (1980) used a numerical ground-water-flow model to simulate aquifer drainage to a proposed open-pit anthracite mine.

Brutsaert and El-Kadi (1984) have shown that neglecting flow in the unsaturated zone in shallow aquifers with a large capillary fringe can lead to large discrepancies in predicting seepage flux and ground-water levels. They concluded that saturated-flow models overestimate the outflow volume and ground-water level and underestimate the duration of flow. Although a few investigators, such as Verma and Brutsaert (1970), have used numerical models that incorporate unsaturated-flow conditions, the results are typically for a limited scale of hydrogeologic properties.

GEOLOGIC SETTING

Techniques presented were developed for Illinois surface coal-mining regions but should be applicable to areas of similar hydrogeology. The coal reserves of Illinois are in Pennsylvanian rocks which underlie the southern three-quarters of the State and extend into Indiana and Kentucky. This region

is the Eastern Interior Coal Field. In Illinois, the surface-minable coal reserves are generally near the periphery of a spoon-shaped structural basin that is oriented north-northwest to south-southeast and has its deepest part, about 750 meters, in southeastern Illinois. Most coals of economic importance in Illinois are in the Spoon and Carbondale Formations (Willman and others, 1975). Coals are underground mined in areas where they lie at depths greater than about 45 meters. Figure 1 shows the areal geology of the consolidated bedrock formations in Illinois that are mostly marine sediments deposited during the Paleozoic Era. Unconsolidated deposits of Quaternary age overlie the Pennsylvanian rocks in much of Illinois. These surficial materials, or overburden, are also important in the hydrogeology of mine drainage. Figure 2 shows the surficial geology of Illinois, and figure 3 shows the general stratigraphic sequence of the rocks of Illinois (Willman and others, 1975).

DESCRIPTION OF TECHNIQUE

The technique is a user's manual of pregenerated head and seepage-flux profiles that can be used to predict changes in seepage flux and head (ground-water level) resulting from ground-water drainage into a surface coal mine. The profiles were generated using a computer model that considers flow in the saturated and unsaturated zones. Two conceptual models were considered: (1) Drainage to a first cut and (2) drainage to multiple cuts.

Conceptual Models

Drainage to a first cut assumed ground-water movement could be represented by flow through a rectangular, vertical cross section perpendicular to the length of the first (box) cut. Seventy-two cross sections, composed of various combinations of the hydrogeologic characteristics of length, thickness, geologic material, and initial head, were chosen to represent aquifers typical of Illinois surface mines.

Drainage to multiple cuts further assumed ground-water drainage to an advancing surface mine could be represented by changing boundary conditions. One hundred and seventy-four combinations of (1) the hydrogeologic characteristics of length, thickness, and geologic material and (2) changing boundaries were chosen to represent aquifers and mining conditions typical of surface mines in Illinois.

Graphs of dimensionless total-head and seepage-flux profiles were constructed using output from a finite-difference, two-dimensional, computer model of variably-saturated, cross-sectional flow. Head profiles at various times and seepage flux as a function of time were obtained for each of the simulated aquifers and are presented in graphical, dimensionless format. These graphs, in conjunction with knowledge of aquifer characteristics at the proposed mine site and estimates of the size and timing of the mine operation, are used to compute water levels and seepage flux for various times and conditions.

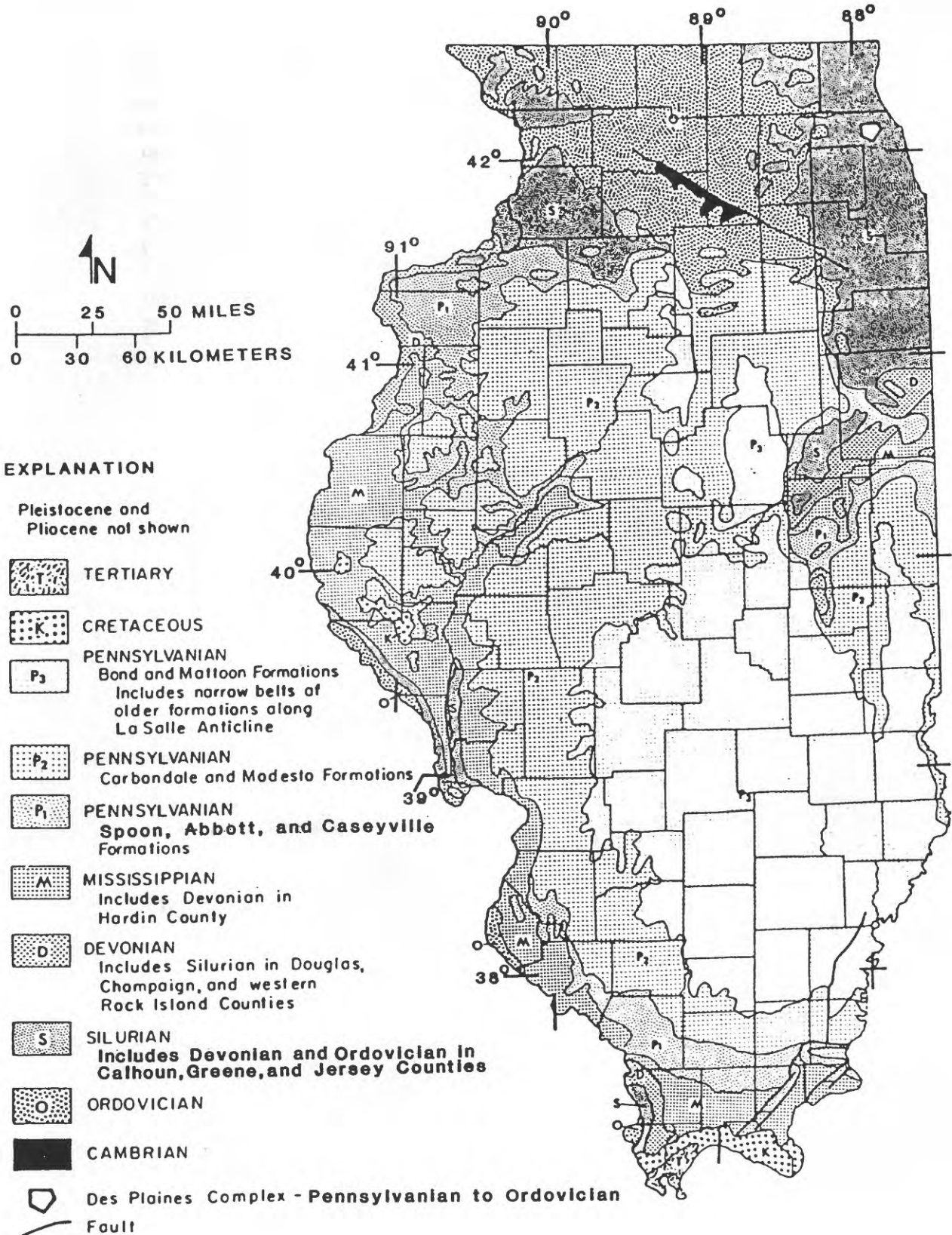


Figure 1.--Generalized bedrock geology of Illinois (from Willman and others, 1975, p. 21).

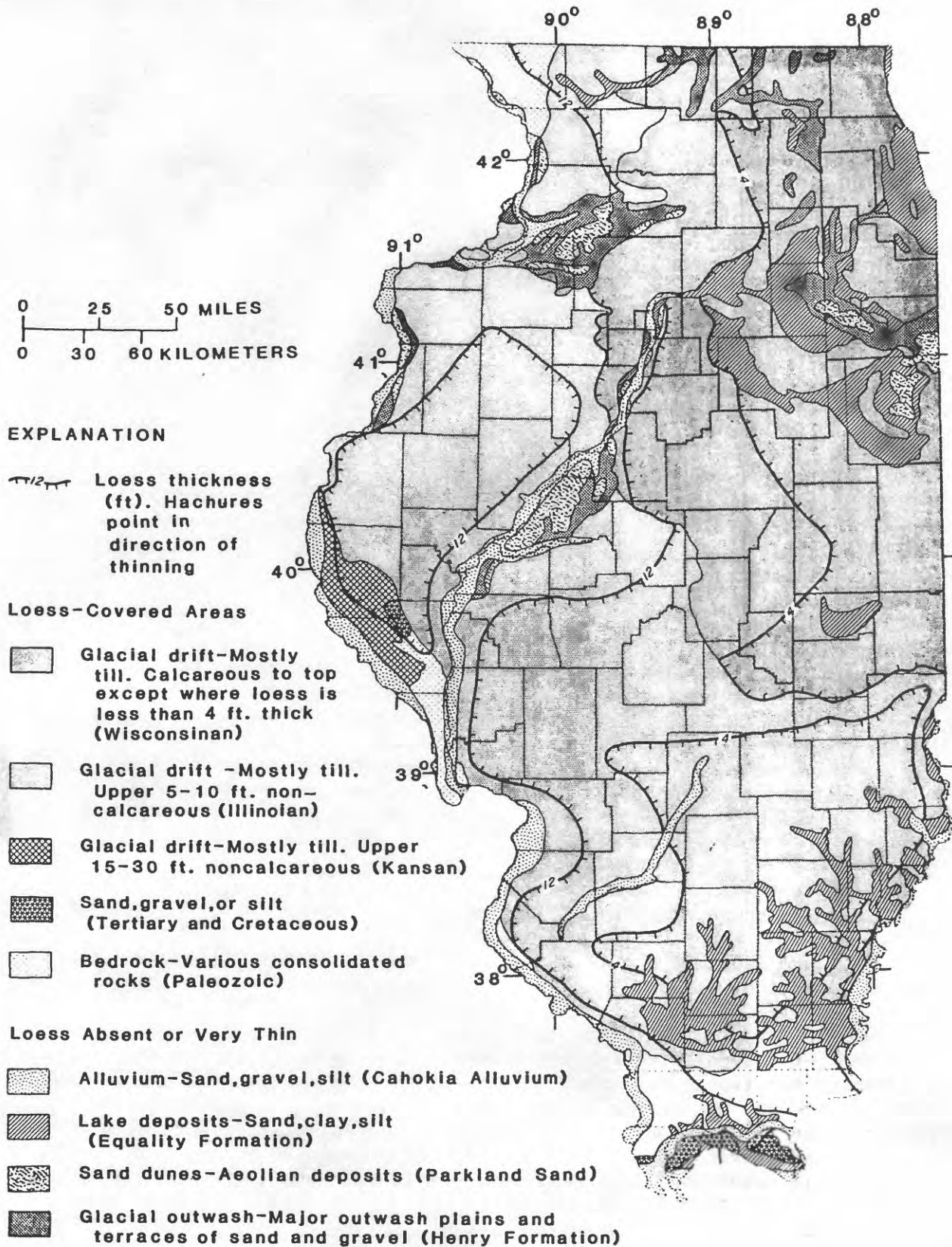


Figure 2.--Generalized surficial geology of Illinois (from Willman and others, 1975, p. 22).

First Cut

Assumptions related to the geometry of the aquifer and the first cut include the first cut is long and linear in shape (fig. 4); the aquifer is approximately rectangular in shape with unit thickness; and the mine is excavated instantaneously and completely penetrates the aquifer. Also, the aquifer cross section and mine face are vertical; the aquifer cross section is perpendicular to the axis of the mine and parallel to the direction of ground-water flow after the mine is emplaced; and the aquifer is extensive laterally to the first cut and is perpendicular to the vertical aquifer cross section.

Assumptions related to properties of the aquifer cross section include the aquifer is homogeneous and isotropic; and the ground-water flow has both horizontal and vertical components and is representative of flow in the aquifer. Also, the unsaturated zone considered is that resulting from drainage from an initially fully-saturated aquifer.

Figure 5a presents the hydrologic conditions, in cross section, of a confined aquifer at the mine cut of figure 4. These conditions consist of no-flow boundaries (CJ, JF, and EF), a seepage face (CE), and potentiometric surfaces at time $t=0$ (AB) and some time later $t=t$ (GHI). Figure 5b presents the hydrologic conditions, in cross section, of an unconfined aquifer at the mine cut of figure 4. These conditions consist of no-flow boundaries (JF, EF), a seepage face (CE), and water table at time $t=0$ (CJ), and some time later $t=t$ (GI). For both figures 5a and 5b, at time $t=t$, the unsaturated portion of the seepage face (CG) at $x=0$ is also considered a no-flow boundary. This boundary does not exist at the instant of the excavation of the first cut, but, in general, its length increases with time. The seepage-face boundary (GE) is a variable-flux boundary through which ground water is discharged from the aquifer. The length of the seepage-face boundary at the instant of excavation equals the initial saturated thickness of the aquifer (CE) and, in general, decreases with time. The unsaturated portion of the aquifer (ACBJ) at $t=0$ is not considered in this analysis.

Initial conditions ($t=0$) in the aquifer cross section (CJEF in figs. 5a and 5b) are (1) the aquifer is initially saturated under the boundary CJ and (2) initial total heads are static and equal throughout the aquifer. Initial total heads are equal to three times the initial saturated thickness for the confined case (fig. 5a) and equal to the aquifer thickness for the unconfined case (fig. 5b).

Seventy-two hypothetical aquifers were selected to represent various combinations of the two initial-head conditions, thickness, length, and geologic material. A suite of various geologic materials (table 1) was chosen to represent a reasonable range of the hydraulic characteristics saturated hydraulic conductivity (K_{sat}) and specific yield (S_y) for geologic materials that typically occur in Illinois surface coal-mining areas (Freeze and Cherry, 1979, p. 29; Bear, 1972, p. 46; Meinzer, 1923, p. 11; and R. W. Healy and J. V. Borghese, U.S. Geological Survey, written commun., 1984). The geologic materials are lettered A through K, where A has the highest K_{sat} and K has the lowest K_{sat} . Lithologies with which these hydraulic characteristics may be

ERA, ERATHEM	PERIOD, SYSTEM	EPOCH, SERIES	ORIGIN AND CHARACTER	GREATEST THICKNESS (m) ¹	AGE (MILLIONS OF YEARS) ²
CENOZOIC	QUATERNARY	Pleistocene	CONTINENTAL - Glacial, river, stream, wind, lake, swamp, colluvial deposits, and soils	180	2
		TERTIARY	Pliocene	CONTINENTAL - River deposits mostly gravel, some sand	15
	Eocene		DELTAIC - Mostly sand, some silt	90	
	Paleocene		MARINE - Mostly clay, some sand	45	
	MESOZOIC	CRETACEOUS	Gulfian	DELTAIC/NEARSHORE MARINE - Sand, silt and clay, locally lignitic	150
PALEOZOIC	PENNSYLVANIAN	Virgilian	MARINE/DELTAIC/CONTINENTAL - Cyclical deposits, mostly shale, sandstone, siltstone, some limestone, coal, clay, black shaly shale; shale over sandstone in lower part, coal in middle, limestone in upper	915	3,138
		Missourian			
		Demoinesian			
		Atokan			
			Morrowan		
	MISSISSIPPIAN	Chesterian	MARINE/DELTAIC - Cyclical deposits of limestone, sandstone, shale	425	330
		Valmeyeran	MARINE/DELTAIC - Limestone, siltstone, shale, chert, sandstone	610	
		Kinderhookian	MARINE - Shale, limestone, siltstone	45	360

ERA, ERATHEM	PERIOD, SYSTEM	EPOCH, SERIES	ORIGIN AND CHARACTER	GREATEST THICKNESS (m) ¹	AGE (MILLIONS OF YEARS) ²
PALEOZOIC	DEVONIAN	Upper	MARINE-Shale, limestone	90	360
		Middle	MARINE-Largely limestone, some shale	135	
		Lower	MARINE-Cherty limestone, chert	400	
	SILURIAN	Cayugan	MARINE-Shale, limestone, siltstone	30	410
		Niagaran	MARINE-Dolomite, limestone, shale, local reefs	300	
		Alexandrian	MARINE-Dolomite, limestone, shale	45	
		Cincinnati	MARINE-Shale, limestone, siltstone, dolomite	90	
	ORDOVICIAN	Champlainian	MARINE-Limestone, dolomite, sandstone	425	435
		Canadian	MARINE-Dolomite, sandstone	300	
	CAMBRIAN	Croloxan	MARINE-Sandstone, dolomite, shale	1220	500
Intrusive igneous rocks--mostly granite				570 ⁴	
PRECAMBRIAN					

EXPLANATION

¹ Greatest thickness in one locality

² Age is beginning of interval and follows U.S. Geological Survey usage

³ Beginning of Cretaceous

⁴ Beginning of Cambrian

----- Denotes unconformity

Figure 3.--Summary of the age, origin, and thickness of Illinois rocks (modified from Willman and others, 1975, p. 10).

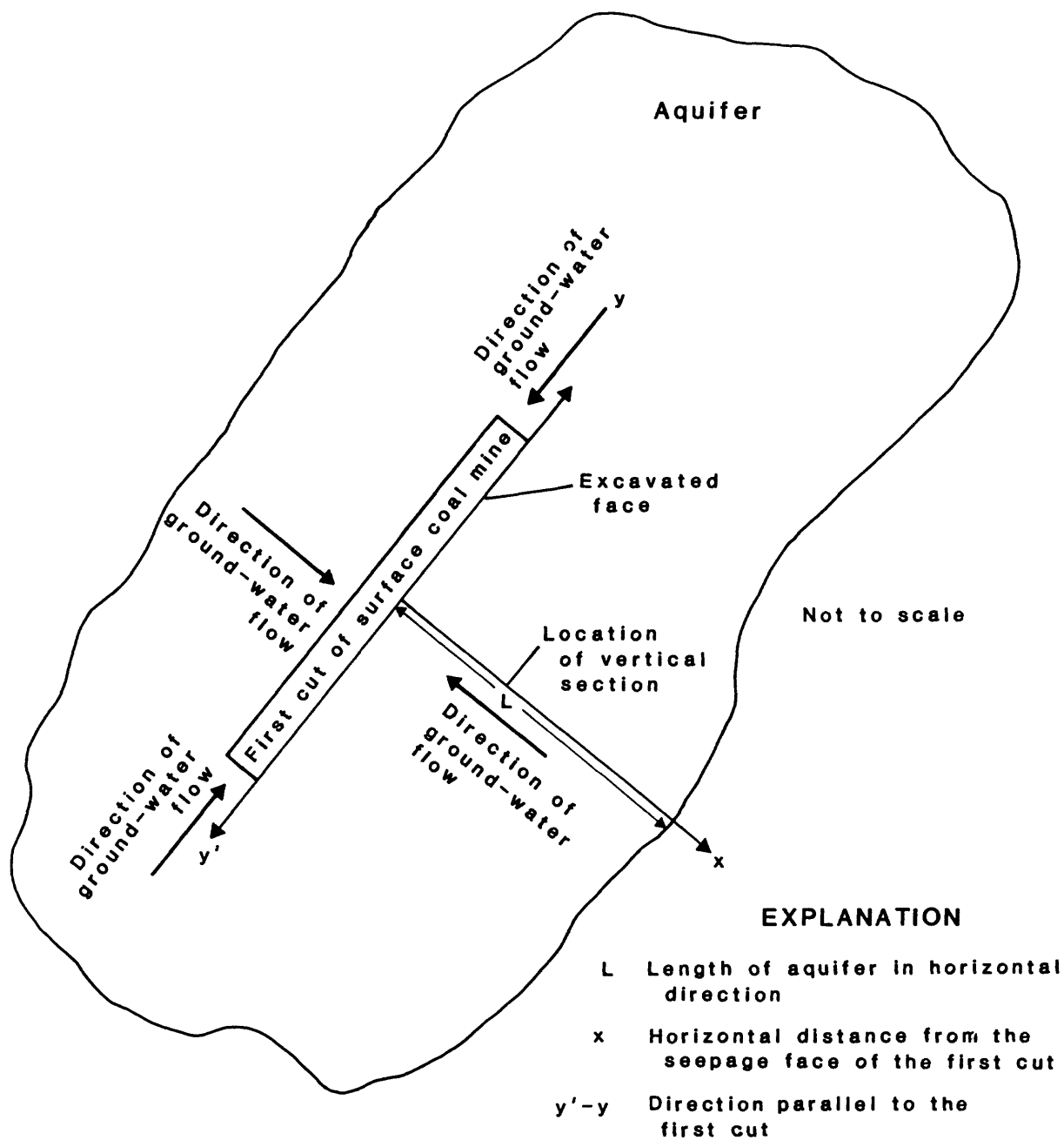
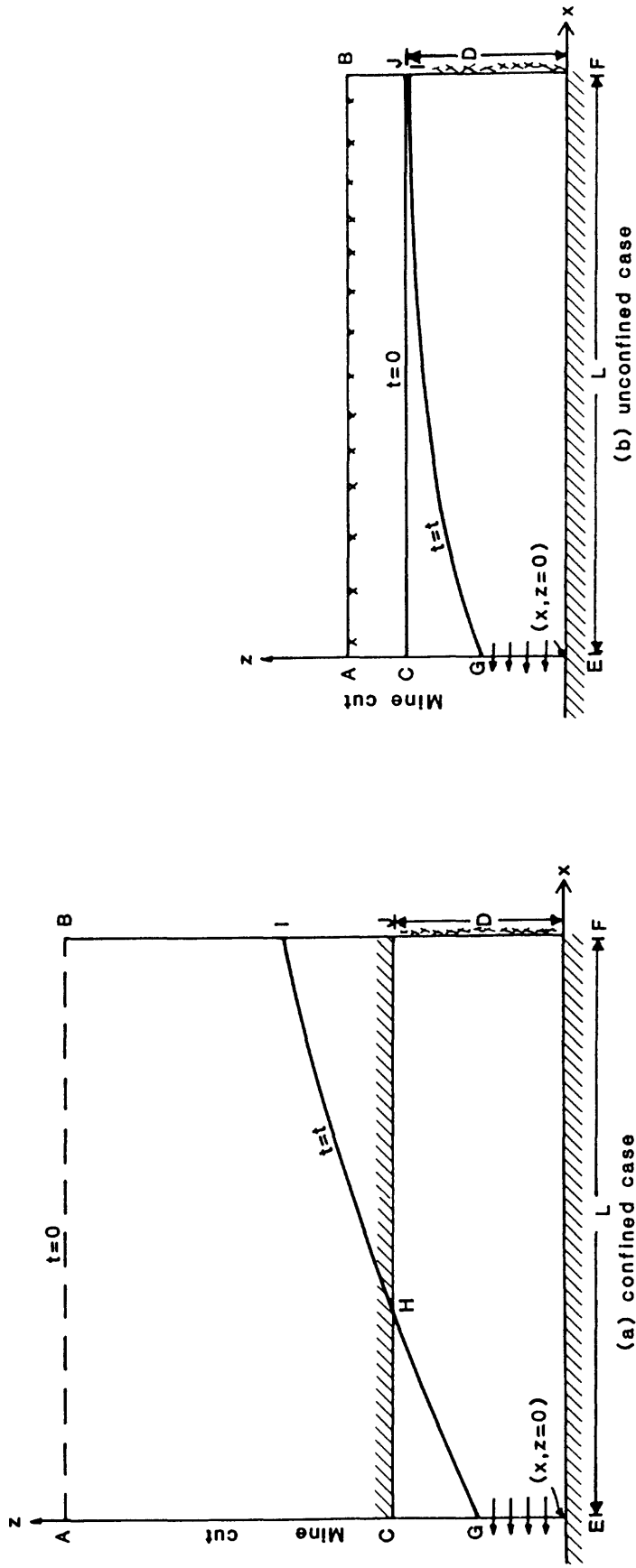


Figure 4.--Plan view of geometry of aquifer and first cut of surface coal mine and location of vertical section.



EXPLANATION

	Aquifer, such as limestone or alluvium	L	Length
CJEF	Aquifer, such as limestone or alluvium	D	Thickness
CE	Seepage face		
JF, EF	No-flow boundaries		
CJ	No-flow boundary (confined case)		
AB	Water table at $t=0$ (unconfined case)		
GH	Potentiometric surface at $t=0$ (confined case)		
HI	Land surface (no recharge or evapotranspiration)(unconfined case)		
GI	Water table at $t=t$ (confined case)		
above line C-J	Potentiometric surface at $t=t$ (confined case)		
above line EF	Water table at $t=t$ (unconfined case)		
below line EF	Initial unsaturated zone (not considered)(unconfined case)		
	Poorly permeable material, such as shale (confined case)		
	Coal bed mined		
	Poorly permeable material, such as underclay		

Figure 5.--Vertical sections of aquifer showing ground-water drainage to first cut.

Table 1.--Geologic materials and hypothetical-aquifer characteristics typical of Illinois surface coal-mining regions
 [m/d, meter per day; m, meter; (m-d²)/g, meter-day squared per gram]

Geologic material	Possible lithologic association	Saturated			Brooks and Corey coefficients			Aquifer compressibility, [(m-d ²)/g]
		hydraulic conductivity, K _{sat} (m/d)	Specific yield, S _y	Porosity, φ	Residual moisture content, θ _r	Bubbling pressure, h _b (m)	Pore-size distribution index, λ	
A	gravel	8.47	0.29	0.30	0.01	-0.10	3.0	1.34 x 10 ⁻²²
B	well-sorted alluvial deposits	2.54	.27	.40	.13	-.15	2.0	1.34 x 10 ⁻²¹
C	poorly-sorted sand and gravel	8.47 x 10 ⁻¹	.28	.35	.07	-.13	2.5	1.34 x 10 ⁻²²
D	clean sand	8.47 x 10 ⁻²	.32	.42	.10	-.17	1.7	1.34 x 10 ⁻²¹
E	limestone	2.54 x 10 ⁻²	.15	.20	.05	-.15	2.0	1.34 x 10 ⁻²²
F	silty sand	8.47 x 10 ⁻³	.35	.45	.10	-.20	1.5	1.34 x 10 ⁻²⁰
G	outwash deposits of silt and clay	2.54 x 10 ⁻³	.12	.30	.18	-.25	1.8	1.34 x 10 ⁻²¹
H	sandstone	2.54 x 10 ⁻⁴	.10	.20	.10	-.60	3.5	1.34 x 10 ⁻²²
I	coal	2.54 x 10 ⁻⁴	.10	.15	.05	-.15	2.5	1.34 x 10 ⁻²²
J	clayey till	2.54 x 10 ⁻⁴	.05	.25	.20	-.90	1.8	1.34 x 10 ⁻²⁰
K	weathered shale	2.54 x 10 ⁻⁶	.05	.06	.01	-.30	2.5	1.34 x 10 ⁻²²

associated include the Pennsylvanian consolidated limestones, shales, coals, underclays, and sandstones normally associated with coals, and the Quaternary unconsolidated clays, sands, and gravels. The lithology and aquifer characteristics associated with table 1 do not imply that clean sand or poorly-sorted sand and gravel deposits, for example, correspond to values in table 1 corresponding to those lithologies. The lithologies should not be taken strictly and are only meant to represent the parameter values that are listed with them. The geologic materials and possible lithologic associations are only meant as convenient labels for the numbers that were used in the hypothetical-aquifer simulations. A suite of aquifer lengths, L , (figs. 4 and 5) and thicknesses, D , (fig. 5) were also selected that are typical of Illinois as described by Pryor (1956). Geometries of hypothetical aquifers were defined by combining aquifer lengths of 75, 150, 450, 800, and 1,500 m (meters) with aquifer thicknesses of 1 and 5 m. Aquifer thickness is defined as the thickness of the initial saturated zone within the geologic-material body, and the aquifer length is the length of the aquifer on the modeled side of the mine.

Multiple Cuts (Unconfined aquifers only)

The conceptual model of drainage to multiple cuts (figs. 6 and 7) assumes that the changing aquifer boundary caused by an area surface mine can be represented by two sets of initial and boundary conditions. Subsequent cuts are parallel to the first. It is assumed that an active area surface mine, in which successive cuts are made, can be approximated by two cutting routines: (1) The first cut (fig. 7a) and (2) any number of subsequent cuts considered together (fig. 7b). The sum of the two cutting routines, or multiple cuts, requires two sets of assumptions including boundaries and initial conditions.

Assumptions related to the geometry of the aquifer and the mine are the same as those for the first cut with the additions that (1) subsequent cuts, after the first, of the mine are represented by one cut excavated instantaneously at time equal to t_0 (CKEP in fig. 7b), and (2) the aquifer cross section is instantaneously shortened by a length corresponding to the width (w_0) of the subsequent cuts (EP). Assumptions related to properties of the aquifer cross section are the same as those related to the first cut except that confined aquifers are not considered.

The second set of assumptions related to the change in boundary conditions after subsequent cuts are instantaneously emplaced (fig. 7b) at t_0 is the side of the section at the multiple mine cuts (KP) is moved to $x = w_0$; and the top and bottom boundaries (KQ and PF) extend from $x = w_0$ to $x = L$.

The second set of initial conditions in the aquifer cross section (fig. 7b) is initial heads are transient heads obtained after drainage to the first cut for time t_0 ; and initial heads vary throughout the aquifer and depend on conditions existing prior to the subsequent cuts.

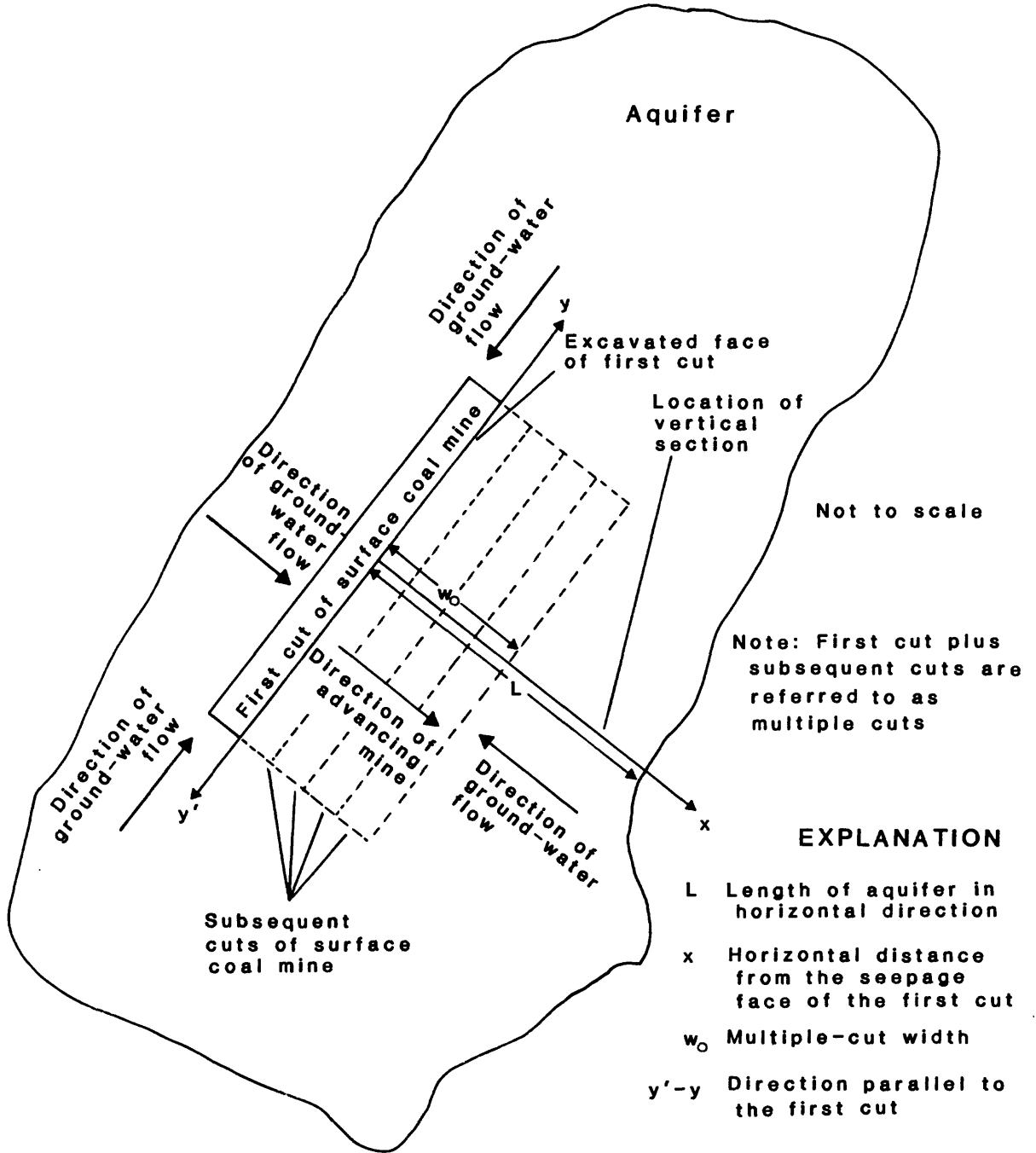
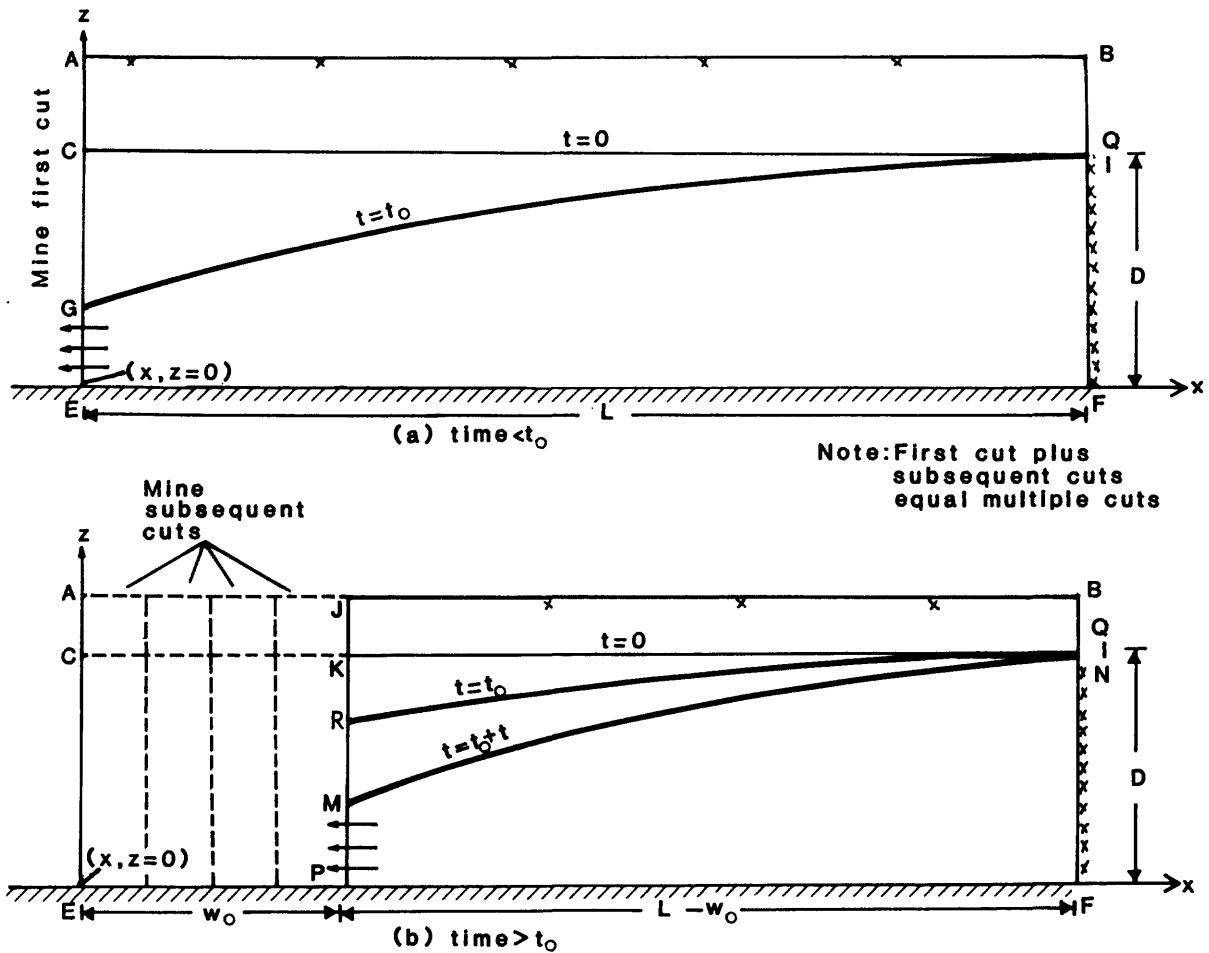


Figure 6.--Plan view of geometry of aquifer and multiple cuts of surface coal mine and location of vertical section.



EXPLANATION

(Note: all cases are unconfined)

- CQEF Aquifer, such as limestone or alluvium, after first cut
- KQPF Aquifer, such as limestone or alluvium, after subsequent cuts
- CE Seepage face, after first cut
- KP Seepage face after multiple cuts
- QF, EF No-flow boundaries
- AB Land surface after first cut (no recharge or evapotranspiration)
- JB Land surface after subsequent cuts (no recharge or evapotranspiration)
- ABCQ Unsaturated zone (not considered) after first cut
- JBKQ Unsaturated zone (not considered) after subsequent cuts
- CQ Water table at $t=0$
- GI, RI Water table at $t=t_0$
- MN Water table at $t>t_0$
- above line EF Coal bed mined
- below line EF Poorly permeable material, such as underclay
- D Thickness
- L Length
- w_0 Width of subsequent cuts

Figure 7.--Vertical sections of aquifer showing ground-water drainage to multiple cuts.

Thirty-two of the 72 hypothetical aquifers used for the first cut were used for the multiple cuts. Only unconfined aquifers (initial head equal to the saturated aquifer thickness) were considered with combinations of thickness, length, and geologic material. Only geologic materials A through F (table 1) were considered because they are the most significant with respect to drainage effects in the time period under consideration. These geologic materials were combined with aquifer lengths of 150, 450, 800, and 1,500 m and with aquifer thicknesses of 1 and 5 m.

Each of the 32 aquifers was modeled with several multiple-cut widths, w_0 , which represented the distance of mine advance from the first cut, and for several multiple-cut times, t_0 , which represented the time for this mine advance. Values of w_0 ranged from 22.5 to 80 m and t_0 ranged from 30 to 270 days. A total of 174 hypothetical-aquifer/multiple-cut combinations were used.

Ground-Water Flow System

Following instantaneous excavation of the mine, a seepage face develops along the boundary between the aquifer and the mine. Ground-water drainage through the seepage face causes decreasing heads in the aquifer and an unsaturated zone develops in the upper part of the aquifer. The water table divides the flow system into the saturated and unsaturated zones.

Total head (H) at any point in the aquifer equals the sum of the pressure head (h_p) and elevation head (h_z). Total head also includes velocity head, which is assumed negligible in ground-water-flow systems (Heath, 1983, p. 10). Total head equals h_z for water-table conditions. Elevation head equals zero at the lower impermeable boundary, $z=0$ (figs. 5 and 7), and increases to D at the top of the saturated portion of the aquifer, $z=D$ (figs. 5 and 7). Pressure head in the saturated zone is greater than atmospheric pressure and proportional to the weight of the water above the measuring point. Although the vertical head distribution generally shows pressure heads increasing with depth, the distribution is not static due to vertical components of flow. Pressure head in the unsaturated zone is less than atmospheric pressure and is also referred to as tension head or suction head.

Computer Models

The U.S. Geological Survey finite-difference model, VS2D (Lappala and others, 1985), that considers variably-saturated, two-dimensional, ground-water flow was used because it simulates flow in the unsaturated zone. Each model simulation required several input variables. The choice of variables was based on a series of test simulations aimed at decreasing mass-balance error and computer time (Appendix A).

First Cut

Saturated hydraulic conductivity (K_{sat}), porosity (ϕ), Brooks and Corey coefficients (θ_r , h_p , λ) (Lappala and others, 1985), and aquifer matrix compressibility (α) were input to the VS2D model to describe the various geologic materials (table 1). Aquifer matrix compressibility must be considered under conditions of large, sudden pressure changes in the water (Brutsaert and El-Kadi, 1984, p. 407). These occur in drainage to surface coal mines from confined aquifers, especially at small times after excavation. Values for α were selected from the literature for the 11 geologic materials (Freeze and Cherry, 1979, p. 55). Fluid compressibility (β) was 5.894×10^{-23} meter-day squared per gram [(m-d²)/g].

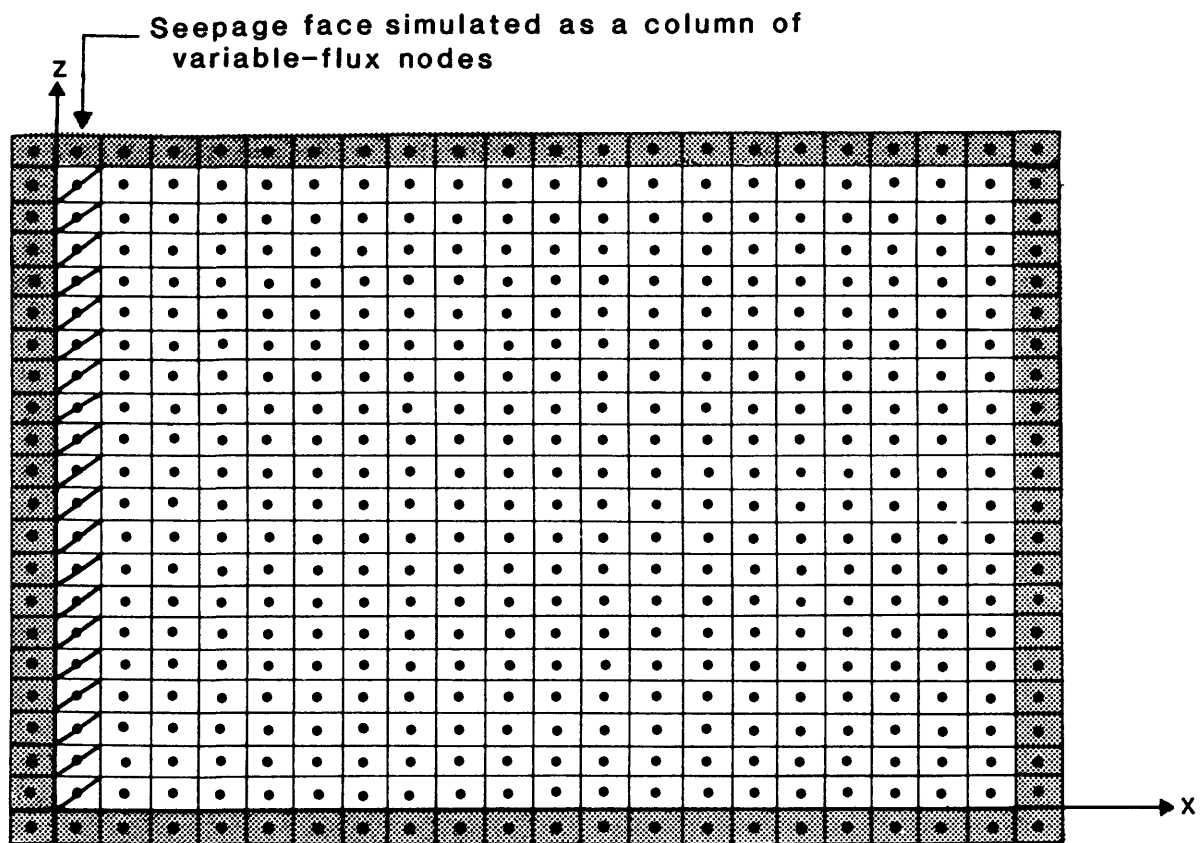
A block-centered, finite-difference grid of 22 nodes by 22 nodes (fig. 8) was used. Because the VS2D model requires a no-flow boundary around the entire domain, the hypothetical aquifer was actually represented by a domain of 20 nodes by 20 nodes. Zero-flux nodes on three sides of the domain were defined using nodes of zero permeability to satisfy the assumptions of impermeable boundaries. The seepage-face boundary was defined by a column of nodes just inside a vertical set of zero-flux nodes (fig. 8). Nodes representing the seepage face were treated as variable-flux nodes. As the potentiometric surface fell during a simulation, the nodes above the potentiometric surface were specified zero flux. Because flow was allowed out of the domain, nodes below the potentiometric surface had flux values greater than zero.

All nodes were equally spaced in the horizontal (x) and vertical (z) directions for a given simulation; however, grid spacing changed from one simulation to another depending on the dimensions of the modeled aquifer. For example, an aquifer 150-m long and 1-m thick had a constant grid spacing of 7.5 m in the x-direction and 0.05 m in the z-direction. An aquifer 450-m long and 5-m thick had a constant grid spacing of 22.5 m in the x-direction and 0.25 m in the z-direction.

Ground-water flow was simulated for times up to 730 days after excavation of the first cut. The initial time step was 0.10 day. This time step was increased by a multiplier equal to 1.75. The maximum time step was 25.0 days, and the minimum was 0.10 day. Total head and seepage flux were calculated for times from 10 to 730 days after excavation of the first cut.

An iterative solution method is used by the VS2D model. Solution was achieved when the maximum total-head change between iterations met the specified closure criterion, 5.0×10^{-4} m in most cases. Simulations with large mass-balance error (Appendix A) had closure criterion decreased to 1.0×10^{-4} m. The relaxation parameter for the numerical matrix-solving method was 0.8. The minimum number of iterations per time step was 3, and the maximum number was 299.

The VS2D model proved inadequate for modeling aquifers of low permeability because of its inability to converge on a solution. Therefore, the Glover linearized saturated-flow solution (Appendix A) was used for simulating flow through geologic materials H through K. Brutsaert and El-Kadi (1984) have



EXPLANATION

-  Zero-flux node
-  Variable-flux node
-  Internal node

Figure 8.--Two-dimensional, block-centered, finite-difference grid for drainage to first cut for model cross section.

shown that when the unsaturated-zone thickness is small and pressure changes are gradual, as is the case for these geologic materials, then the governing differential equation for saturated flow (Bear, 1972) holds. The effect of neglecting flow in the unsaturated zone for these geologic materials is insignificant.

In total, 64 simulations were made using VS2D and 8 were made using the Glover solution. Total head at each node and seepage flux at specified times from 10 to 730 days were output from the VS2D simulations. Only total head for unconfined aquifers was output from the Glover simulations.

Multiple Cuts

Saturated hydraulic conductivity, porosity, and Brooks and Corey coefficients for geologic materials A through F (table 1) were used for the multiple-cut simulations. Compressibility values were assumed to be zero because only unconfined aquifers were considered.

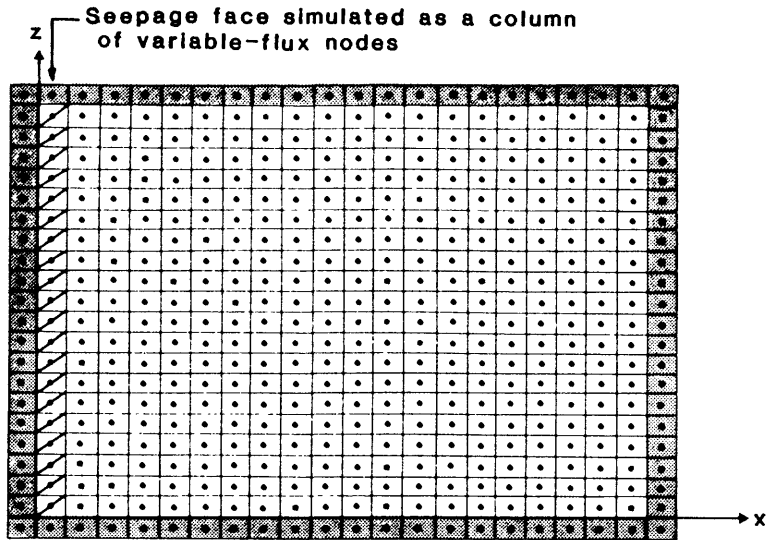
Two finite-difference grids were used in sequence for each multiple-cut simulation. The first grid (fig. 9a) represented an aquifer draining to a first cut from time zero to time t_0 . The domain of internal nodes was surrounded with nodes of zero permeability (zero flux) to represent impermeable boundaries on three sides of the domain. The seepage-face boundary was the column of variable-flux nodes just inside the vertical set of zero-flux nodes at the left of the domain. Ground-water flow through the figure 9a grid was simulated until time t_0 (30, 90, 180, or 270 days), when output heads were saved and input as initial conditions to the interior nodes of the second grid (fig. 9b). The change of grids at time t_0 represents when all subsequent cuts of combined width w_0 are instantaneously emplaced. Subsequent cuts were modeled by redefining the nodes representing the cuts to zero-permeability (zero-flux) nodes, and respecifying the location of the seepage-face nodes to $x=w_0$ at $t=t_0$. Simulation proceeded to 730 days.

Multiple-cut widths ranged from 22.5 to 80.0 m, depending on the aquifer length. The widths were assigned dimensions of multiple whole grid spacing to simplify input data specification. For example, horizontal grid spacing for an aquifer 450-m long was 22.5 m (20 nodes times 22.5 m equals 450 m). Multiple-cut widths for this length were whole multiples of 22.5 m. Thus, w_0 equal to 22.5 m, 45.0 m, and 62.5 m were chosen for aquifers 450-m long. Other aquifer lengths were treated similarly.

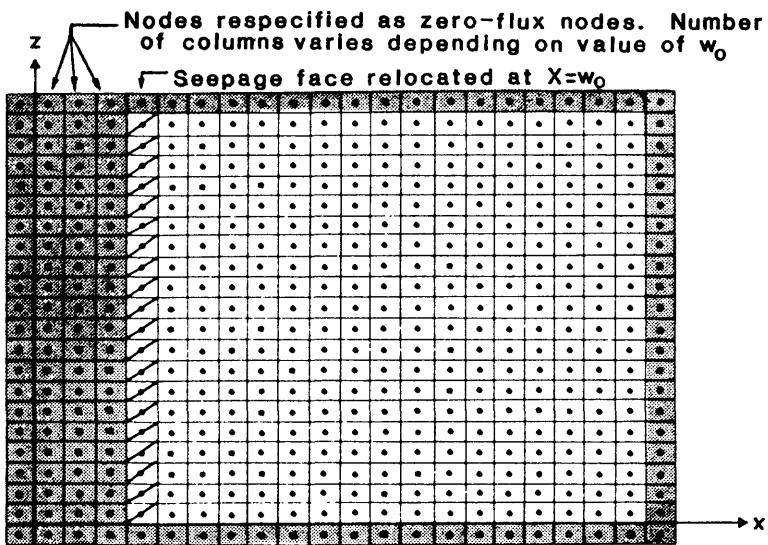
The output from the 174 multiple-cut simulations were total head at each node and seepage flux at specified times of drainage to the first cut from 10 to 730 days. Graphs were constructed using output from these simulations and the 72 first-cut simulations and were used in example computations.

Limitations

Assumptions of the conceptual and computer models used to develop the technique and simplifications required to match field conditions are as follows:



(a) Drainage to first cut (time $\geq t_0$)



(b) Drainage to subsequent cuts (time $\geq t_0$)

EXPLANATION

-  Zero-flux node
-  Variable-flux node
-  Internal node

Note: First cut plus subsequent cuts are referred to as multiple cuts

Figure 9.--Two-dimensional, block-centered, finite-difference grids for drainage to multiple cuts for model cross sections.

The conceptual model assumes a two-dimensional, vertical aquifer cross section and instantaneous excavation. This conceptualization precludes flow to the excavation from aquifers outside the modeled cross section. This causes seepage flux into the mine and head declines in the aquifer to be underestimated at small times and overestimated at large times.

The conceptual model assumes that the initial head in the aquifer is everywhere equal, the gradient is initially flat, and the pressure change at the seepage face is sudden. Deviations from the flat-gradient initial condition may yield some differences in heads and seepage fluxes, especially near the seepage face at small times. The differences would depend on the initial gradients relative to the gradient induced by mining. The orientation of the mine in relation to the direction of ground-water flow might also be significant.

Heads and seepage fluxes were computed neglecting leakage and recharge. No recharge to an aquifer means that predicted water levels and seepage fluxes will be lower than if recharge were included. Recharge should be considered if the recharge flux is significant relative to the seepage flux. Leakage to or from an aquifer may significantly affect head and seepage flux. The amount of leakage would have to be estimated to assess the potential impacts on the predicted head and seepage flux. If recharge and leakage are significant, the technique should only be used as a rough estimate.

Fracture flow is not considered. This limitation may be especially important in limestone aquifers and near excavations due to highwall-blasting-induced fractures. The technique should not be used for fractured media with a strong anisotropy of permeability.

The conceptualized aquifer is assumed to be initially fully saturated. Thus, the unsaturated zone above the water table is not considered. If the initial unsaturated zone contains moisture in excess of the moisture-retention capability, this water could infiltrate deeper as the water table falls and could contribute to the seepage flux.

It is assumed that the excavations penetrate layered and horizontal strata, and aquifer properties are assumed to be constant throughout the cross section. These may be limiting assumptions, especially for glacial drift.

A constant-head boundary, such as a final-cut lake or flooded underground mine, is not considered. Constant-head boundaries within 1,500 m could affect mine drainage.

Simulation of drainage through the hypothetical aquifers using the VS2D model depended on various numerical choices, such as node number and spacing, finite-difference spatial and temporal discretization, matrix-solving technique, closure criterion, time-step multiplier, seepage-face algorithm, or computational procedure. Final choice of these variables was based on considerations of consistency, reasonable results, good mass balance, and minimum computer time. Other choices may have given different total-head and seepage-flux profiles, especially near the seepage face.

Evaluation of the technique through comparison of results with saturated-flow solutions and measured data was limited to evaluation of predicted heads for an unconfined aquifer at one field site. No seepage-flux data were available for testing.

Only unconfined aquifers were considered for multiple cuts. If the aquifer at the proposed mine is confined, the first-cut-only technique should be used.

APPLICATION OF TECHNIQUE

Measurements, simplifications, and judgments must be made to make predictions at a proposed mine site. Predicted heads and seepage fluxes are sensitive to estimates of aquifer permeability. Measurements of saturated hydraulic conductivity and specific yield at the mine are preferable to estimates. The reader is referred to Ground-Water Manual (U.S. Department of the Interior, 1981), Ground-Water Hydraulics (Lohman, 1972), Aquifer-Test Design, Observation and Data Analysis (Stallman, 1976), and Theory of Aquifer Tests (Ferris and others, 1962) for more information.

Field measurement of saturated hydraulic conductivity can be done with a single-well aquifer test although multiple-well tests give more reliable results. Saturated hydraulic conductivity may also be measured by injection tests and slug tests. Laboratory measurements, in lieu of or in addition to field tests, are usually less reliable because of the small rock volumes tested. Many laboratory methods are available for measuring permeabilities in rock cores extracted from the field site. Other methods based on grain-size analyses have been used to compute saturated-rock permeability (Freeze and Cherry, 1979).

Specific yield can be determined from aquifer tests or laboratory measurements. At least two wells are necessary to determine S_y . Laboratory measurements of porosity and residual moisture content may be made on core samples and S_y may be calculated by subtracting residual moisture content from porosity (American Society of Testing Materials, 1967). Specific yield may also be estimated from a hydrologic budget analysis.

Permeabilities may be determined for individual strata penetrated by the mine or collectively to obtain an average for the saturated zone. An average permeability would probably be appropriate if there is leakage between the layers and their hydraulic conductivities are of the same order of magnitude. However, if vertically adjacent aquifers have K_{sat} differing by one or more orders of magnitude, a composite one-layer analysis would not be appropriate. A well penetrating strata of highly differing K_{sat} would be representative of the most conductive aquifer, and the predicted drawdown and seepage flux would be overestimated. In this case, each aquifer should be considered independent and analyzed separately.

Stratigraphic information, well-water levels, and water-quality information should be used to identify individual aquifers. Areal definition of the aquifer will aid in determining saturated thickness.

Aquifer boundaries should be determined using geologic, topographic, and water-level information. If the hypothetical aquifer length, L , is shorter than the field length and drawdown occurs at the boundary of the hypothetical aquifer at the selected time, then a longer length should also be used and predicted drawdown interpolated from the results. If the proposed mine site has an aquifer length greater than the largest modeled length, only times less than those for which the model predicts drawdown at the boundary may be used.

Seepage flux into the mine is predicted for one side of the mine only. For first cuts, seepage fluxes for both sides must be added to obtain the predicted total flux into the mine at a specified time. No way is provided to estimate seepage flux into the filled side of the mine for multiple cuts.

Use of Model Output

Results of computer modeling were converted to dimensionless (non-dimensional) units for application to field conditions different from the hypothetical aquifers. Dimensionless values are used in the computations and converted to dimensioned values for proposed mine sites.

Model results for total head at various distances from the seepage face at specified times and seepage flux at specified times were converted to dimensionless units using characteristics of the simulated hypothetical aquifers. Dimensionless total head was computed by

$$h' = H/D$$

where H is the output total head, in meters. Dimensionless seepage flux was computed by

$$q' = \frac{(S_y)q}{(K_{sat})D}$$

where q is the model output seepage flux per unit length, in meters squared per day (m^2/d). Dimensionless distance was computed by

$$x' = x/D.$$

Dimensionless time was computed by

$$t' = \frac{(K_{sat})t}{(S_y)D}.$$

The above equations were used by Yeh (1970) and Verma and Brutsaert (1970) and are similar to those used by Ibrahim and Brutsaert (1965). Thickness was used for nondimensionalization since it is more important than length in unsaturated drainage.

Pressure heads at each node were calculated by the VS2D model at specified times after excavation of the first cut. Nodes with zero pressure heads defined the potentiometric surface. Dimensionless total heads at these nodes were plotted as a function of dimensionless distance from the seepage face of the first cut for each specified dimensionless time. Dimensionless seepage fluxes were plotted as a function of dimensionless time.

Appendixes B and C contain profiles of dimensionless head as a function of dimensionless distance and dimensionless seepage flux as a function of dimensionless time for drainage to a first cut for each hypothetical-aquifer simulation. The graphs are arranged in the following order: (1) Geologic material A through K, (2) initial saturated thickness of 1 or 5 m, (3) initial head of 1, 3, 5, or 15 m, and (4) aquifer length of 75, 150, 450, 800, or 1,500 m. Appendixes D and E contain dimensionless profiles for multiple cuts. The graphs are arranged in the following order: (1) Geologic material A through F, (2) aquifer length of 150, 450, 800, or 1,500 m, (3) initial saturated thickness of 1 or 5 m, (4) multiple-cut width from 22.5 to 80.0 m, and (5) multiple-cut time of 30, 90, 180, or 270 days.

For aquifers that are not similar to the modeled aquifers, head and seepage flux can be predicted by using additive and interpolative methods.

The first step in applying the technique is to decide which of the two conceptual models, drainage to a first cut or drainage to multiple cuts, is to be used. Drainage to multiple cuts should be used if the aquifer at the proposed mine is similar to the given hypothetical aquifers and the proposed mining operation is similar to the given multiple cuts, since this conceptual model is more realistic. However, the possibilities are more limited for the multiple-cut conceptual model. Thus, the first-cut conceptual model should be used if the multiple-cut hypothetical aquifers do not describe the aquifer at the proposed mine or if the proposed mining operation is not available. Once the conceptual model is chosen, the conditions at the proposed mine site must be matched with one or more of the hypothetical aquifers.

First Cut

If the first-cut conceptual model is chosen, the user must

1. Determine the hydraulic characteristics and geometry of the aquifer at the proposed mine site.
2. Choose a hypothetical aquifer (table 1 and Appendixes B, C) that is approximately equivalent to the aquifer at the site. If aquifer characteristics at the site fall between values for two hypothetical aquifers, the computations should be made for the two hypothetical aquifers that bracket the aquifer at the mine. The results may be interpolated for the proposed mine conditions.

3. Choose a time after excavation of the first cut for which seepage flux into the mine and heads in the aquifer are desired. Convert the time to dimensionless units by substituting values for the aquifer at the site into the equation

$$t' = \frac{(K_{sat})t}{(S_y)D} .$$

4. Choose a distance from the planned seepage face for which head is required at the chosen time. Convert the distance to dimensionless units by substituting values for the aquifer at the site into the equation

$$x' = x/D .$$

5. Using graphs in Appendix B, find dimensionless head, h' , in the hypothetical aquifers selected in step 1 for dimensionless time and distance calculated in steps 3 and 4.

6. Dimension head using the equation

$$H = h'D .$$

This is the predicted head in the aquifer at the proposed site at the distance from the seepage face and time chosen in steps 3 and 4.

7. Using graphs in Appendix C, find dimensionless seepage flux, q' , for the value of dimensionless time calculated in step 3.

8. Dimension seepage flux using the equation

$$q = \frac{q'(K_{sat})D}{S_y} .$$

This is the predicted seepage flux per unit length into the mine at the time chosen in step 3. Flux into the mine through the excavated face is calculated by multiplying q times the mine length.

Interpolate heads and seepage fluxes computed in steps 6 and 8 for characteristics of two hypothetical aquifers that bracket the aquifer characteristics at the site. Interpolations should be approached in the following order: (1) Geologic-material characteristics K_{sat} and S_y , (2) initial head, (3) thickness, and (4) length. The following four examples illustrate some of the choices that could occur to the user in applying the outlined steps. Since so many variations are possible, the examples, presented in order from the least to the most complicated, demonstrate how the user should logically approach a particular situation. Example 1 illustrates an aquifer identical to a hypothetical aquifer; Example 2 illustrates an aquifer with initial head bracketed by initial heads of two hypothetical aquifers; Example 3 illustrates an aquifer with K_{sat} and S_y values bracketed by two geologic materials; and Example 4 illustrates two aquifer layers, one layer that has K_{sat} and S_y , D , and L bracketed by hypothetical aquifers, and one layer that has K_{sat} and S_y , and IH bracketed by hypothetical aquifers.

Example 1.--Preliminary drilling and aquifer testing at a proposed mine show that the mine will penetrate an unconfined, well-sorted, alluvial aquifer (fig. 10). Specific yield from aquifer tests ranges from 0.26 to 0.29 and averages 0.27. Saturated hydraulic conductivity from aquifer tests ranges from 0.91 to 5.42 m/d and averages 2.54 m/d. The aquifer thickness is 2.10 m and the water table is 0.90 m below the land surface to give a saturated thickness of 1.20 m. The alluvial deposit pinches out 160 m measured perpendicular to the planned excavation. The length of the first cut of the mine will be about 100 m.

Field-determined values of K_{sat} and S_y are compared to values listed in table 1 to determine the geologic material. Field values are identical to values for geologic material B.

The attributes of the aquifer at the proposed mine site are (1) geologic material B, (2) initial head of 1 times the aquifer thickness, because this is an unconfined aquifer, (3) saturated thickness of 1.20 m, close to the hypothetical-aquifer thickness 1 m (the reader is referred to Appendix A for a discussion of sensitivity pertaining to aquifer thickness), and (4) length of 160 m, which is close to the hypothetical-aquifer length 150 m. These attributes are described by the hypothetical aquifer of graphs B17 and C17 (Appendixes B and C).

A time of 90 days after initial excavation is selected for predicting drainage into the mine. Dimensionless time is calculated using the equation

$$t' = \frac{(K_{sat})t}{(S_y)D} = \frac{(2.54 \text{ m/d})(90 \text{ d})}{(0.27)(1.20 \text{ m})} \cong 710.$$

It is desired to predict the water level in a well located 30 m from the mine after 90 days of drainage. Dimensionless distance is calculated using the equation

$$x' = x/D = (30 \text{ m})/(1.20 \text{ m}) = 25.$$

From Appendix B, dimensionless head, read from graph B17 for a dimensionless time of 710 and a dimensionless distance of 25, is 0.52. Head in the private well at 90 days is determined using the equation

$$H = h'D = (0.52)(1.20 \text{ m}) \cong 0.62 \text{ m}.$$

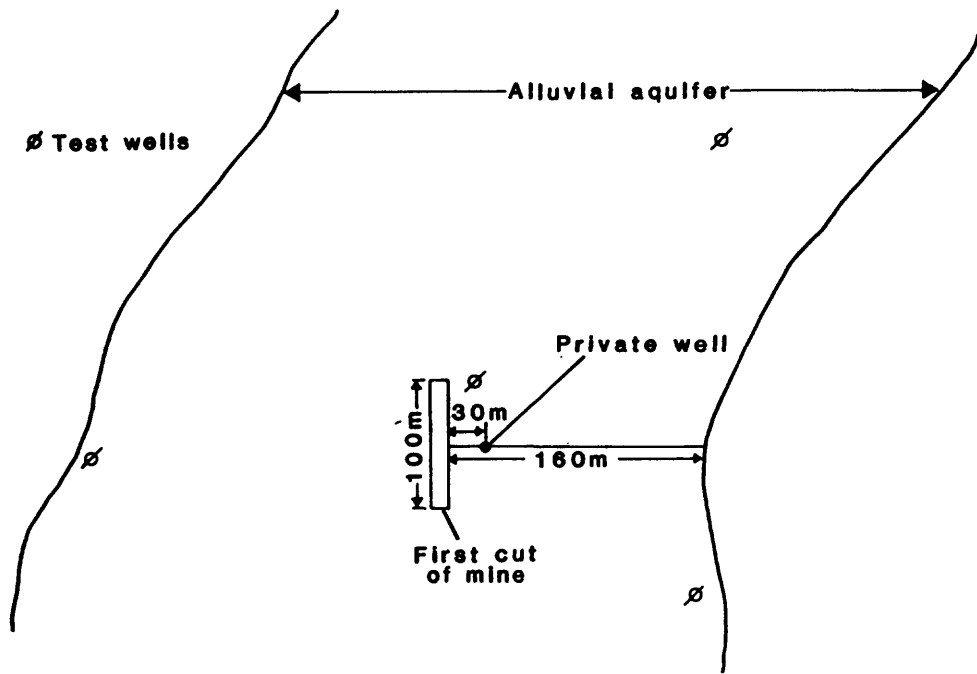
Thus, the water level is predicted to change from 1.20 m to 0.62 m, a decline of 0.58 m.

From Appendix C, dimensionless seepage flux, read from graph C17 for a dimensionless time of 710, is 2.33×10^{-3} . The seepage flux per unit length of excavation at 90 days is calculated using the equation

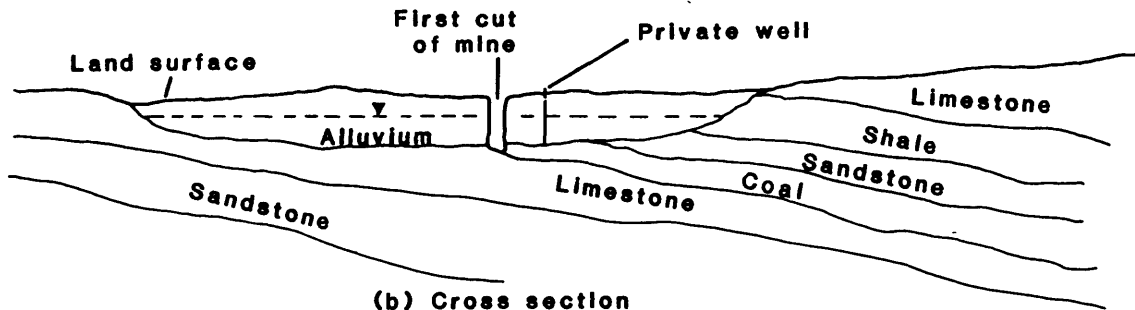
$$q = \frac{q'(K_{sat})D}{S_y} = \frac{(2.33 \times 10^{-3})(2.54 \text{ m/d})(1.20 \text{ m})}{0.27} \cong 2.63 \times 10^{-2} \text{ m}^2/\text{d}.$$

Thus, the flux into the mine along the 100 m of one excavated face is

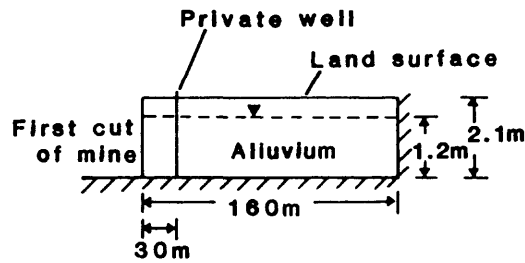
$$(2.63 \times 10^{-2} \text{ m}^2/\text{d})(100 \text{ m}) \cong 2.6 \text{ cubic meter per day (m}^3/\text{d)}.$$



(a) Plan view



(b) Cross section



(c) Simplified cross section

Figure 10.--Diagram of preliminary information for Example 1--First cut.

Example 2.--A proposed mine will penetrate an alluvial aquifer confined by low-permeability till (fig. 11). Aquifer tests indicate a K_{sat} value of 2.54 m/d and 0.27 for S_y . Thickness of the aquifer is 1.20 m and initial head is 2.00 m. There is a topographic high, considered a ground-water divide, 1,600 m from the proposed mine. The length of the aquifer is thus chosen to be 1,600 m. The length of the first cut will be approximately 100 m.

Field-determined values of K_{sat} and S_y are identical to those listed for geologic material B (table 1). Aquifer thickness and length of 1.20 m and 1,600 m are close to dimensions of hypothetical aquifers 1-m thick and 1,500-m long. The head in the aquifer, 2.00 m, is between the two initial head conditions of 1 and 3 times the hypothetical aquifer thickness of 1 m, or 1 m and 3 m. Therefore, the two hypothetical aquifers of graphs B20 and C20 and B24 and C24 (Appendixes B and C) will be used and results interpolated.

It is desired to predict drainage into the mine and the potentiometric surface at a private well located 1,000 m from the mine 12 days after initial excavation. Dimensionless time is calculated using the equation

$$t' = \frac{(K_{sat})t}{(S_y)D} = \frac{(2.54 \text{ m/d})(12 \text{ d})}{(0.27)(1.20 \text{ m})} \cong 94.$$

Dimensionless distance is calculated using the equation

$$x' = x/D = (1000 \text{ m})/(1.20 \text{ m}) \cong 830.$$

Dimensionless heads for a dimensionless time of 94 and a dimensionless distance of 830 are 1.00 from graph B20 and 1.94 from graph B24. Heads from each hypothetical aquifer are dimensioned using the equations

$$H = h'D = (1.00)(1.20 \text{ m}) = 1.20 \text{ m for graph B20; and}$$

$$H = h'D = (1.94)(1.20 \text{ m}) \cong 2.33 \text{ m for graph B24.}$$

The two heads are used to compute head in the private well. Corresponding initial heads are defined as 1 times the aquifer thickness for B20 and 3 times the aquifer thickness for B24. Initial heads of 1.20 and 3.60 m, respectively, are used in the interpolation

$$\frac{H_{B24} - H_{PW}}{IH_{B24} - IH_{PW}} = \frac{H_{B24} - H_{B20}}{IH_{B24} - IH_{B20}}$$

where H refers to head, IH refers to initial head, and PW refers to the private well. Thus,

$$\frac{2.33 \text{ m} - H_{PW}}{3.60 \text{ m} - 2.00 \text{ m}} = \frac{2.33 \text{ m} - 1.20 \text{ m}}{3.60 \text{ m} - 1.20 \text{ m}}$$

or head in the private well approximately equals 1.58 m. Thus, after 12 days, the potentiometric surface is predicted to change from 2.00 m to 1.58 m, a decline of 0.42 m.

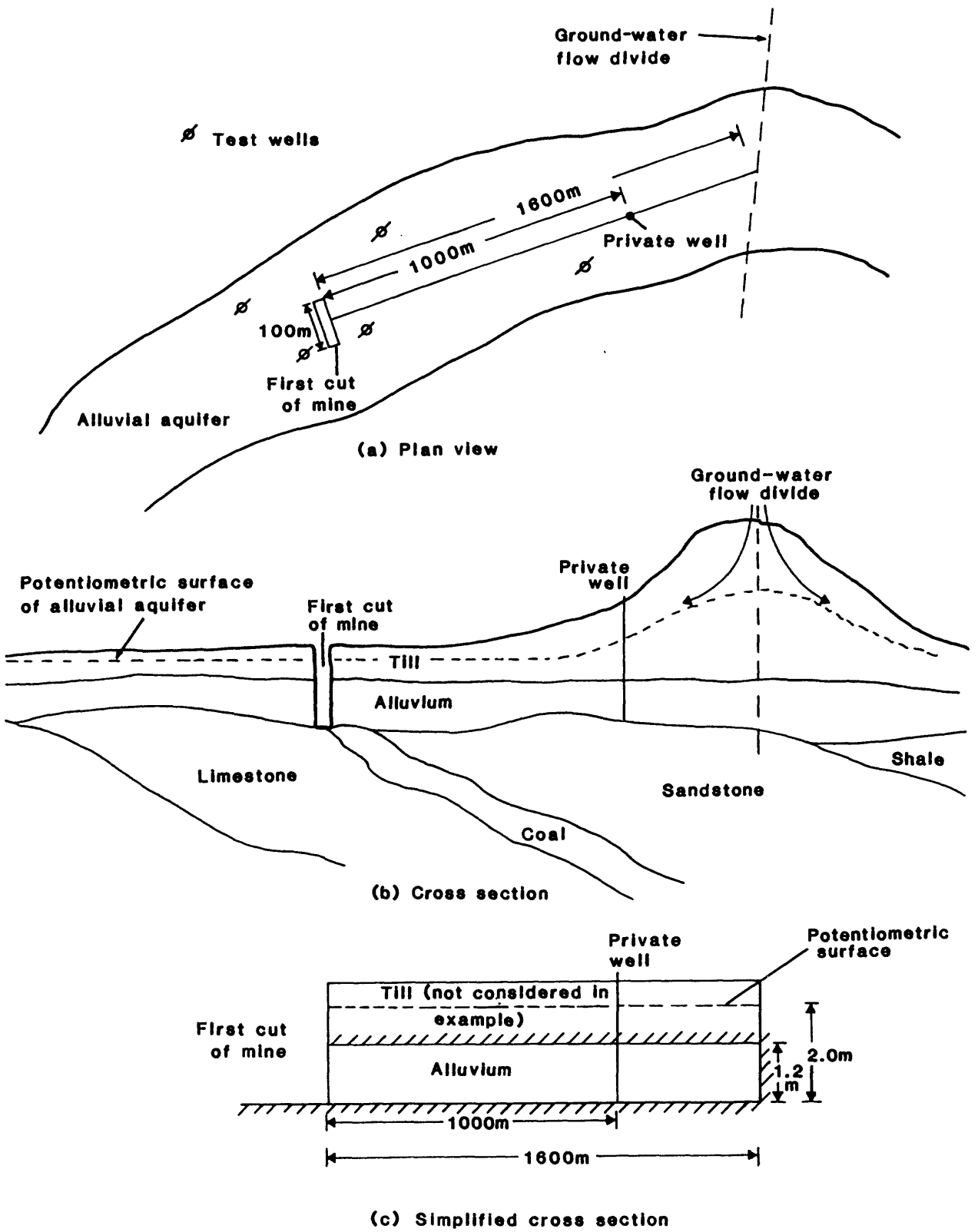


Figure 11.--Diagram of preliminary information for Example 2--First cut.

Dimensionless seepage flux for a dimensionless time of 94 is 1.26×10^{-3} from graph C20 (IH=1) and 1.29×10^{-3} from graph C24 (IH=3). The seepage flux per unit length at 12 days using graph C20 is

$$q = \frac{q'(K_{\text{sat}})^D}{S_y} = \frac{(1.26 \times 10^{-3})(2.54 \text{ m/d})(1.20 \text{ m})}{0.27} \cong 1.42 \times 10^{-2} \text{ m}^2/\text{d}.$$

The seepage flux per unit length at 12 days using graph C24 is

$$q = \frac{q'(K_{\text{sat}})^D}{S_y} = \frac{(1.29 \times 10^{-3})(2.54 \text{ m/d})(1.20 \text{ m})}{0.27} \cong 1.46 \times 10^{-2} \text{ m}^2/\text{d}.$$

The computed seepage fluxes and initial heads based on both aquifers are used to interpolate seepage into the proposed mine. Initial heads are 1.20 m for graph C20 and 3.60 m for graph C24.

$$\frac{q_{\text{C24}} - q_{\text{PW}}}{\text{IH}_{\text{C24}} - \text{IH}_{\text{PW}}} = \frac{q_{\text{C24}} - q_{\text{C20}}}{\text{IH}_{\text{C24}} - \text{IH}_{\text{C20}}}$$

where q refers to seepage flux per unit length. Thus,

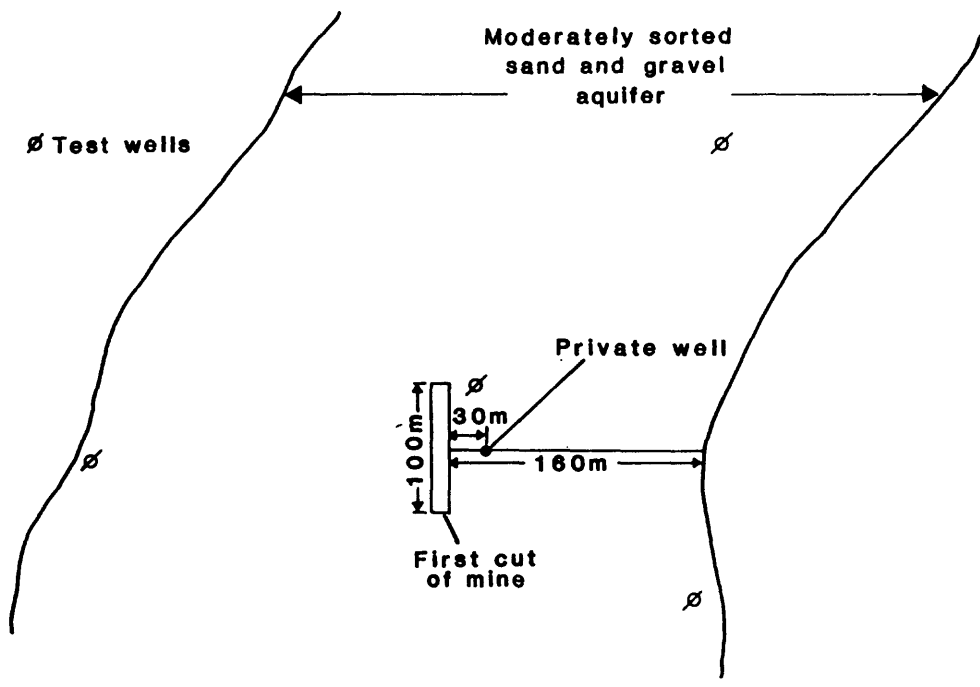
$$\frac{1.46 \times 10^{-2} \text{ m}^2/\text{d} - q_{\text{PW}}}{3.60 \text{ m} - 2.00 \text{ m}} = \frac{1.46 \times 10^{-2} \text{ m}^2/\text{d} - 1.42 \times 10^{-2} \text{ m}^2/\text{d}}{3.60 \text{ m} - 1.20 \text{ m}}$$

or seepage flux per unit length after 12 days is approximately $1.43 \times 10^{-2} \text{ m}^2/\text{d}$. The flux into the mine along the 100 m of one excavated face is

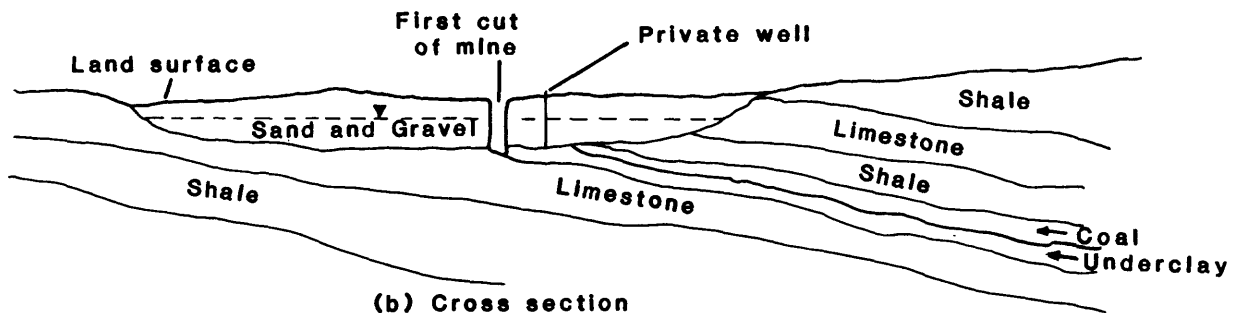
$$(1.43 \times 10^{-2} \text{ m}^2/\text{d})(100 \text{ m}) \cong 1.4 \text{ m}^3/\text{d}.$$

Example 3.--A proposed mine will penetrate an unconfined aquifer of moderately-sorted sand and gravel (fig. 12). Aquifer tests indicate a K_{sat} value of 2.00 m/d and 0.27 for S_y . The aquifer thickness is 2.10 m and the water table is 0.90 m below the land surface to give a saturated thickness of 1.20 m. The sand and gravel deposit pinches out 160 m measured perpendicular to the planned excavation. The length of the first cut of the mine will be about 100 m.

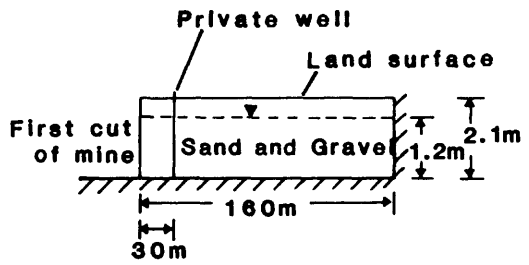
Aquifer thickness and length of 1.20 m and 160 m are close to dimensions of hypothetical aquifers 1-m thick and 150-m long. The initial head is 1 times the aquifer thickness because it is an unconfined aquifer. Field-determined values for K_{sat} and S_y for the sand and gravel aquifer, 2.00 m/d and 0.27, are between K_{sat} and S_y values of 2.54 m/d and 0.27 for geologic material B and 8.47×10^{-1} m/d and 0.28 for geologic material C (table 1). Therefore, the two hypothetical aquifers of graphs B17 and C17, and B33 and C33 (Appendixes B and C) will be used and the results interpolated. Interpolation will be made using dimensionless time because the aquifer characteristics K_{sat} and S_y are both incorporated into t' .



(a) Plan view



(b) Cross section



(c) Simplified cross section

Figure 12.--Diagram of preliminary information for Example 3--First cut.

It is desired to predict the drainage into the mine and the water level in a private well located 30 m from the mine after 90 days from initial excavation. Dimensionless time for graphs B17 and C17 is

$$t' = \frac{(K_{sat})t}{(S_y)D} = \frac{(2.54 \text{ m/d})(90 \text{ d})}{(0.27)(1.20 \text{ m})} \approx 710.$$

Dimensionless time for graphs B33 and C33 is

$$t' = \frac{(K_{sat})t}{(S_y)D} = \frac{(0.847 \text{ m/d})(90 \text{ d})}{(0.28)(1.20 \text{ m})} \approx 230.$$

Dimensionless time for the aquifer at the mine is

$$t' = \frac{(K_{sat})t}{(S_y)D} = \frac{(2.00 \text{ m/d})(90 \text{ d})}{(0.27)(1.20 \text{ m})} \approx 560.$$

Dimensionless distance is

$$x' = x/D = (30 \text{ m})/(1.20 \text{ m}) = 25.$$

Dimensionless head from graph B17 for a dimensionless time of 710 and a dimensionless distance of 25 is 0.52. Dimensionless head from graph B33 for a dimensionless time of 230 and a dimensionless distance of 25 is 0.70. Heads are dimensioned from each of the dimensionless heads using the equations

$$H = h'D = (0.52)(1.20 \text{ m}) \approx 0.62 \text{ m for graph B17, and}$$

$$H = h'D = (0.70)(1.20 \text{ m}) = 0.84 \text{ m for graph B33.}$$

Head in the private well is interpolated using the computed heads and dimensionless times for graphs B17 and B33. Dimensionless times are 710 for graph B17, 230 for graph B33, and 560 for the aquifer at the proposed mine. Thus,

$$\frac{H_{B17} - H_{PW}}{t'_{B17} - t'_{PW}} = \frac{H_{B17} - H_{B33}}{t'_{B17} - t'_{B33}}$$

where H refers to head, t' refers to dimensionless time, and PW refers to the private well. Thus,

$$\frac{0.62 \text{ m} - H_{PW}}{710 - 560} = \frac{0.62 \text{ m} - 0.84 \text{ m}}{710 - 230}$$

or head in the private well approximately equals 0.69 m. The water level is predicted to change from 1.20 to 0.69 m, a decline of 0.51 m, after 90 days of drainage.

Dimensionless seepage fluxes are 2.5×10^{-3} from graph C17 (geologic material B) using a dimensionless time of 710, and 5.5×10^{-3} from graph C33 (geologic material C) using a dimensionless time of 230. The seepage flux per unit length at 90 days using graph C17 is

$$q = \frac{q'(K_{sat})D}{S_y} = \frac{(2.5 \times 10^{-3})(2.54 \text{ m/d})(1.20 \text{ m})}{0.27} \cong 2.82 \times 10^{-2} \text{ m}^2/\text{d}.$$

The seepage flux per unit length at 90 days using graph C33 is

$$q = \frac{q'(K_{sat})D}{S_y} = \frac{(5.5 \times 10^{-3})(0.847 \text{ m/d})(1.20 \text{ m})}{0.28} \cong 2.00 \times 10^{-2} \text{ m}^2/\text{d}.$$

Computed seepage fluxes and dimensionless times for graphs C17 and C33 are used to compute seepage into the mine at 90 days. Dimensionless times of 710 for graph C17, 230 for graph C33, and 560 for the aquifer at the mine are used in the interpolation

$$\frac{q_{C17} - q_{PW}}{t'_{C17} - t'_{PW}} = \frac{q_{C17} - q_{C33}}{t'_{C17} - t'_{C33}}.$$

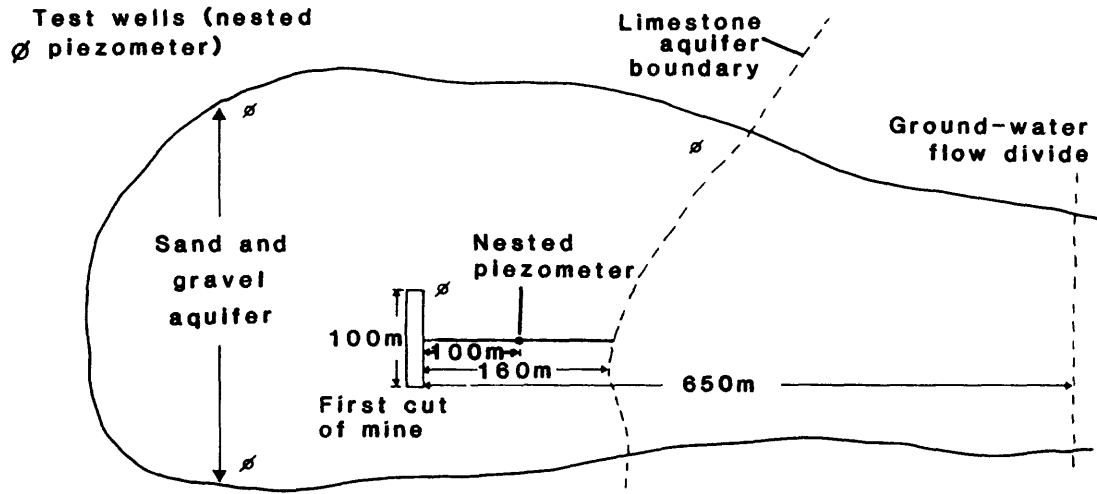
$$\text{Thus, } \frac{(2.82 \times 10^{-2} \text{ m}^2/\text{d}) - q_{PW}}{710 - 560} = \frac{(2.82 \times 10^{-2} \text{ m}^2/\text{d}) - (2.00 \times 10^{-2} \text{ m}^2/\text{d})}{710 - 230}$$

or seepage flux per unit length after 90 days approximately equals $2.6 \times 10^{-2} \text{ m}^2/\text{d}$. The flux into the mine along the 100 m of one excavated face is

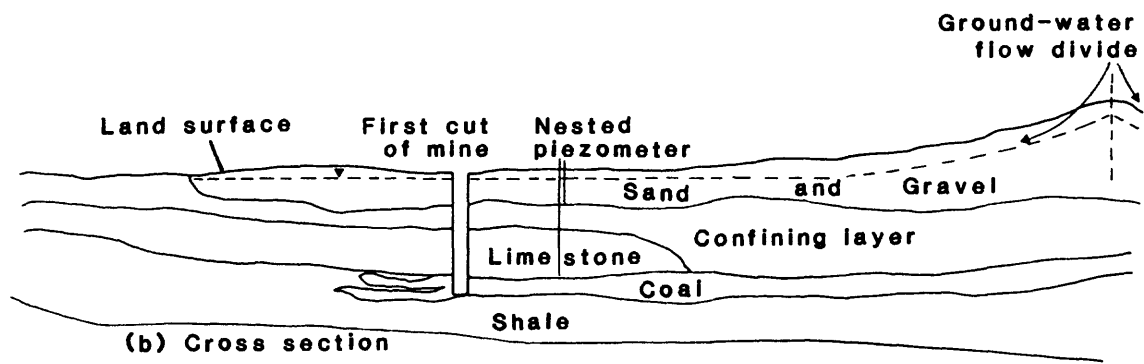
$$(2.6 \times 10^{-2} \text{ m}^2/\text{d})(100 \text{ m}) = 2.6 \text{ m}^3/\text{d}.$$

Example 4.--This example illustrates a proposed mine that penetrates a confined aquifer overlain by an unconfined aquifer. Aquifer hydraulic and geometric characteristics are bracketed by, but not equal to, those of the hypothetical aquifers. Only two layers are considered. However, the technique may be extended to any number of layers.

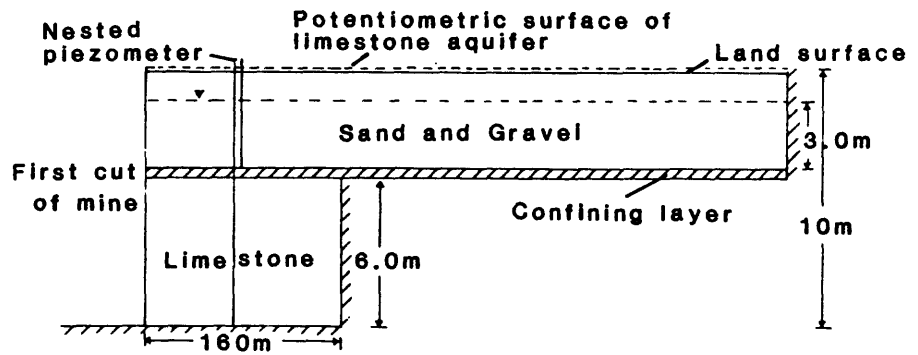
A mine is proposed that will penetrate strata composed of a limestone aquifer overlain by a confining layer, overlain by an unconfined aquifer of moderately sorted sand and gravel (fig. 13). Aquifer tests give a K_{sat} value of 1.80 m/d and 0.27 for S_y for the sand and gravel, and a K_{sat} value of 4.00×10^{-2} m/d and 0.20 for S_y for the limestone. The confining layer is assumed to be impermeable and no ground-water discharge from this layer is considered in the analysis. Thickness of the unconfined sand and gravel is 3.9 m. The water table is 0.90 m below land surface to give a saturated thickness of 3.0 m. Thickness of the confined limestone is 6.00 m and the initial head is 10.0 m. The limestone layer pinches out 160 m measured perpendicular to the planned excavation. The length of the limestone layer is thus chosen to be 160 m. A topographic high about 650 m from the proposed mine is considered a ground-water-flow divide so the length of the unconfined sand and gravel is 650 m. The first cut will be approximately 100 m.



(a) Plan view



(b) Cross section



(c) Simplified cross section

Figure 13.--Diagram of preliminary information for Example 4--First cut.

It is desired to predict drainage into the mine 90 days from initial excavation. It is also desired to predict the effect of drainage on the water level in each of two piezometers located 100 m from the proposed mine, one open to the sand and gravel and one open to the limestone, at 90 days. The two aquifer layers are considered separately. Seepage flux for the entire system will be combined at the end of the problem.

Field-determined values for K_{sat} and S_y for the sand and gravel aquifer, 1.80 m/d and 0.27, are between K_{sat} and S_y values of 2.54 m/d and 0.27 for geologic material B and 8.47×10^{-1} m/d and 0.28 for geologic material C (table 1). The saturated thickness of 3.00 m is between the two hypothetical-aquifer thicknesses of 1 and 5 m. The aquifer length of 650 m is between the two hypothetical-aquifer lengths of 450 and 800 m. Three steps of interpolation will thus be necessary: (1) K_{sat} and S_y using dimensionless time, (2) initial saturated thickness, and (3) aquifer length. Eight hypothetical aquifers based on the hydraulic and geometric characteristics (fig. 14) will be used.

Dimensionless times for geologic materials B and C and the sand and gravel aquifer are calculated by

$$t' = \frac{(K_{sat})t}{(S_y)D} = \frac{(2.54 \text{ m/d})(90 \text{ d})}{(0.27)(3.00 \text{ m})} \cong 280$$

for graphs 18, 19, 26, 27 in Appendixes B and C for geologic material B;

$$t' = \frac{(K_{sat})t}{(S_y)D} = \frac{(0.847 \text{ m/d})(90 \text{ d})}{(0.28)(3.00 \text{ m})} \cong 91$$

for graphs 34, 35, 42, 43 in Appendixes B and C for geologic material C; and

$$t' = \frac{(K_{sat})t}{(S_y)D} = \frac{(1.80 \text{ m/d})(90 \text{ d})}{(0.27)(3.00 \text{ m})} = 200$$

for the sand and gravel.

Dimensionless distance is calculated using the equation

$$x' = x/D = (100 \text{ m})/(3.00 \text{ m}) \cong 33.$$

Using a dimensionless time of 280 and a dimensionless distance of 33, dimensionless head is read from graphs B18, B19, B26, and B27 (hypothetical aquifers with geologic material B). Using a dimensionless time of 91 and a dimensionless distance of 33, dimensionless head is read from graphs B34, B35, B42, and B43 (hypothetical aquifers with geologic material C) (table 2). Heads are dimensioned from each of the dimensionless heads using the equation $H = h'D$ and are also given in table 2.

Table 2.--Calculations from

[m/d, meter per day; m, meter; d, day;

Aquifer designation (graph number in Appendixes B and C)	Geologic material	Saturated hydraulic conductivity, K_{sat} (m/d)	Specific yield, S_y	Saturated thickness, D	Length, L (m)	Initial head, IH (m)
Aquifers of Example 4						
Sand and gravel		1.80	0.27	3	650	3
Limestone		.04	.20	6	160	10
SAND AND						
Hypothetical aquifers used for calculations						
18	B	2.54	0.27	1	450	1
19	B	2.54	.27	1	800	1
26	B	2.54	.27	5	450	5
27	B	2.54	.27	5	800	5
34	C	.847	.28	1	450	1
35	C	.847	.28	1	800	1
42	C	.847	.28	5	450	5
43	C	.847	.28	5	800	5
LIME						
Hypothetical aquifers used for calculations						
51	D	0.0847	.32	5	150	5
52	D	.0847	.32	5	150	15
55	E	.0254	.15	5	150	5
56	E	.0254	.15	5	150	15

Example 4--First cut

m²/d, meter squared per day]

Time	Distance	Head	Seepage flux x 10 ⁻³	Time (d)	Distance (m)	Head (m)	Seepage flux x 10 ⁻² (m ² /d)
------	----------	------	------------------------------------	-------------	-----------------	-------------	---

GRAVEL

Dimensionless results				Dimensioned results			
280	33	0.67	2.74	90	100	2.01	7.73
280	33	.73	1.89	90	100	2.19	5.33
280	33	.86	7.12	90	100	2.58	20.1
280	33	.84	5.54	90	100	2.52	15.6
91	33	.77	3.95	90	100	2.31	3.58
91	33	.72	2.71	90	100	2.16	2.46
91	33	.95	9.61	90	100	2.85	8.72
91	33	.93	9.09	90	100	2.79	8.25

STONE

Dimensionless results				Dimensioned results			
4.0	17	0.96	50.1	90	100	5.76	7.96
4.0	17	.95	49.9	90	100	5.70	7.92
2.5	17	.97	26.5	90	100	5.82	2.69
2.5	17	.97	29.0	90	100	5.82	2.95

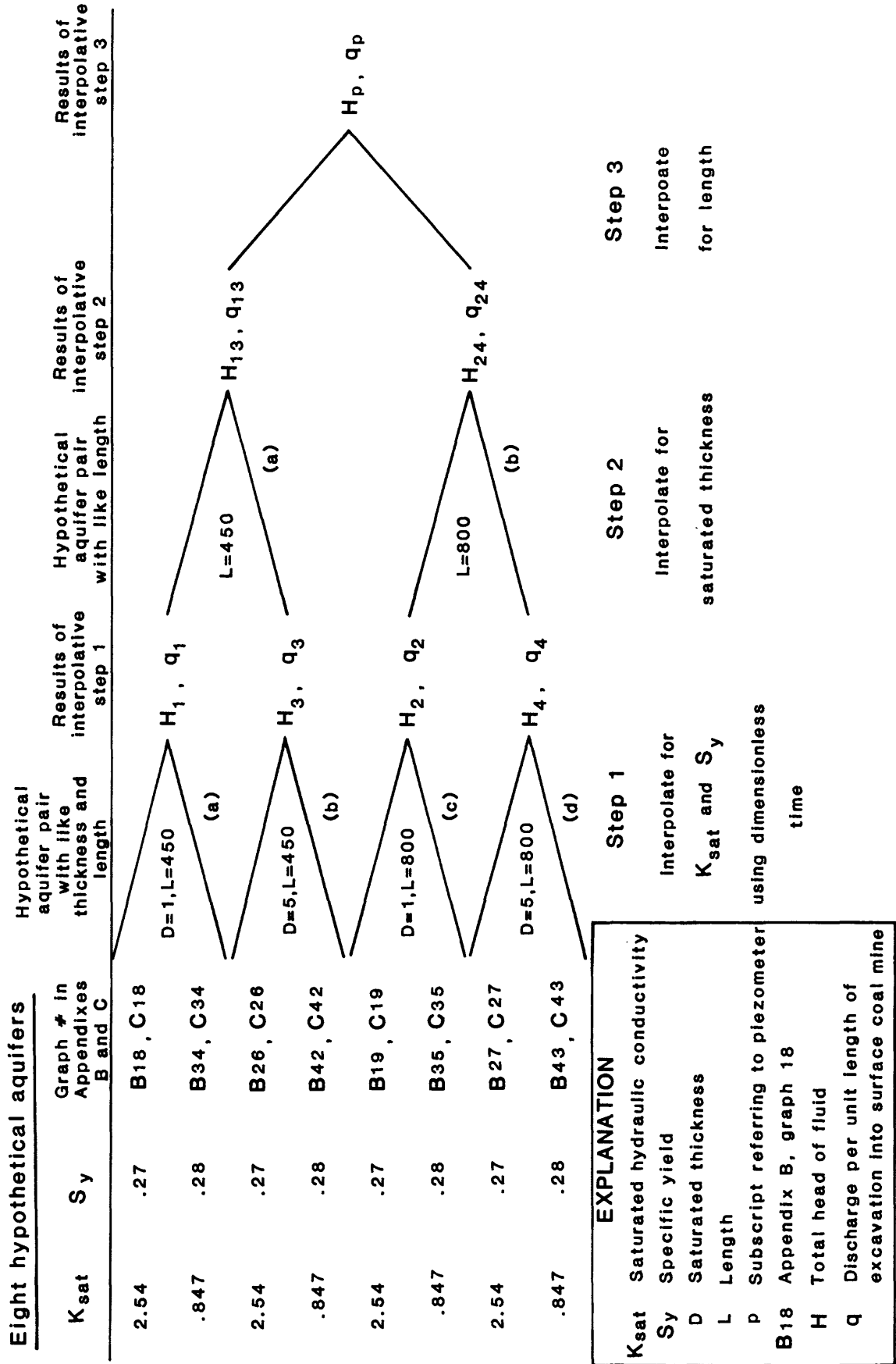


Figure 14.--Interpolative steps for unconfined aquifer portion of Example 4--First cut.

Heads and dimensionless times for hypothetical aquifers with geologic materials B and C having like thicknesses and lengths are used to interpolate head for geologic material. Interpolation equations for step 1 (fig. 14) are

$$(a) \quad \frac{H_{B18} - H_1}{t'_{B18} - t'} = \frac{H_{B18} - H_{B34}}{t'_{B18} - t'_{B34}} .$$

$$\text{Thus,} \quad \frac{2.01 \text{ m} - H_1}{280 - 200} = \frac{2.01 \text{ m} - 2.31 \text{ m}}{280 - 91}$$

$$\text{or} \quad H_1 \cong 2.14 \text{ m.}$$

$$(b) \quad \frac{H_{B19} - H_2}{t'_{B19} - t'} = \frac{H_{B19} - H_{B35}}{t'_{B19} - t'_{B35}} .$$

$$\text{Thus,} \quad \frac{2.19 \text{ m} - H_2}{280 - 200} = \frac{2.19 \text{ m} - 2.16 \text{ m}}{280 - 91}$$

$$\text{or} \quad H_2 \cong 2.18 \text{ m.}$$

$$(c) \quad \frac{H_{B26} - H_3}{t'_{B26} - t'} = \frac{H_{B26} - H_{B42}}{t'_{B26} - t'_{B42}} .$$

$$\text{Thus,} \quad \frac{2.58 \text{ m} - H_3}{280 - 200} = \frac{2.58 \text{ m} - 2.85 \text{ m}}{280 - 91}$$

$$\text{or} \quad H_3 \cong 2.69 \text{ m.}$$

$$(d) \quad \frac{H_{B27} - H_4}{t'_{B27} - t'} = \frac{H_{B27} - H_{B43}}{t'_{B27} - t'_{B43}} .$$

$$\text{Thus,} \quad \frac{2.52 \text{ m} - H_4}{280 - 200} = \frac{2.52 \text{ m} - 2.79 \text{ m}}{280 - 91}$$

$$\text{or} \quad H_4 \cong 2.63 \text{ m.}$$

Computed heads from step 1 and initial saturated thickness for hypothetical aquifers having like length are used to interpolate for thickness. Equations for step 2 are

$$\frac{H_1 - H_{13}}{D_1 - D} = \frac{H_1 - H_3}{D_1 - D_3}$$

where H_1 and H_3 were calculated in step 1, D_1 and D_3 are hypothetical aquifer thicknesses corresponding to these heads, D is the initial saturated thickness of the aquifer at the proposed mine, and H_{13} is the desired head. Thus,

$$(a) \quad \frac{2.14 \text{ m} - H_{13}}{1.00 \text{ m} - 3.00 \text{ m}} = \frac{2.14 \text{ m} - 2.69 \text{ m}}{1.00 \text{ m} - 5.00 \text{ m}}$$

or $H_{13} \cong 2.42 \text{ m}.$

$$(b) \quad \frac{H_2 - H_{24}}{D_2 - D} = \frac{H_2 - H_4}{D_2 - D_4}.$$

Thus,
$$\frac{2.18 \text{ m} - H_{24}}{1.00 \text{ m} - 3.00 \text{ m}} = \frac{2.18 \text{ m} - 2.63 \text{ m}}{1.00 \text{ m} - 5.00 \text{ m}}$$

or $H_{24} \cong 2.41 \text{ m}.$

Length is interpolated using computed heads from step 2 and lengths for corresponding hypothetical aquifers. Step 3 is

$$\frac{H_{13} - H_p}{L_{13} - L} = \frac{H_{13} - H_{24}}{L_{13} - L_{24}}$$

where H_p is the required head in the piezometer and L is the length of the aquifer at the proposed mine. Thus,

$$\frac{2.42 \text{ m} - H_p}{450 \text{ m} - 650 \text{ m}} = \frac{2.42 \text{ m} - 2.41 \text{ m}}{450 \text{ m} - 800 \text{ m}}$$

or predicted head at the piezometer is approximately 2.41 m. Thus, the water level in the unconfined aquifer at the piezometer is predicted to change from 3.00 to 2.41 m after 90 days of drainage, a decline of 0.59 m.

Dimensionless seepage fluxes are read from Appendix C for a dimensionless time of 280 for hypothetical aquifers with geologic material B (graphs C18, C19, C26, and C27) and for a dimensionless time of 91 for hypothetical aquifers with geologic material C (graphs C34, C35, C42, and C43). Dimensionless seepage fluxes from Appendix C are given in table 2. The seepage fluxes per unit length at 90 days for each hypothetical aquifer are obtained from $q = q'(K_{sat})D/S_y$ and are also given in table 2. The computed seepage fluxes and dimensionless times are used to interpolate seepage fluxes for pairs of hypothetical aquifers with like thickness and length. Equations for step 1 (fig. 14) are

$$(a) \quad \frac{q_{C18} - q_1}{t'_{C18} - t'} = \frac{q_{C18} - q_{C34}}{t'_{C18} - t'_{C34}}.$$

$$\text{Thus, } \frac{(7.73 \times 10^{-2} \text{ m}^2/\text{d}) - q_1}{280 - 200} = \frac{(7.73 \times 10^{-2} \text{ m}^2/\text{d}) - (3.58 \times 10^{-2} \text{ m}^2/\text{d})}{280 - 91}$$

$$\text{or } q_1 \cong 5.97 \times 10^{-2} \text{ m}^2/\text{d}.$$

$$(b) \quad \frac{q_{C19} - q_2}{t'_{C19} - t'} = \frac{q_{C19} - q_{C35}}{t'_{C19} - t'_{C35}} .$$

$$\text{Thus, } \frac{(5.33 \times 10^{-2} \text{ m}^2/\text{d}) - q_2}{280 - 200} = \frac{(5.33 \times 10^{-2} \text{ m}^2/\text{d}) - (2.46 \times 10^{-2} \text{ m}^2/\text{d})}{280 - 91}$$

$$\text{or } q_2 \cong 4.12 \times 10^{-2} \text{ m}^2/\text{d}.$$

$$(c) \quad \frac{q_{C26} - q_3}{t'_{C26} - t'} = \frac{q_{C26} - q_{C42}}{t'_{C26} - t'_{C42}} .$$

$$\text{Thus, } \frac{(2.01 \times 10^{-1} \text{ m}^2/\text{d}) - q_3}{280 - 200} = \frac{(2.01 \times 10^{-1} \text{ m}^2/\text{d}) - (8.72 \times 10^{-2} \text{ m}^2/\text{d})}{280 - 91}$$

$$\text{or } q_3 \cong 1.53 \times 10^{-1} \text{ m}^2/\text{d}.$$

$$(d) \quad \frac{q_{C27} - q_4}{t'_{C27} - t'} = \frac{q_{C27} - q_{C43}}{t'_{C27} - t'_{C43}} .$$

$$\text{Thus, } \frac{(1.56 \times 10^{-1} \text{ m}^2/\text{d}) - q_4}{280 - 200} = \frac{(1.56 \times 10^{-1} \text{ m}^2/\text{d}) - (8.25 \times 10^{-2} \text{ m}^2/\text{d})}{280 - 91}$$

$$\text{or } q_4 \cong 1.25 \times 10^{-1} \text{ m}^2/\text{d}.$$

The computed seepage fluxes from step 1 and initial saturated thicknesses for hypothetical aquifers of like length are used to interpolate for thickness. Equations for step 2 are

$$(a) \quad \frac{q_1 - q_{13}}{D_1 - D} = \frac{q_1 - q_3}{D_1 - D_3}$$

where q_1 and q_3 were calculated in step 1, D_1 and D_3 are hypothetical-aquifer thicknesses corresponding to these seepage fluxes, D is the initial saturated thickness of the aquifer at the proposed mine, and q_{13} is the desired seepage flux. Thus,

$$\frac{(5.97 \times 10^{-2} \text{ m}^2/\text{d}) - q_{13}}{1.00 \text{ m} - 3.00 \text{ m}} = \frac{(5.97 \times 10^{-2} \text{ m}^2/\text{d}) - (1.53 \times 10^{-1} \text{ m}^2/\text{d})}{1.00 \text{ m} - 5.00 \text{ m}}$$

or $q_{13} \cong 1.06 \times 10^{-1} \text{ m}^2/\text{d}.$

$$(b) \quad \frac{q_2 - q_{24}}{D_2 - D} = \frac{q_2 - q_4}{D_2 - D_4}.$$

Thus, $\frac{(4.12 \times 10^{-2} \text{ m}^2/\text{d}) - q_{24}}{1.00 \text{ m} - 3.00 \text{ m}} = \frac{(4.12 \times 10^{-2} \text{ m}^2/\text{d}) - (1.25 \times 10^{-1} \text{ m}^2/\text{d})}{1.00 \text{ m} - 5.00 \text{ m}}$

or $q_{24} \cong 8.31 \times 10^{-2} \text{ m}^2/\text{d}.$

Computed seepage fluxes q_{13} and q_{24} and aquifer lengths of the hypothetical aquifers corresponding to these seepage fluxes are used to interpolate length. An equation for step 3 is

$$\frac{q_{13} - q_p}{L_{13} - L} = \frac{q_{13} - q_{24}}{L_{13} - L_{24}}$$

where q_p is the seepage flux into the excavation at 90 days. Thus,

$$\frac{(1.06 \times 10^{-1} \text{ m}^2/\text{d}) - q_p}{450 \text{ m} - 650 \text{ m}} = \frac{(1.06 \times 10^{-1} \text{ m}^2/\text{d}) - (8.31 \times 10^{-2} \text{ m}^2/\text{d})}{450 \text{ m} - 800 \text{ m}}$$

or q_p approximately equals $9.29 \times 10^{-2} \text{ m}^2/\text{d}$. Thus, the flux into the mine along the 100 m of one excavated face from the unconfined aquifer is

$$(9.29 \times 10^{-2} \text{ m}^2/\text{d})(100 \text{ m}) \cong 9.3 \text{ m}^3/\text{d}.$$

Field-determined values for K_{sat} and S_y for the confined limestone aquifer (table 2) are between K_{sat} and S_y values of geologic materials D and E (tables 1 and 2). Aquifer thickness and length of 6.00 m and 160 m, respectively, are close to dimensions of hypothetical aquifers 5-m thick and 150-m long. The head in the aquifer, 10.0 m, is between the two initial head conditions for the hypothetical aquifers of 1 and 3 times the aquifer thickness, or 6.00 m and 18.0 m, respectively. Two interpolative steps will thus be necessary to solve the problem: (1) Interpolating for K_{sat} and S_y using dimensionless time, and (2) interpolating for initial head. The four hypothetical aquifers and the scheme for the interpolations are shown in figure 15.

It is desired to predict drainage into the mine and head in a nested piezometer open to the limestone and located 100 m from the proposed mine after 90 days. Dimensionless times for the confined limestone aquifer and geologic materials D and E are

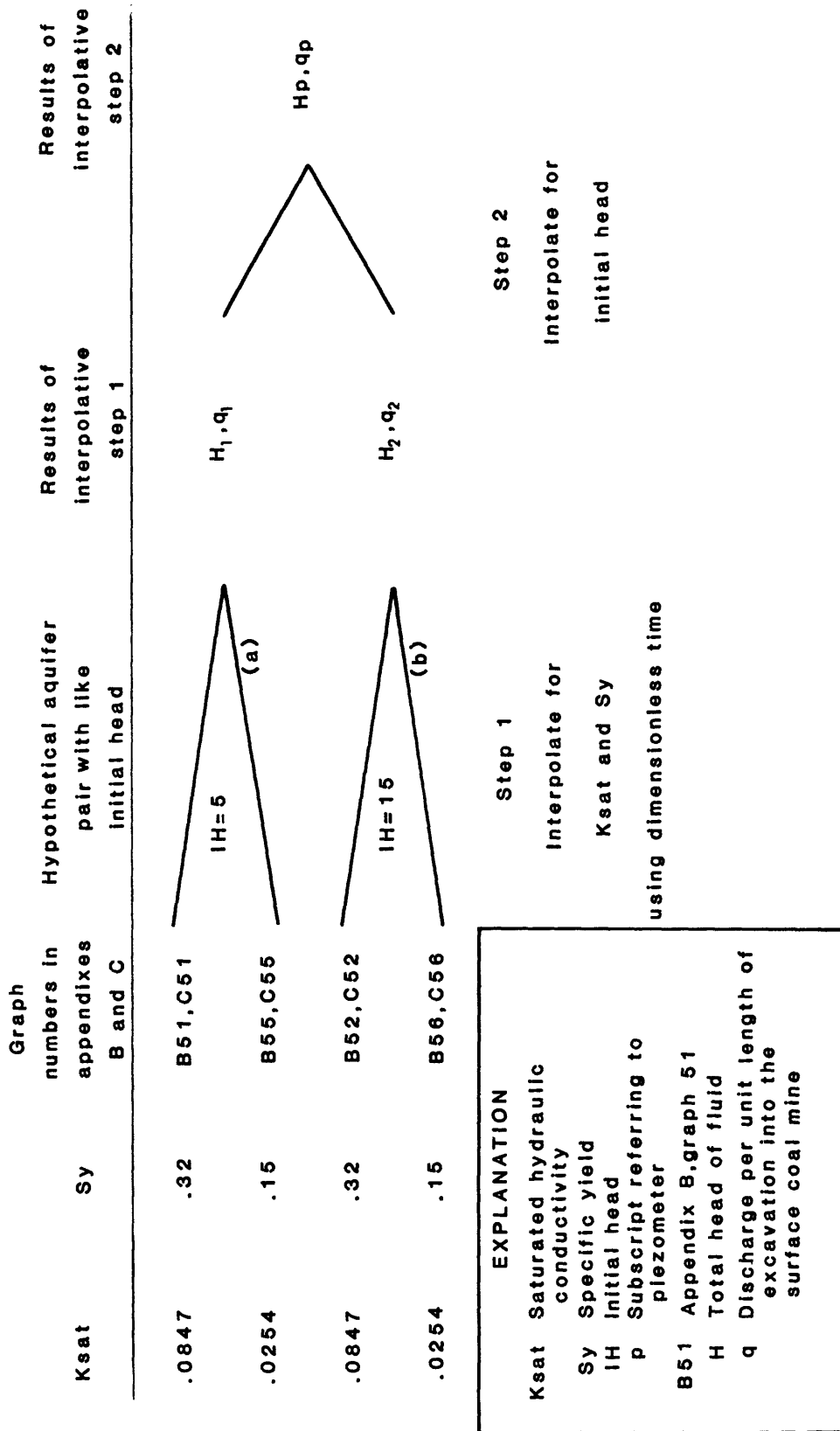


Figure 15.--Interpolative steps for confined aquifer portion of Example 4--First cut.

$$t' = \frac{(K_{sat})t}{(S_y)D} = \frac{(8.47 \times 10^{-2} \text{ m/d})(90 \text{ d})}{(0.32)(6.00 \text{ m})} \cong 4.0$$

for graphs 51 and 52 in Appendixes B and C;

$$t' = \frac{(K_{sat})t}{(S_y)D} = \frac{(2.54 \times 10^{-2} \text{ m/d})(90 \text{ d})}{(0.15)(6.00 \text{ m})} \cong 2.5$$

for graphs 55 and 56 in Appendixes B and C; and

$$t' = \frac{(K_{sat})t}{(S_y)D} = \frac{(4.00 \times 10^{-2} \text{ m/d})(90 \text{ d})}{(0.20)(6.00 \text{ m})} \cong 3.0$$

for the limestone. Dimensionless distance is calculated using the equation

$$x' = x/D = (100 \text{ m})/(6.00 \text{ m}) \cong 17.$$

Dimensionless head is read from graphs B51 and B52 for a dimensionless time of 4.0 and a dimensionless distance of 17 (hypothetical aquifers with geologic material D), and from graphs B55 and B56 for a dimensionless time of 2.5 and a dimensionless distance of 17 (hypothetical aquifers with geologic material E). Dimensionless heads are listed in table 2. Heads are dimensioned from each of the dimensionless heads using the equation $H = h'D$ and are included in table 2.

The computed heads and dimensionless times for pairs of hypothetical aquifers with like initial heads are used to interpolate head for geologic material. Equations for step 1 (fig. 15) are

$$(a) \quad \frac{H_{B51} - H_1}{t'_{B51} - t'} = \frac{H_{B51} - H_{B55}}{t'_{B51} - t'_{B55}}$$

$$\text{Thus,} \quad \frac{5.76 \text{ m} - H_1}{4.0 - 3.0} = \frac{5.76 \text{ m} - 5.82 \text{ m}}{4.0 - 2.5}$$

$$\text{or} \quad H_1 = 5.80 \text{ m.}$$

$$(b) \quad \frac{H_{B52} - H_2}{t'_{B52} - t'} = \frac{H_{B52} - H_{B56}}{t'_{B52} - t'_{B56}}$$

$$\text{Thus,} \quad \frac{5.70 \text{ m} - H_2}{4.0 - 3.0} = \frac{5.70 \text{ m} - 5.82 \text{ m}}{4.0 - 2.5}$$

$$\text{or} \quad H_2 = 5.78 \text{ m.}$$

The predicted head in the piezometer 100 m from the proposed mine and open to the limestone is interpolated from these computed heads and the initial heads in the hypothetical aquifers. Step 2 is

$$\frac{H_1 - H_p}{IH_1 - IH} = \frac{H_1 - H_2}{IH_1 - IH_2}$$

where H_1 and H_2 were computed in step 1, IH_1 and IH_2 are initial heads of the hypothetical aquifers corresponding to the computed heads, IH is the initial head of the aquifer at the mine, and H_p is the predicted head in the piezometer after 90 days. Thus,

$$\frac{5.80 \text{ m} - H_p}{6.00 \text{ m} - 10.0 \text{ m}} = \frac{5.80 \text{ m} - 5.78 \text{ m}}{6.00 \text{ m} - 18.0 \text{ m}}$$

or head in the piezometer approximately equals 5.79 m. The potentiometric surface in the confined aquifer at the piezometer is predicted to change from 10.0 to 5.79 m, a decline of 4.21 m, after 90 days of drainage.

Dimensionless seepage fluxes are read from Appendix C for a dimensionless time of 4.0 for hypothetical aquifers with geologic material D (graphs C51 and C52) and a dimensionless time of 2.5 for hypothetical aquifers with geologic material E (graphs C55 and C56). Dimensionless seepage fluxes from Appendix C are listed in table 2. The seepage fluxes per unit length after 90 days for each hypothetical aquifer are obtained from $q = q'(K_{sat})D/S_y$ and are also given in table 2.

The computed seepage fluxes and dimensionless times are used to interpolate seepage fluxes for pairs of hypothetical aquifers with like initial heads. Equations for step 1 (fig. 15) are

$$(a) \quad \frac{q_{C51} - q_1}{t'_{C51} - t'} = \frac{q_{C51} - q_{C55}}{t'_{C51} - t'_{C55}}$$

$$\text{Thus,} \quad \frac{(7.96 \times 10^{-2} \text{ m}^2/\text{d}) - q_1}{4.0 - 3.0} = \frac{(7.96 \times 10^{-2} \text{ m}^2/\text{d}) - (2.69 \times 10^{-2} \text{ m}^2/\text{d})}{4.0 - 2.5}$$

$$\text{or} \quad q_1 \cong 4.45 \times 10^{-2} \text{ m}^2/\text{d}.$$

$$(b) \quad \frac{q_{C52} - q_2}{t'_{C52} - t'} = \frac{q_{C52} - q_{C56}}{t'_{C52} - t'_{C56}}$$

$$\text{Thus,} \quad \frac{(7.92 \times 10^{-2} \text{ m}^2/\text{d}) - q_2}{4.0 - 3.0} = \frac{(7.92 \times 10^{-2} \text{ m}^2/\text{d}) - (2.95 \times 10^{-2} \text{ m}^2/\text{d})}{4.0 - 2.5}$$

$$\text{or} \quad q_2 \cong 4.61 \times 10^{-2} \text{ m}^2/\text{d}.$$

The computed seepage fluxes from step 1 and initial heads are used to interpolate seepage flux into the mine from the confined limestone. An equation for step 2 is

$$\frac{q_1 - q_p}{IH_1 - IH} = \frac{q_1 - q_2}{IH_1 - IH_2}$$

where q_1 and q_2 are seepage fluxes calculated in step 1, IH_1 and IH_2 are initial heads of the hypothetical aquifers corresponding to the computed seepage fluxes, IH is the initial head of the aquifer at the mine, and q_p is the seepage flux into the excavation after 90 days. Thus,

$$\frac{(4.45 \times 10^{-2} \text{ m}^2/\text{d}) - q_p}{6.00 \text{ m} - 10.0 \text{ m}} = \frac{(4.45 \times 10^{-2} \text{ m}^2/\text{d}) - (4.61 \times 10^{-2} \text{ m}^2/\text{d})}{6.00 \text{ m} - 18.0 \text{ m}}$$

or q_p approximately equals $4.50 \times 10^{-2} \text{ m}^2/\text{d}$. The flux into the mine after 90 days along the 100 m of one excavated face from the confined aquifer is

$$(4.50 \times 10^{-2} \text{ m}^2/\text{d})(100 \text{ m}) = 4.5 \text{ m}^3/\text{d}.$$

The total seepage flux into the mine along the 100 m of one excavated face from both the unconfined and confined aquifers after 90 days is found by summing the individual seepage fluxes. Thus,

$$9.3 \text{ m}^3/\text{d} + 4.5 \text{ m}^3/\text{d} = 14 \text{ m}^3/\text{d}.$$

Multiple Cuts

If the multiple-cut conceptual model is chosen, the user must

1. Determine the hydraulic characteristics and geometry of the aquifer at the proposed mine.
2. Estimate the size and timing of the proposed mine operation.
3. Choose a hypothetical-aquifer/multiple-cut combination (Appendixes D and E) that is approximately equivalent to the aquifer at the proposed mine and the proposed mine operation. A general algorithm that may be used as a guide to choosing a multiple cut is (a) compare the time, in days, at which head and seepage flux are required with the predicted time for the final cut. Let the smaller of the two times be t^* . (b) Calculate the average daily rate of mine advancement. Compute the distance that the mine will have moved in time t^* . Call this distance x^* . (c) Select the times (multiple-cut denominators, t_0) nearest to t^* for the appropriate hypothetical aquifers from the available multiple cuts (Appendixes D and E). All times selected must be less than or equal to the time at which head and seepage flux are

desired. (d) Select the widths (multiple-cut numerators, w_0) nearest to x^* from the available multiple cuts. (e) Examine each possible combination of t_0 and w_0 in terms of physical similarity to the proposed mine operation. Rate is suggested as a determinant of suitability because multiple cuts in Appendixes D and E were chosen based on selected times and distances. The interpolation procedure uses the rates, or time or distance if the rates are identical, for two multiple cuts.

4. Choose an elapsed time after excavation of the first cut for which seepage flux into the mine and heads in the aquifer are desired. Convert the time to dimensionless units by substituting appropriate values for the aquifer at the site into the equation

$$t' = \frac{(K_{sat})t}{(S_y)D} .$$

5. Choose a distance from the planned seepage face of the first cut for which head is desired at the chosen time. Convert the distance to dimensionless units by substituting values for the aquifer at the site into the equation

$$x' = x/D.$$

6. Find dimensionless head, h' , using graphs in Appendix D, for values of dimensionless time and distance calculated in steps 4 and 5.
7. Dimension head using the equation

$$H = h'D.$$

This is the predicted head in the aquifer at the proposed mine site at the distance from the seepage face of the first cut and the elapsed time chosen in steps 4 and 5.

8. Find dimensionless seepage flux, q' , using graphs in Appendix E, for the dimensionless time calculated in step 4.
9. Dimension seepage flux using the equation

$$q = \frac{q'(K_{sat})D}{S_y} .$$

This is the predicted seepage flux per unit length into the proposed mine at the elapsed time chosen in step 4. Flux into the mine through one entire excavated face is calculated by multiplying q times the mine length.

Interpolate or average the heads and seepage fluxes computed in steps 7 and 9 for two hypothetical aquifers or two multiple cuts that bracket the aquifer at the mine. Interpolation for hypothetical-aquifer characteristics

should precede interpolation for multiple-cut characteristics when both are required. The following four examples illustrate some of the choices that could occur to the user in applying the outlined steps. Since so many variations are possible, the examples, presented in order from the least to the most complicated, demonstrate how the user should logically approach a particular situation. Example 1 illustrates an aquifer and mining operation identical to a hypothetical aquifer and multiple cut; Example 2 illustrates an aquifer identical to a hypothetical aquifer but with a mining operation bracketed by two multiple cuts; Example 3 illustrates an aquifer with K_{sat} and S_y bracketed by geologic materials of two hypothetical aquifers and mining operation bracketed by multiple cuts; Example 4 illustrates required times that are before and after t_0 values used for the multiple cuts.

Example 1.--Preliminary drilling and aquifer testing at a proposed mine indicate that a weathered limestone aquifer (fig. 16) has a K_{sat} of 2.54×10^{-2} m/d and an S_y of 0.15. The aquifer thickness is 8.50 m and the water table is 2.95 m below land surface to give a saturated thickness of 5.55 m. The initial cut will be 160 m from a ground-water divide measured perpendicular to the first cut. The length of the mine (y-y'-direction, fig. 6) is to be about 250 m. The mine will advance (x-direction, fig. 6) about 60 m in 180 days. It is desired to predict drainage into the mine and the water level in a well located 130 m from the first cut after 2 years or 730 days.

The aquifer thickness of 5.55 m is close to the hypothetical-aquifer thickness of 5 m, and the length of 160 m is close to the hypothetical-aquifer length of 150 m. Field values for K_{sat} and S_y of 2.54×10^{-2} m/d and 0.15 are identical to those of geologic material E (table 1). Graphs 157 through 162 (Appendixes D and E) are thus possible choices.

The time at which head and seepage flux are desired is 730 days, and the predicted time for the final cut is 180 days. The smaller of these two times is 180 days. Thus, t^* equals 180 days. The average daily rate of mine advancement is 0.33 m/d (60 m/180 d). The distance the mine will have moved is calculated using the equation

$$x^* = (180 \text{ d})(0.33 \text{ m/d}) \cong 60 \text{ m.}$$

The possible hypothetical multiple cuts (graphs 157 to 162) and their average daily rates are as follows: (30 m/30 d) = 1.0 m/d; (30 m/90 d) = 0.33 m/d; (60 m/30 d) = 2.0 m/d; (60 m/90 d) = 0.67 m/d; (60 m/180 d) = 0.33 m/d; and (60 m/270 d) = 0.22 m/d. The hypothetical multiple cuts have possible times (t_0) of 30, 90, 180, or 270 days. The time, t_0 , closest to t^* is 180 days. The hypothetical multiple cuts have possible widths (w_0) of 30 and 60 m. The width, w_0 , closest to x^* is 60 m. The proposed mining rate of 0.33 m/d is identical to the multiple cut (60 m/180 d) of graph 161.

Dimensionless time for the 730 days is

$$t = \frac{(K_{sat})t}{(S_y)D} = \frac{(2.54 \times 10^{-2} \text{ m/d})(730 \text{ d})}{(0.15)(5.55 \text{ m})} \cong 22.$$

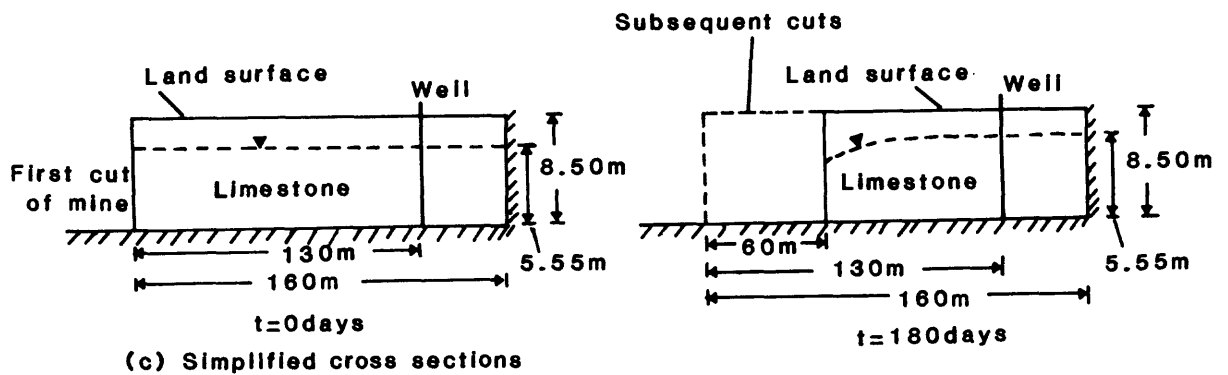
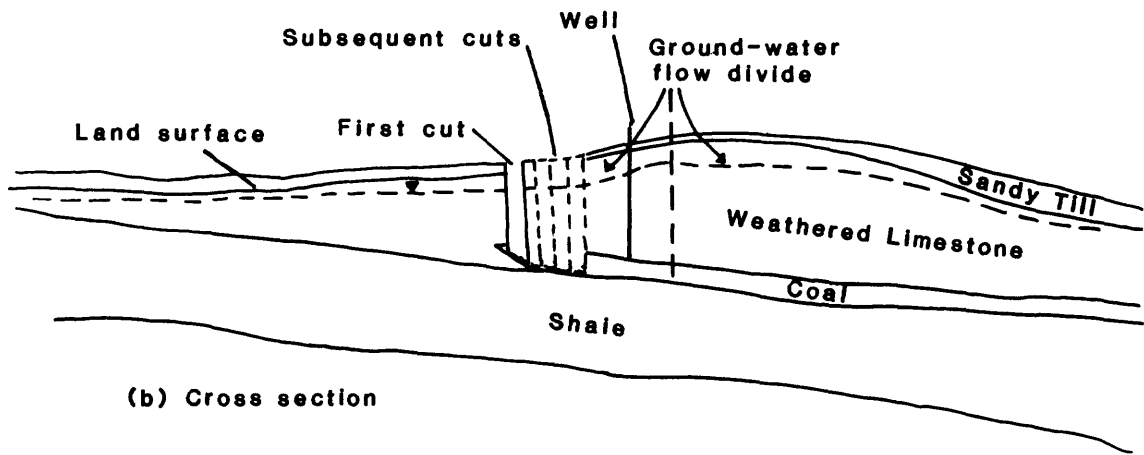
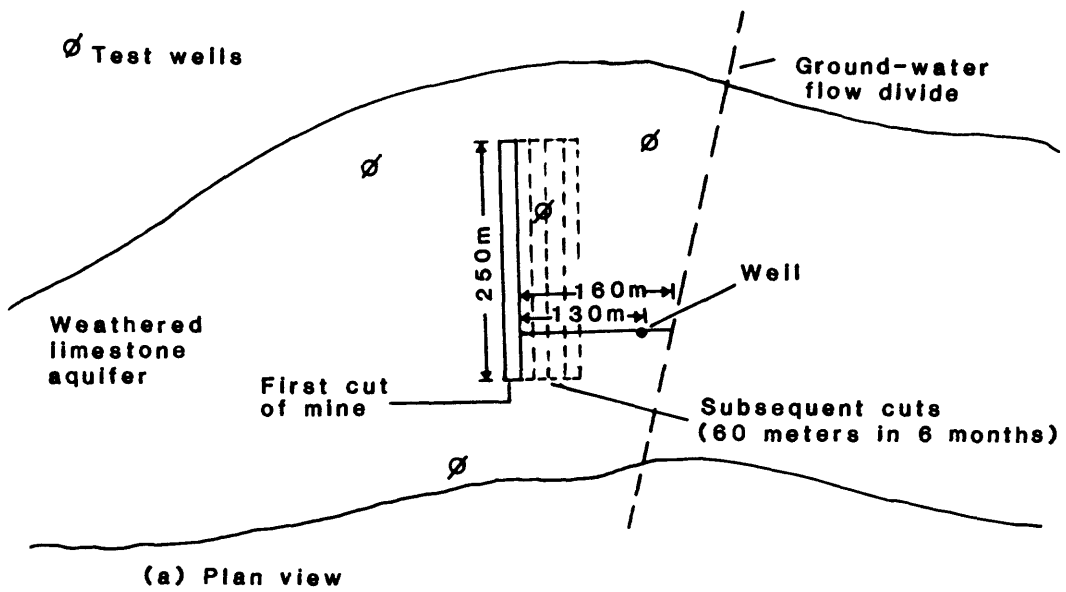


Figure 16.--Diagram of preliminary information for Example 1--Multiple cuts.

Dimensionless distance for the well 130 m from the first cut is

$$x' = x/D = 130 \text{ m}/5.55 \text{ m} \cong 23.$$

Dimensionless head from graph D161 for a dimensionless time of 22 and a dimensionless distance of 23 is 0.92. Head in the well after 730 days is

$$H = h'D = (0.92)(5.55 \text{ m}) \cong 5.11 \text{ m}.$$

Thus, the water level is predicted to change from 5.55 to 5.11 m, a decline of 0.44 m.

Dimensionless seepage flux from graph E161 for a dimensionless time of 22 is 1.33×10^{-2} . The seepage flux per unit length of excavation after 730 days is

$$q = \frac{q'(K_{\text{sat}})^D}{S_y} = \frac{(1.33 \times 10^{-2})(2.54 \times 10^{-2} \text{ m/d})(5.55 \text{ m})}{0.15} \cong 1.25 \times 10^{-2} \text{ m}^2/\text{d}.$$

Thus, the flux into the mine along the 250 m of one excavated face is predicted to be

$$(1.25 \times 10^{-2} \text{ m}^2/\text{d})(250 \text{ m}) \cong 3.1 \text{ m}^3/\text{d}.$$

Example 2.--Preliminary drilling and aquifer testing at a proposed mine site indicate that the mine will penetrate an unconfined, poorly-sorted, sand and gravel aquifer (fig. 17). Aquifer tests indicate an S_y of 0.28 and a K_{sat} of 0.85 m/d. The aquifer is 2.10 m thick and the water table is 0.90 m below land surface to give a saturated thickness of 1.20 m. The sand and gravel deposit pinches out 160 m measured perpendicular to the planned excavation. The length of the first cut will be about 1,000 m. Subsequent cuts during 1 month of mining will advance the mine a distance of 50 m perpendicular to the axis of the first cut. It is desired to predict drainage into the mine and the water level in a well located 100 m from the excavated face of the first cut after 6 months, or 180 days, from the start of excavation.

Field values for K_{sat} of 0.85 m/d and S_y of 0.28 are similar to values for geologic material C, in which K_{sat} equals 0.847 m/d and S_y equals 0.28. The saturated thickness of 1.20 m and length of 160 m are close to the thickness and length of hypothetical aquifers 1-m thick and 150-m long. Graphs 93 through 98 (Appendixes D and E) are thus possible choices.

The proposed mining plan is for the mine to advance at the rate of 50 m in 30 days or 1.67 m/d. The time at which head and seepage flux are required is 180 days, and the predicted time for the final cut is 30 days. The smaller of these, 30 days, is t^* . At the average daily rate of 1.67 m/d the mine will have moved $x^* = (30 \text{ d})(1.67 \text{ m/d}) = 50 \text{ m}$ in 30 days. The multiple cuts (graphs 93 to 98) have possible times (t_o) of 30, 90, 180, and 270 days and possible widths (w_o) of 30 and 60 m. The t_o closest to t^* is 30 days. The two values of w_o bracket x^* equal to 50 m. The possible combinations of t_o and w_o and

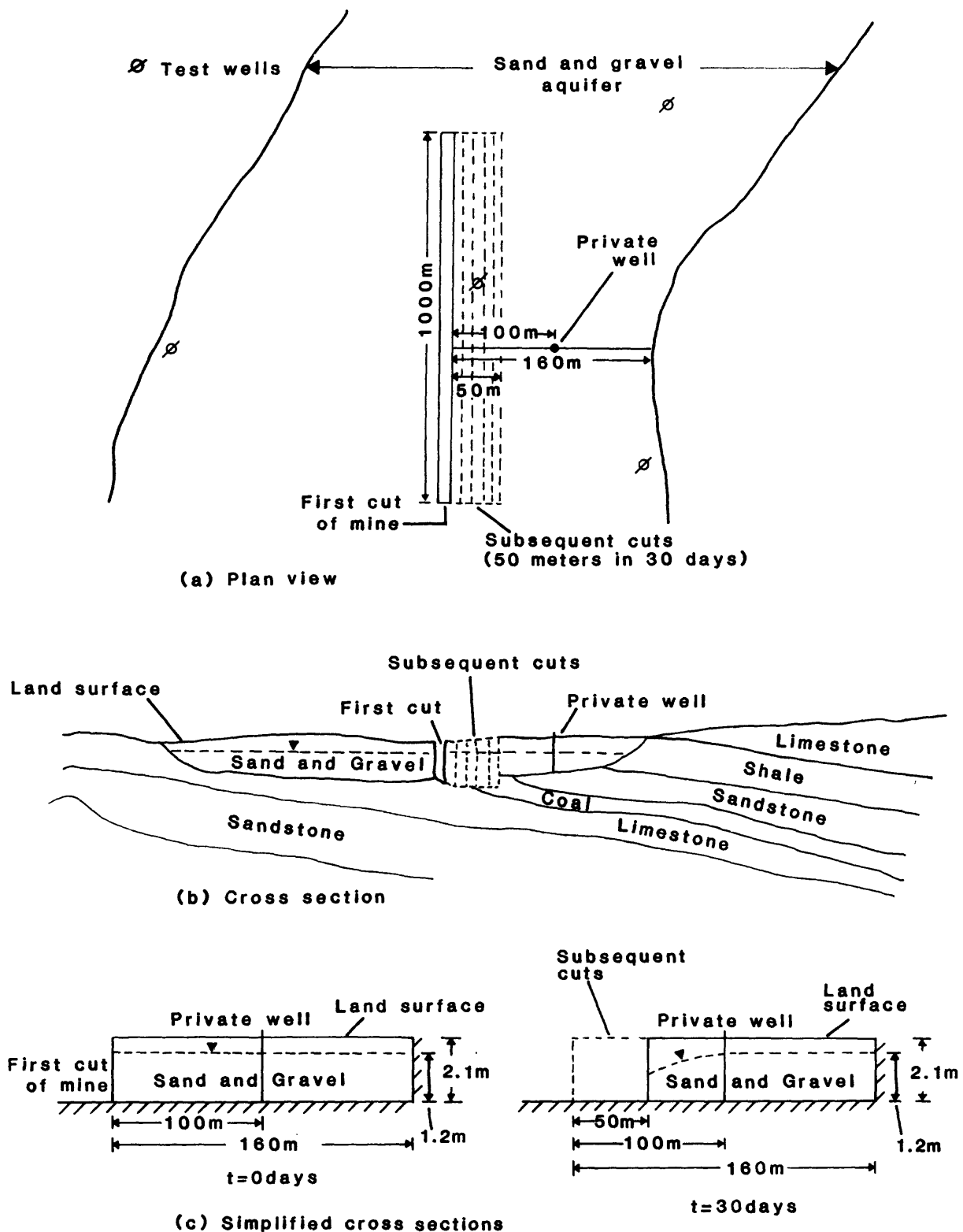


Figure 17.--Diagram of preliminary information for Example 2--Multiple cuts.

their average daily rates of (30 m/30 d) = 1.00 m/d and (60 m/30 d) = 2.00 m/d are best represented by graphs 93 and 95. The proposed average daily rate of 1.67 m/d is between 2.00 and 1.00 m/d, so interpolation is required.

Dimensionless time is

$$t' = \frac{(K_{sat})t}{(S_y)D} = \frac{(8.47 \times 10^{-1} \text{ m/d})(180 \text{ d})}{(0.28)(1.20 \text{ m})} \cong 450,$$

and dimensionless distance is

$$x' = x/D = 100 \text{ m}/1.20 \text{ m} \cong 83.$$

Dimensionless head for dimensionless time 450 and dimensionless distance 83 is 0.81 from graph D93 and 0.66 from graph D95. Heads are dimensioned with the equations

$$H = h'D = (0.81)(1.20 \text{ m}) \cong 0.97 \text{ for graph D93; and}$$

$$H = h'D = (0.66)(1.20 \text{ m}) \cong 0.79 \text{ for graph D95.}$$

Average daily mining rates based on the two multiple cuts are used in the interpolation

$$\frac{H_{D93} - H_{PW}}{r_{D93} - r_P} = \frac{H_{D93} - H_{D95}}{r_{D93} - r_{D95}}$$

where H refers to head, r refers to average daily mining rate, PW refers to the private well, and P refers to the proposed mine. Thus,

$$\frac{0.97 \text{ m} - H_{PW}}{1.00 \text{ m/d} - 1.67 \text{ m/d}} = \frac{0.97 \text{ m} - 0.79 \text{ m}}{1.00 \text{ m/d} - 2.00 \text{ m/d}}$$

or head in the private well approximately equals 0.85 m. Thus, after 180 days, the water level is predicted to change from 1.20 to 0.85 m, a decline of 0.35 m.

Dimensionless seepage flux for a dimensionless time of 450 is 4.00×10^{-3} from graph E93 and 4.10×10^{-3} from graph E95. Seepage flux per unit length at 180 days for graph E93 is

$$q = \frac{q'(K_{sat})D}{S_y} = \frac{(4.00 \times 10^{-3})(8.47 \times 10^{-1} \text{ m/d})(1.20 \text{ m})}{0.28} \cong 1.45 \times 10^{-2} \text{ m}^2/\text{d}$$

and for graph E95 is

$$q = \frac{q'(K_{sat})D}{S_y} = \frac{(4.10 \times 10^{-3})(8.47 \times 10^{-1} \text{ m/d})(1.20 \text{ m})}{0.28} \cong 1.49 \times 10^{-2} \text{ m}^2/\text{d}.$$

The interpolation is made using the computed seepage fluxes and average daily mining rates based on the two multiple cuts. An equation that may be used is

$$\frac{q_{E93} - q_{PW}}{r_{E93} - r_p} = \frac{q_{E93} - q_{E95}}{r_{E93} - r_{E95}}$$

where q refers to seepage flux per unit length of excavation, and P and PW are as defined above. Thus,

$$\frac{1.45 \times 10^{-2} \text{ m}^2/\text{d} - q_{PW}}{1.00 \text{ m/d} - 1.67 \text{ m/d}} = \frac{1.45 \times 10^{-2} \text{ m}^2/\text{d} - 1.49 \times 10^{-2} \text{ m}^2/\text{d}}{1.00 \text{ m/d} - 2.00 \text{ m/d}}$$

or seepage flux per unit length after 180 days is approximately $1.48 \times 10^{-2} \text{ m}^2/\text{d}$. The flux into the mine along the 1,000 m of one excavated face is

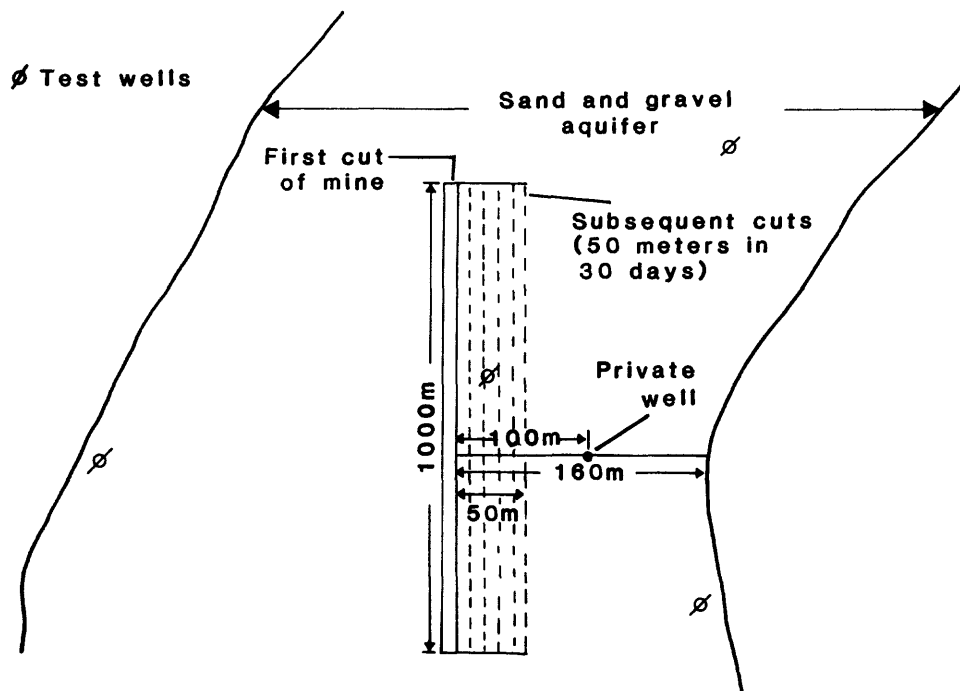
$$(1.48 \times 10^{-2} \text{ m}^2/\text{d})(1,000 \text{ m}) \cong 15 \text{ m}^3/\text{d}.$$

Example 3.--Preliminary drilling and aquifer testing at a proposed mine site indicate that the mine will penetrate an unconfined aquifer of moderately-sorted sand and gravel (fig. 18). Aquifer tests indicate a K_{sat} value of 1.80 m/d and 0.27 for S_y . The aquifer thickness is 2.10 m and the water table is 0.90 m below land surface to give a saturated thickness of 1.20 m. The sand and gravel deposit pinches out 160 m measured perpendicular to the planned excavation. The length of the first cut of the mine will be about 1,000 m. Subsequent cuts during 1 month, or 30 days, will advance the mine a distance of 50 m perpendicular to the axis of the first cut. It is desired to predict drainage into the mine and the water level in a well located 100 m from the excavated face of the first cut after 6 months, or 180 days, from the start of excavation.

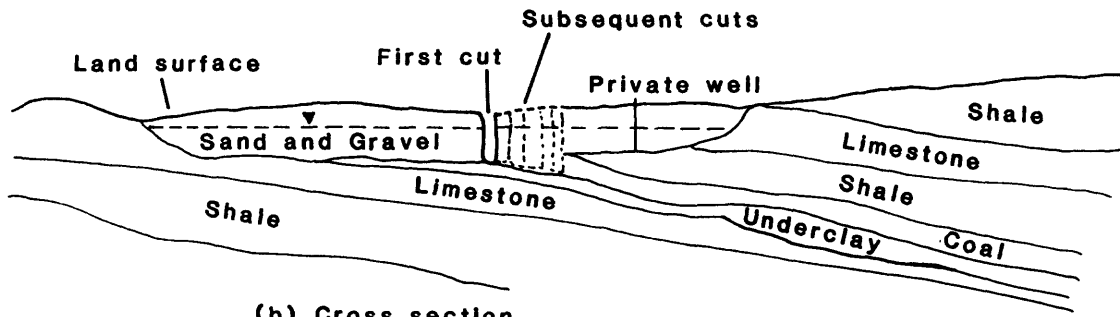
Aquifer thickness and length of 1.20 m and 160 m are close to dimensions of hypothetical aquifers 1-m thick and 150-m long. Field-determined K_{sat} and S_y values of 1.80 m/d and 0.27 are between K_{sat} and S_y values of two geologic materials. K_{sat} and S_y are 2.54 m/d and 0.27 for geologic material B and 8.47×10^{-1} m/d and 0.28 for geologic material C. Geologic material B and a thickness of 1 m and length of 150 m are represented in graphs 47 through 52 (Appendixes D and E). Geologic material C and a thickness of 1 m and length of 150 m are represented in graphs 93 through 98 (Appendixes D and E).

The proposed plan is for the mine to advance at the rate of 50 m in 30 d or 1.67 m/d. The time at which head and seepage flux are desired is 180 days, and the predicted time for the final cut is 30 days. The smaller of these, 30 days, is t^* . At the average rate of 1.67 m/d, the mine will have moved $x^* = (30 \text{ d})(1.67 \text{ m/d}) \cong 50 \text{ m}$ in 30 days.

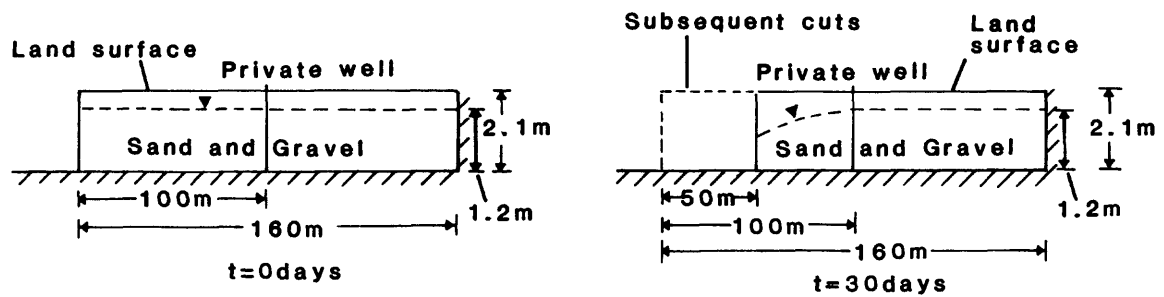
Multiple cuts (graphs 47-52, 93-98) have possible times (t_o) of 30, 90, 180, and 270 days and possible widths (w_o) of 30 and 60 m. The t_o closest to t^* is 30 days. The two values of w_o bracket x^* equal to 50 m. The possible



(a) Plan view



(b) Cross section



(c) Simplified cross sections

Figure 18.--Diagram of preliminary information for Example 3--Multiple cuts.

combinations of t_0 and w_0 and their average daily rates of (30 m/30 d) = 1.00 m/d and (60 m/30 d) = 2.00 m/d are represented in graphs 47, 49, 93, and 95. The proposed average daily rate of mine advancement of 1.67 m/d is between 2.00 and 1.00 m/d. Two interpolations are required: (1) Interpolation using dimensionless time for the aquifer characteristics K_{sat} and S_y , and (2) interpolation for average daily rate.

Dimensionless time is calculated by

$$t' = \frac{(K_{sat})t}{(S_y)D} \quad \text{or}$$

$$\frac{(2.54 \text{ m/d})(180 \text{ d})}{(0.27)(1.20 \text{ m})} \cong 1,400 \text{ for graphs 47 and 49;}$$

$$\frac{(8.47 \times 10^{-1} \text{ m/d})(180 \text{ d})}{(0.28)(1.20 \text{ m})} \cong 450 \text{ for graphs 93 and 95; and}$$

$$\frac{(1.80 \text{ m/d})(180 \text{ d})}{(0.27)(1.20 \text{ m})} = 1,000 \text{ for the proposed mine.}$$

Dimensionless distance is

$$x' = x/D = 100 \text{ m} / 1.20 \text{ m} = 83.$$

Dimensionless head is read from graphs D47 and D49 for a dimensionless time of 1,400 and a dimensionless distance of 83, and from graphs D93 and D95 for a dimensionless time of 450 and a dimensionless distance of 83. Dimensionless heads are 0.68, 0.48, 0.81, and 0.66, respectively. Heads are dimensioned using the equation $H = h'D$ and are approximately 0.82 m, 0.58 m, 0.97 m, and 0.79 m, respectively. The computed heads and dimensionless times for the hypothetical-aquifer/multiple-cut combinations paired by like average daily mining rates are used to interpolate for head in the rock at the mine site. Dimensionless times are 1,400 for geologic material B (graphs 47 and 49), 450 for geologic material C (graphs 93 and 95), and 1,000 for the aquifer at the proposed mine. Interpolation equations are

$$\frac{H_{D47} - H_1}{t'_{D47} - t'} = \frac{H_{D47} - H_{D93}}{t'_{D47} - t'_{D93}} .$$

Thus,

$$\frac{0.82 \text{ m} - H_1}{1,400 - 1,000} = \frac{0.82 \text{ m} - 0.97 \text{ m}}{1,400 - 450}$$

or

$$H_1 = 0.88 \text{ m}.$$

$$\frac{H_{D49} - H_2}{t'_{D49} - t'} = \frac{H_{D49} - H_{D95}}{t'_{D49} - t'_{D95}} .$$

Thus,
$$\frac{0.58 \text{ m} - H_2}{1,400 - 1,000} = \frac{0.58 \text{ m} - 0.79 \text{ m}}{1,400 - 450}$$

or
$$H_2 \cong 0.67 \text{ m} .$$

The computed heads and the average mining rates are used to interpolate head between rates. An interpolation equation is

$$\frac{H_1 - H_{PW}}{r_1 - r} = \frac{H_1 - H_2}{r_1 - r_2}$$

where H_1 and H_2 were calculated in step 1, r_1 and r_2 are mining rates corresponding to the calculated heads, r is the average daily rate of the proposed mine, and H_{PW} is the required head in the private well. Thus,

$$\frac{0.88 \text{ m} - H_{PW}}{1.00 \text{ m/d} - 1.67 \text{ m/d}} = \frac{0.88 \text{ m} - 0.67 \text{ m}}{1.00 \text{ m/d} - 2.00 \text{ m/d}}$$

or head in the private well approximately equals 0.74 m. Thus, after 180 days, the water level is predicted to change from 1.20 to 0.74 m, a decline of 0.46 m.

Dimensionless seepage fluxes from graphs E47 and E49 for a dimensionless time of 1,400 and from graphs E93 and E95 for a dimensionless time of 450, are 2.27×10^{-3} , 2.33×10^{-3} , 4.00×10^{-3} , and 4.10×10^{-3} , respectively. Seepage fluxes per unit length are dimensioned using the equation $q = q'(K_{sat})D/S_y$ and are approximately $2.56 \times 10^{-2} \text{ m}^2/\text{d}$, $2.63 \times 10^{-2} \text{ m}^2/\text{d}$, $1.45 \times 10^{-2} \text{ m}^2/\text{d}$, and $1.49 \times 10^{-2} \text{ m}^2/\text{d}$, respectively.

The computed seepage fluxes and dimensionless times for the hypothetical-aquifer/multiple-cut combinations paired by like average daily mining rates are used to interpolate for seepage flux between geologic materials. Dimensionless times are 1,400 for geologic material B (graphs E47 and E49), 450 for geologic material C (graphs E93 and E95), and 1,000 for the aquifer at the proposed mine. Interpolation equations are

$$\frac{q_{E47} - q_1}{t'_{E47} - t'} = \frac{q_{E47} - q_{E93}}{t'_{E47} - t'_{E93}} .$$

Thus,
$$\frac{(2.56 \times 10^{-2} \text{ m}^2/\text{d}) - q_1}{1,400 - 1,000} = \frac{(2.56 \times 10^{-2} \text{ m}^2/\text{d}) - (1.45 \times 10^{-2} \text{ m}^2/\text{d})}{1,400 - 450}$$

or
$$q_1 \cong 2.09 \times 10^{-2} \text{ m}^2/\text{d} .$$

$$\frac{q_{E49} - q_2}{t'_{E49} - t'} = \frac{q_{E49} - q_{E95}}{t'_{E49} - t'_{E95}} .$$

$$\text{Thus, } \frac{(2.63 \times 10^{-2} \text{ m}^2/\text{d}) - q_2}{1,400 - 1,000} = \frac{(2.63 \times 10^{-2} \text{ m}^2/\text{d}) - (1.49 \times 10^{-2} \text{ m}^2/\text{d})}{1,400 - 450}$$

$$\text{or } q_2 \cong 2.15 \times 10^{-2} \text{ m}^2/\text{d}.$$

The interpolation uses the computed seepage fluxes and average daily mining rates. An equation is

$$\frac{q_1 - q_{PW}}{r_1 - r} = \frac{q_1 - q_2}{r_1 - r_2} .$$

$$\text{Thus, } \frac{(2.09 \times 10^{-2} \text{ m}^2/\text{d}) - q_{PW}}{1.00 - 1.67} = \frac{(2.09 \times 10^{-2} \text{ m}^2/\text{d}) - (2.15 \times 10^{-2} \text{ m}^2/\text{d})}{1.00 - 2.00}$$

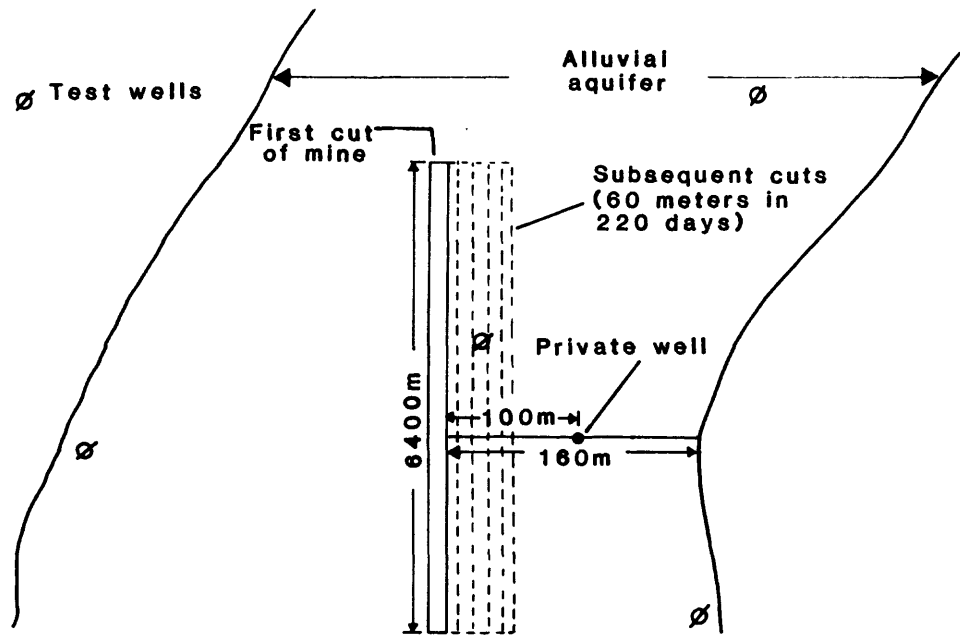
or seepage flux per unit length into the excavation after 180 days is approximately $2.13 \times 10^{-2} \text{ m}^2/\text{d}$. The flux into the mine along the 1,000 m of one excavated face is predicted to be

$$(2.13 \times 10^{-2} \text{ m}^2/\text{d})(1,000 \text{ m}) \cong 21 \text{ m}^3/\text{d}.$$

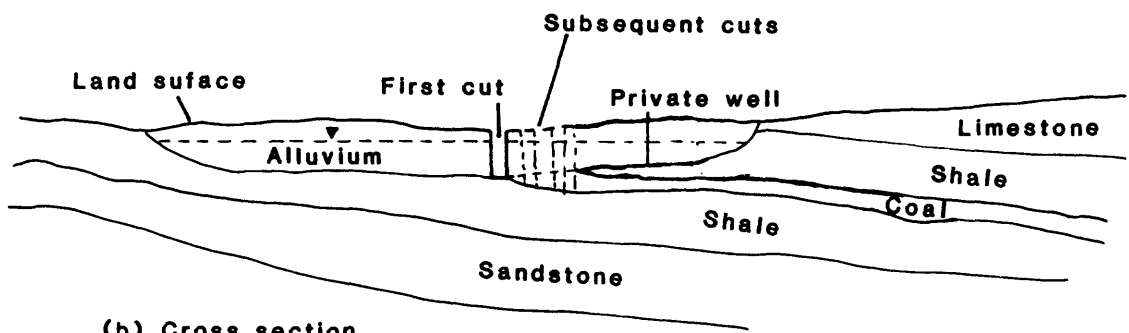
Example 4.--Preliminary drilling at a proposed mine site indicates that the mine will penetrate an unconfined aquifer composed of well-sorted alluvial deposits (fig. 19). Aquifer tests indicate a K_{sat} value of 2.54 m/d and 0.27 for S_y . The aquifer thickness is 2.10 m and the water table is 0.90 m below land surface to give a saturated thickness of 1.20 m. The alluvial deposit pinches out 160 m measured perpendicular to the planned excavation. The length of the first cut will be about 6,400 m. Subsequent cuts during 220 days of mining will advance the mine a distance of 60 m perpendicular to the axis of the first cut. It is desired to predict drainage into the mine and the water level in a well located 100 m from the excavated face of the first cut after 120 and 365 days from the start of excavation.

Field-determined K_{sat} and S_y values of 2.54 m/d and 0.27 are identical to K_{sat} and S_y values for geologic material B. Aquifer thickness and length of 1.20 m and 160 m are close to dimensions of hypothetical aquifers 1-m thick and 150-m long. Geologic material B and a thickness of 1 m and length of 150 m are represented in graphs 47 through 52 (Appendixes D and E).

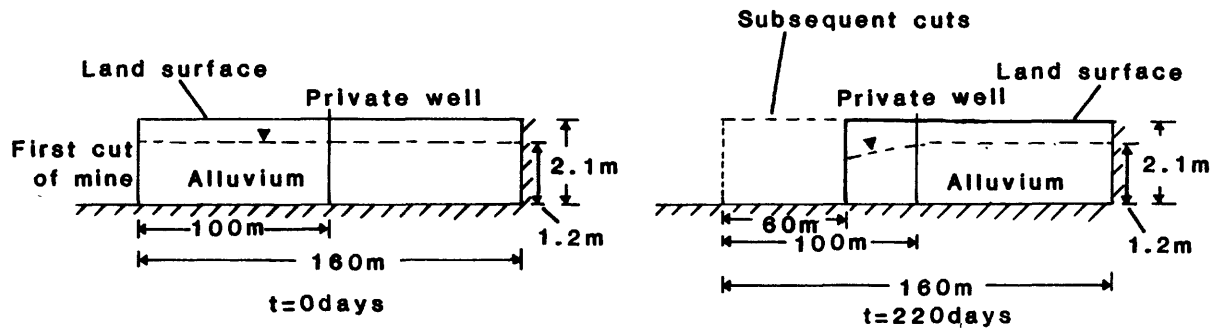
The proposed plan is for the mine to advance 60 m in 220 days (0.27 m/d). The times at which head and seepage flux are desired are 120 days (T1) and 365 days (T2), and the predicted time for the final cut is 220 days. The time 120



(a) Plan view



(b) Cross section



(c) Simplified cross sections

Figure 19.--Diagram of preliminary information for Example 4--Multiple cuts.

days is smaller than 220 days, so t^*_1 is 120 days. The time 365 days is larger than 220 days, so t^*_2 is 220 days. At the average rate of 0.27 m/d, the mine will have moved

$$x^*_1 = (120 \text{ d})(0.27 \text{ m/d}) \cong 32 \text{ m in 120 days}$$

and

$$x^*_2 = (220 \text{ d})(0.27 \text{ m/d}) \cong 59 \text{ m in 220 days.}$$

Multiple cuts (graphs 47 to 52) have possible times (t_o) of 30, 90, 180, and 270 days and possible widths (w_o) of 30 and 60 m. The values of t_o of 90 and 180 days bracket t^*_1 of 120 days. Ninety days is less than the 120 days at which head and seepage flux are to be predicted, but 180 days is not. The values of t_o of 180 and 270 days bracket t^*_2 of 220 days. Both 180 and 270 days are less than the 365 days at which head and seepage flux are to be predicted. The width closest to x^*_1 equal to 32 m is w_o of 30 m. The width closest to x^*_2 equal to 59 m is w_o of 60 m.

The possible combinations of t_o and w_o and their average daily rates are (30 m/90 d) = 0.33 m/d for case 1; and (60 m/180 d) = 0.33 m/d and (60 m/270 d) = 0.22 m/d for case 2. The appropriate multiple cut for case 1 is represented in graph 48, and the appropriate multiple cuts for case 2 are represented in graphs 50 and 51. The proposed average rate of mine advancement of 0.27 m/d is between 0.22 and 0.33 m/d. Head and seepage flux for case 2 must be interpolated using average daily rates.

Dimensionless times are

$$t'_1 = \frac{(K_{sat})t}{(S_y)D} = \frac{(2.54 \text{ m/d})(120 \text{ d})}{(0.27)(1.20 \text{ m})} \cong 940$$

and

$$t'_2 = \frac{(K_{sat})t}{(S_y)D} = \frac{(2.54 \text{ m/d})(365 \text{ d})}{(0.27)(1.20 \text{ m})} \cong 2,900.$$

Dimensionless distance is

$$x' = x/D = 100 \text{ m}/1.20 \text{ m} \cong 83.$$

Dimensionless head is read from graph D48 for a dimensionless time of 940 and a dimensionless distance of 83, and from graphs D50 and D51 for a dimensionless time of 2,900 and a dimensionless distance of 83. Dimensionless heads are 0.78, 0.42, and 0.49, respectively. Heads are dimensioned using $H = h'D$ and are approximately 0.94 m, 0.50 m, and 0.59 m, respectively. The water level in the private well after 12 days is predicted to change from 1.20 to 0.94 m, a decline of 0.26 m (case 1). An equation to interpolate for case 2 is

$$\frac{H_{D50} - H_{PW}}{r_{D50} - r_P} = \frac{H_{D50} - H_{D51}}{r_{D50} - r_{D51}}$$

where H is head, r is average daily mining rate, PW is the private well after 365 days of drainage, and P refers to the proposed mine. Thus,

$$\frac{0.50 \text{ m} - H_{PW}}{0.33 \text{ m/d} - 0.27 \text{ m/d}} = \frac{0.50 \text{ m} - 0.59 \text{ m}}{0.33 \text{ m/d} - 0.22 \text{ m/d}}$$

or head in the private well approximately equals 0.55 m. Thus, after 365 days, the water level is predicted to change from 1.20 to 0.55 m, a decline of 0.65 m (case 2).

Dimensionless seepage fluxes from graph E48 for a dimensionless time of 940 and from graphs E50 and E51 for a dimensionless time of 2,900 are 2.65×10^{-3} , 1.57×10^{-3} , and 2.17×10^{-3} , respectively. Seepage fluxes per unit length of excavation are dimensioned using $q = q'(K_{sat})D/S_y$, and are approximately $2.99 \times 10^{-2} \text{ m}^2/\text{d}$ after 120 days (case 1), and $1.77 \times 10^{-2} \text{ m}^2/\text{d}$ and $2.45 \times 10^{-2} \text{ m}^2/\text{d}$ after 365 days (case 2). The seepage flux into the mine along the 6,400 m of one excavated face at 120 days (case 1) is predicted to be

$$(2.99 \times 10^{-2} \text{ m}^2/\text{d})(6,400 \text{ m}) \cong 190 \text{ m}^3/\text{d}.$$

Seepage flux is interpolated for 365 days (case 2) by

$$\frac{q_{E50} - q_{PW}}{r_{E50} - r_P} = \frac{q_{E50} - q_{E51}}{r_{E50} - r_{E51}}.$$

Thus,

$$\frac{(2.90 \times 10^{-2} \text{ m}^2/\text{d}) - q_{PW}}{0.33 \text{ m/d} - 0.27 \text{ m/d}} = \frac{(1.77 \times 10^{-2} \text{ m}^2/\text{d}) - (2.45 \times 10^{-2} \text{ m}^2/\text{d})}{0.33 \text{ m/d} - 0.22 \text{ m/d}}$$

or seepage flux per unit length into the excavation at 365 days is approximately $3.27 \times 10^{-2} \text{ m}^2/\text{d}$. The flux into the mine along the 6,400 m of one excavated face at 365 days (case 2) is predicted to be

$$(3.27 \times 10^{-2} \text{ m}^2/\text{d})(6,400 \text{ m}) \cong 209 \text{ m}^3/\text{d}.$$

SUMMARY

Changes in seepage flux and head (ground-water level) that result from ground-water drainage into a surface coal mine can be predicted by a technique that considers drainage from the unsaturated zone. Consideration of flow in the saturated and unsaturated zones gives a more realistic model of ground-water drainage. The complex solution to the variably-saturated, ground-water drainage problem is simplified through the use of computer-generated head and seepage flux profiles that can be applied to a range of mine-drainage problems.

It was assumed that hydrogeologic conditions and mining operations at a proposed mine site could be represented by two simplified conceptual models: (1) Drainage to a first cut, and (2) drainage to multiple cuts, in which drainage effects of an area surface mine are included. Numerous simulations were made of ground-water flow in selected hypothetical aquifers. For drainage to a first cut, aquifers at a proposed mine site were represented by one or more of 72 hypothetical aquifers. For drainage to multiple cuts, each of

32 of the hypothetical aquifers was coupled with several hypothetical area surface mines to give a total of 174 hypothetical-aquifer/multiple-cut combinations. A finite-difference model that considers variably-saturated, two-dimensional, ground-water flow, VS2D, was used for the simulations. Computed heads and seepage fluxes were presented as graphs in nondimensional units.

Users are required to know geologic and hydrologic data typically available prior to mining. If multiple cuts are considered, the user also is required to estimate the size and timing of the proposed mine operation. The user then matches conditions at the proposed site to the hypothetical aquifers. Dimensionless heads and seepage fluxes from the graphs are dimensioned using field-determined data. Head and seepage flux in aquifers at proposed mine sites can be predicted by applying additive and interpolative methods. Measured heads resulting from drainage into a surface coal mine near Industry, Illinois (Appendix A), were compared to predicted heads computed using this technique. Because each layer is considered separately, the technique is applicable to many variations in geologic strata.

The technique is limited to hydrogeologic settings and surface-mining methods common to Illinois. Application of the technique is limited to the ranges of aquifer geometries, geologic materials, initial-head conditions, and mining operations considered. Fracture flow, recharge, and leakage are not considered. The conceptual model on which the technique is based is limited to a two-dimensional, cross-sectional analysis of drainage. Sensitivity analyses (Appendix A) indicate that the most sensitive model parameter is saturated hydraulic conductivity and that neglecting recharge may be a significant limitation.

REFERENCES CITED

- American Society of Testing Materials, 1967, Permeability and capillarity of soils: Philadelphia, Pa., ASTM, 210 p.
- Bair, E. S., 1980, Numerical simulation of the hydrogeological effects of open pit anthracite mining: Ph.D. dissertation, Pennsylvania State University, 230 p.
- Bear, Jacob, 1972, Dynamics of fluids in porous media: New York, American Elsevier, 764 p.
- Boussinesq, J., 1877, Du mouvement non permanent des eaux souterraines: Essai sur la theorie des eaux courantes, Memoires presentes par divers savants a l'Academie des Sciences de l'Institut de France, v. 23, no. 1, 680 p.
- 1904, Recherches theoriques sur l'ecoulement des nappes d'eau infiltrées dans le solet sur le debit des sources: Journal de Mathematiques pures et appliquees, v. 10, sme serie, p. 5-78.
- Brutsaert, W. F., and El-Kadi, A. I., 1984, The relative importance of compressibility and partial saturation in unconfined groundwater flow: Water Resources Research, v. 20, no. 3, p. 400-408.

- Ferris, J. G., Knowles, D. B., Brown, R. H., and Stallman, R. W., 1962, Theory of aquifer tests: U.S. Geological Survey Water-Supply Paper 1536-E, 174 p.
- Freeze, R. A., and Cherry, J. A., 1979, Groundwater: Englewood Cliffs, N.J., Prentice-Hall, 604 p.
- Glover, R. E., 1964, Ground-water movement: Engineering Monograph No. 31, Office of Chief Engineer, Bureau of Reclamation, U.S. Department of the Interior, Denver, Colorado.
- Hamilton, D. A., and Wilson, J. L., 1977, A generic study of strip mining impacts on groundwater resources: Cambridge, Massachusetts Institute of Technology Report No. 229, 156 p.
- Haushild, William, and Kruse, Gorden, 1962, Unsteady flow of ground water into a surface reservoir: Transactions, American Society of Civil Engineers, v. 127, part I, p. 408-415.
- Heath, R. C., 1983, Basic ground-water hydrology: U.S. Geological Survey Water-Supply Paper 2220, 84 p.
- Ibrahim, H. A., and Brutsaert, W. F., 1965, Inflow hydrographs from large unconfined aquifers: Journal of the Irrigation and Drainage Division - Proceedings of the American Society of Civil Engineers, v. 91, no. IR2, p. 21-38.
- Lappala, E. G., Healy, R. W., and Weeks, E. P., 1985, Documentation of computer program VS2D to solve the equations of fluid flow in variably saturated porous media: U.S. Geological Survey Water-Resources Investigations Report 83-4099, 200 p.
- Lohman, S. W., 1972, Ground-water hydraulics: U.S. Geological Survey Professional Paper 708, 70 p.
- Meinzer, O. E., 1923, The occurrence of groundwater in the United States, with a discussion of principles: U.S. Geological Survey Water-Supply Paper 489, 321 p.
- National Research Council, 1981, Coal mining and ground-water resources in the United States, a report prepared by the committee on ground-water resources in relation to coal mining: National Academy Press, Washington, D.C., 197 p.
- Nawrocki, M. A., 1979, Groundwater monitoring to fulfill U. S. Office of Surface Mining regulations: Symposium on surface mining hydrology, sedimentology and reclamation: University of Kentucky, Lexington, Kentucky, p. 139-143.
- Pryor, W. A., 1956, Groundwater geology in southern Illinois: Illinois State Geological Survey Circular 212, 25 p.
- Stallman, R. W., 1976, Aquifer-test design, observation and data analysis: U.S. Geological Survey Techniques of Water-Resources Investigations, Book 3, Chapter B1, 26 p.

U.S. Department of the Interior, Water and Power Resources Service, 1981, Ground-water manual: New York, John Wiley and Sons, 480 p.

Verma, R. D., and Brutsaert, W. F., 1970, Unconfined aquifer seepage by capillary flow theory: Journal of the Hydraulics Division - Proceedings of the American Society of Civil Engineers, v. 96, no. HY6, p. 1331-1344.

----- 1971, Unsteady free surface ground water seepage: Journal of the Hydraulics Division - Proceedings of the American Society of Civil Engineers, v. 97, no. HY8, p. 1213-1229.

Willman, H. B., and others, 1975, Handbook of Illinois stratigraphy: Illinois State Geological Survey Bulletin 95, Illinois Department of Registration and Education, 261 p.

Yeh, William W. G., 1970, Nonsteady flow to surface reservoir: Journal of the Hydraulics Division - Proceedings of the American Society of Civil Engineers, v. 96, no. HY3, p. 609-619.

GLOSSARY OF TECHNICAL TERMS

ALGORITHM is a recursive computational procedure.

ANISOTROPY is that condition in which significant properties may not be independent of direction.

AQUIFER is a water-bearing layer of rock that will yield water in a usable quantity to a well or spring.

AREA SURFACE MINING is a mining method in which (1) a cut is made and the overburden is removed to expose the coal; (2) the coal is removed and a second cut is excavated adjacent to the first cut; (3) the overburden from the second cut is deposited as spoil into the previous cut; (4) the sequence of cuts is continued until a boundary is reached or it is uneconomical to continue.

CONFINED AQUIFER is an aquifer that is bounded above and below by impermeable beds, or by beds of distinctly lower permeability than that of the aquifer itself. A confined aquifer contains ground water under pressure significantly greater than atmospheric. The upper surface of the confined ground water is the bottom of a poorly permeable confining layer.

CONFINING BED is a layer of rock having very low hydraulic conductivity that hampers the movement of water into and out of an aquifer.

DIMENSIONLESS is a physical property consisting of length, mass, and time combined such that units cancel and a fundamental measure with no units is formed.

FINITE-DIFFERENCE is a method to calculate approximately the solution of partial differential equations. Derivatives at a point are replaced by ratios of the changes in appropriate variables over a small but finite interval.

GEOLOGIC MATERIALS are rocks and unconsolidated deposits described by hydraulic characteristics including saturated hydraulic conductivity and specific yield. They represent aquifer properties typical of Illinois surface coal-mining areas.

GROUND-WATER DRAINAGE is the gravity removal of excess ground water from the porous medium of a penetrated aquifer.

HEAD of a liquid at a given point is the sum of three components:
(1) Elevation head, which is equal to the elevation of the point above a datum,
(2) pressure head, which is the height of a column of static water that can be supported by the static pressure at the point, and (3) velocity head, which is the height the kinetic energy of the liquid is capable of lifting the liquid.

HOMOGENEITY is a property that describes a material with identical hydrologic properties everywhere. Homogeneity is synonymous with hydrologic uniformity.

HYDRAULIC GRADIENT is the change in head per unit of distance in the direction of the steepest change.

IMPERMEABLE BOUNDARY is a boundary that does not permit water to move through it perceptibly under the head differences ordinarily found in subsurface water. The flow lines adjacent to the boundary are parallel to it, and the equipotential lines meet the boundary at right angles.

ISOTROPY is that condition in which all significant properties are independent of direction.

MULTIPLE CUTS are representations of first and subsequent cuts of hypothetical active area surface mines. Multiple-cut widths represent the total distance of mine advance from the first cut. Multiple-cut times represent the time for this mine advance.

OVERBURDEN is material that overlies a deposit of useful materials, ores, or coal, especially those deposits that are mined from the surface by open cuts.

POROSITY is a property describing the voids or openings in a rock. Porosity may be expressed quantitatively as the ratio of the volume of openings in a rock to the total volume of the rock.

POTENTIOMETRIC SURFACE is the total head in an aquifer, or the height above a datum at which the water level stands in tightly cased wells that penetrate the aquifer; a potentiometric surface for an unconfined aquifer is called a water table.

SATURATED HYDRAULIC CONDUCTIVITY is the volume of water at the existing kinematic viscosity that will move in unit time under a unit hydraulic gradient through a unit area measured at right angles to the direction of flow for an isotropic medium and homogeneous fluid.

SATURATED ZONE is the subsurface zone in which all openings are full of water.

SEEPAGE FACE is a boundary from which water emerges from the flow region at atmospheric pressure.

SEEPAGE FLUX is the discharge of ground water leaving the aquifer through the seepage-face boundary.

SPECIFIC YIELD is the ratio of the ultimate volume of water that will drain under the influence of gravity to the volume of saturated rock.

SPOIL is the overburden or waste material excavated by mining.

TOTAL HEAD see **HEAD**.

TRANSIENT FLOW is flow that occurs when at any point in a flow field the magnitude or direction of the flow velocity changes with time.

UNCONFINED AQUIFER is an aquifer having a water table.

UNSATURATED ZONE is the subsurface zone, usually starting at the land surface, that contains both water and air in the pores.

WATER TABLE is the water level in the saturated zone at which the pressure is equal to the atmospheric pressure in an unconfined aquifer.

APPENDIXES

SYMBOLS USED IN APPENDIXES

<u>Symbol</u>	<u>Dimension</u>	<u>Description</u>
h_c	L	Level in surface reservoir above the impermeable layer in Boussinesq, Glover, and Haushild and Kruse solutions
C	-	Subscript used in sensitivity analysis to represent values obtained using the control parameters
D	L	Initial saturated thickness of the aquifer in the vertical direction; initial height of the water table above the impermeable layer in Boussinesq solution
GM	-	Geologic material
H_{ave}	L	Average height of free surface above impermeable layer in Boussinesq solution
IH	L	Initial head of aquifer
K_{sat}	LT^{-1}	Saturated hydraulic conductivity
L	L	Length of aquifer in horizontal direction
N	-	Subscript used in sensitivity analysis to represent new values after increase or decrease in parameter value
S_y	-	Specific yield
VS2D	-	Variably-saturated, two-dimensional, ground-water flow, finite-difference, numerical model
a^*	L^2T^{-1}	Equal to $K_{sat}D/S_y$ in Glover solution
exp	-	Equal to e to the exponent which follows error function
erf	-	Error function
h	L	Height of water table above the impermeable layer in Boussinesq solution
h^*	L	Linearized height of water table above the impermeable layer in Glover solution
h'	-	Dimensionless total head of fluid

SYMBOLS USED IN APPENDIXES

<u>Symbol</u>	<u>Dimension</u>	<u>Description</u>
$\Delta h'$	-	Percentage change in dimensionless total head of fluid; used in sensitivity analysis
h_b	L	Bubbling or air entry pressure head of fluid; Brooks and Corey coefficient
q'	-	Dimensionless discharge, or seepage flux, into the surface coal mine
$\Delta q'$	-	Percentage change in dimensionless seepage flux; used in sensitivity analysis
t	T	Elapsed time of drainage since excavation of the first cut
t'	-	Dimensionless time
t_0	T	Multiple-cut time
w_0	L	Multiple-cut width
x	L	Horizontal distance from the seepage face of the first cut from $x=0$ to $x=L$
x'	-	Dimensionless distance
z	L	Vertical distance from the impermeable bed at $z=0$ to $z=D$
α	LT^2M^{-1}	Aquifer matrix compressibility
β	LT^2M^{-1}	Fluid compressibility
λ	-	Pore-size distribution index; Brooks and Corey coefficient
ϕ	-	Porosity, equal to the moisture content at saturation
θ_r	-	Residual moisture content at which the capillary conductivity may be considered infinitesimal; Brooks and Corey coefficient

APPENDIX A

Technique Evaluation

Comparison with other Techniques

Head profiles calculated using the technique (first cut only) for a sample problem were compared with profiles calculated using several other solution methods. The problem considered was an unconfined aquifer with S_y equal to 0.28, K_{sat} equal to 8.47×10^{-1} m/d, and aquifer saturated thickness and length equal to 1.20 and 450 m, respectively. The objective was to predict the water-table (head) profiles after 90 and 630 days of drainage into a surface coal mine (or surface reservoir of water depth equal to zero).

Figures A1 and A2 show head profiles for different solution methods at 90 days (fig. A1) and 630 days (fig. A2). The solution methods, unless otherwise stated, assume saturated-flow conditions.

Boussinesq (1877, 1904) developed a differential equation incorporating the Dupuit assumptions governing horizontal, ground-water flow to a surface reservoir. He linearized the equation by assuming a negligible water-table slope at an average height above an impermeable layer. Boussinesq's Fourier-series solution is

$$h-h_C = (D-h_C) \frac{4}{\pi} \sum_{n=1}^{\infty} \frac{1}{n} \sin \frac{n\pi x}{2L} \exp \frac{-n^2 \pi^2 K_{sat} H_{ave} t}{4 L^2 S_y}, \quad (A1)$$

$$n = 1, 3, 5, \text{ etc.}$$

in which h is the height of the water table above the impermeable layer (L); h_C is the level in the surface reservoir above the impermeable layer (L) (equal to zero for the problem under consideration); D is the initial height of the water table above the impermeable layer (L); and H_{ave} is the average height of the water table above the the impermeable layer (L).

Eleven terms were used in the summation for the profiles labeled "Boussinesq 1" (figs. A1 and A2). For the "Glover" solution, the Boussinesq equation is solved for only the first term in the series (Dumm, 1954).

Glover also solved the problem by linearizing the governing second-order, nonlinear, partial differential equation (Glover, 1964). The solution is

$$h^* = h_C + (D - h_C) \operatorname{erf} \frac{x}{(4a^*t)^{0.5}} \quad (A2)$$

in which a^* equals $(K_{sat} D)/(S_y)$ and h^* is the linearized height of the water table above the impermeable layer (L). These water-table profiles are labeled "Glover linearized."

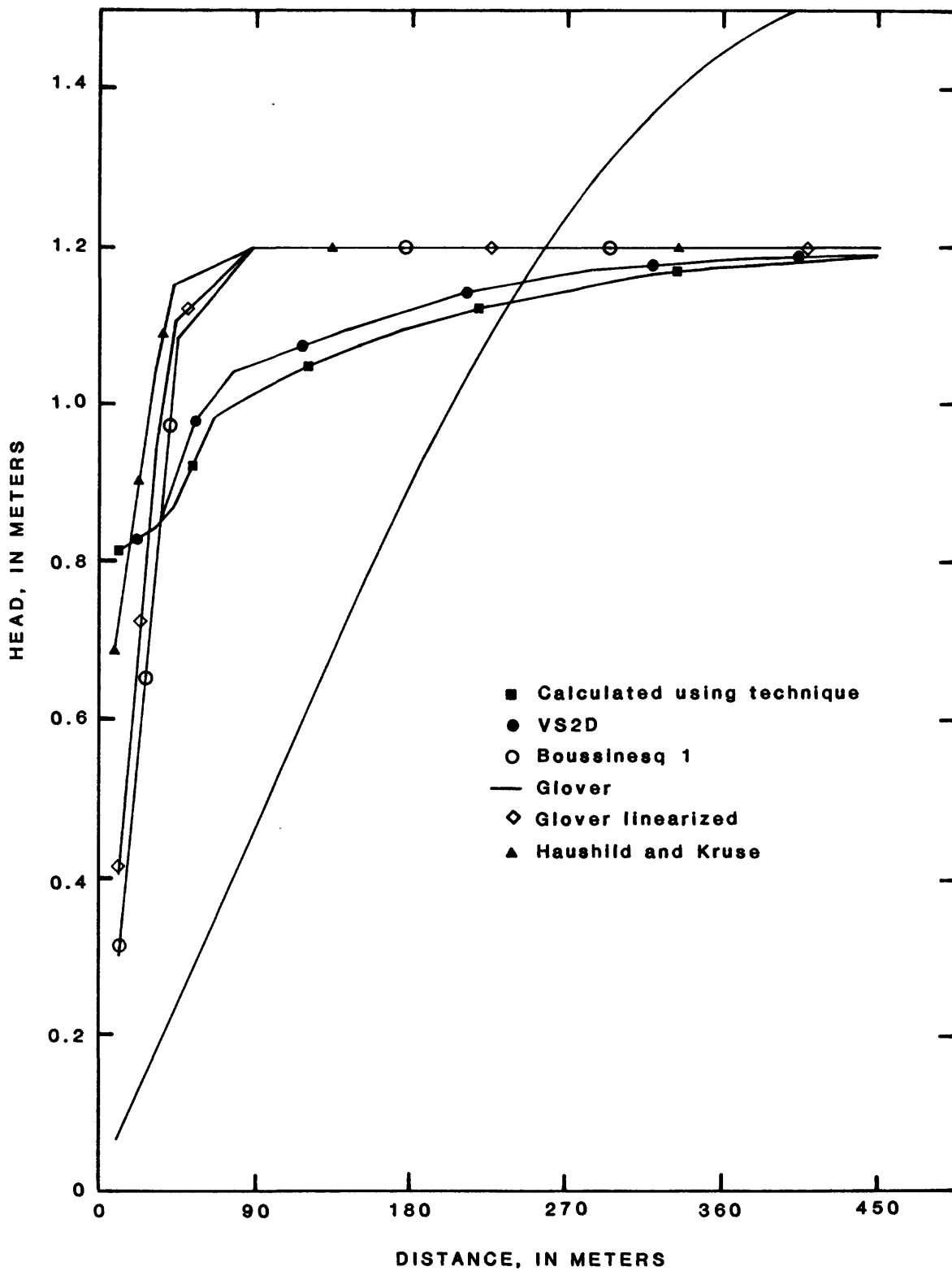


Figure A1.--Head profiles for sample problem at time 90 days.

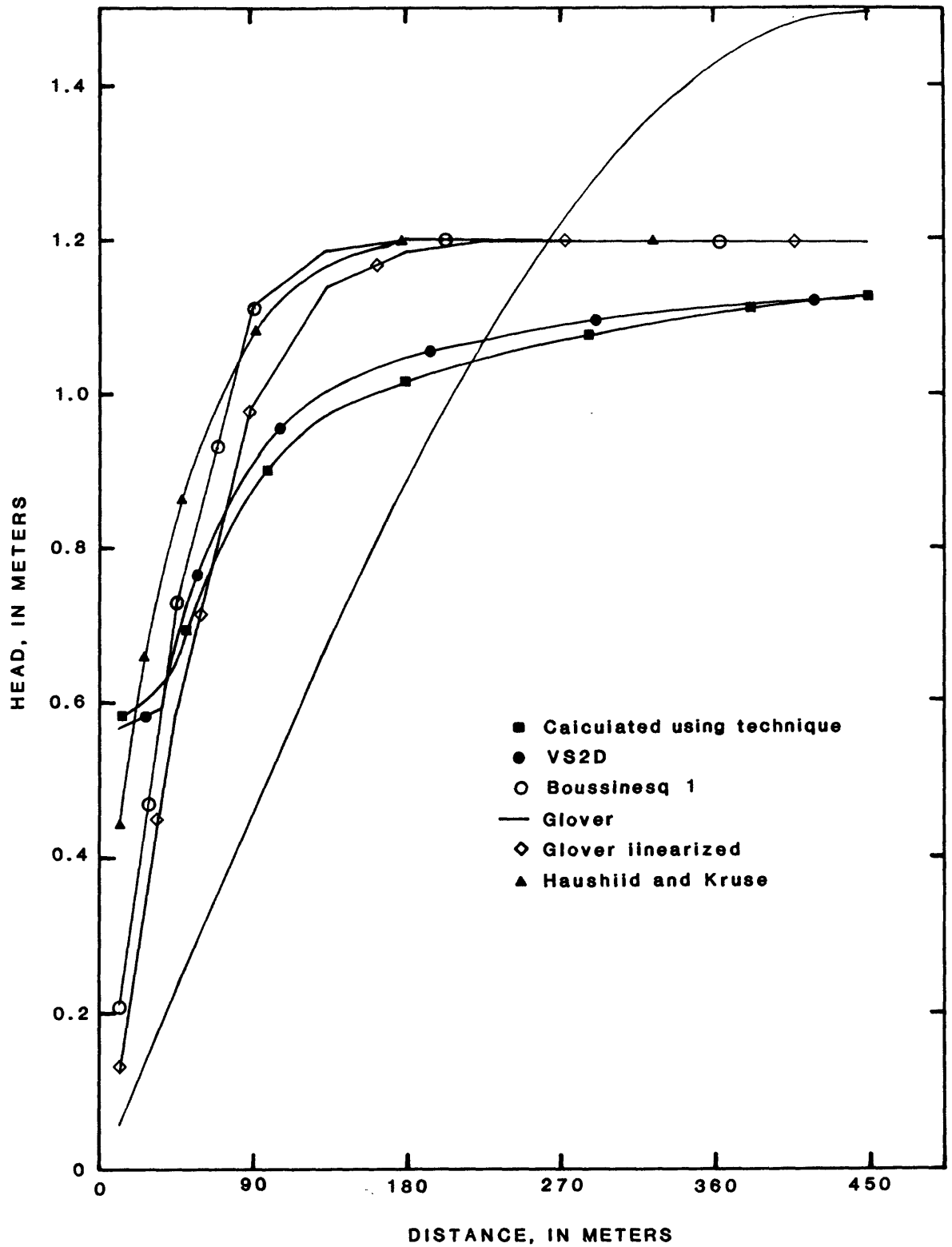


Figure A2.--Head profiles for sample problem at time 630 days.

The "Haushild and Kruse" (1962) solution of the nonlinear partial differential equation is

$$h = \{2[h_c + 1/2 (D-h_c)] h_3 + h_c^2 - h_c\}^{0.5} \quad (A3)$$

in which

$$h_3 = (D-h_c) \operatorname{erf} \frac{x}{(4a^*t)^{0.5}} \quad (A4)$$

Aquifer hydraulic conductivity and specific yield were identical to those of geologic material C (table 1). Brooks and Corey (1964) coefficients for geologic material C were used for the VS2D-model (Lappala and others, 1985) solution. Heads (figs. A1 and A2) labeled "VS2D" were determined using the VS2D model. Heads labeled "technique" were calculated using the hypothetical aquifer of graph B34 (Appendix B).

Heads calculated using the technique compare reasonably with those obtained using other methods. The variably-saturated flow heads (VS2D model and technique) tend to be greater near the seepage face and smaller farther from the seepage face than the saturated-flow heads. The VS2D-model and technique solutions are similar to each other but differ from the saturated-flow solutions more with increasing distance from the seepage face and increasing time. Close to the seepage face, the VS2D-model and technique solutions converge on the saturated-flow solutions with increasing time. This is in agreement with Brutsaert and El-Kadi (1984).

Although not shown in figures A1 and A2, variably-saturated and saturated-head profiles deviated more for more permeable geologic materials and shorter aquifer lengths. Brutsaert and El-Kadi (1984) observed that neglect of flow in the unsaturated zone can lead to large discrepancies in the prediction of seepage fluxes and heads, especially in shallow aquifers with a large unsaturated-zone relative thickness.

The shapes of the water-table profiles near the seepage face for the VS2D solutions may be concave upward. This shape has been noted elsewhere (Freeze and Cherry, 1979, p. 186-188; Cooley, 1983, p. 1276).

Comparison of technique results with results from other available solutions shows that the technique provides a satisfactory method for predicting water-level changes resulting from ground-water drainage. Because the technique considers variably-saturated flow, results should be more accurate than results obtained when only the saturated zone is considered.

Field Test

Data from a surface coal mine located near Industry, Illinois, in McDonough County (fig. A3) were used to compare computed and measured heads. The mine is operated by the Freeman United Coal Mining Company. Information from the site was obtained by the U.S. Geological Survey with the cooperation of Freeman United Coal Mining Company.

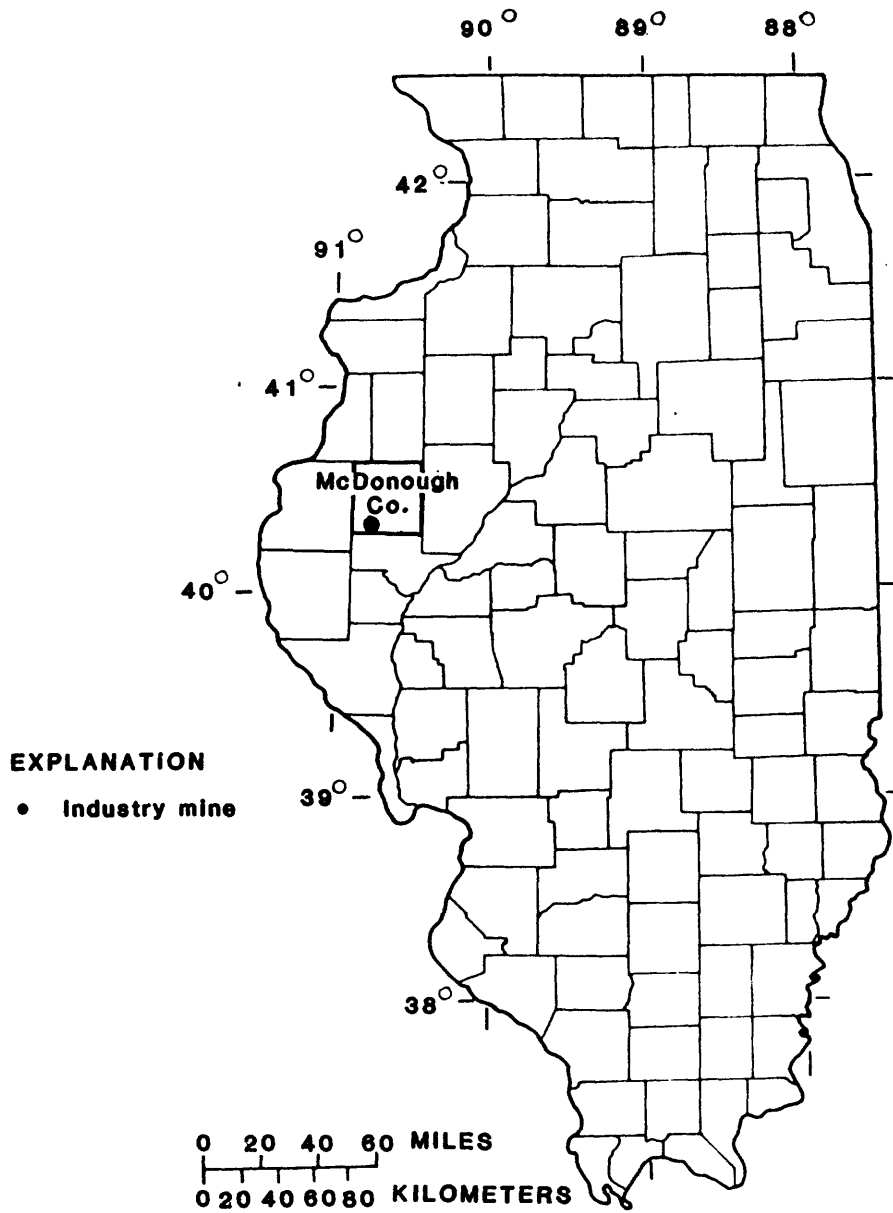


Figure A3.--Location of Industry Mine in McDonough County, Illinois.

The geologic strata in the vicinity of the mine are nearly horizontal. Figure A4 shows a stratigraphic sequence of the geologic units found in the area of the mine. Unconsolidated glacial deposits overlie much of the area. The predominant till is the Kellerville Till Member of the Illinoian Glasford Formation. This till consists of discontinuous intercalated zones of sand and gravel outwash and silt. The till is overlain by the Francis Creek Shale Member of the Pennsylvanian Carbondale Formation. The shale is medium-gray, silty, and finely banded, and contains thin, discontinuous, gray silty sandstone units. The Francis Creek Shale Member also contains thin, discontinuous, highly laminated and argillaceous shale beds. It is the uppermost bedrock unit in the area. The Francis Creek Shale Member overlies the Colchester (No. 2) Coal Member of the Carbondale. The underclay associated with the No. 2 coal is light gray to white and contains coal flecks and pyritic inclusions. A gray shaly siltstone is below the underclay. This siltstone belongs to the Browning Sandstone Member of the Pennsylvanian Spoon Formation.

Heads measured in wells tapping the coal were taken to be representative of heads in the water table. Ground-water level measurements in wells completed in the coal, the overlying Francis Creek Shale Member and the underlying Browning Sandstone Member, and results from a numerical ground-water flow model indicate that the coal and the shale were connected hydraulically. Results also indicate that the underclay was an effective impermeable barrier.

An observation well, designated 8002, was drilled approximately 152 m from the mine by Freeman United Coal Mining Company in May 1980 to provide detailed water-level data. The Colchester (No. 2) Coal Member was approximately 16.4 m below land surface. The well was completed in the coal and was open to the coal through an isolated 1.20-m screened interval. Ground-water levels at the well were measured once or twice monthly until December 1982, when the well was destroyed by mining.

The first cut at the Industry Mine was excavated in January 1982. For the year prior to excavation, the average water level in well 8002, referenced to the base of the aquifer, was approximately 7.76 m, although seasonal variations occurred in the water levels. Figure A5 shows a schematic diagram of a geologic section of the aquifer. The aquifer is assumed laterally extensive. A ground-water flow divide occurs approximately 1,600 m upgradient from the location of the first cut. Approximate field initial water-table and land-surface altitudes at the mine and at the water-table divide are given in figure A5(a). An assumption of the technique is that the initial water table is horizontal in the aquifer. The idealized initial water-table altitudes (fig. A5(b)) used in the analysis are extensions in the horizontal (x) direction from altitude measurements at the well. The deviation in assumed geometry should be noted.

Saturated hydraulic conductivity ranged from 0.396 to 1.10 m/d. Hydraulic conductivity was determined by applying the Bouwer and Rice method (1976). Average K_{sat} (7.48×10^{-1} m/d) was close to K_{sat} of geologic material C (8.47×10^{-1} m/d). Specific yield was not measured so a value of 0.28 (S_y associated with geologic material C) was assumed (table 1). Initial head at the well was 7.76 m. The aquifer was unconfined so D was 7.76 m. The hypothetical aquifer thickness of 5 m was close to 7.76 m. A hypothetical aquifer

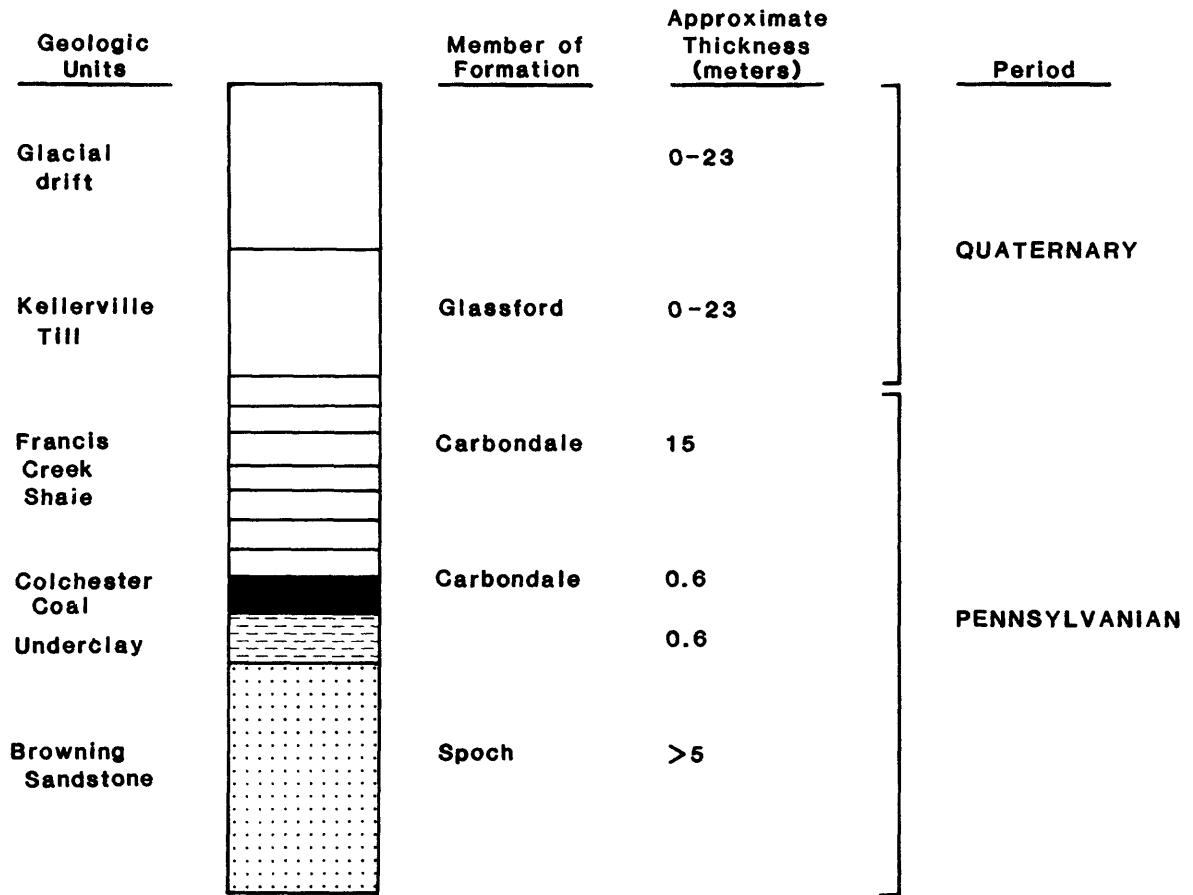
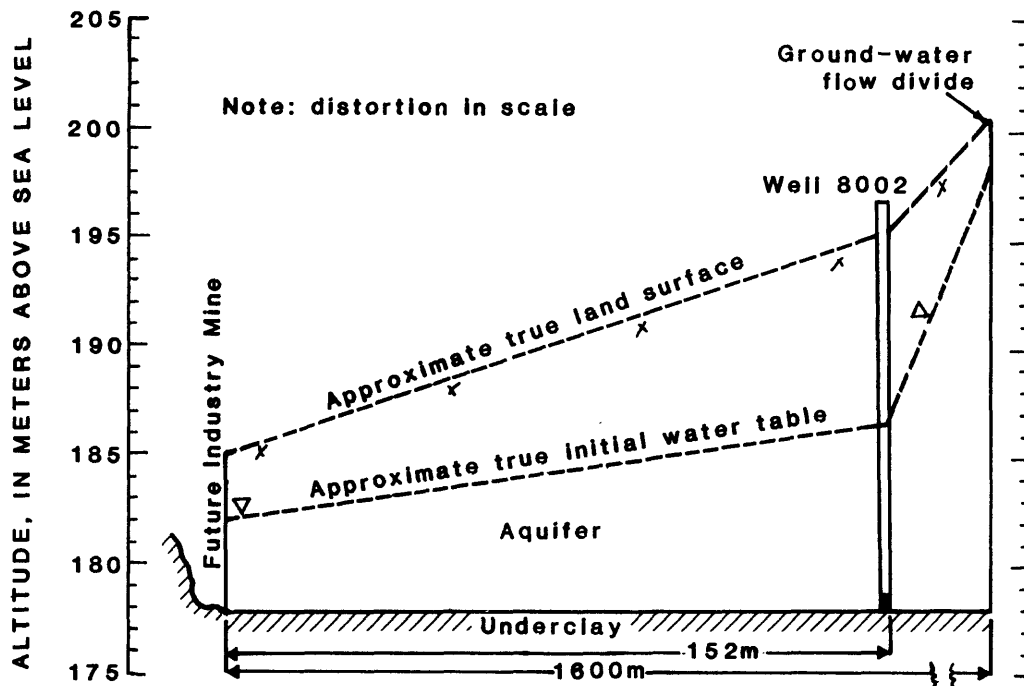
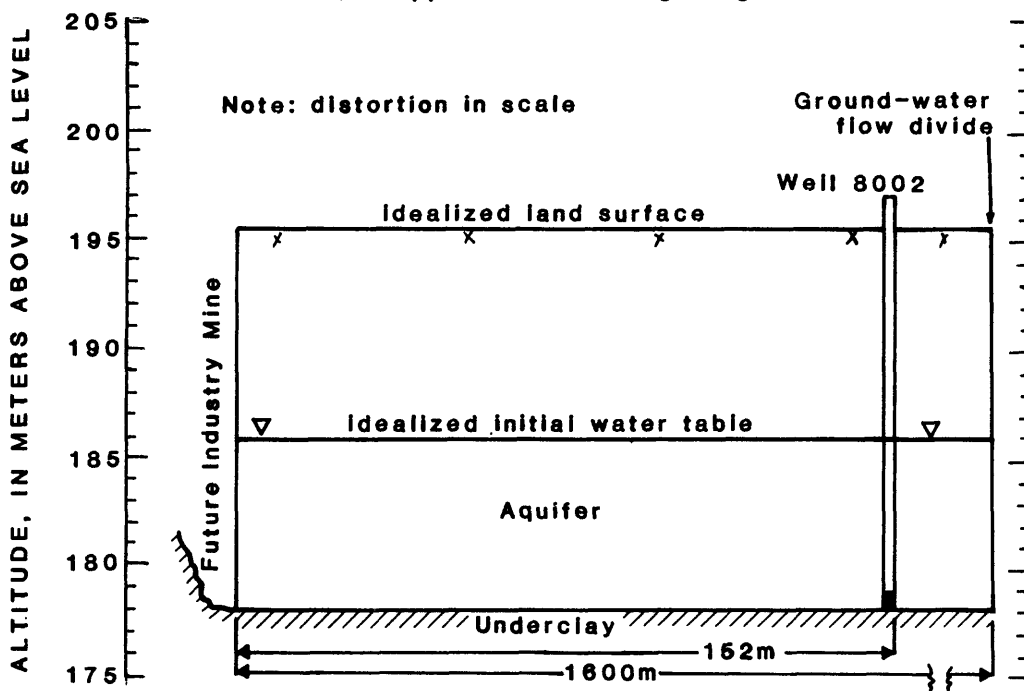


Figure A4.--Stratigraphic column showing geologic units found in the area of Industry Mine.



(a) Approximate true geologic section



(b) Idealized geologic section (used in solution of Industry Mine example)

Figure A5.--Geologic section of aquifer at Industry Mine, McDonough County.

length of 1,500 m was chosen. This is close to the approximately 1,500 m distance between the first cut and a water-table divide. This distance was measured along a flow streamline determined from the 1981 water-year average annual water-table map. Therefore, the hypothetical aquifer of graph 44 (Appendixes B and C) was selected to represent hydrogeologic conditions at the Industry Mine site (first cut only). If multiple cuts are considered, the aquifer is represented by graphs 136 through 138 (Appendixes D and E). Area surface mining at the Industry Mine moved the mine 152 m in 1 year. The multiple cut (75 m/180 d) is similar to this rate of mine advancement. Graph 137 was the hypothetical-aquifer/multiple-cut combination used. The objective was to estimate the head in well 8002, located 152 m from the first cut of the surface mine. Dimensionless times were calculated at 90, 166, 196, 275, 308, and 334 days after initial excavation, when water-level measurements at the well were made.

Figure A6 shows heads measured at the well, calculated using the technique, both first and multiple cuts, and calculated using some saturated-flow solutions. Measured water levels are plotted beginning 1 year prior to the first cut and ending 334 days after the first cut, when the well was destroyed. A constant water level of 7.76 m is plotted for the year preceding the first cut, and calculated heads are plotted for the 334 days after the first cut.

Calculated heads are smaller than measured heads for approximately 200 days after initial excavation. Field measurements were taken in spring and early summer when the water table is highest in response to snowmelt and spring rainfall. Because seasonal variations are not considered, it is reasonable to calculate heads that are smaller than measured heads.

Heads calculated using the technique (first cut only) and calculated using saturated-flow solutions are larger than measured heads beginning approximately 200 days after initial excavation of the mine. Heads calculated using the technique (multiple cuts) match measured heads well for the period beginning approximately 200 days after excavation of the first cut. Cuts made during the first year moved the boundary of the mine southward towards the well. Heads match measured heads better when the mine operation is considered than when only the first cut is considered.

Figure A7 shows calculated seepage fluxes into Industry Mine. Seepage fluxes calculated without incorporating effects of the mine operation may be underpredicted. Measured seepage-flux data from Industry Mine were not available for comparison.

Sensitivity Analysis

Sensitivity analyses are performed to determine the variability of calculated results due to the variability of input parameters. Sensitivity of dimensionless head and seepage flux, h' and q' , calculated using VS2D for the hypothetical aquifers (drainage to a first cut) was evaluated by varying input aquifer characteristics. Many possible variations in aquifer geometric and hydrogeologic characteristics exist. However, two sets of characteristics

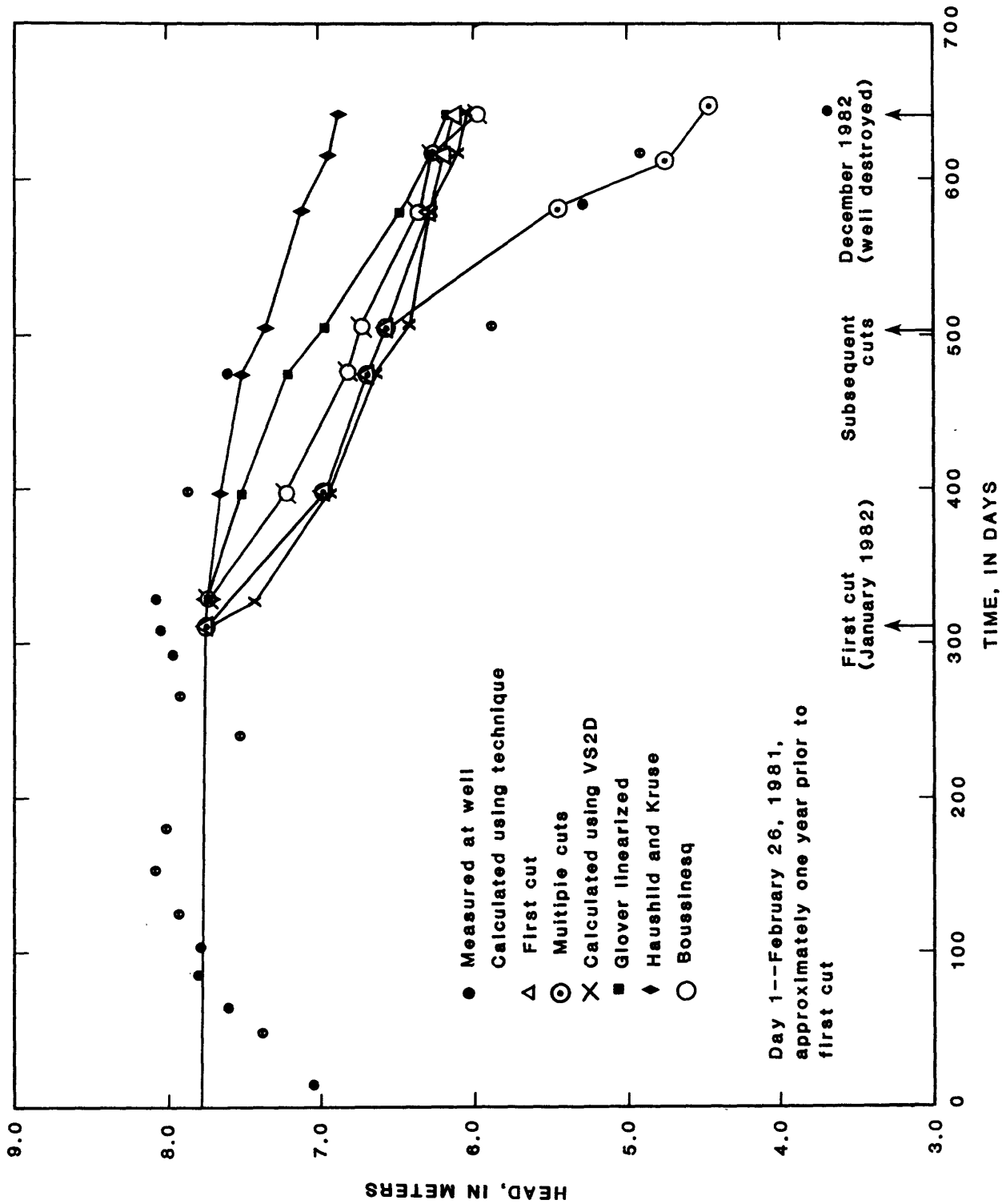


Figure A6.--Measured and calculated heads for well 8002.

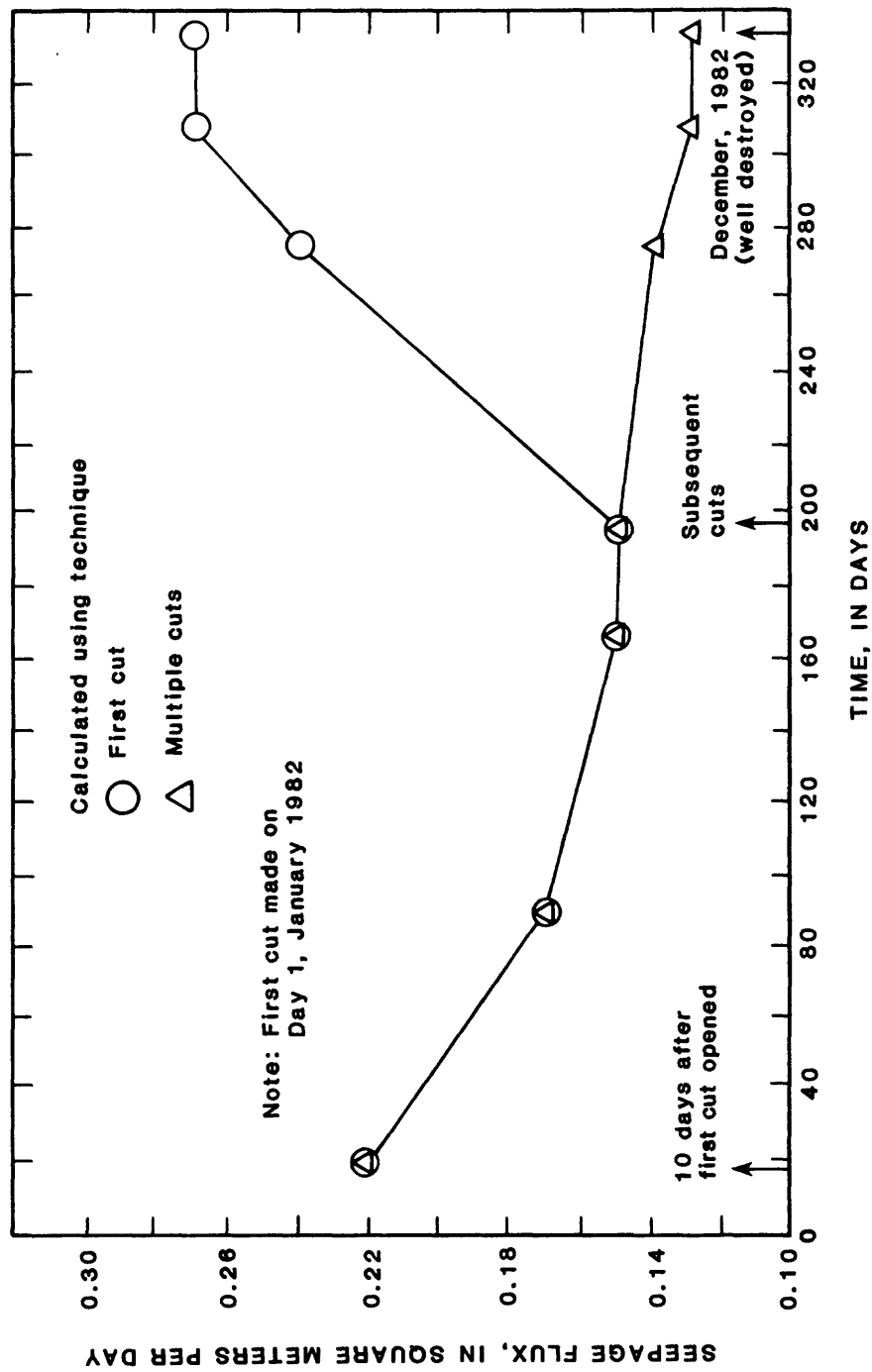


Figure A7.--Calculated seepage fluxes into Industry Mine.

were considered to have the most significant impact on the h' and q' profiles generated by VS2D and on the subsequent use of the profiles as part of the technique. Simulations were run in which (1) aquifer thickness and (2) saturated hydraulic conductivity and coefficients in the Brooks and Corey moisture-characteristic relations were varied. Sensitivity of h' and q' to matrix compressibility and recharge were also examined.

To evaluate the applicability of the hypothetical aquifer thicknesses of 1 and 5 m to field-determined saturated aquifer thicknesses outside of this range, simulations were run in which an unconfined aquifer 150-m long drained to a surface mine for 90 days. Geologic materials B, C, and E were examined for thicknesses of 0.5, 1.0, 5.0, 15.0, and 50.0 m. Figures A8 and A9 show h' as a function of distance from the seepage face, in meters, for geologic material C at 10 and 90 days, respectively. Figure A10 shows q' as a function of time (in days) for geologic material C.

Sensitivity of h' and q' to variations in aquifer moisture-characteristic input data (for VS2D) was evaluated using an unconfined aquifer 150-m long and 5-m thick. Simulations were made in which the aquifer drained to a surface mine for 90 days. Aquifer characteristics (table 1) for geologic materials B, C, and E were used for the control simulations. Brooks and Corey coefficients, porosity, and saturated hydraulic conductivity for the control geologic materials are given in table A1. Fluid and aquifer matrix compressibility, β and α , respectively, and leakage and recharge were zero for the control simulations. Each control-parameter value was increased and decreased, while all other parameters remained the same. Figures A11 and A12 show h' as a function of dimensionless distance, x' , for increases in geologic-material moisture characteristics for geologic material C at 10 and 90 days. Figures A13 and A14 show h' as a function of x' for decreases in geologic-material moisture characteristics for geologic material C at 10 and 90 days. Figures A15 and A16 show q' as a function of dimensionless time, t' , for increases and decreases, respectively, in geologic-material moisture characteristics for geologic material C.

The change in dimensionless head, as a percentage of the control head, is

$$\frac{h'_N - h'_C}{h'_C} * 100 = \Delta h' \quad (A5)$$

and the change in dimensionless seepage flux, as a percentage of the control seepage flux, is

$$\frac{q'_N - q'_C}{q'_C} * 100 = \Delta q' \quad (A6)$$

in which C is a subscript representing head and seepage-flux values obtained using the control parameters, N is a subscript representing the new head and seepage-flux values after an increase or decrease in parameter values, $\Delta h'$ is the percentage change in dimensionless head of fluid, and $\Delta q'$ is the percentage change in dimensionless seepage flux. Table A1 contains percentage change of geologic-material moisture characteristic parameters from control values

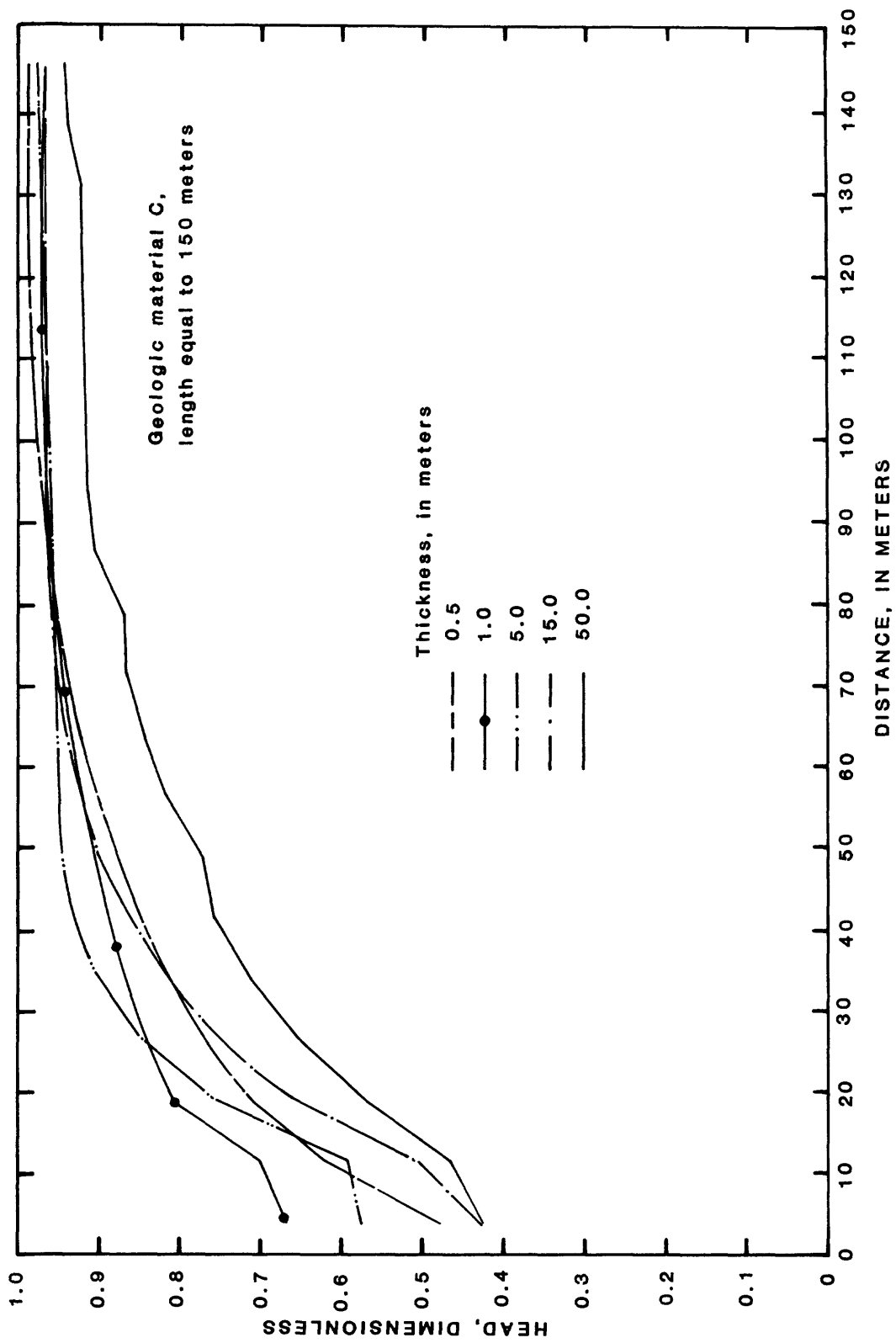


Figure A8.--Dimensionless heads at time 10 days for thickness sensitivity.

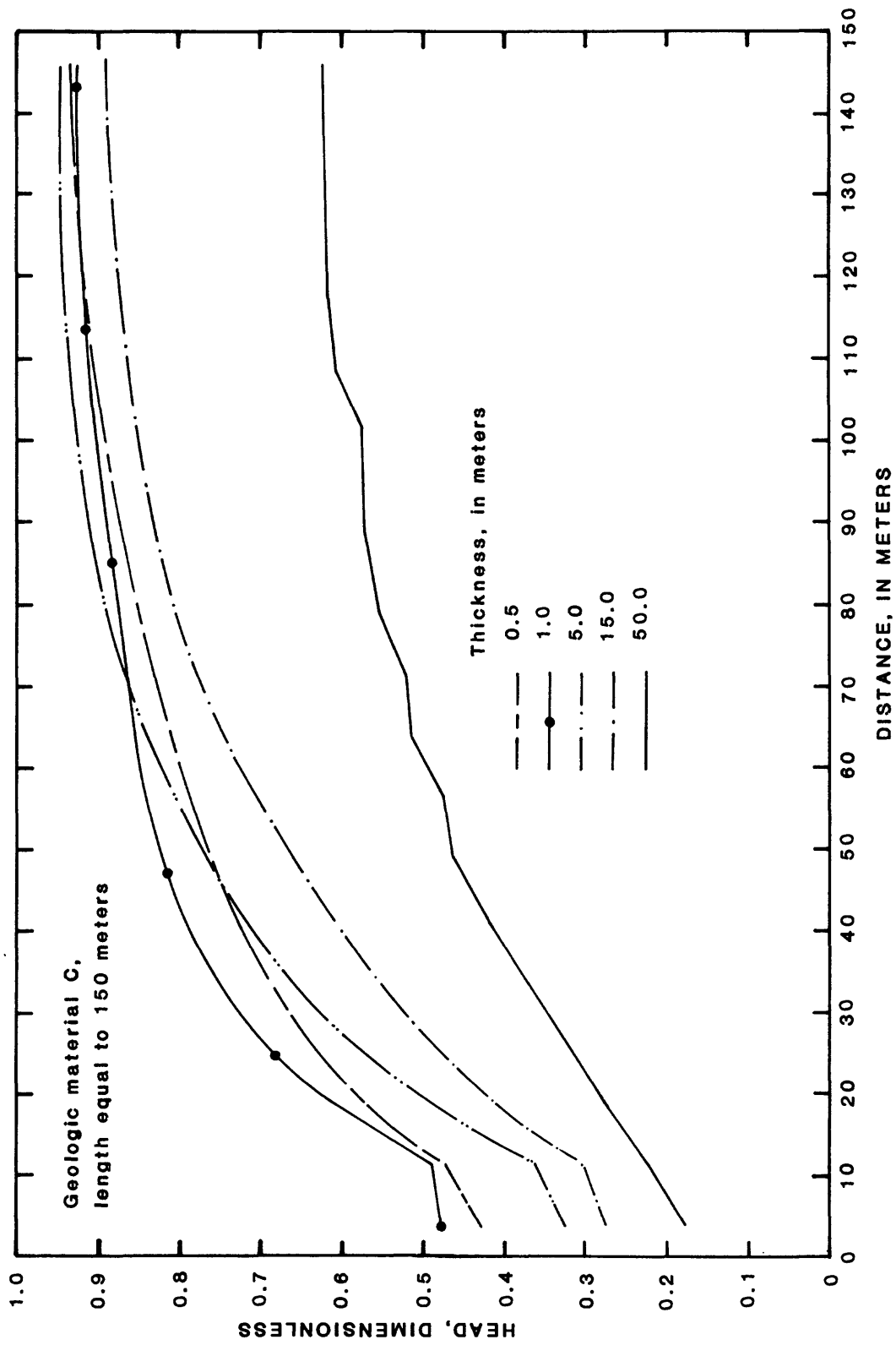


Figure A9.--Dimensionless heads at time 90 days for thickness sensitivity.

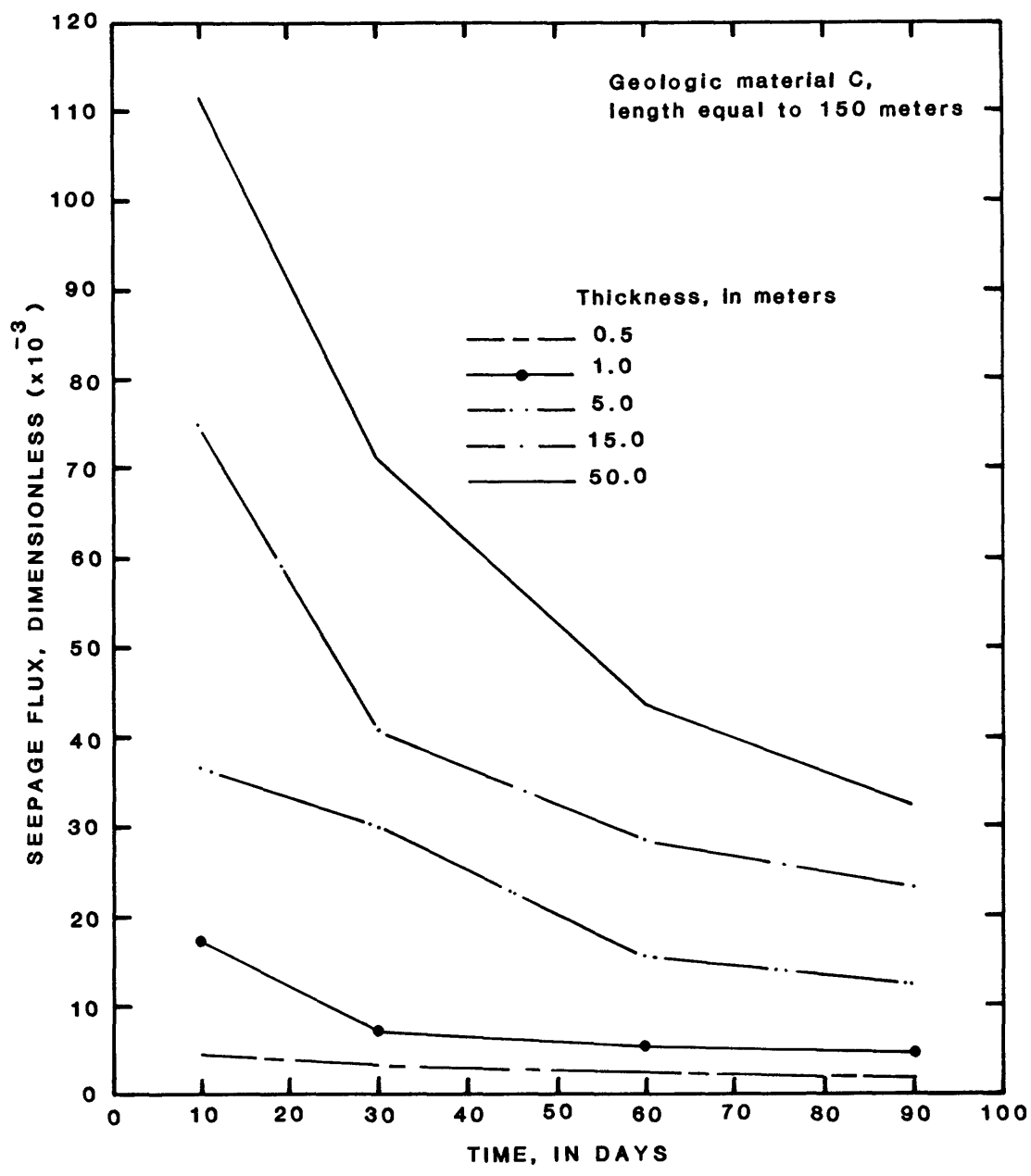


Figure A10.--Dimensionless seepage fluxes for thickness sensitivity.

Table A1.--Control-parameter values and percentage change from control values for the various geologic materials in sensitivity analysis

[m/d, meter per day; m, meter]

Aquifer characteristics	Geologic material		
	B	C	E
	(Percentage change from control value)		
Saturated hydraulic conductivity, K_{sat} (m/d)	2.54 (+900,-90)	8.47×10^{-1} (+900,-90)	2.54×10^{-2} (+900,-90)
Porosity, ϕ	0.40 (+25,-25)	0.35 (+29,-29)	0.20 (+50,-50)
Bubbling pressure, h_b (m)	-0.15 (+67,-67)	-0.13 (+77,-77)	-0.15 (+67,-67)
Residual moisture content, θ_r	0.13 (+77,-77)	0.07 (+71,-71)	0.05 (+80,-80)
Pore-size distribution index, λ	2.0 (+50,-50)	2.5 (+40,-40)	2.0 (+50,-50)

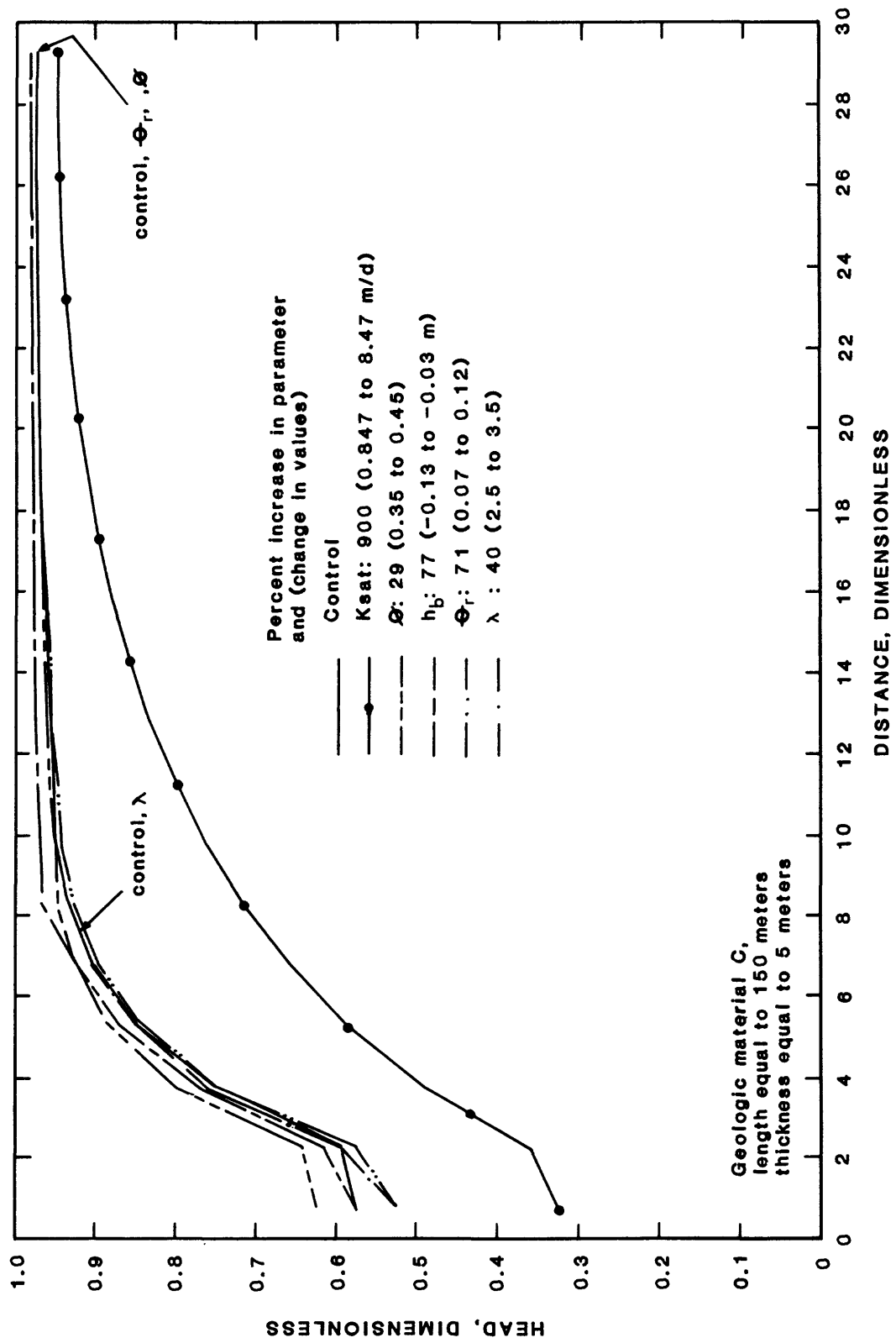


Figure All.--Dimensionless-head profiles at time 10 days for increases in geologic-material moisture characteristics for sensitivity analysis.

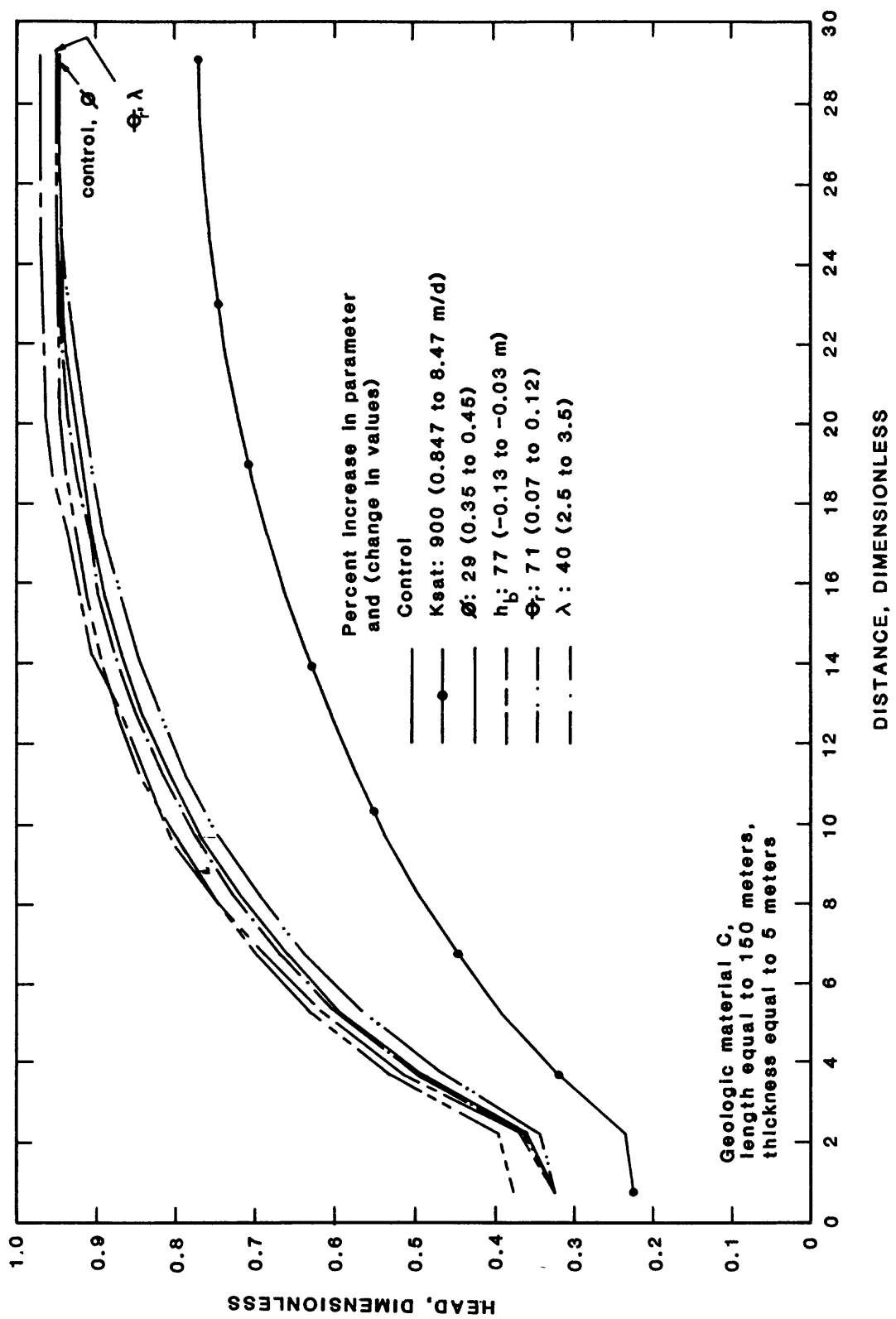


Figure A12.--Dimensionless-head profiles at time 90 days for increases in geologic-material moisture characteristics for sensitivity analysis.

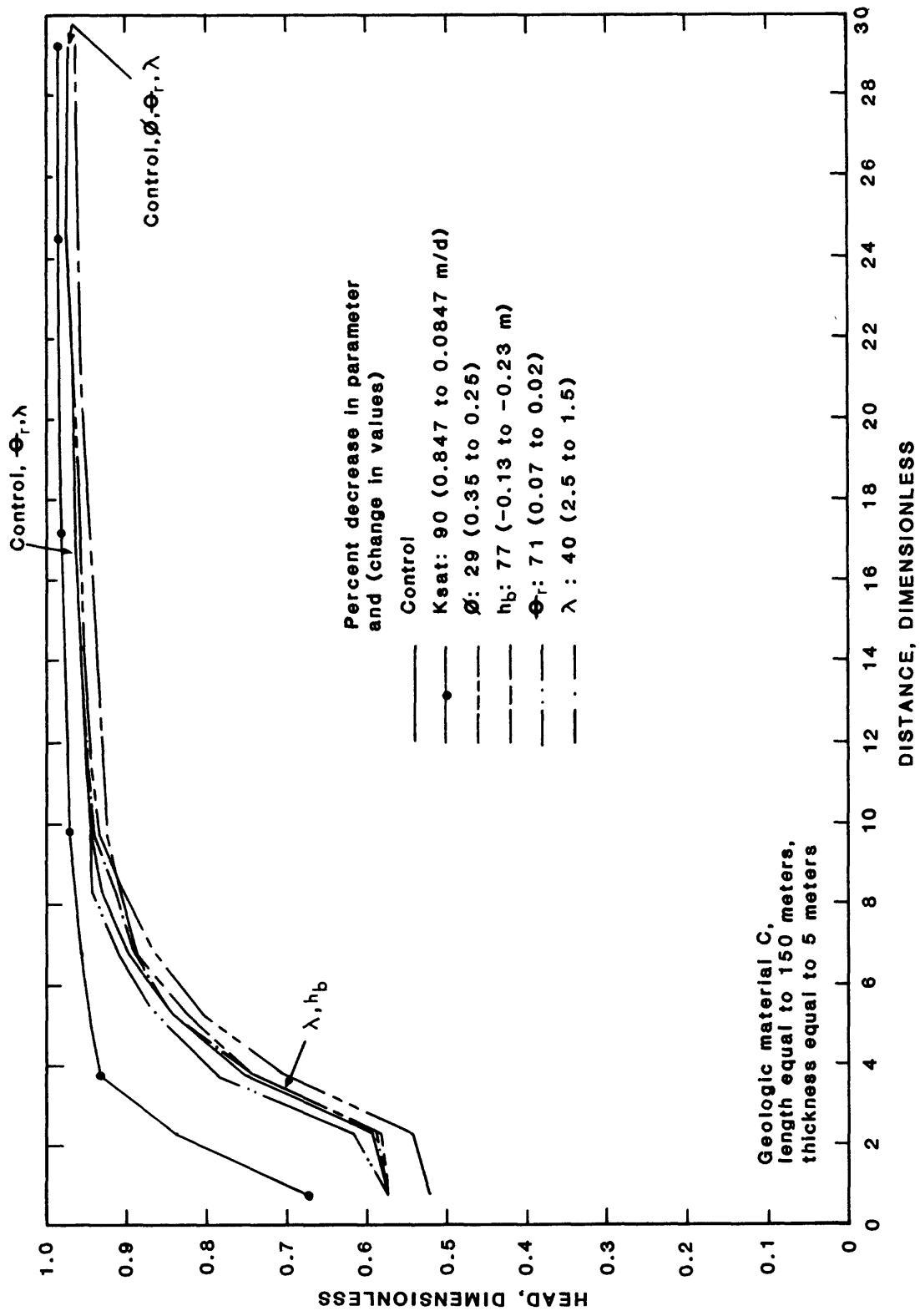


Figure A13.--Dimensionless-head profiles at time 10 days for decreases in geologic-material moisture characteristics for sensitivity analysis.

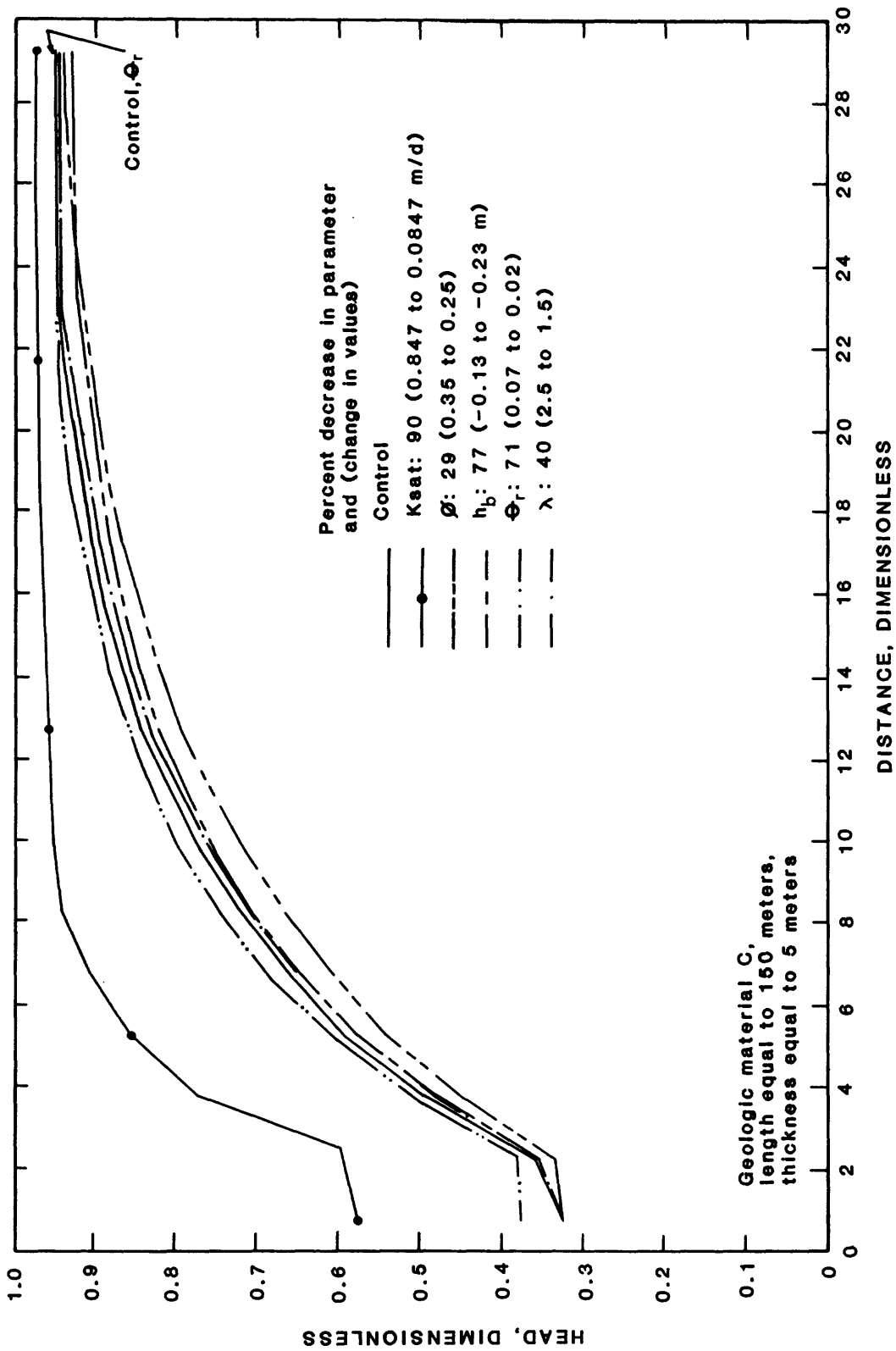


Figure A14.--Dimensionless-head profiles at time 90 days for decreases in geologic-material moisture characteristics for sensitivity analysis.

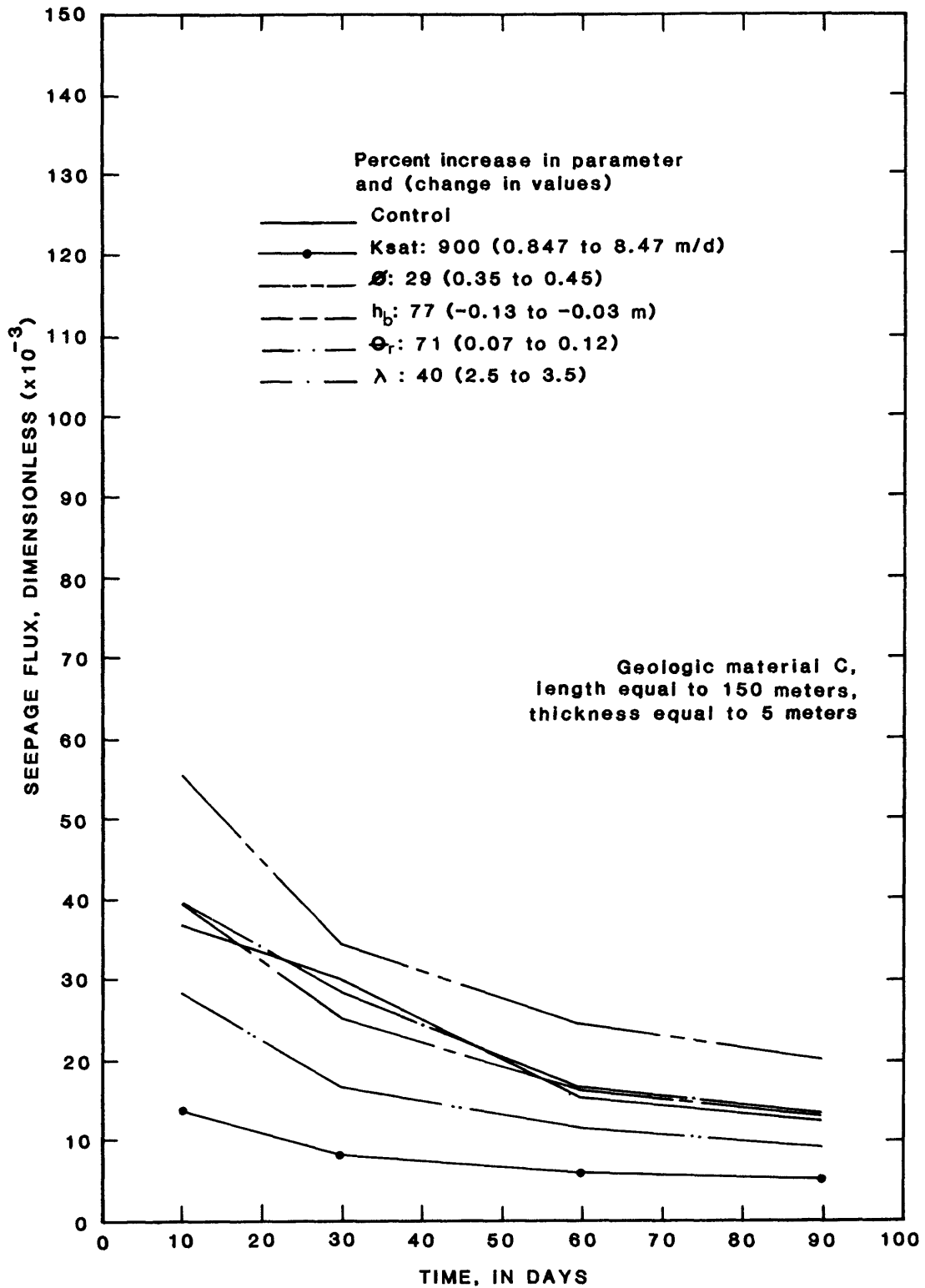


Figure A15.--Dimensionless seepage-flux profiles for increases in geologic-material moisture characteristics for sensitivity analysis.

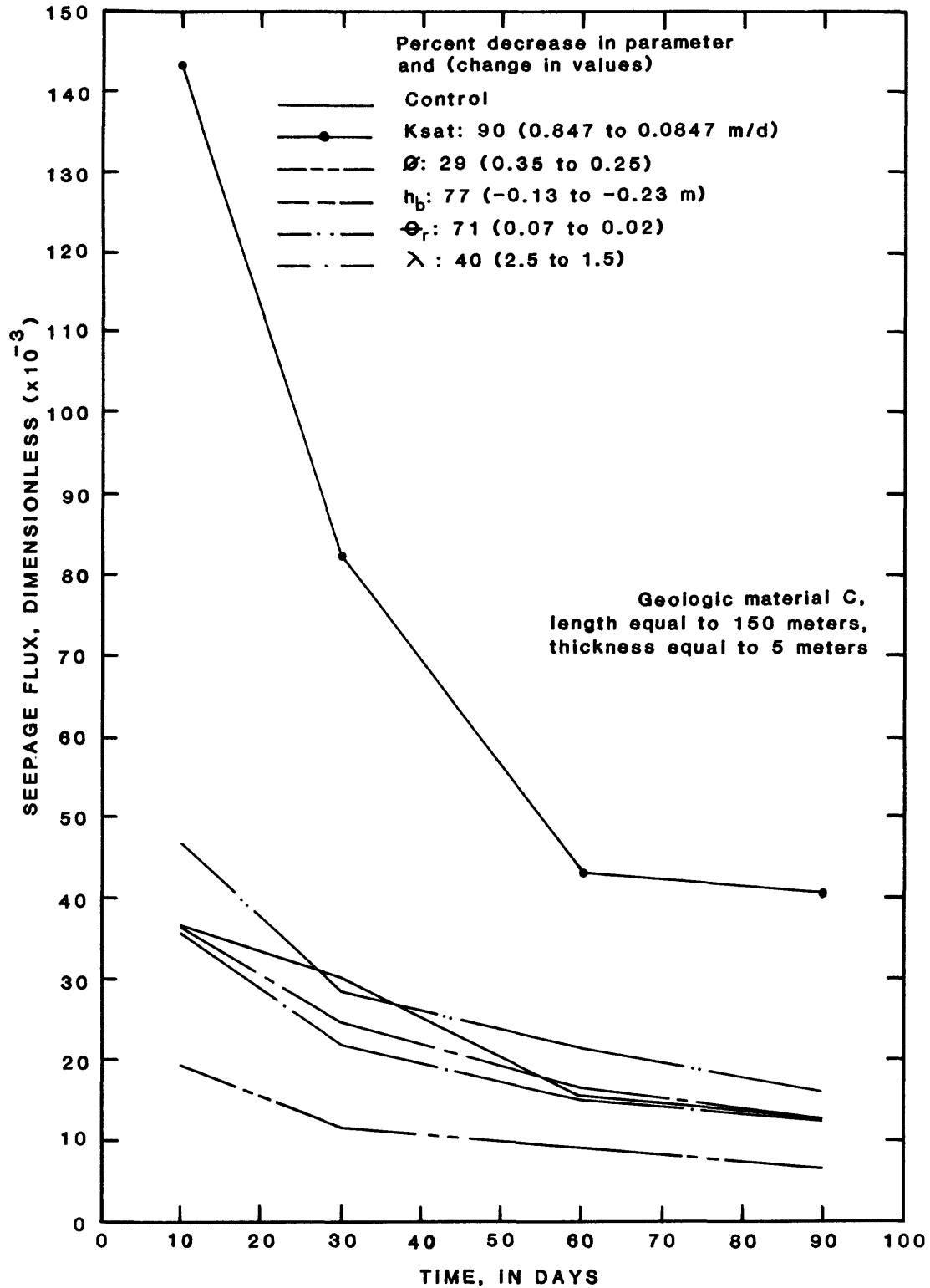


Figure A16.--Dimensionless seepage-flux profiles for decreases in geologic-material moisture characteristics for sensitivity analysis.

used in the sensitivity analysis. The ranges in percentage change from each control parameter were chosen to represent variations due to measurement inaccuracies and seasonal variations.

Two control values were used for the thickness sensitivity. Saturated thickness, D , of 1.0 m was used for the control in conjunction with the decreased D of 0.5 m (equal to -50 percent change from the control value of 1.0 m). Five m were used for the control D in conjunction with the increased D of 15.0 and 50.0 m (equal to +200 and +900 percent change from the control value of 5.0 m).

Recharge sensitivity was analyzed using the control hypothetical aquifers of table A1. Recharge was increased from the control value of 0.0 m/d to 1.74×10^{-4} m/d, 3.48×10^{-4} m/d, and 6.96×10^{-4} m/d. Recharge was simulated with a row of variable-flux nodes at the top of the aquifer.

Matrix compressibility was analyzed using the control hypothetical aquifers of table A1, except with an initial head condition of $3 \times D$, or 15 m. Fluid compressibility was 5.89×10^{-23} (m-d²)/g, and aquifer matrix compressibility was 1.34×10^{-21} (m-d²)/g for geologic material B, 1.34×10^{-22} (m-d²)/g for geologic material C, and 1.34×10^{-22} (m-d²)/g for geologic material E (table 1). Each matrix compressibility value was increased and decreased an order of magnitude.

Sensitivity was quantified by defining the maximum and minimum differences in h' and q' obtained for each varied parameter from h' and q' obtained for the control simulations. Maximum and minimum head differences were noted at 10 and 90 days, and at distances from the seepage face ranging from 4 to 146 m. Maximum and minimum seepage-flux differences were defined at 10, 30, 60, or 90 days. Equation A5 was used to determine relative percentage change in h' for maximum and minimum h' differences. Table A2 contains these results for geologic materials B, C, and E. Equation A6 was used to determine relative percentage change in q' for maximum and minimum q' differences. Table A3 contains these results for geologic materials B, C, and E.

The following are results of the sensitivity analyses:

1. Decreasing aquifer saturated thickness, D , from 1 to 0.5 m (-50 percent) yields a range in magnitude of relative change in h' (table A2) from (1) 29 to 0.02 percent for geologic material C; (2) 41 to 0.07 percent for geologic material E; and (3) 15 to 0.40 percent for geologic material B. Changes indicate a general trend of decreasing sensitivity with time and distance from the seepage face for geologic materials C and E. Results for geologic material B indicate decreasing sensitivity with time near the seepage face and increasing sensitivity with time far from the seepage face.

Decreasing D from 1 to 0.5 m yields a range in magnitude of relative change in q' (table A3) from (1) 73 to 54 percent for geologic material C; (2) 437 to 38 percent for geologic material E; and (3) 71 to 51 percent for geologic material B. Seepage fluxes for all three geologic materials are sensitive to a 50 percent decrease in D and exhibit the same trend of decreasing sensitivity with time.

Table A2.--Relative sensitivity of dimensionless head to selected changes in aquifer characteristics

[t, time (days) since first cut was made; x, distance (meters) from seepage face; m/d, meter per day; m, meter; (m-d²)/g, meter-day squared per gram]

Aquifer characteristic	Percentage change from control value	Percentage change in dimensionless head [$\Delta(h')$ @ x]			
		t = 10 days		t = 90 days	
		maximum h' _N -h' _C	minimum h' _N -h' _C	maximum h' _N -h' _C	minimum h' _N -h' _C
GEOLOGIC MATERIAL B					
Initial saturated thickness, D = 1.0 m	- 50	-13 @ 34	-1.2 @ 146	-15 @ 146	+0.4 @ 4
Initial saturated thickness, D = 5.0 m	+200	-16 @ 34	-.18 @ 109	-8.7 @ 49	-9.1 @ 11
	+900	-32 @ 41	-14 @ 116	-59 @ 146	-61 @ 11
Saturated hydraulic conductivity, K _{sat} (m/d)	+900	-32 @ 34	-8.6 @ 146	-61 @ 146	-65 @ 19
	- 90	+71 @ 4	+13 @ 41	+54 @ 34	+12 @ 146
Porosity, ϕ	+ 25	+12 @ 4	+0.32 @ 146	+8.2 @ 79	0 @ 4
	- 25	-8.1 @ 26	-.6 @ 146	-19 @ 4	-9.2 @ 11
Bubbling pressure, h _b (m)	+ 67	+4.5 @ 26	0 @ 4	+5.7 @ 79	0 @ 4
	- 67	-2.7 @ 71	0 @ 4	-18 @ 4	-4.7 @ 11
Residual moisture content, θ_r	+ 77	-9.9 @ 19	-0.52 @ 101	-12 @ 146	-15 @ 11
	- 77	+12 @ 4	+0.32 @ 146	+8.7 @ 71	0 @ 4
Pore-size distribution index, λ	+ 50	+0.87 @ 26	0 @ 4	+1.7 @ 86	0 @ 4
	- 50	-3.2 @ 26	0 @ 4	-18 @ 4	-5.6 @ 11
Recharge (actual change from control = 0.0 m/d)	+1.74x10 ⁻⁴ m/d	+11 @ 49	+3.2 @ 11	+58 @ 49	+36 @ 4
	+3.48x10 ⁻⁴ m/d	+11 @ 49	+3.2 @ 11	+58 @ 49	+36 @ 4
	+6.96x10 ⁻⁴ m/d	+16 @ 41	+2.0 @ 146	+70 @ 41	+14 @ 146
Matrix compressibility, α (percentage change from control = 1.34x10 ⁻²¹ (m-d ²)/g)	+900	+12 @ 4	+0.76 @ 79	-0.24 @ 116	0 @ 4
	- 90	-0.22 @ 146	0 @ 4	+4.8 @ 139	0 @ 4

Table A2.--Relative sensitivity of dimensionless head to selected changes in aquifer characteristics--Continued

Aquifer characteristic	Percentage change from control value	Percentage change in dimensionless head [$\Delta(h')$ @ x]			
		t = 10 days		t = 90 days	
		maximum $h'_N - h'_C$	minimum $h'_N - h'_C$	maximum $h'_N - h'_C$	minimum $h'_N - h'_C$
GEOLOGIC MATERIAL C					
Initial saturated thickness, D = 1.0 m	- 50	-29 @ 4	+9 @ 94	-9 @ 41	-0.02 @ 116
Initial saturated thickness, D = 5.0 m	+200	-26 @ 4	-0.01 @ 86	-14 @ 64	-15 @ 34
	+900	-23 @ 26	-2.9 @ 146	-38 @ 101	-39 @ 11
Saturated hydraulic conductivity, K_{sat} (m/d)	+900	-35 @ 19	-2.7 @ 146	-28 @ 64	-31 @ 4
	- 90	+41 @ 11	+1.3 @ 146	+56 @ 19	+2.7 @ 139
Porosity, ϕ	+ 29	+8.7 @ 4	+0.04 @ 131	+15 @ 4	+0.03 @ 146
	- 29	-8.4 @ 11	-0.11 @ 146	-7.8 @ 41	0 @ 4
Bubbling pressure, h_b (m)	+ 77	+3.2 @ 41	0 @ 4	+4.3 @ 71	0 @ 4
	- 77	-2.5 @ 41	0 @ 4	-2.8 @ 109	0 @ 4
Residual moisture content, θ_r	+ 71	-8.7 @ 4	-0.04 @ 146	-3.4 @ 34	0 @ 4
	- 71	-14 @ 19	-1.1 @ 146	+15 @ 4	+0.02 @ 146
Pore-size distribution index, λ	+ 40	-8.7 @ 4	+0.01 @ 139	+1.0 @ 34	0 @ 4
	- 40	-1.0 @ 19	0 @ 4	-2.8 @ 79	0 @ 4
Recharge (actual change from control = 0.0 m/d)	+1.74x10 ⁻⁴ m/d	+4.6 @ 41	0 @ 4	+36 @ 41	+3.8 @ 146
	+3.48x10 ⁻⁴ m/d	+8.6 @ 34	0 @ 4	+48 @ 34	+2.8 @ 146
	+6.96x10 ⁻⁴ m/d	+8.6 @ 34	0 @ 4	+48 @ 34	+2.8 @ 146
Matrix compressibility, α (percentage change from control = 1.34x10 ⁻²² (m-d ²)/g)	+900	+0.30 @ 19	0 @ 4	+0.31 @ 64	0 @ 4
	- 90	-0.099 @ 11	0 @ 4	-0.29 @ 11	0 @ 4

Table A2.--Relative sensitivity of dimensionless head to selected changes
in aquifer characteristics--Continued

Aquifer characteristic	Percentage change from control value	Percentage change in dimensionless head [$\Delta(h')$ @ x]			
		t = 10 days		t = 90 days	
		maximum $ h'_N - h'_C $	minimum $ h'_N - h'_C $	maximum $ h'_N - h'_C $	minimum $ h'_N - h'_C $
GEOLOGIC MATERIAL E					
Initial saturated thickness, D = 1.0 m	- 50	-41 @ 4	-0.1 @ 19	-37 @ 4	+0.07 @ 49
Initial saturated thickness, D = 5.0 m	+200	-18 @ 4	-0.43 @ 34	-24 @ 4	-0.21 @ 64
	+900	-6.1 @ 4	-0.94 @ 64	-19 @ 26	-0.89 @ 124
Saturated hydraulic conductivity, K_{sat} (m/d)	+900	-24 @ 11	-1.2 @ 139	-33 @ 19	+3.0 @ 146
	- 90	+12 @ 4	+0.53 @ 19	+31 @ 11	+0.92 @ 94
Porosity, ϕ	+ 50	+6.1 @ 4	+0.04 @ 41	+9.0 @ 11	+0.07 @ 94
	- 50	-9.4 @ 11	-0.07 @ 49	-19 @ 11	-0.23 @ 101
Bubbling pressure, h_b (m)	+ 67	+3.5 @ 11	0 @ 4	-8.0 @ 4	+0.13 @ 139
	- 67	-2.2 @ 19	0 @ 4	-2.3 @ 34	0 @ 4
Residual moisture content, θ_r	+ 80	-12 @ 4	+0.002 @ 124	-8.0 @ 4	-0.07 @ 124
	- 80	-12 @ 4	+0.008 @ 49	+10 @ 11	+0.21 @ 94
Pore-size distribution index, λ	+ 50	-12 @ 4	-0.004 @ 34	+7.9 @ 11	0 @ 4
	- 50	-1.6 @ 11	0 @ 4	-3.1 @ 11	0 @ 4
Recharge (actual change from control = 0.0 m/d)	+1.74x10 ⁻⁴ m/d	+3.8 @ 19	0 @ 4	+18 @ 19	+0.029 @ 94
	+3.48x10 ⁻⁴ m/d	+6.1 @ 4	+0.015 @ 49	+18 @ 19	+0.029 @ 94
	+6.96x10 ⁻⁴ m/d	+12 @ 11	+0.015 @ 49	+46 @ 11	+0.029 @ 94
Matrix compressibility, α (percentage change from control = 1.34x10 ⁻²² (m-d ²)/g)	+900	+48 @ 146	0 @ 4	+0.86 @ 11	0 @ 4
	- 90	-3.4 @ 146	0 @ 4	-0.11 @ 19	0 @ 4

Table A3.--Relative sensitivity of dimensionless seepage flux to selected changes in aquifer characteristics

[t, time (days) since first cut was made; m/d, meter per day;
m, meter; (m-d²)/g, meter-day squared per gram]

Aquifer characteristic	Percentage change from control value	Percentage change in dimensionless seepage flux [$\Delta(q') @ t$]	
		maximum $ q'_N - q'_C $	minimum $ q'_N - q'_C $
GEOLOGIC MATERIAL B			
Initial saturated thickness, D = 1.0 m	- 50	-71 @ 10	-51 @ 90
Initial saturated thickness, D = 5.0 m	+200 +900	+78 @ 10 +176 @ 10	+63 @ 30 +48 @ 90
Saturated hydraulic conductivity, K _{sat} (m/d)	+900 - 90	-67 @ 10 +131 @ 10	-86 @ 90 +167 @ 30
Porosity, ϕ	+ 25 - 25	+59 @ 10 -50 @ 10	+54 @ 60 -45 @ 90
Bubbling pressure, h _b (m)	+ 67 - 67	+3.5 @ 10 -11 @ 30	+1.8 @ 90 -4.9 @ 60
Residual moisture content, θ_r	+ 77 - 77	-43 @ 10 +59 @ 10	-54 @ 90 +67 @ 90
Pore-size distribution index, λ	+ 50 - 50	+1.6 @ 10 -6.9 @ 10	+0.8 @ 30 +0.98 @ 90
Recharge (actual change from control = 0.0 m/d)	+1.74x10 ⁻⁴ m/d +3.48x10 ⁻⁴ m/d +6.96x10 ⁻⁴ m/d	-53 @ 10 -53 @ 10 -55 @ 10	-95 @ 90 -94 @ 90 -92 @ 90
Matrix compressibility, α (percentage change from control = 1.34x10 ⁻²¹ (m-d ²)/g)	+900 - 90	-5.2 @ 10 +9.9 @ 60	+0.091 @ 90 +0.92 @ 10

Table A3.--Relative sensitivity of dimensionless seepage flux to selected changes in aquifer characteristics--Continued

Aquifer characteristic	Percentage change from control value	Percentage change in dimensionless seepage flux [$\Delta(q')$ @ t]	
		maximum	minimum
		$ q'_N - q'_C $	$ q'_N - q'_C $
GEOLOGIC MATERIAL C			
Initial saturated thickness, D = 1.0 m	- 50	-73 @ 10	-54 @ 60
Initial saturated thickness, D = 5.0 m	+200	+104 @ 10	+83 @ 90
	+900	+204 @ 10	+154 @ 90
Saturated hydraulic conductivity, K_{sat} (m/d)	+900	-64 @ 10	-59 @ 90
	- 90	+290 @ 10	+177 @ 60
Porosity, ϕ	+ 29	+50 @ 10	+14 @ 30
	- 29	-62 @ 30	-48 @ 90
Bubbling pressure, h_b (m)	+ 77	-16 @ 30	+2.3 @ 90
	- 77	-19 @ 30	+0.63 @ 90
Residual moisture content, θ_r	+ 71	-45 @ 30	-27 @ 90
	- 71	+28 @ 10	-5.4 @ 30
Pore-size distribution index, λ	+ 40	+6.4 @ 10	+2.0 @ 90
	- 40	-27 @ 30	-0.02 @ 90
Recharge (actual change from control = 0.0 m/d)	+1.74x10 ⁻⁴ m/d	-68 @ 30	-9.9 @ 10
	+3.48x10 ⁻⁴ m/d	-65 @ 30	-22 @ 10
	+6.96x10 ⁻⁴ m/d	-71 @ 30	-31 @ 10
Matrix compressibility, α (percentage change from control = 1.34x10 ⁻²² (m-d ²)/g)	+900	-9.6 @ 90	-0.20 @ 30
	- 90	+18 @ 30	+2.2 @ 60

Table A3.--Relative sensitivity of dimensionless seepage flux to selected changes in aquifer characteristics--Continued

Aquifer characteristic	Percentage change from control value	Percentage change in dimensionless seepage flux [$\Delta(q') @ t$]	
		maximum $ q'_N - q'_C $	minimum $ q'_N - q'_C $
GEOLOGIC MATERIAL E			
Initial saturated thickness, D = 1.0 m	- 50	+437 @ 10	-38 @ 30
Initial saturated thickness, D = 5.0 m	+200 +900	+71 @ 10 +200 @ 60	+70 @ 90 +70 @ 10
Saturated hydraulic conductivity, K_{sat} (m/d)	+900 - 90	-57 @ 10 +469 @ 90	-57 @ 60 +22 @ 10
Porosity, ϕ	+ 50 - 50	+62 @ 10 -80 @ 10	+59 @ 30 -80 @ 90
Bubbling pressure, h_b (m)	+ 67 - 67	+22 @ 60 -91 @ 10	+5.3 @ 90 -91 @ 90
Residual moisture content, θ_r	+ 80 - 80	-49 @ 30 +105 @ 10	-32 @ 90 +20 @ 90
Pore-size distribution index, λ	+ 50 - 50	+60 @ 10 -8.0 @ 10	-6.7 @ 90 -4.5 @ 90
Recharge (actual change from control = 0.0 m/d)	+1.74x10 ⁻⁴ m/d +3.48x10 ⁻⁴ m/d +6.96x10 ⁻⁴ m/d	-70 @ 90 -41 @ 10 -86 @ 10	-16 @ 10 -21 @ 30 -78 @ 90
Matrix compressibility, α (percentage change from control = 1.34x10 ⁻²² (m-d ²)/g)	+900 - 90	-38 @ 10 -27 @ 10	+10 @ 90 +0.51 @ 60

2. Increasing D from 5 to 15 m (+200 percent) yields a range in magnitude of relative change in h' from (1) 26 to 0.01 percent for geologic material C; (2) 41 to 0.07 percent for geologic material E; and (3) 16 to 0.18 percent for geologic material B. ("Maximum" and "minimum" in tables A2 and A3 refer to the differences in h' or q' values, and not to the relative percentage changes. Some relative percentage sensitivity values corresponding to maximum h' or q' differences may have smaller magnitudes than those corresponding to minimum h' or q' differences. An example is the 8.7 percent at 90 days and 49 m corresponding to maximum $|h'_N - h'_C|$ and the 9.1 percent at 90 days and 11 m corresponding to minimum $|h'_N - h'_C|$ for a +200 percent change in D for geologic material B). At 10 days, all three geologic materials exhibit largest sensitivity near the seepage face and smallest sensitivity away from the seepage face. This is true at 90 days for geologic material E but geologic materials B and C exhibit a magnitude of relative percentage change at 90 days that is fairly constant for the entire domain.

Increasing D from 5 to 15 m yields a range in magnitude of relative change in q' from (1) 104 to 83 percent for geologic material C; (2) 71 to 70 percent for geologic material E; and (3) 78 to 63 percent for geologic material B. Seepage flux for all three geologic materials exhibits the same general trend of decreasing sensitivity with time. Dimensionless seepage flux is sensitive to a +200 percent increase in D for the three geologic materials.

Similar general trends in relative sensitivity of h' and q' exist but are more pronounced when D is increased from 5 to 50 m (900 percent).

3. Increasing and decreasing K_{sat} an order of magnitude yields a range in magnitude of relative change in h' from (1) 56 to 1.3 percent for geologic material C; (2) 33 to 0.53 percent for geologic material E; and (3) 71 to 8.6 percent for geologic material B. Relative sensitivity, in most cases, decreases with distance from the seepage face and increases with time. Decreasing K_{sat} an order of magnitude for geologic material E yields unstable results (VS2D has difficulty converging on a solution for less permeable geologic materials).

Increasing and decreasing K_{sat} an order of magnitude yields a range in magnitude of relative change in q' from (1) 290 to 59 percent for geologic material C; (2) 469 to 22 percent for geologic material E; and (3) 167 to 67 percent for geologic material B. In most cases, q' is more sensitive to an order-of-magnitude decrease in K_{sat} than to an order-of-magnitude increase.

4. Increasing and decreasing ϕ by 0.1 yields a range in magnitude of relative change in h' from (1) 15 to 0 percent for geologic material C; (2) 19 to 0.04 percent for geologic material E; and (3) 19 to 0 percent for geologic material B. In general, magnitude of relative change in h' decreases with distance from the seepage face. Some heads experienced no change at the seepage face.

Increasing and decreasing ϕ by 0.1 yields a range in magnitude of relative change in q' from (1) 62 to 14 percent for geologic material C; (2) 80 to 59 percent for geologic material E; and (3) 59 to 45 percent for geologic material B. Dimensionless seepage flux is sensitive to variations in ϕ for all three geologic materials.

5. Increasing and decreasing h_b by 0.1 m yields a range in magnitude of relative change in h' from (1) 4.3 to 0 percent for geologic material C; (2) 8.0 to 0 percent for geologic material E; and (3) 18 to 0 percent for geologic material B. In most cases, h' is most sensitive to variations in h_b near the center of the aquifer domain. The magnitude of relative percentage change increases with distance from the seepage face.

Increasing and decreasing h_b by 0.1 m yields a range in magnitude of relative change in q' from (1) 19 to 0.63 percent for geologic material C; (2) 91 to 5.3 percent for geologic material E; and (3) 11 to 1.8 percent for geologic material B. Sensitivity of q' to variations in h_b increases with decreasing permeability and decreases with time.

6. Increasing and decreasing θ_r by 0.1 for geologic material B, 0.05 for geologic material C, and 0.04 for geologic material E yields a range in magnitude of relative change in h' from (1) 15 to 0 percent for geologic material C; (2) 12 to 0.002 percent for geologic material E; and (3) 15 to 0 percent for geologic material B. Sensitivity, in most cases, decreases with distance from the seepage face.

Increasing and decreasing θ_r by 0.1 for geologic material B, 0.05 for geologic material C, and 0.04 for geologic material E yields a range in magnitude of relative change in q' from (1) 45 to 5.4 percent for geologic material C; (2) 105 to 20 percent for geologic material E; and (3) 67 to 43 percent for geologic material B. Seepage flux is sensitive to variations in θ_r for the three geologic materials.

7. Increasing and decreasing λ by 1.0 yields a range in magnitude of relative change in h' from (1) 8.7 to 0 percent for geologic material C; (2) 12 to 0 percent for geologic material E; and (3) 18 to 0 percent for geologic material B. In most cases, h' is least sensitive to variations in λ near the seepage face.

Increasing and decreasing λ by 1.0 yields a range in magnitude of relative change in q' from (1) 27 to 0.02 percent for geologic material C; (2) 60 to 4.5 percent for geologic material E; and (3) 6.9 to 0.8 percent for geologic material B. Sensitivity decreases with time. Dimensionless seepage flux is more sensitive to a decrease in λ for geologic materials B and C and to an increase in λ for geologic material E.

8. Increasing recharge from 0.0 to 1.74×10^{-4} m/d yields a range in magnitude of relative change in h' from (1) 36 to 0 percent for geologic material C; (2) 18 to 0 percent for geologic material E; and (3) 58 to 3.2 percent for geologic material B. Changes indicate a trend of increasing sensitivity with time.

Increasing recharge from 0.0 to 1.74×10^{-4} m/d yields a range in magnitude of relative change in q' from (1) 68 to 9.9 percent for geologic material C; (2) 70 to 16 percent for geologic material E; and (3) 95 to 53 percent for geologic material B. Seepage fluxes exhibit a trend of increasing sensitivity with time.

Similar trends in relative sensitivity of h' and q' exist when recharge is increased from 0.0 to 3.48×10^{-4} m/d and 6.96×10^{-4} m/d.

9. Increasing and decreasing aquifer matrix compressibility α an order of magnitude from each geologic material value of α for the confined aquifer sensitivity simulations yields a range in magnitude of relative change in h' from (1) 0.31 to 0 percent for geologic material C; (2) 48 to 0 percent for geologic material E; and (3) 12 to 0 percent for geologic material B. Relative sensitivity is often 0 percent at the seepage face, and generally increases (slightly) with distance from the seepage face.

Increasing and decreasing α an order of magnitude yields a range in magnitude of relative change in q' from (1) 18 to 0.20 percent for geologic material C; (2) 38 to 0.51 percent for geologic material E; and (3) 9.9 to 0.091 percent for geologic material B. General trends show decreasing sensitivity with time.

The following conclusions are based on the results of the sensitivity analyses and additional simulations not previously discussed:

1. Dimensionless heads far from the seepage face are insensitive to a decrease in D from 1.0 to 0.5 m, especially as time increases. Dimensionless heads are more sensitive near the seepage face, especially for less permeable geologic materials. Dimensionless seepage flux is sensitive to this decrease in D for all geologic materials. The user should exercise caution in extending 1-m h' results to aquifers of D less than 0.5 m, especially near the seepage face. The user should not extend q' results to D less than 0.5 m.

2. Dimensionless heads are sensitive to an increase in D from 5 to 15 m. Dimensionless heads are less sensitive to this change far from the seepage face at small times for the more permeable geologic materials, and at all times for the less permeable geologic materials. Seepage flux is sensitive to this change in D for all cases. Sensitivity of both h' and q' increases when D is increased from 5 to 50 m for all cases. The user should exercise caution in extending 5-m h' results to aquifers of D greater than 15 m, especially near the seepage face. The user should not extend 5-m q' results to aquifers of D greater than 15 m.

3. Dimensionless head and seepage flux are sensitive to variations in K_{sat} more than to other geologic-material moisture characteristics. Seepage flux is also sensitive to variations in ϕ and θ_r . Head and seepage flux are insensitive to variations in h_D and λ , within limits imposed by measurement techniques or variability in field conditions.

Head and seepage flux obtained using the technique may be used for the ranges of physical properties indicated in the sensitivity analysis (extended to the remaining geologic materials). The user is forewarned that K_{sat} and S_y (equal to ϕ minus θ_r) may be critical to the calculated head and seepage flux. Users of the technique should perform measurements to obtain best estimates of K_{sat} and S_y at the proposed mine site.

4. Simulations performed on each geologic material to test the effect of order-of-magnitude changes in α on h' and q' in confined aquifers indicate that head and seepage flux are not strongly sensitive to changes in aquifer matrix compressibility for the confined aquifers that were considered.

5. Simulations were performed on each geologic material to test the effect of recharge on h' and q' . Representative recharge rates of 1.74×10^{-4} m/d, 3.48×10^{-4} m/d, and 6.96×10^{-4} m/d were selected. Dimensionless head may be sensitive to recharge, depending on the aquifer characteristics, especially at large times. Sensitivity increases with increasing geologic-material permeability. Dimensionless seepage flux is very sensitive to recharge, particularly at large times and for more permeable geologic materials. The user is forewarned that the neglect of recharge in the formulation of the technique may be a limitation that should be noted.

6. Head and seepage flux may be sensitive to leakage between aquifers, which was also not taken into consideration in the formulation of the technique.

Mass Balance

A "mass-balance" calculation, based on the conservation of mass, balances fluxes into and out of the system against the change in storage in the system. These calculations are performed to check the accuracy of the finite-difference solution to the governing equations, subject to the associated initial and boundary conditions. A large mass-balance error may be an indication that there is an error in the numerical solution technique.

Because leakage and recharge are not considered, there is only flux out of the aquifer through the seepage face into the mine. Mass-balance error is calculated in VS2D by subtracting the total flux out of the nodes on the seepage face from the change in storage in the aquifer at specified times. This error in mass balance is computed as a volume percent.

Mass-balance error is directly related to the closure criterion used for the numerical solution method. Closure criterion is a user-specified tolerance that determines when convergence is achieved. A larger value of closure criterion yields larger mass-balance error, but convergence may be faster. A smaller value of closure criterion yields smaller mass-balance error and usually longer convergence times. It was necessary to reduce mass balance error as much as possible and yet maintain economic use of computer time. The closure criterion was specified as 0.5 millimeter (mm) for most simulations. Some cross sections were simulated using a closure criterion of 0.1 mm to reduce mass-balance error to an acceptable level. Mass balance ranged from 0.005 percent to a maximum of approximately 10 percent for some simulations.

Figure A17 shows q' as a function of dimensionless time, t' , for the hypothetical aquifer of graph C21 (Appendix C), simulated using two closure criteria. Small changes in the profiles were observed when the closure criteria were varied. Most aquifers were simulated with the larger closure criterion because of the large increase in computer time that resulted when the closure criterion was decreased. As a result it was necessary to smooth some q' profiles in Appendixes C and E. The small variations that occurred in q' when mass balance error was decreased indicated that use of the larger closure criterion was justified.

Differences obtained for the two closure criteria for the h' profiles in Appendixes B and D were negligible.

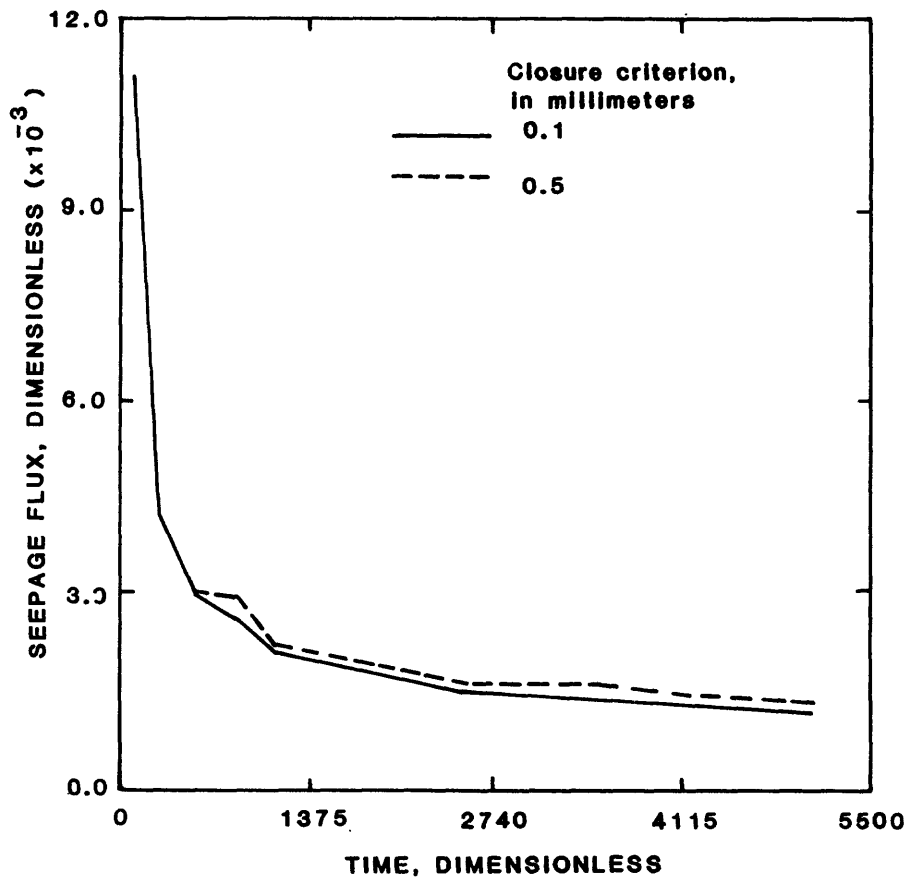


Figure A17.--Dimensionless seepage-flux profiles, with closure criteria of 0.1 millimeter and 0.5 millimeter.

REFERENCES CITED

- Boussinesq, J., 1877, Du mouvement non permanent des eaux souterraines: Essai sur la theorie des eaux courantes, Memoires presentes par divers savants a l'Academie des Sciences de l'Institut de France, v. 23, no. 1, 680 p.
- 1904, Recherches theoriques sur l'ecoulement des nappes d'eau infiltrées dans le solet sur le debit des sources: Journal de Mathematiques pures et appliquees, v. 10, sme serie, p. 5-78.
- Bouwer, H., and Rice, R. C., 1976, A slug test for determining hydraulic conductivity of unconfined aquifers with completely or partially penetrating wells: Water Resources Research, v. 12, no. 3, p. 423-428.
- Brooks, R. H., and Corey, A. T., 1964, Hydraulic properties of porous media: Fort Collins, Colorado State University Hydrology Paper 3, 27 p.
- Brutsaert, W. F., and El-Kadi, A. I., 1984, The relative importance of compressibility and partial saturation in unconfined groundwater flow: Water Resources Research, v. 20, no. 3, p. 400-408.
- Cooley, R. L., 1983, Some new procedures for numerical solution of variably saturated flow problems: Water Resources Research, v. 19, no. 5, p. 1271-1285.
- Dumm, L. D., 1954, New formula for determining depth and spacing of surface drains in irrigated lands: Agricultural Engineering, v. 35.
- Freeze, R. A., and Cherry, J. A., 1979, Groundwater: Englewood Cliffs, N.J., Prentice-Hall, 604 p.
- Glover, R. E., 1964, Ground-water movement: Engineering Monograph No. 31, Office of Chief Engineer, Bureau of Reclamation, U.S. Department of the Interior, Denver, Colorado.
- Haushild, William, and Kruse, Gorden, 1962, Unsteady flow of ground water into a surface reservoir: Transactions, American Society of Civil Engineers, v. 127, part I, p. 408-415.
- Lappala, E. G., Healy, R. W., and Weeks, E. P., 1985, Documentation of computer program VS2D to solve the equations of fluid flow in variably saturated porous media: U.S. Geological Survey Water-Resources Investigations Report 83-4099, 200 p.

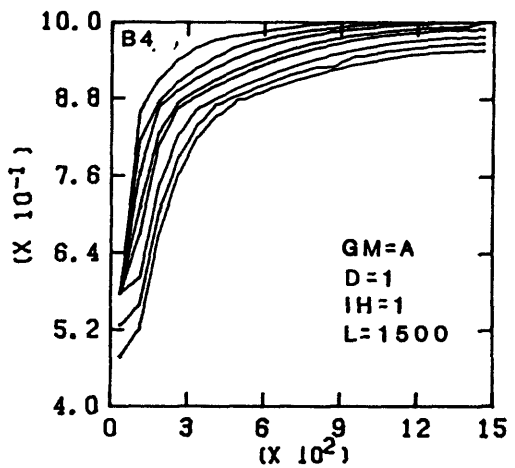
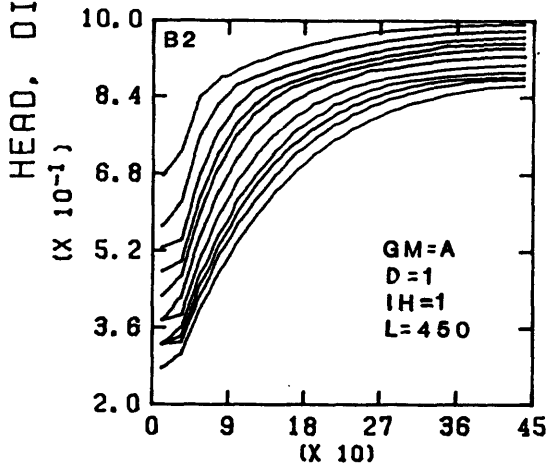
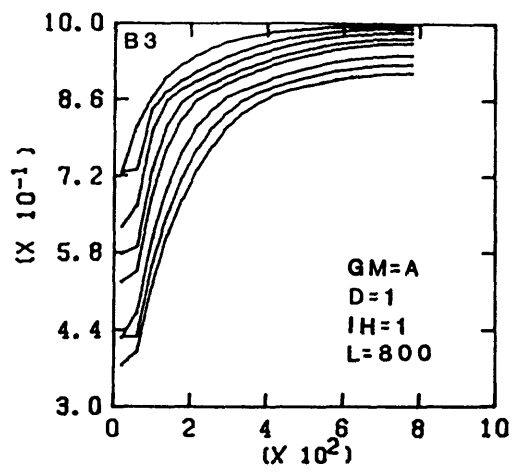
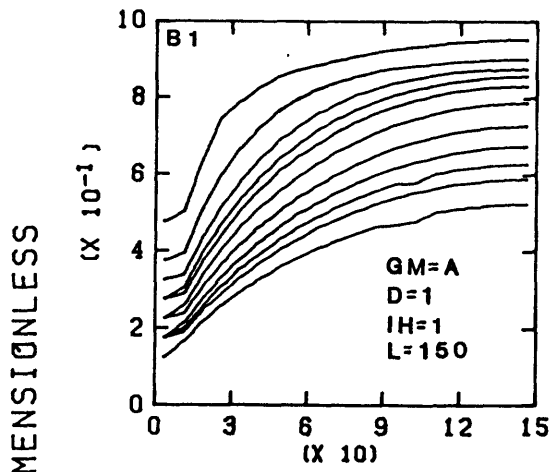
APPENDIX B

Dimensionless total-head profiles for the hypothetical aquifers.

Symbols.--The following symbols appear with graphs B1 through B72 of Appendix B:

<u>Symbol</u>	<u>Explanation</u>
GM	Geologic material (table 1).
D	Initial saturated thickness, in meters.
IH	Initial head, in meters.
L	Length, in meters.

Note: Maximum head values in many figures coincide with top of graphs.



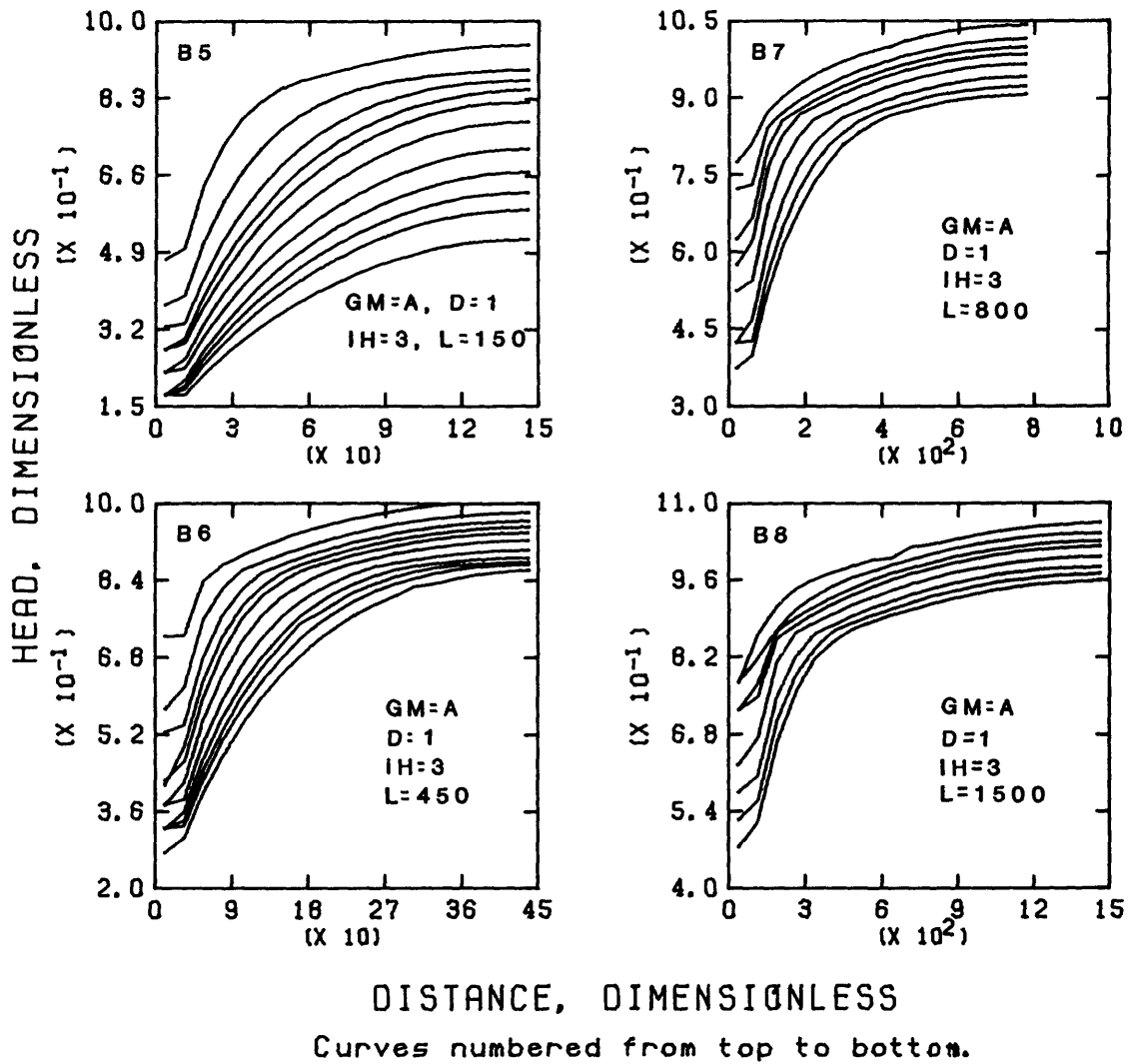
DISTANCE, DIMENSIONLESS
Curves numbered from top to bottom.

Graphs B1 and B2

Curve	Dimensionless time
1	292
2	875
3	1750
4	2630
5	3500
6	5260
7	7880
8	10500
9	13100
10	15800
11	21300

Graphs B3 and B4

Curve	Dimensionless time
1	292
2	876
3	1750
4	3500
5	5260
6	10500
7	15800
8	21300



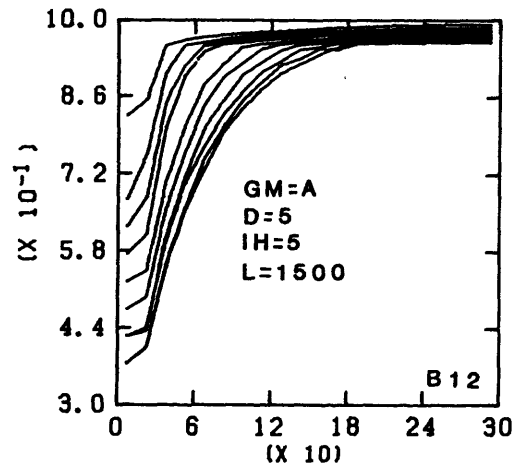
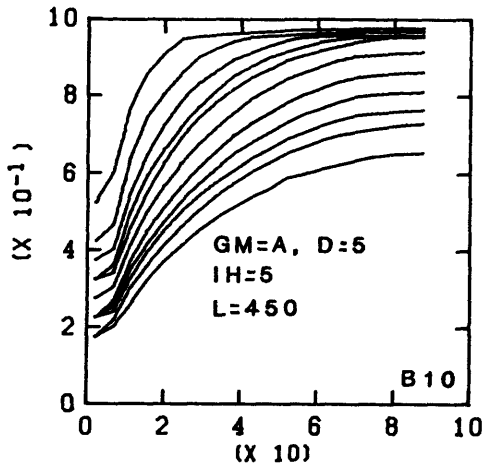
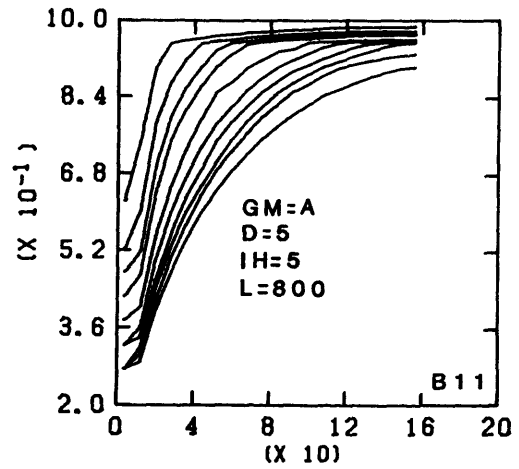
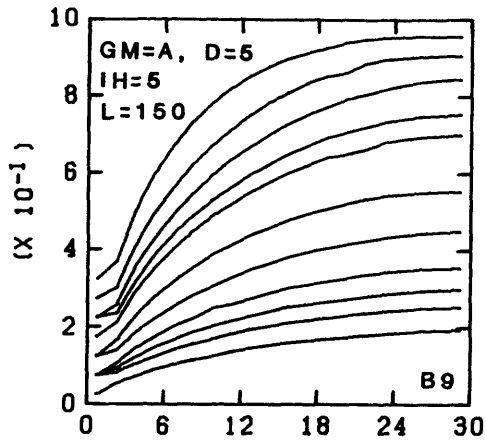
Graphs B5 and B6

Curve	Dimensionless time
1	292
2	876
3	1750
4	2630
5	3500
6	5260
7	7880
8	10500
9	13100
10	15800
11	21300

Graphs B7 and B8

Curve	Dimensionless time
1	292
2	876
3	1752
4	2628
5	5256
6	10510
7	15770
8	21310

HEAD, DIMENSIONLESS



DISTANCE, DIMENSIONLESS

Curves numbered from top to bottom.

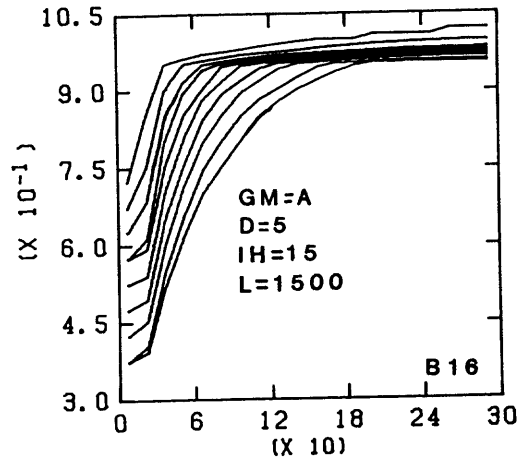
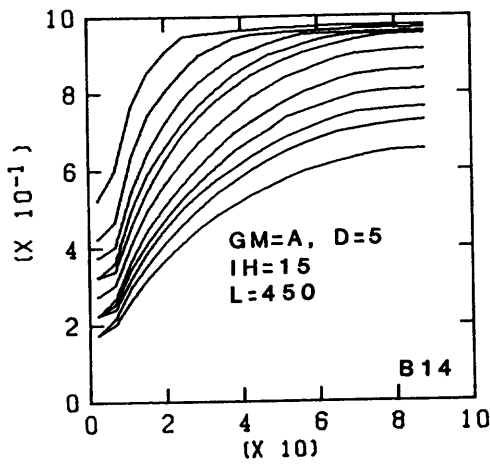
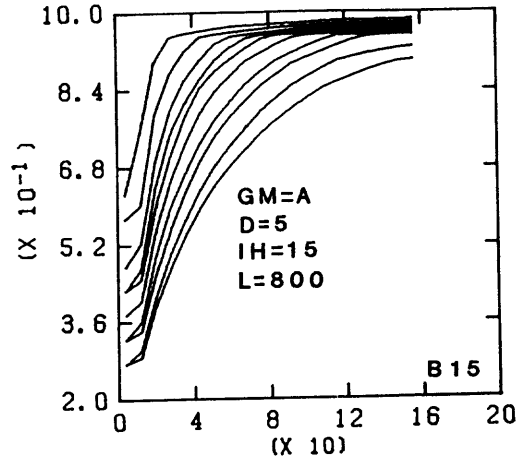
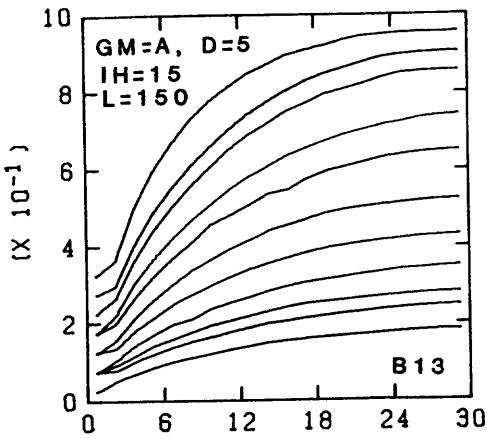
Graphs B9 and B10
Curve Dimensionless time

1	58
2	175
3	350
4	526
5	701
6	1050
7	1580
8	2190
9	2630
10	3150
11	4260

Graphs B11 and B12
Curve Dimensionless time

1	58
2	175
3	350
4	526
5	1050
6	1580
7	2100
8	2630
9	3150
10	3680

HEAD, DIMENSIONLESS
(X 10⁻¹)



DISTANCE, DIMENSIONLESS

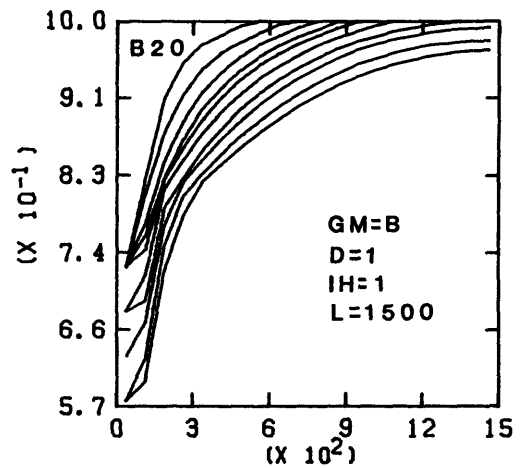
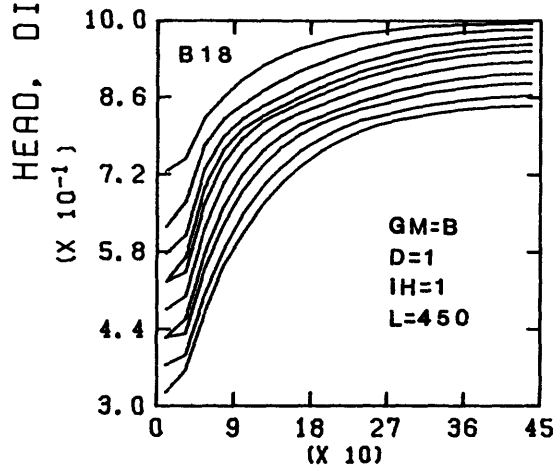
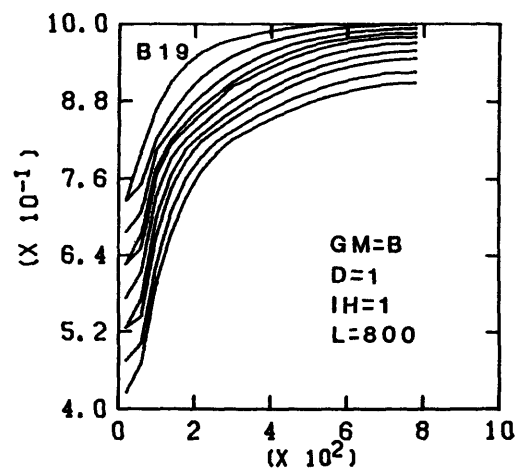
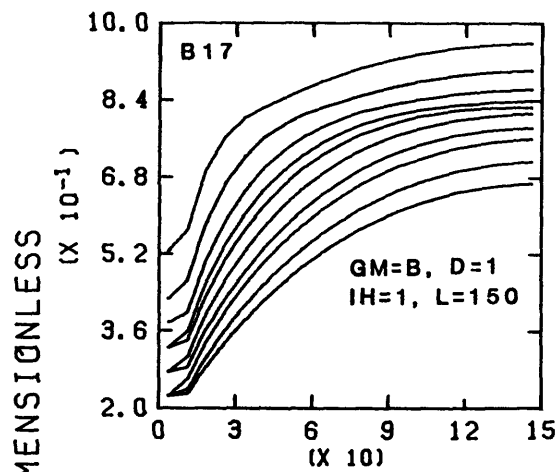
Curves numbered from top to bottom.

Graphs B13 and B14

Curve	Dimensionless time
1	58
2	175
3	350
4	526
5	701
6	1050
7	1580
8	2100
9	2630
10	3150
11	4260

Graphs B15 and B16

Curve	Dimensionless time
1	58
2	175
3	350
4	526
5	701
6	1050
7	1580
8	2100
9	3150
10	4260



DISTANCE, DIMENSIONLESS

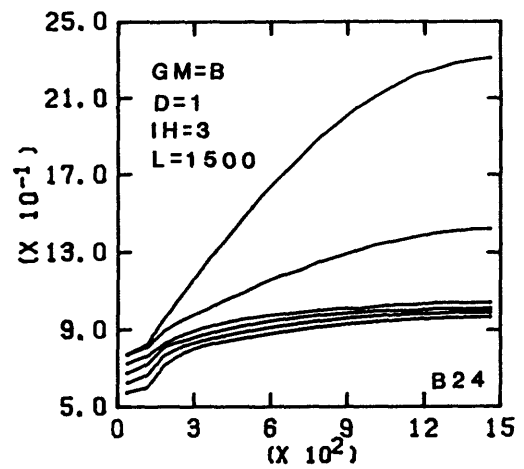
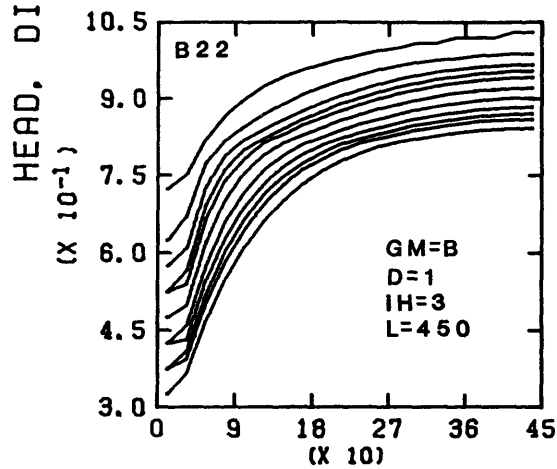
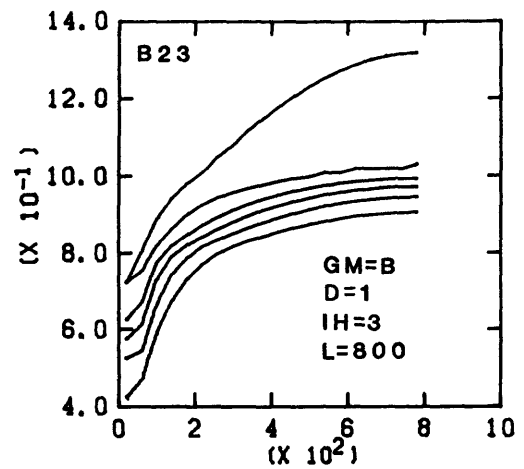
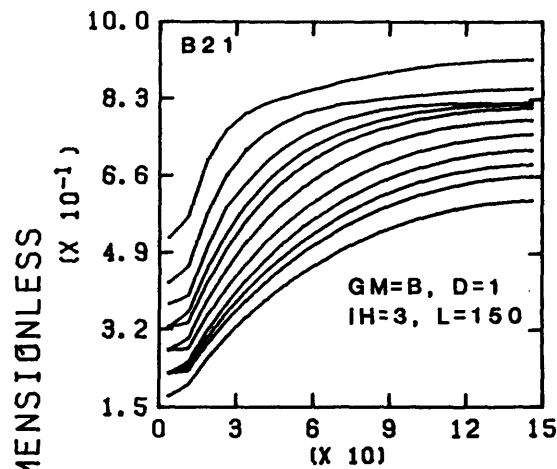
Curves numbered from top to bottom.

Graphs B17 and B18
 Curve Dimensionless time

1	94
2	282
3	564
4	847
5	1130
6	1690
7	2540
8	3390
9	5080
10	6870

Graphs B19 and B20
 Curve Dimensionless time

1	94
2	282
3	564
4	847
5	1130
6	1690
7	2540
8	3390
9	5080
10	6870



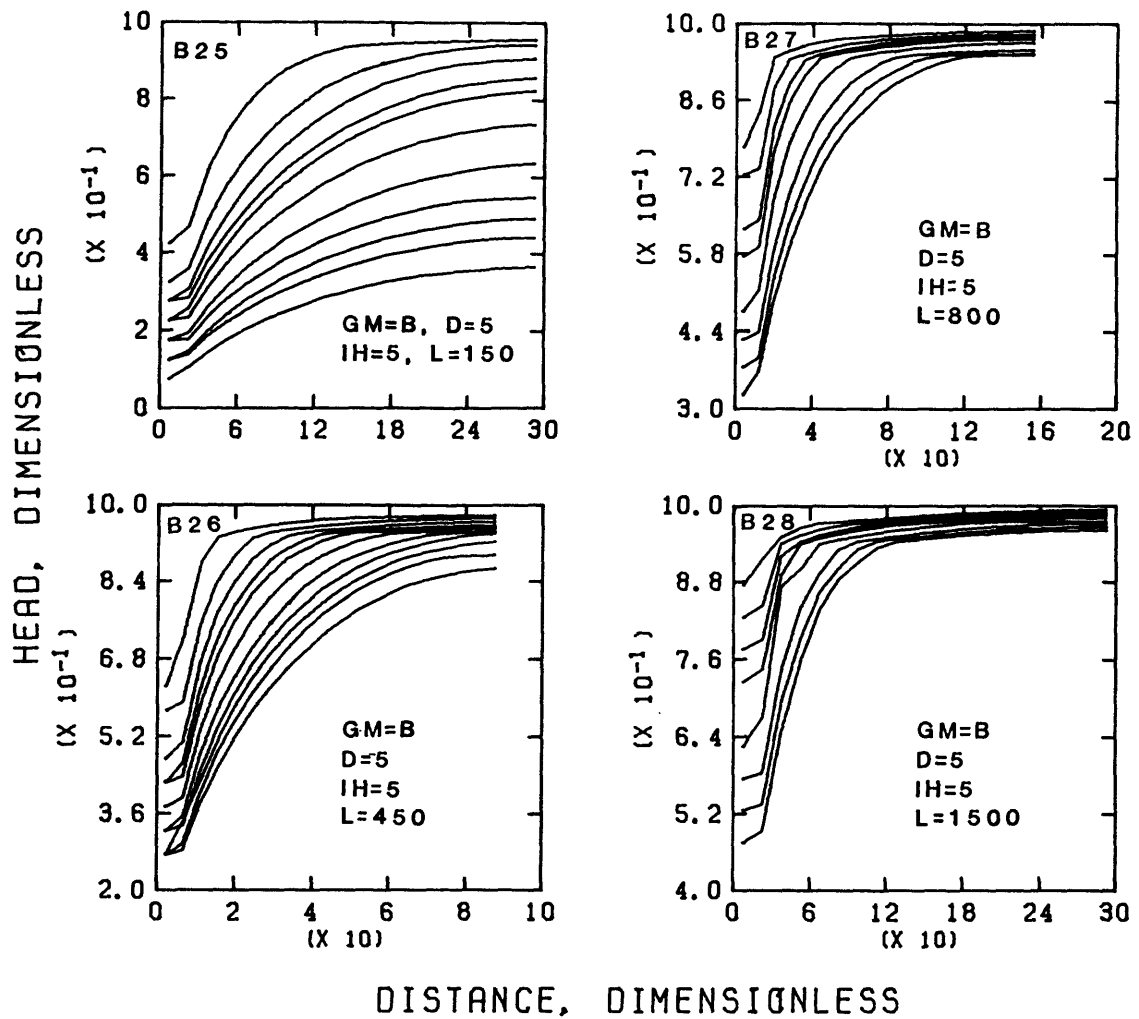
DISTANCE, DIMENSIONLESS
 Curves numbered from top to bottom.

Graphs B21 and B22
 Curve Dimensionless time

1	94
2	282
3	564
4	847
5	1130
6	1690
7	2540
8	3390
9	4230
10	5080
11	6870

Graphs B23 and B24
 Curve Dimensionless time

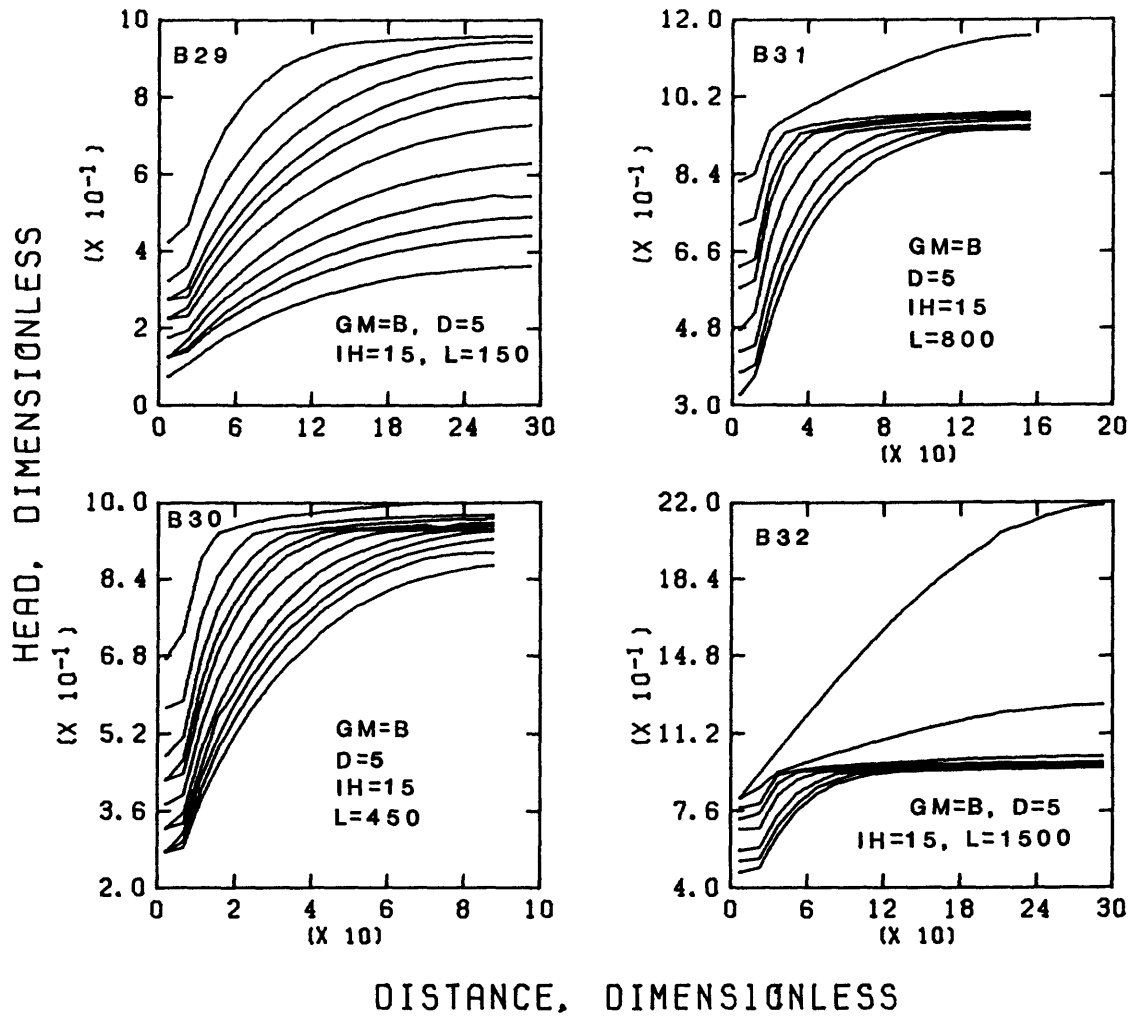
1	94
2	282
3	847
4	1690
5	3390
6	6870



Curves numbered from top to bottom.

Graphs B25 and B26	
Curve	Dimensionless time
1	19
2	56
3	113
4	169
5	226
6	339
7	508
8	677
9	847
10	1020
11	1370

Graphs B27 and B28	
Curve	Dimensionless time
1	19
2	56
3	113
4	169
5	339
6	677
7	1020
8	1370



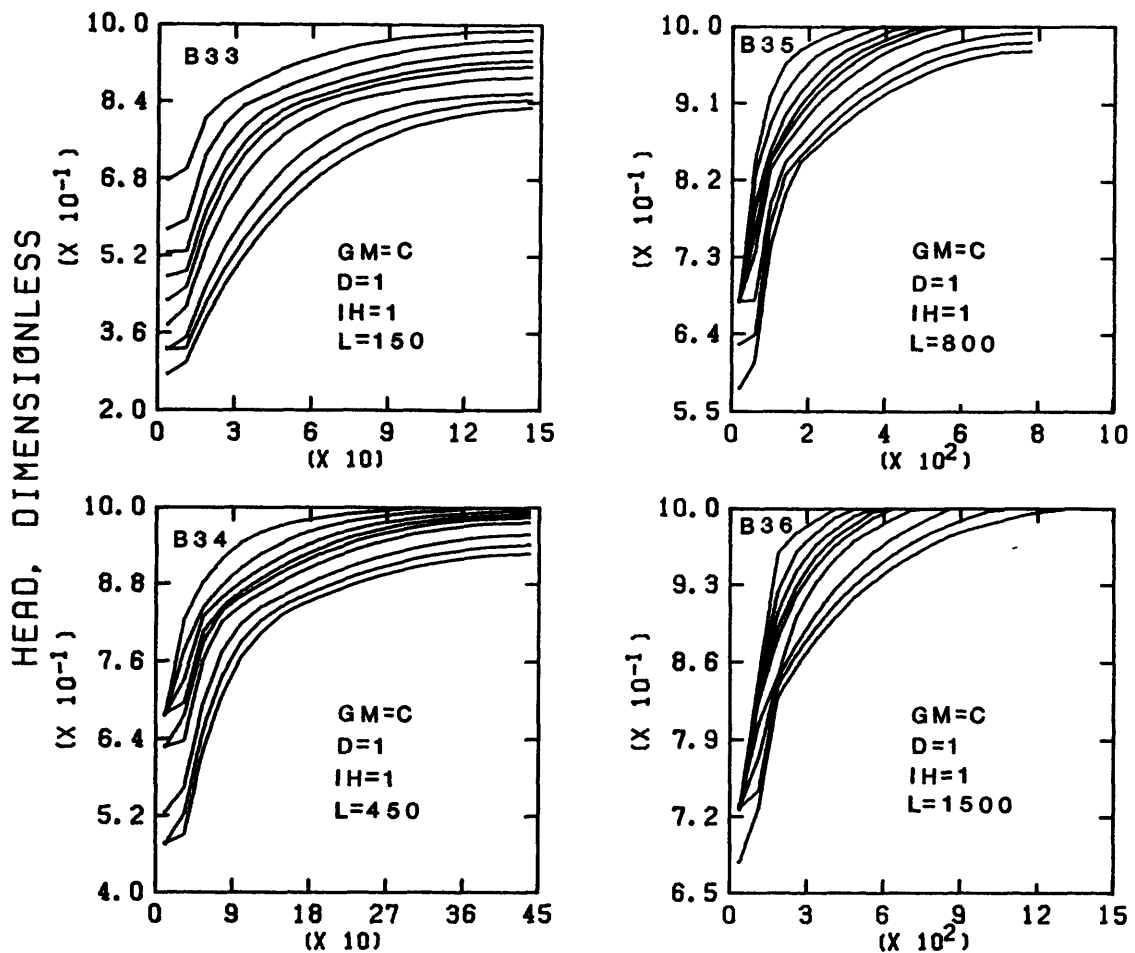
Curves numbered from top to bottom.

Graphs B29 and B30
Curve Dimensionless time

1	19
2	56
3	113
4	169
5	226
6	339
7	508
8	677
9	847
10	1020
11	1370

Graphs B31 and B32
Curve Dimensionless time

1	19
2	56
3	112
4	169
5	339
6	677
7	1020
8	1370



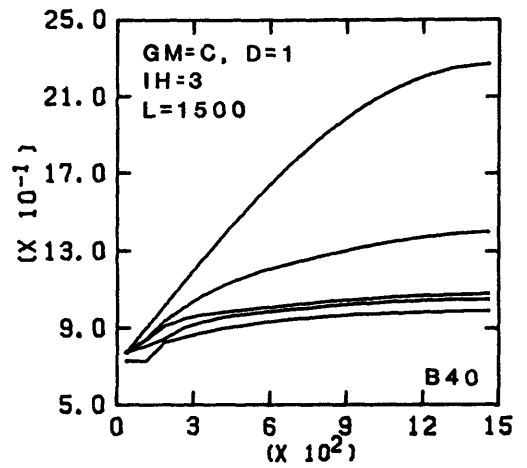
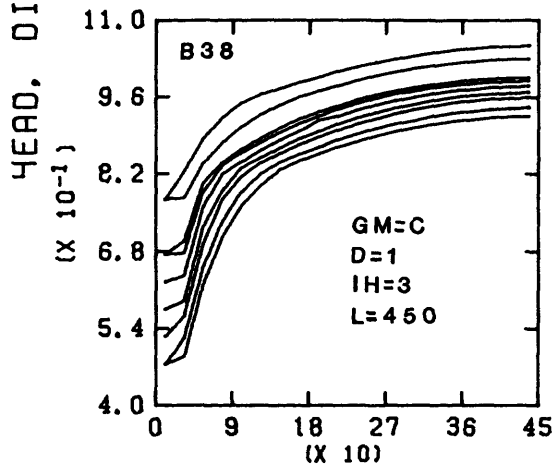
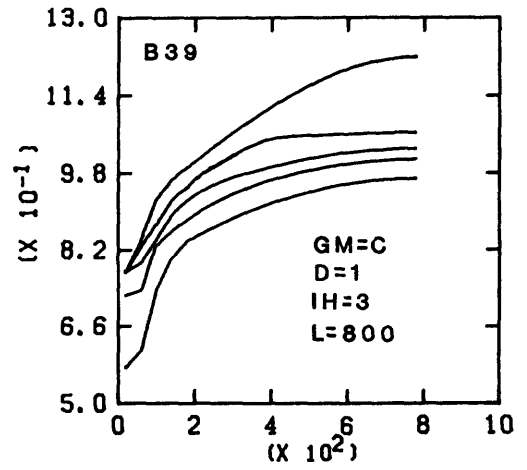
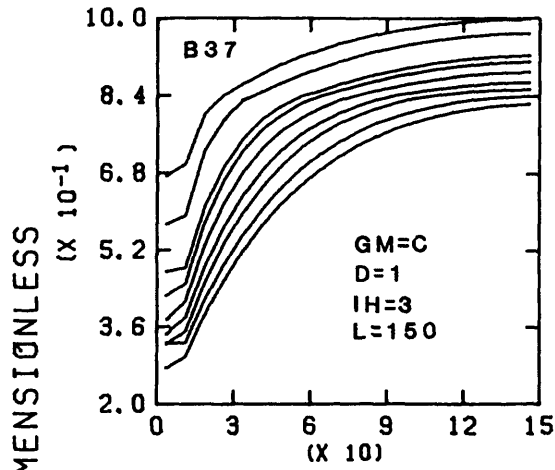
DISTANCE, DIMENSIONLESS
Curves numbered from top to bottom.

Graphs B33 and B34
Curve Dimensionless time

1	30
2	91
3	181
4	272
5	363
6	544
7	1090
8	1630
9	2210

Graphs B35 and B36
Curve Dimensionless time

1	30
2	91
3	181
4	272
5	363
6	544
7	1090
8	1630
9	2210



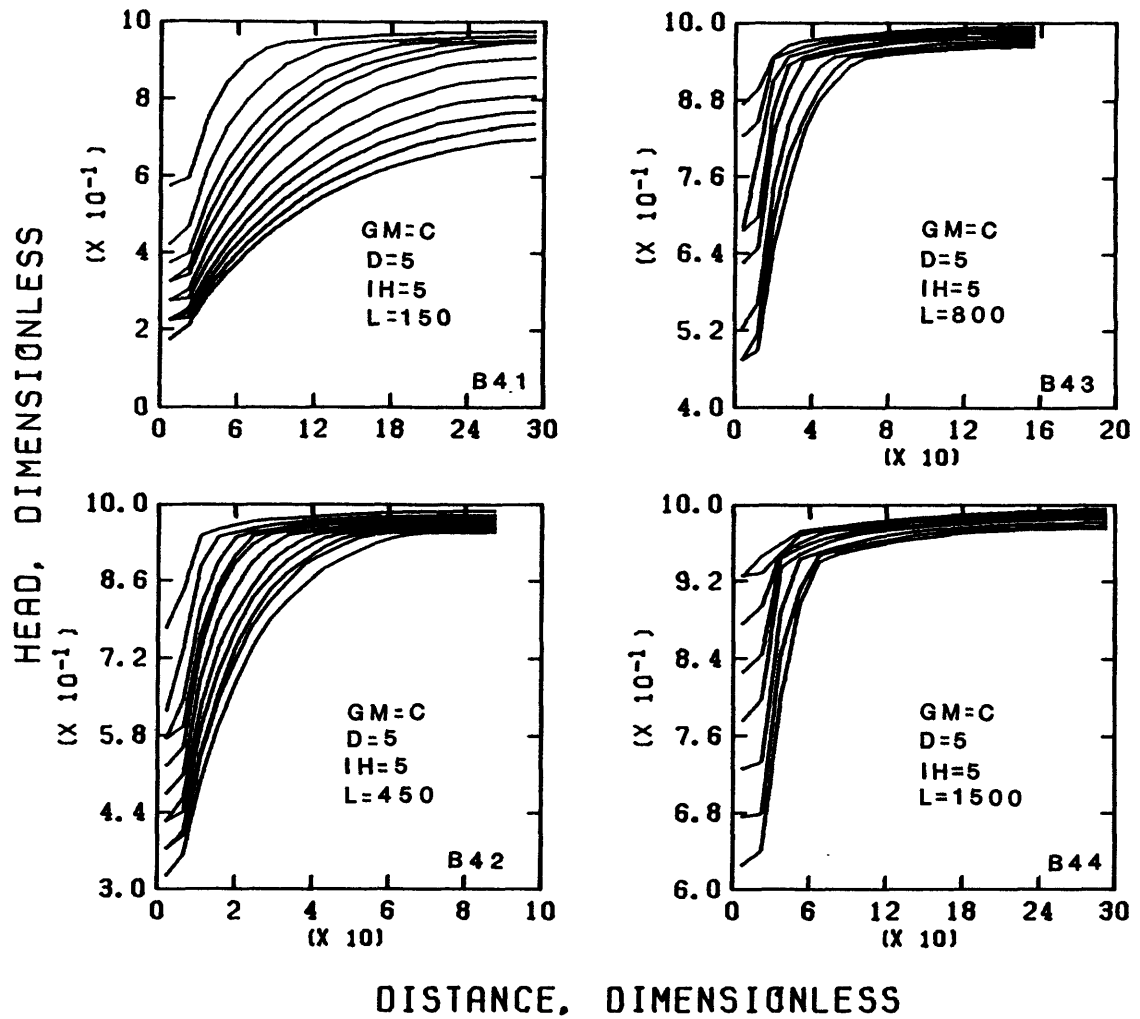
DISTANCE, DIMENSIONLESS
 Curves numbered from top to bottom.

Graphs B37 and B38

Curve	Dimensionless time
1	30
2	91
3	272
4	363
5	544
6	816
7	1090
8	1630
9	2210

Graphs B39 and B40

Curve	Dimensionless time
1	30
2	91
3	181
4	544
5	2210



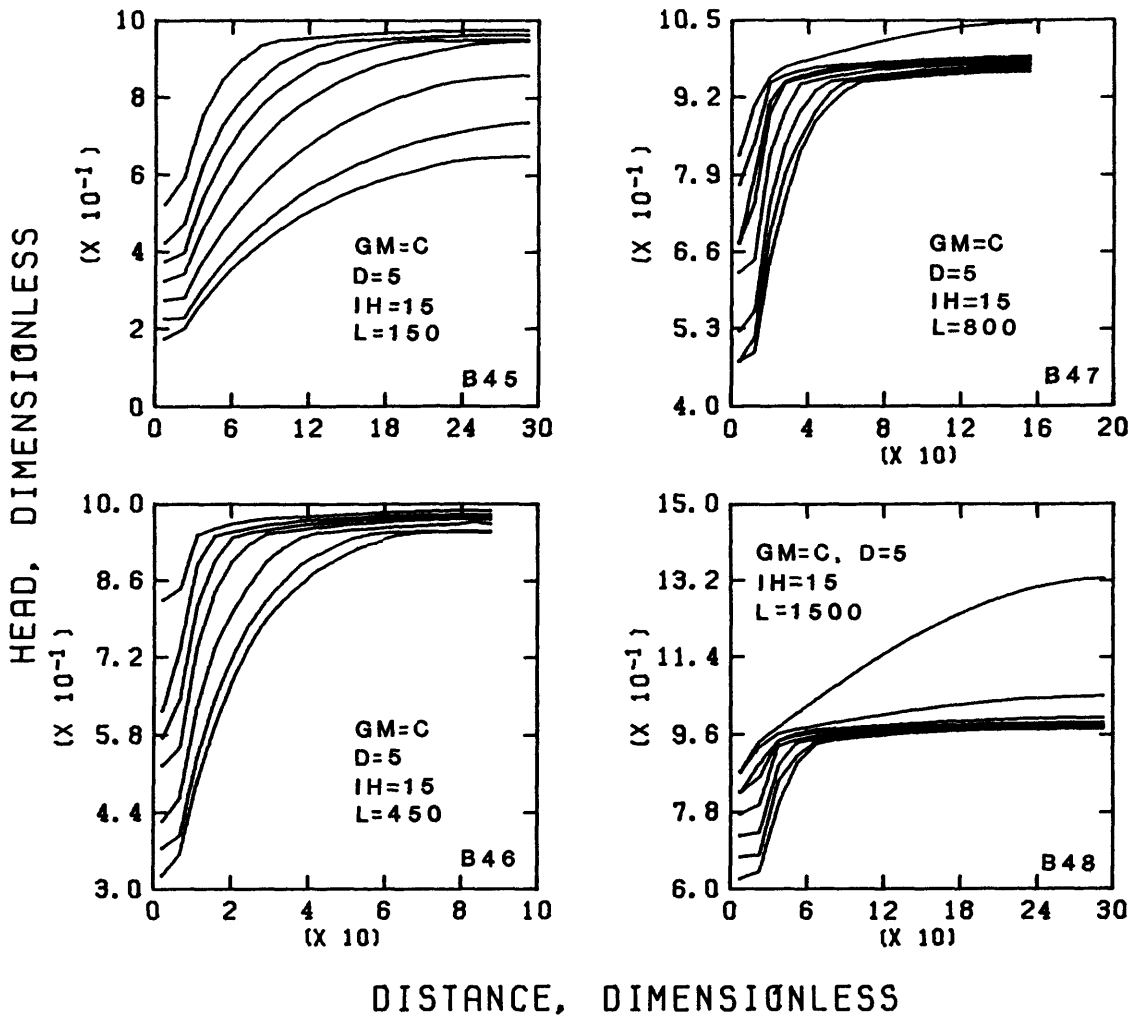
Curves numbered from top to bottom.

Graphs B41 and B42
Curve Dimensionless time

1	6.0
2	18
3	36
4	54
5	73
6	109
7	163
8	218
9	272
10	327
11	442

Graphs B43 and B44
Curve Dimensionless time

1	6.0
2	18
3	36
4	73
5	109
6	218
7	327
8	441



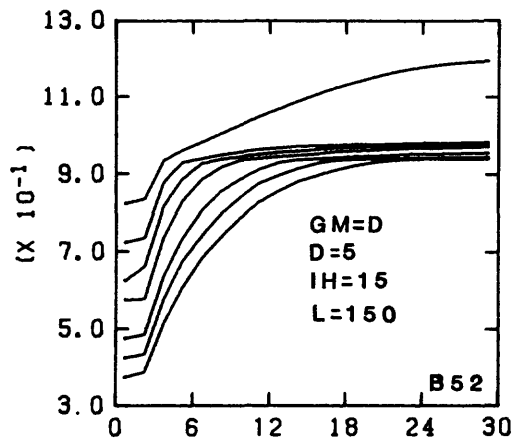
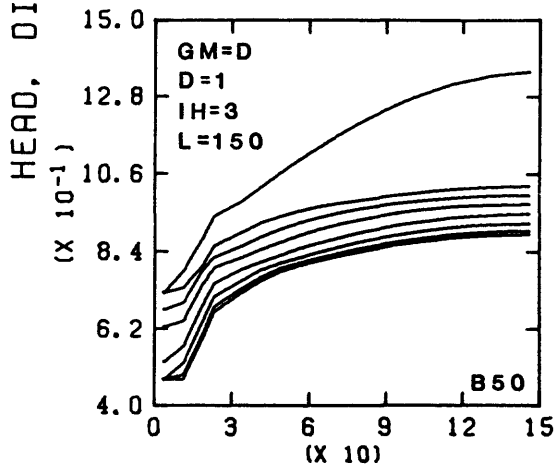
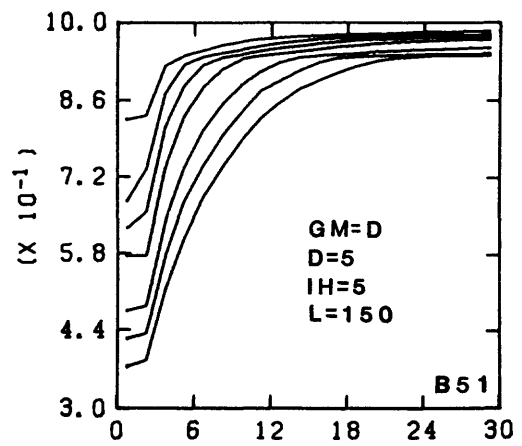
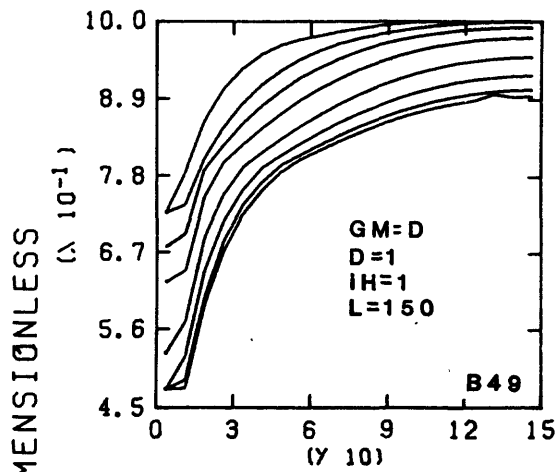
Curves numbered from top to bottom.

Graphs B45 and B46

Curve	Dimensionless time
1	6.0
2	18
3	36
4	73
5	163
6	327
7	441

Graphs B47 and B48

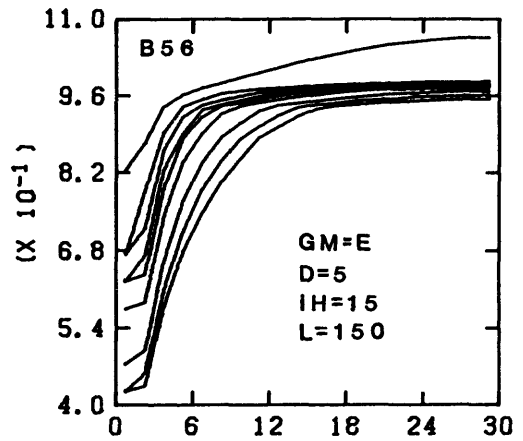
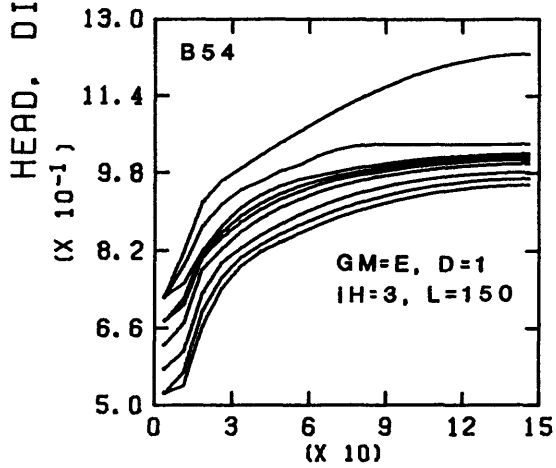
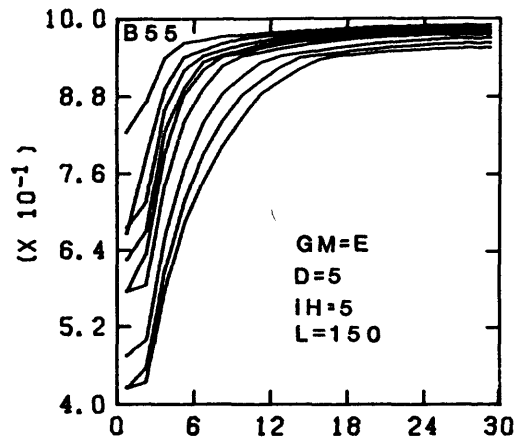
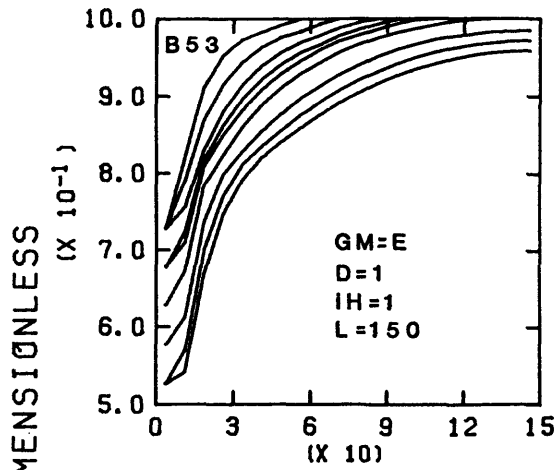
Curve	Dimensionless time
1	6.0
2	18
3	36
4	54
5	109
6	218
7	327
8	441



DISTANCE, DIMENSIONLESS
Curves numbered from top to bottom.

Graphs B49 and B50	
Curve	Dimensionless time
1	2.6
2	7.9
3	16
4	32
5	71
6	119
7	167
8	193

Graphs B51 and B52	
Curve	Dimensionless time
1	0.53
2	1.6
3	3.2
4	6.3
5	14
6	24
7	39



DISTANCE, DIMENSIONLESS

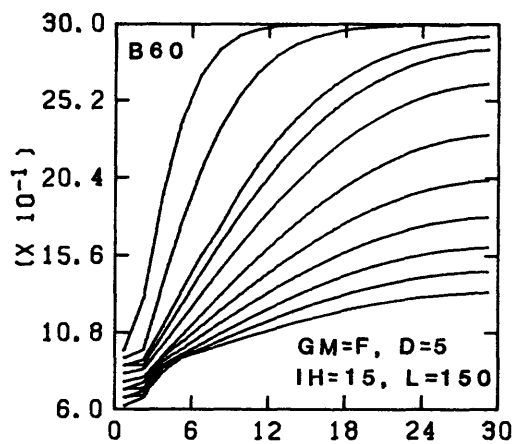
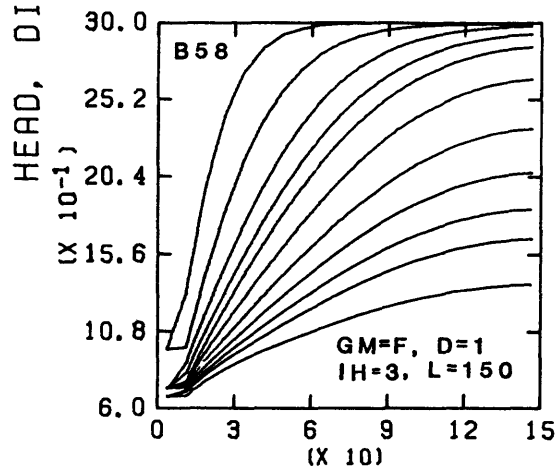
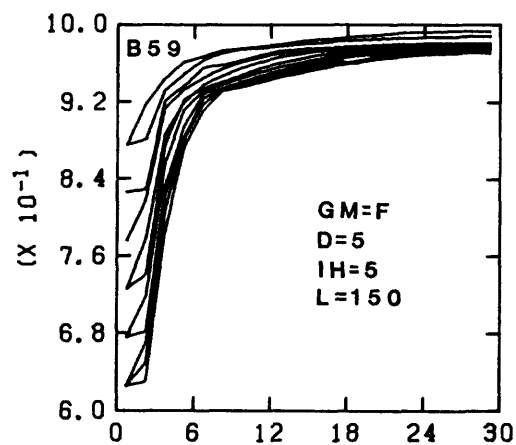
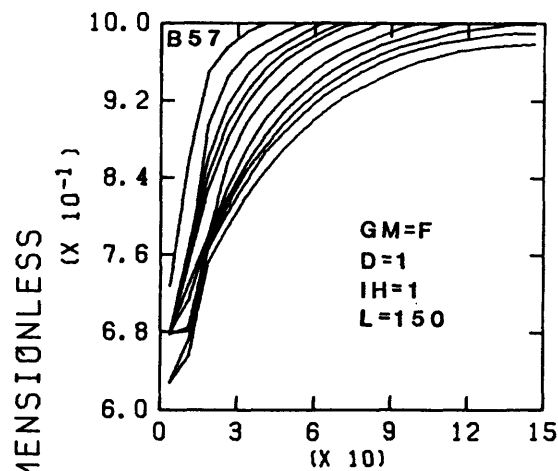
Curves numbered from top to bottom.

Graphs B53 and B54
 Curve Dimensionless time

1	1.7
2	5.1
3	10
4	15
5	20
6	31
7	61
8	91
9	124

Graphs B55 and B56
 Curve Dimensionless time

1	0.34
2	1.0
3	2.0
4	3.0
5	4.1
6	6.1
7	12
8	18
9	25



DISTANCE, DIMENSIONLESS

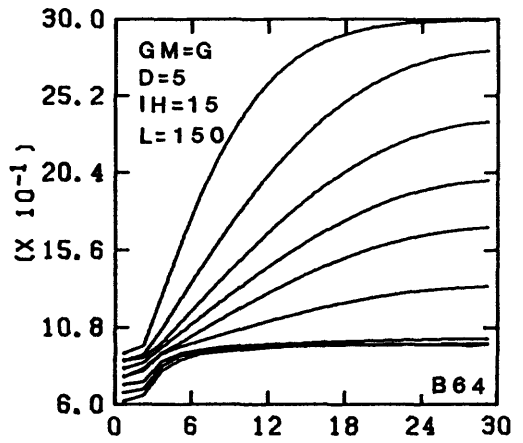
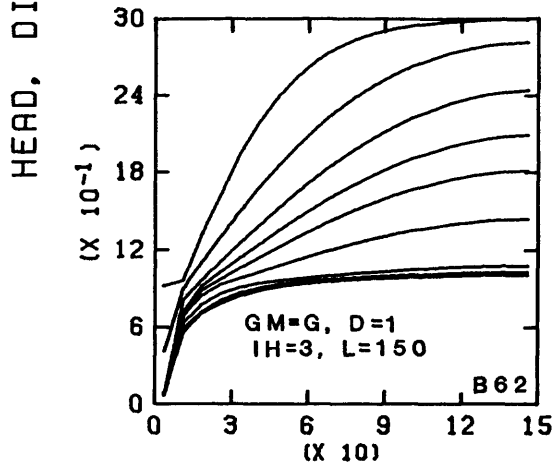
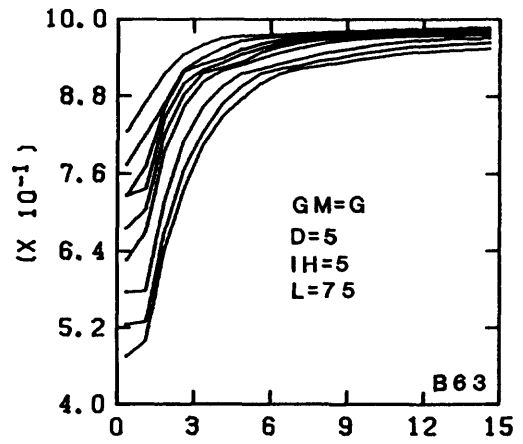
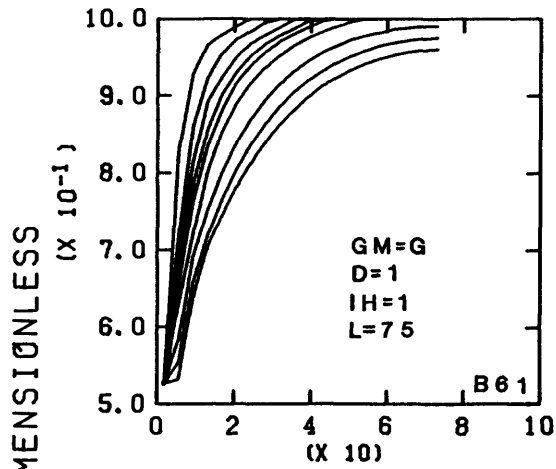
Curves numbered from top to bottom.

Graphs B57 and B58
 Curve Dimensionless time

1	0.24
2	0.73
3	1.5
4	2.2
5	2.9
6	4.3
7	6.5
8	8.7
9	11
10	13
11	18

Graphs B59 and B60
 Curve Dimensionless time

1	0.05
2	0.15
3	0.44
4	0.58
5	0.81
6	1.3
7	1.7
8	2.2
9	2.6
10	3.0
11	3.5



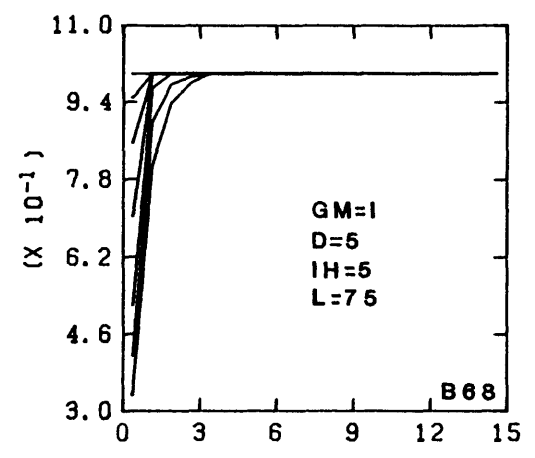
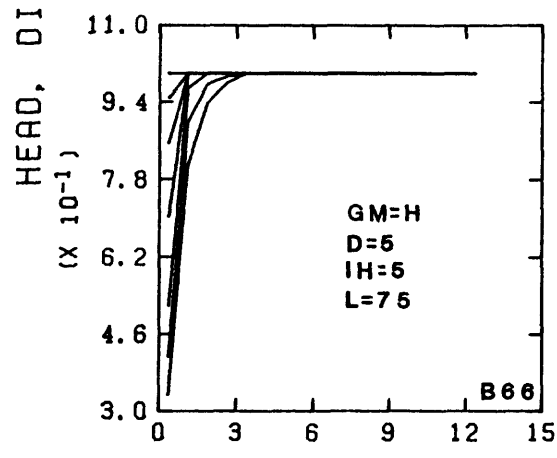
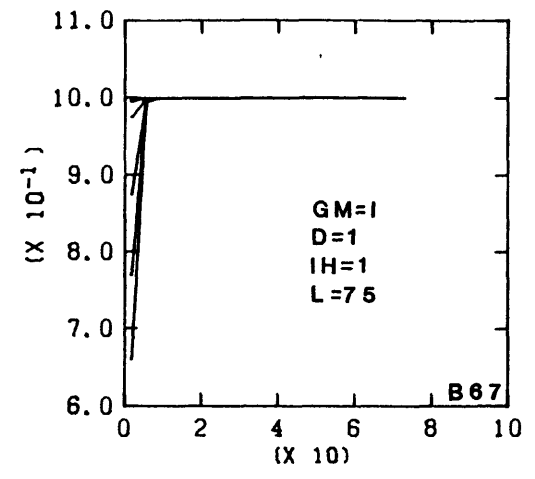
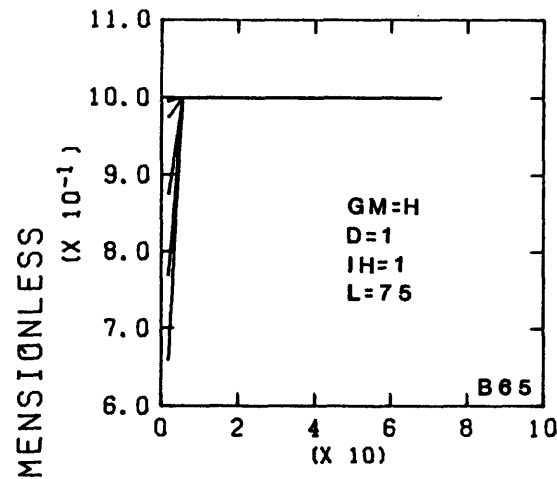
DISTANCE, DIMENSIONLESS
Curves numbered from top to bottom.

Graphs B61 and B62
Curve Dimensionless time

1	0.21
2	0.64
3	1.3
4	1.9
5	2.5
6	3.8
7	7.6
8	11
9	15

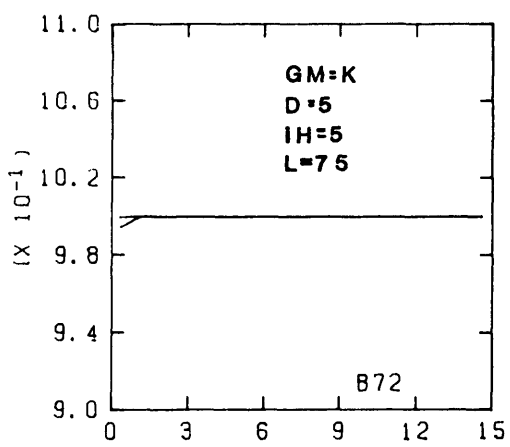
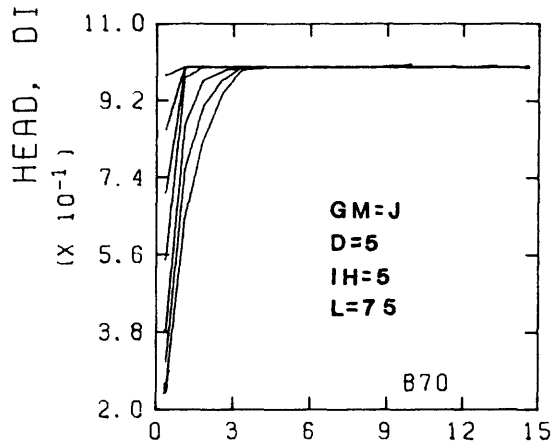
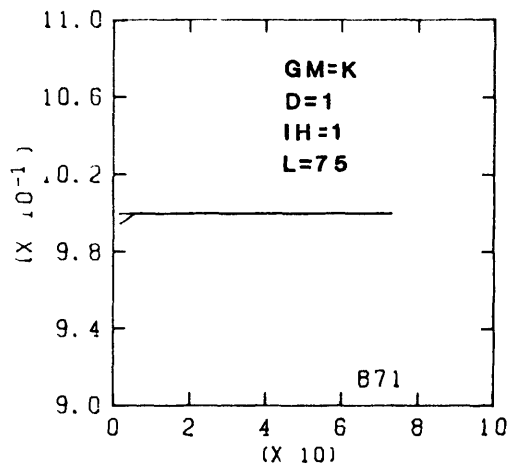
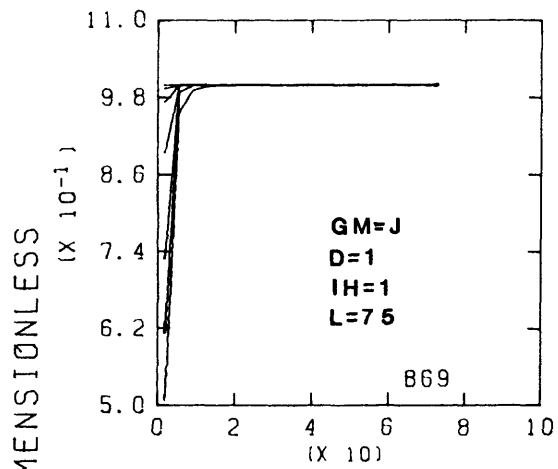
Graphs B63 and B64
Curve Dimensionless time

1	0.04
2	0.13
3	0.25
4	0.38
5	0.51
6	0.76
7	1.5
8	2.3
9	3.1



DISTANCE, DIMENSIONLESS
Curves numbered from top to bottom.

Graphs B65 and B66		Graphs B67 and B68	
Curve	Dimensionless time	Curve	Dimensionless time
1	0.005	1	0.005
2	0.015	2	0.015
3	0.030	3	0.030
4	0.061	4	0.061
5	0.14	5	0.14
6	0.23	6	0.23
7	0.37	7	0.39



DISTANCE, DIMENSIONLESS

Curves numbered from top to bottom.

Graphs B69 and B70

Graphs B71 and B72

Curve Dimensionless time

Curve Dimensionless time

1	0.010
2	0.030
3	0.061
4	0.12
5	0.27
6	0.46
7	0.74

1	0.000
2	0.007

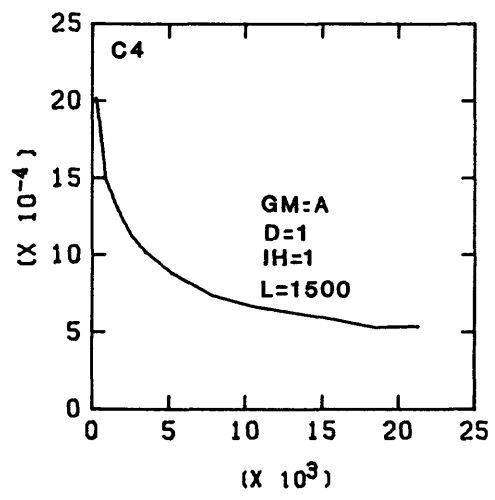
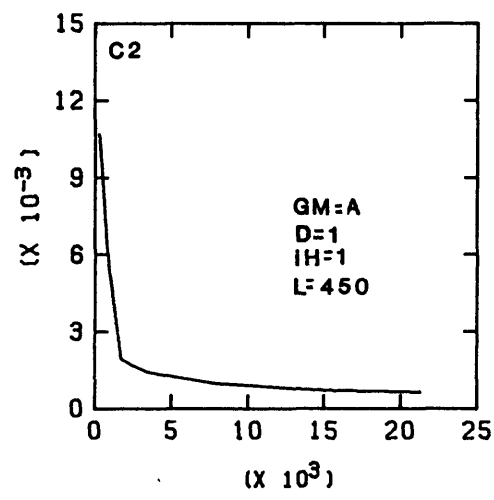
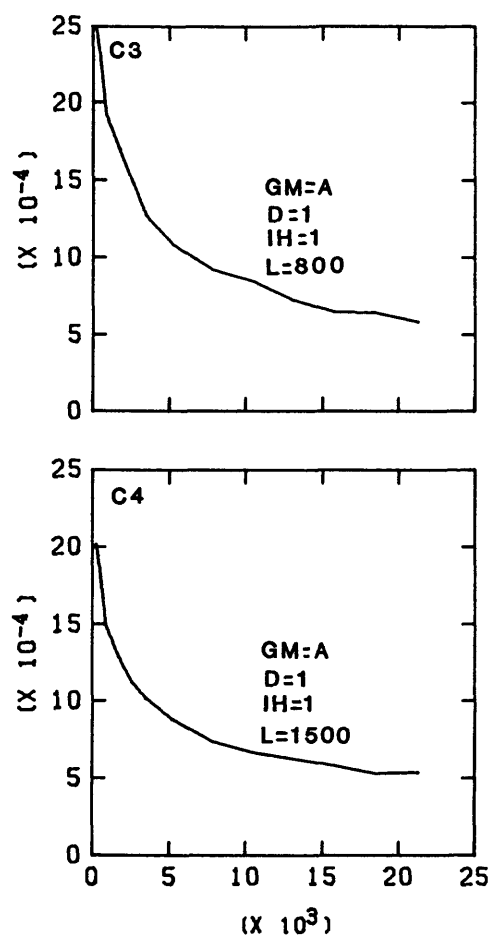
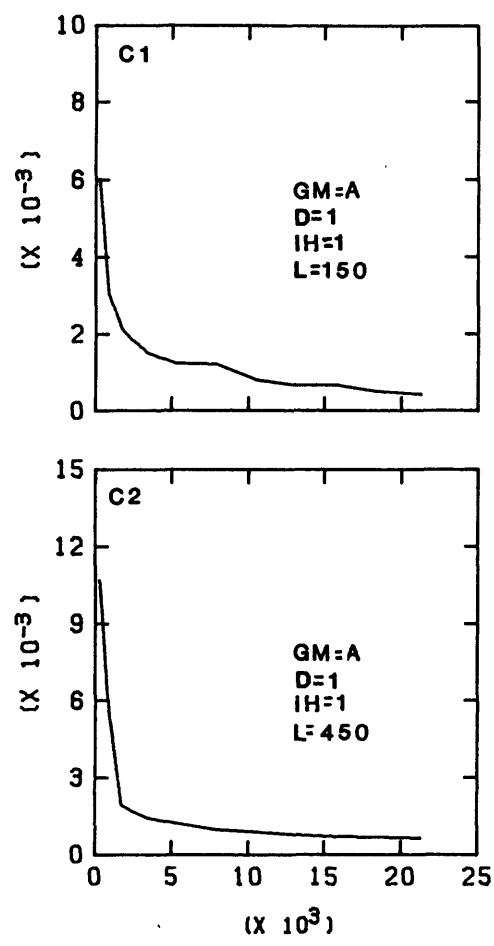
APPENDIX C

Dimensionless seepage-flux profiles for the hypothetical aquifers.

Symbols.--The following symbols appear with graphs C1 through C64 of Appendix C:

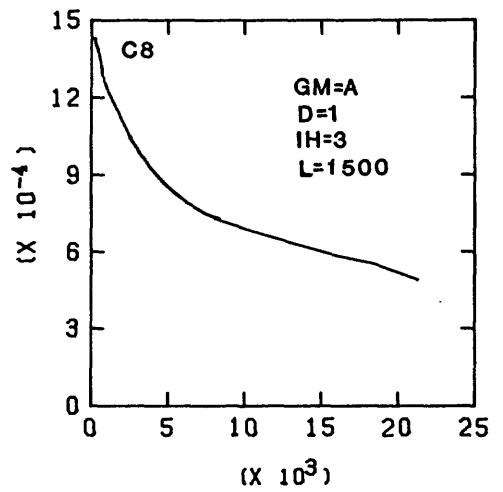
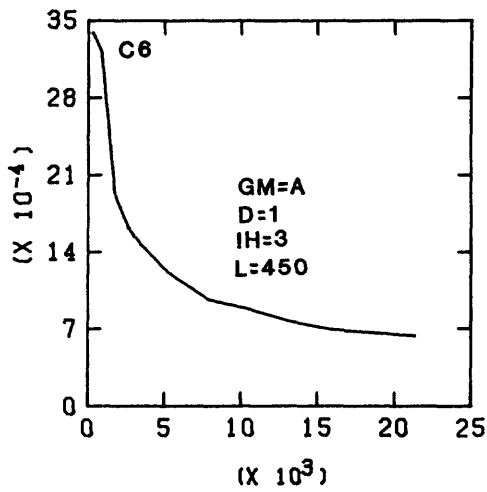
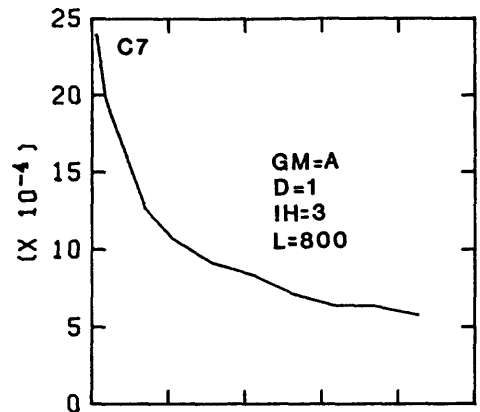
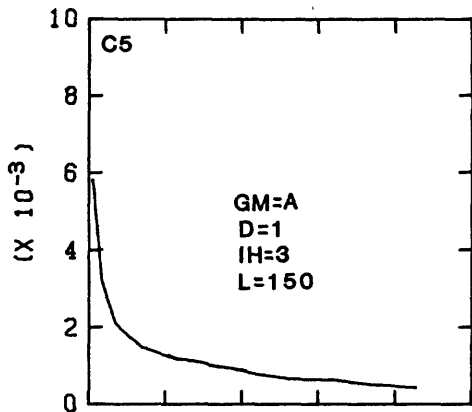
<u>Symbol</u>	<u>Explanation</u>
GM	Geologic material (table 1).
D	Initial saturated thickness, in meters.
IH	Initial head, in meters.
L	Length, in meters.

SEEPAGE FLUX, DIMENSIONLESS



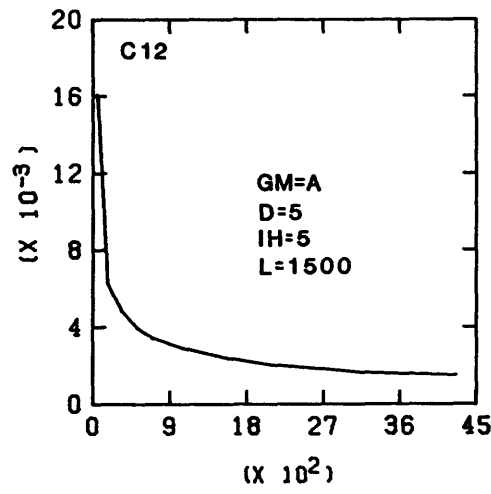
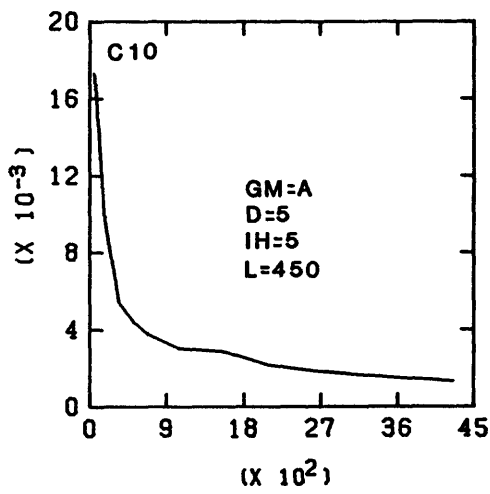
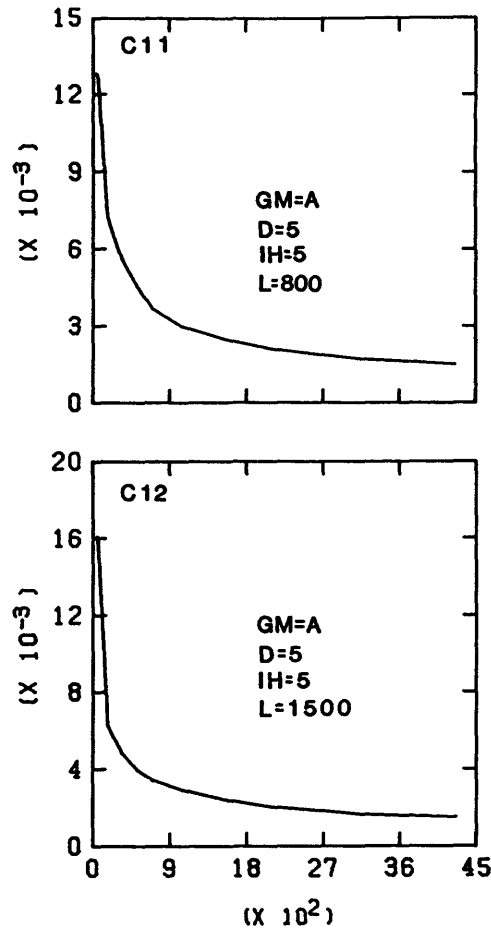
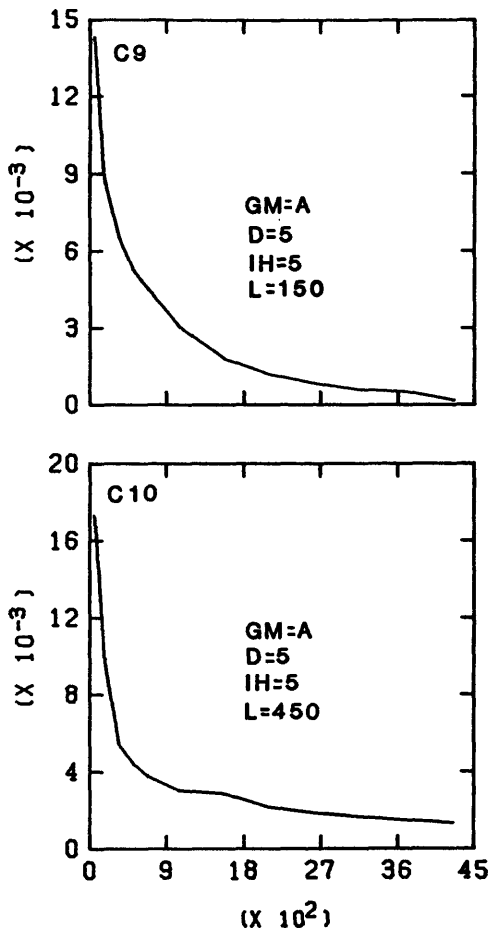
TIME, DIMENSIONLESS

SEEPAGE FLUX, DIMENSIONLESS



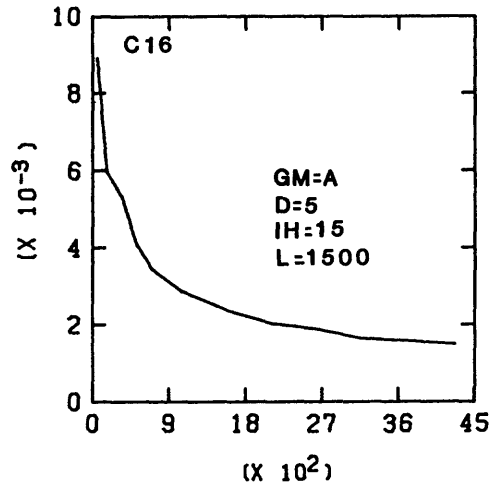
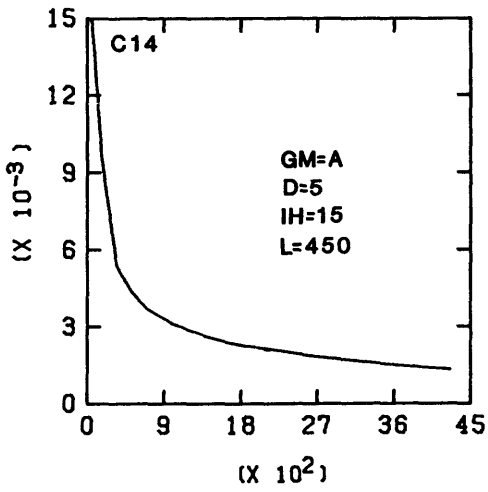
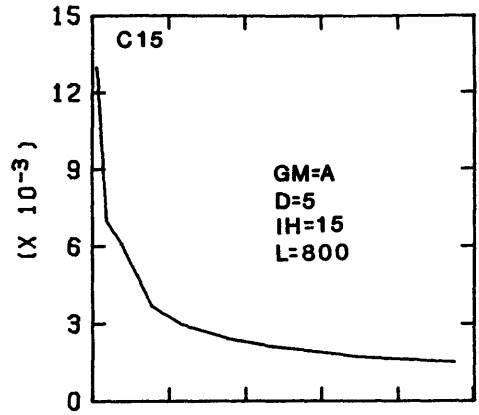
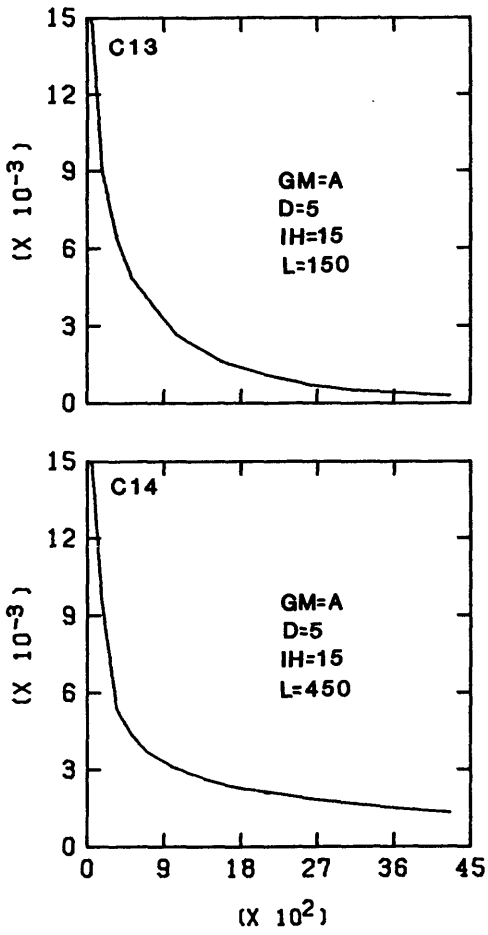
TIME, DIMENSIONLESS

SEEPAGE FLUX, DIMENSIONLESS



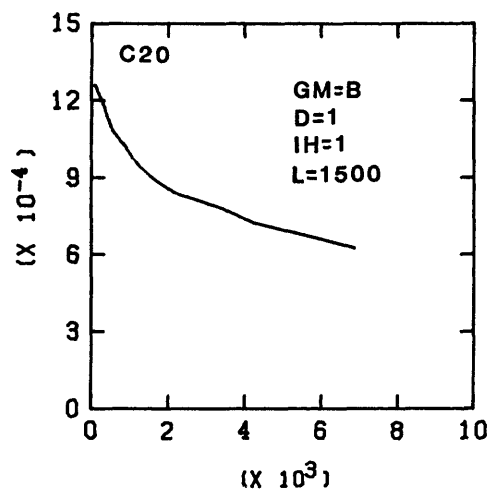
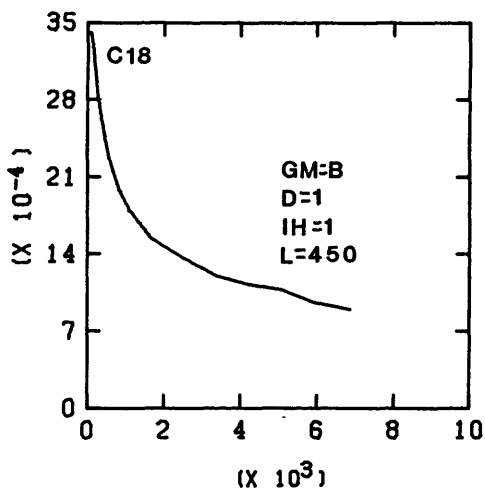
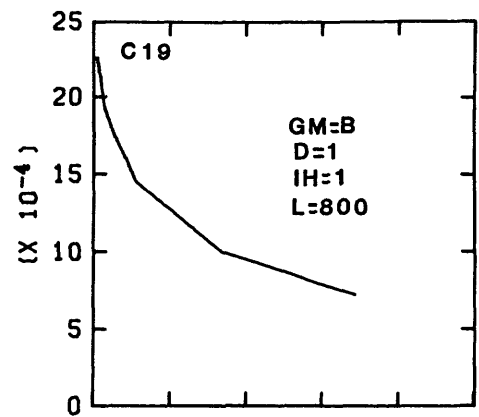
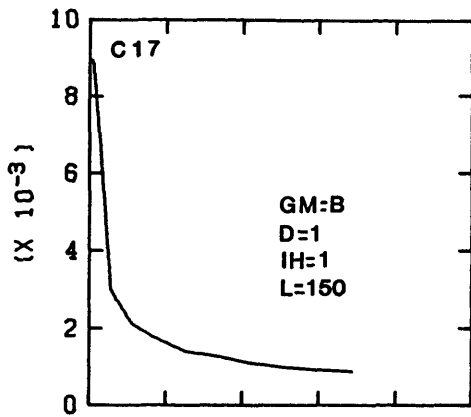
TIME, DIMENSIONLESS

SEEPAGE FLUX, DIMENSIONLESS



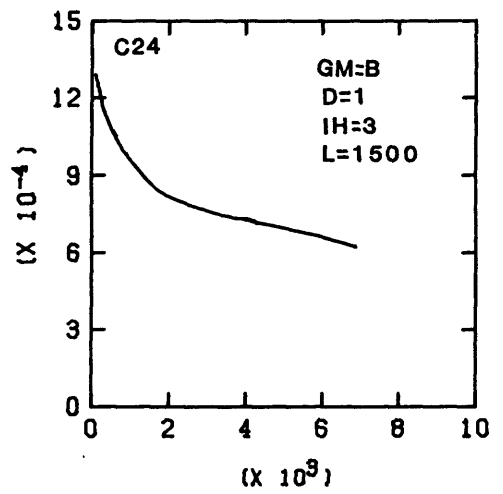
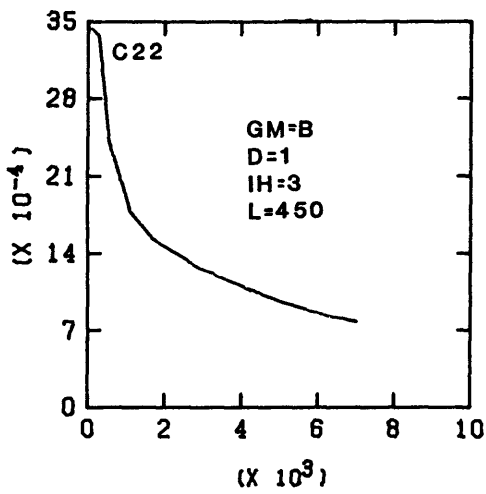
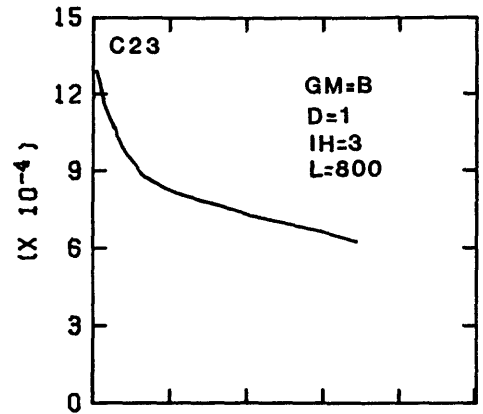
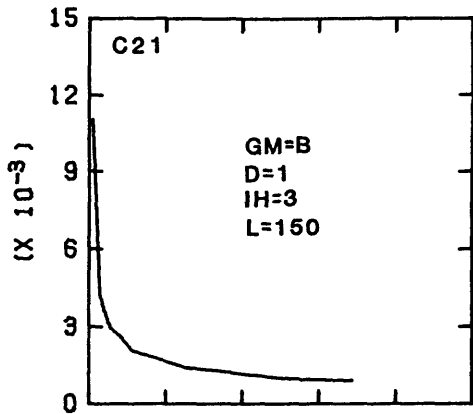
TIME, DIMENSIONLESS

SEEPAGE FLUX, DIMENSIONLESS



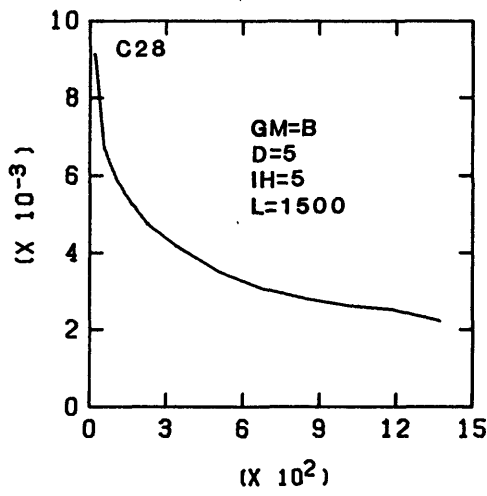
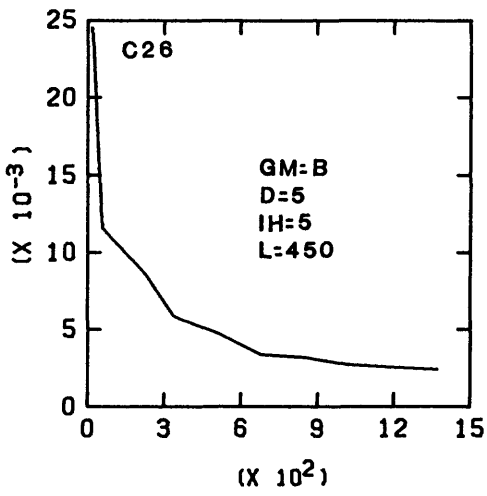
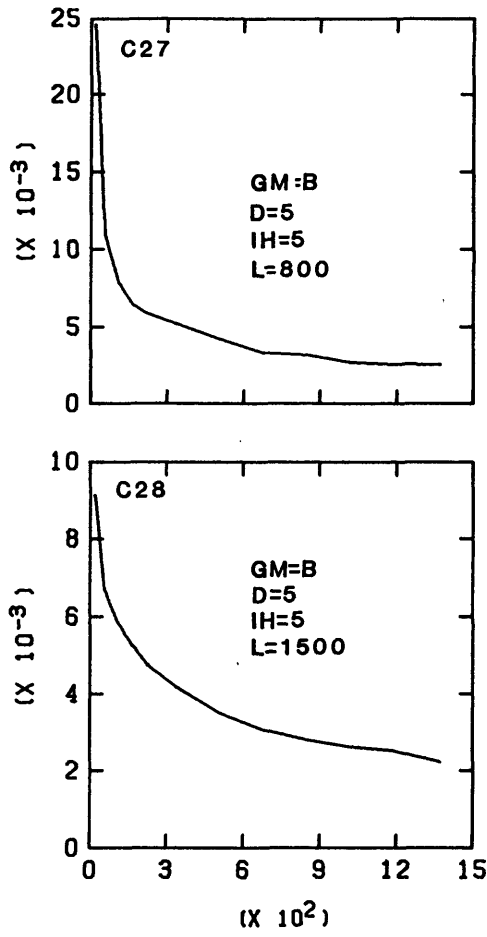
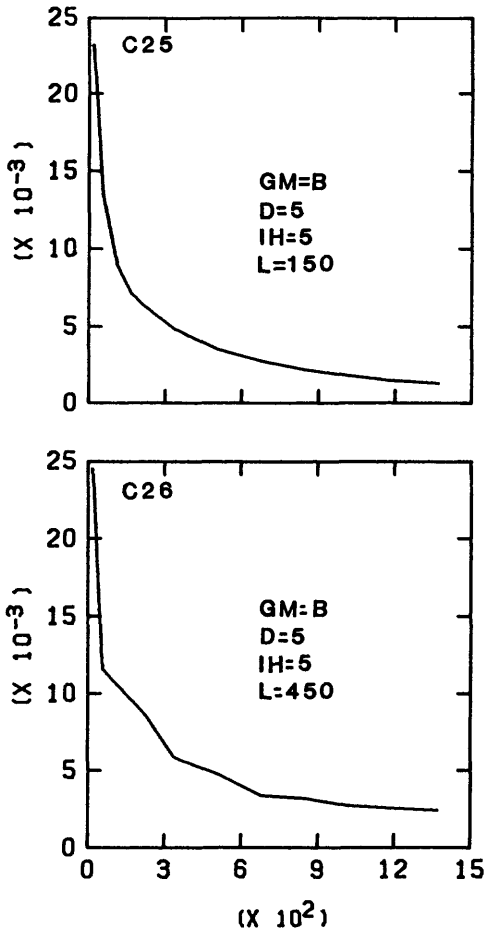
TIME, DIMENSIONLESS

SEEPAGE FLUX, DIMENSIONLESS



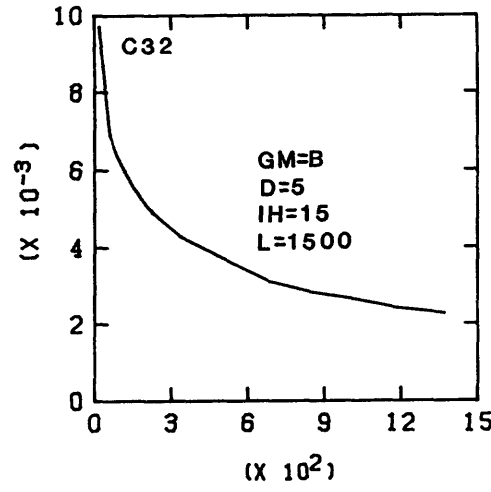
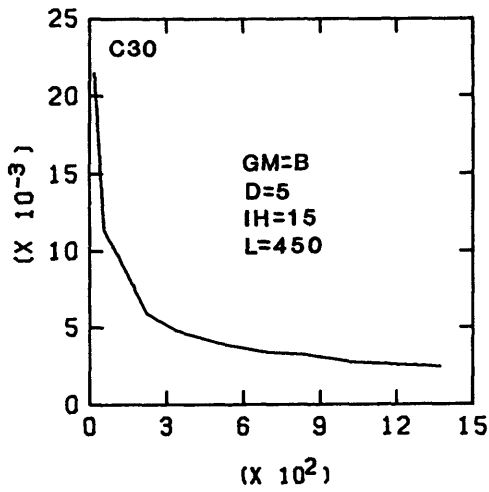
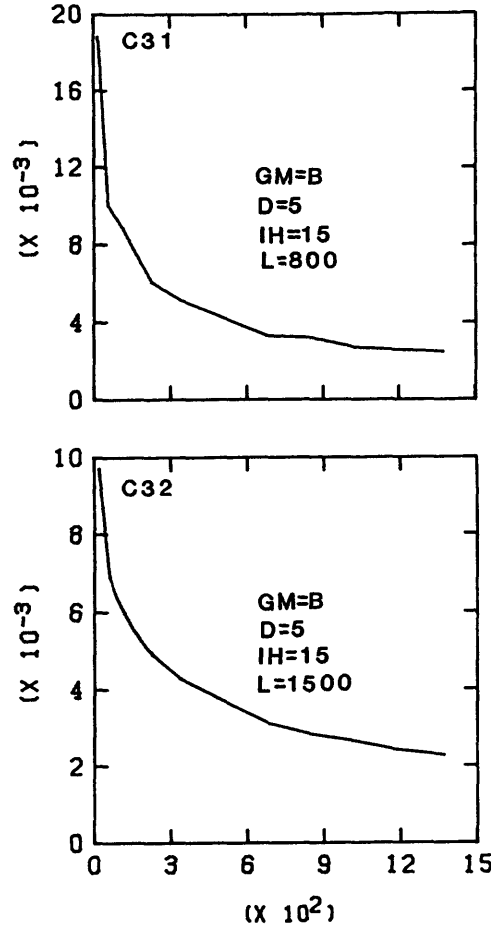
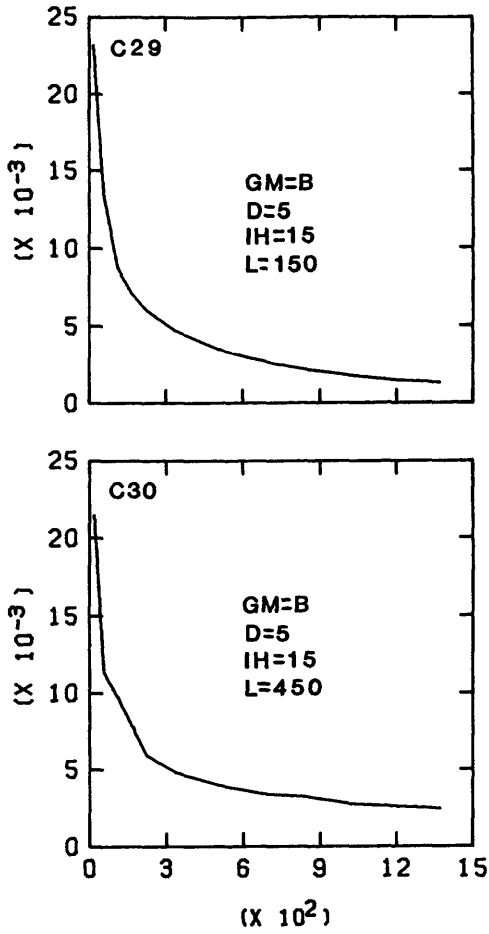
TIME, DIMENSIONLESS

SEEPAGE FLUX, DIMENSIONLESS



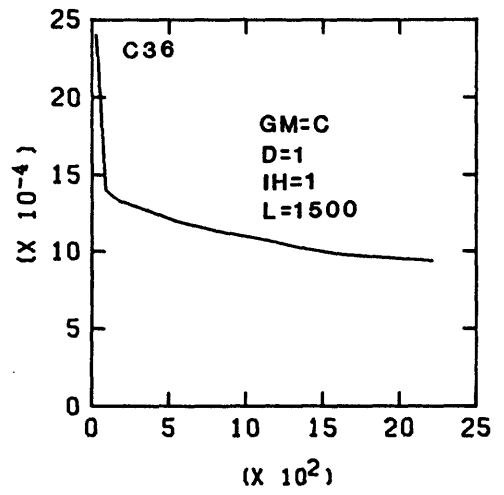
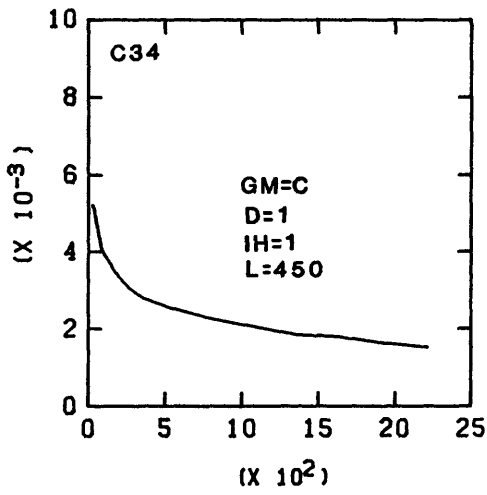
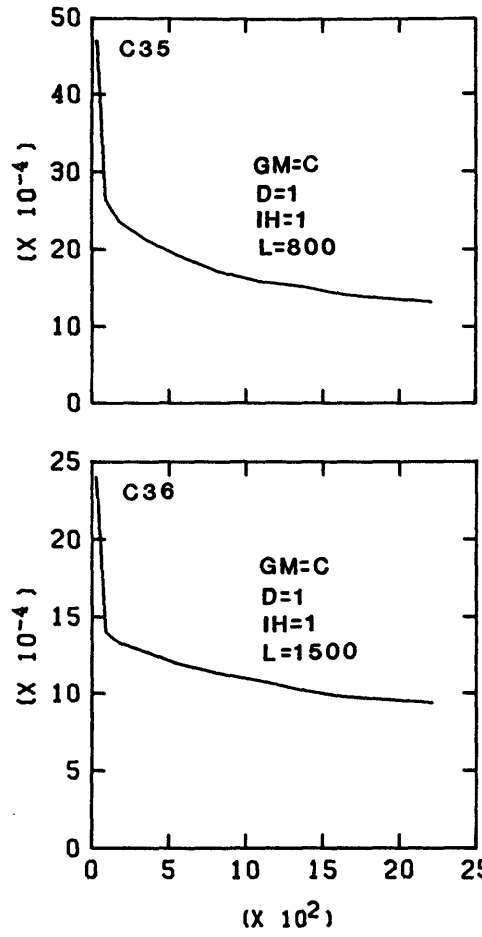
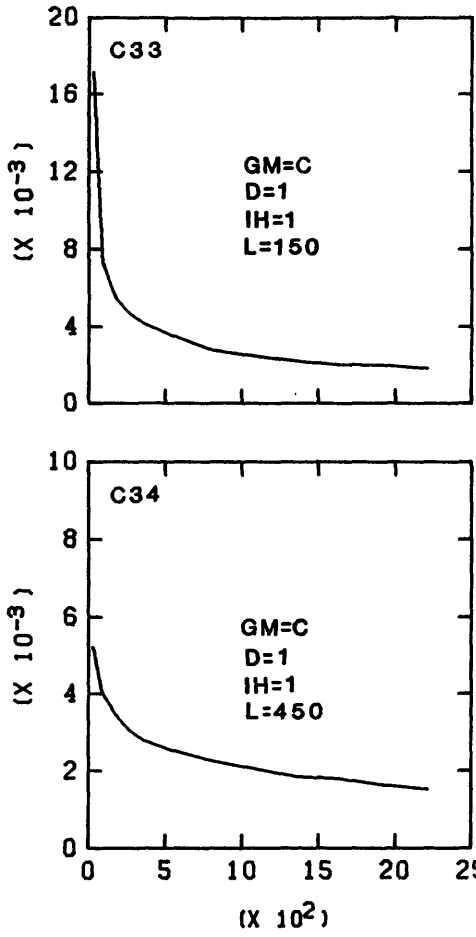
TIME, DIMENSIONLESS

SEEPAGE FLUX, DIMENSIONLESS



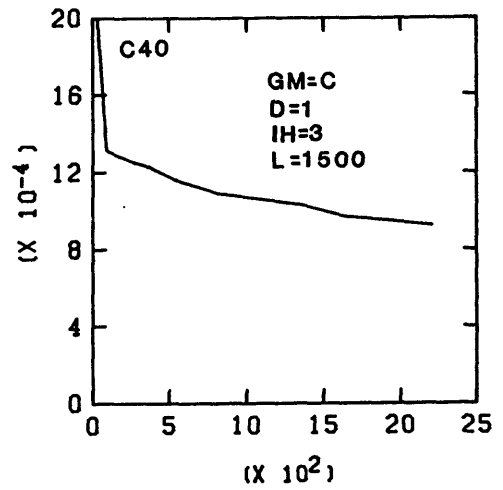
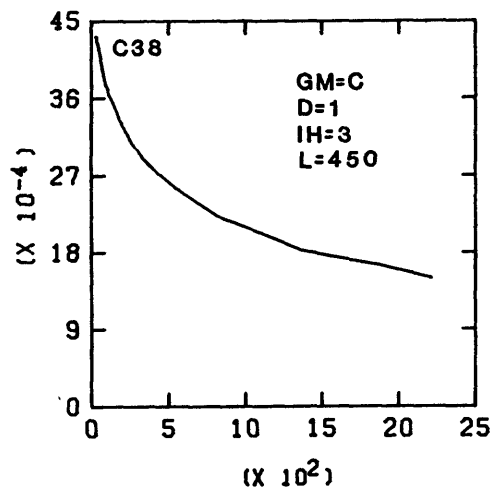
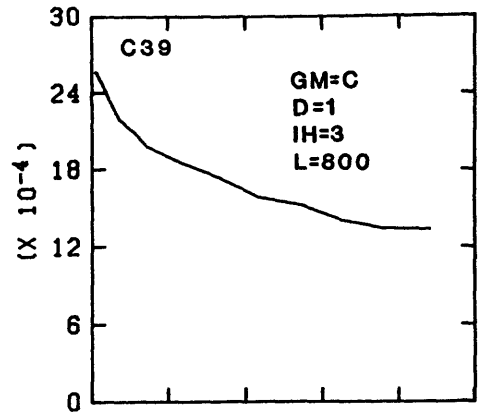
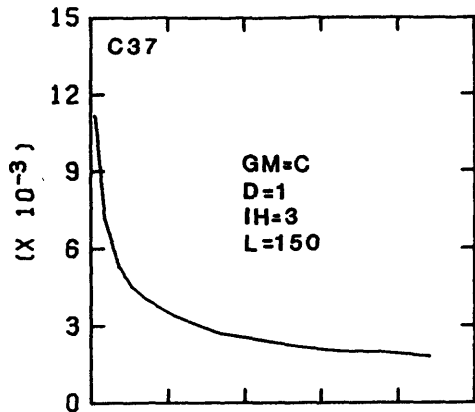
TIME, DIMENSIONLESS

SEEPAGE FLUX, DIMENSIONLESS



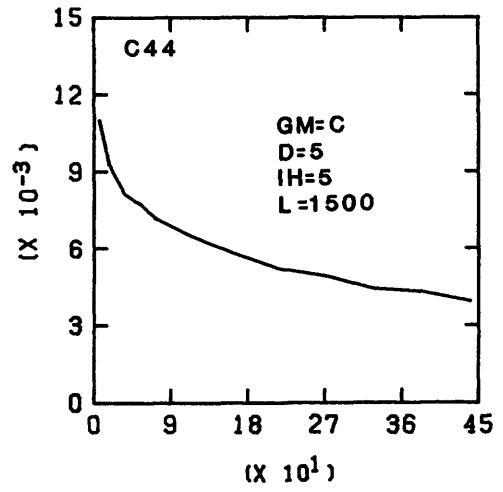
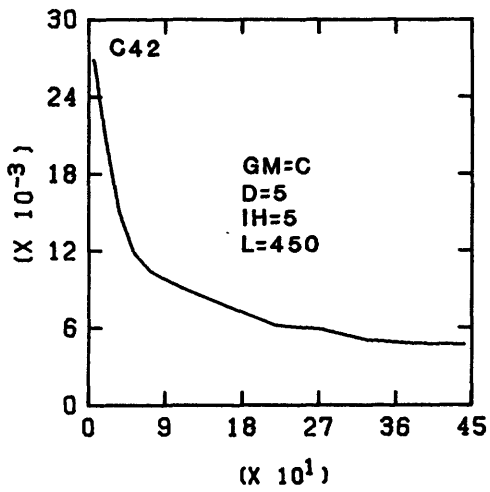
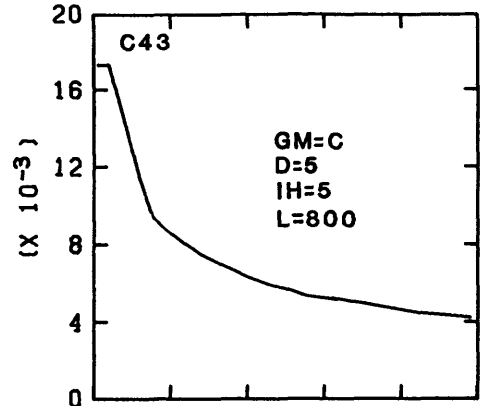
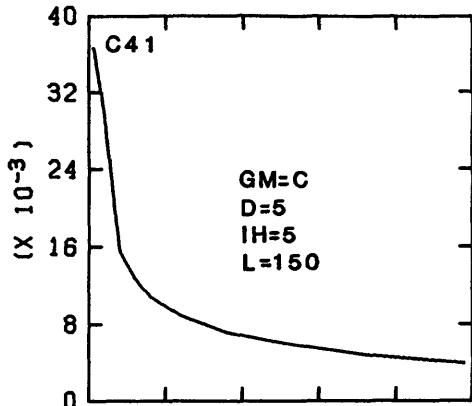
TIME, DIMENSIONLESS

SEEPAGE FLUX, DIMENSIONLESS



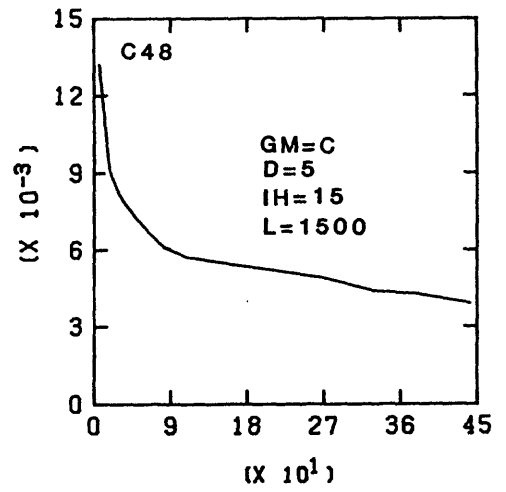
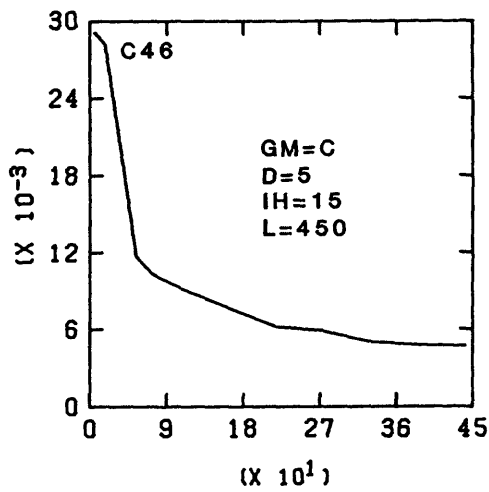
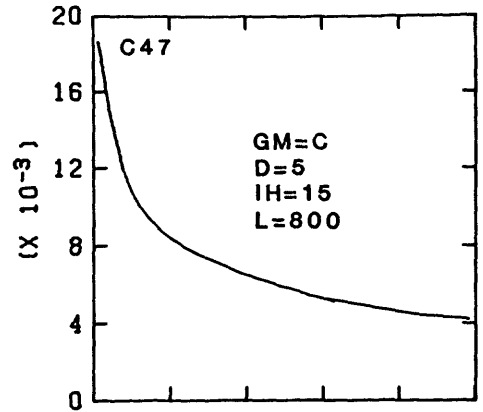
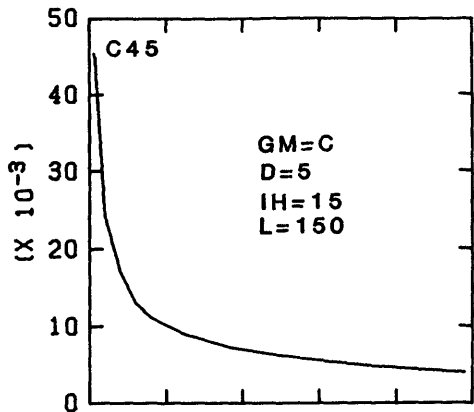
TIME, DIMENSIONLESS

SEEPAGE FLUX, DIMENSIONLESS



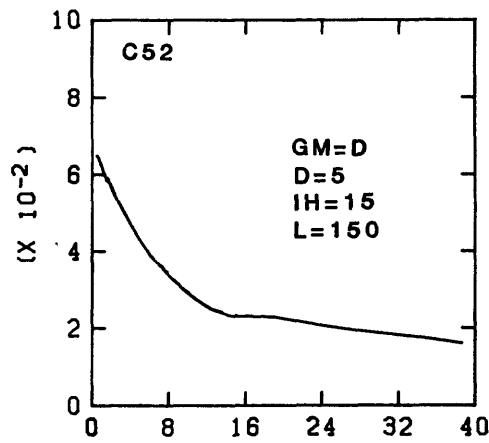
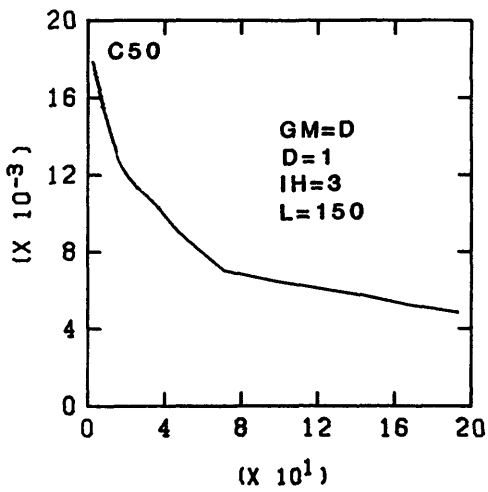
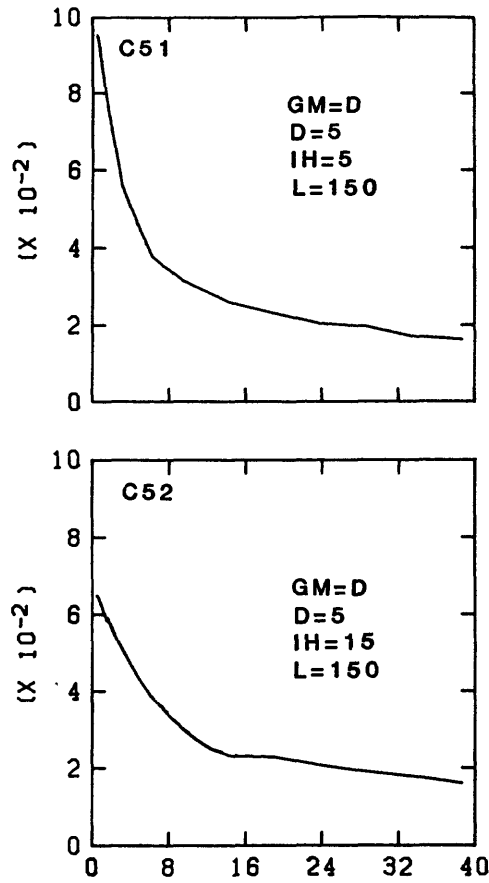
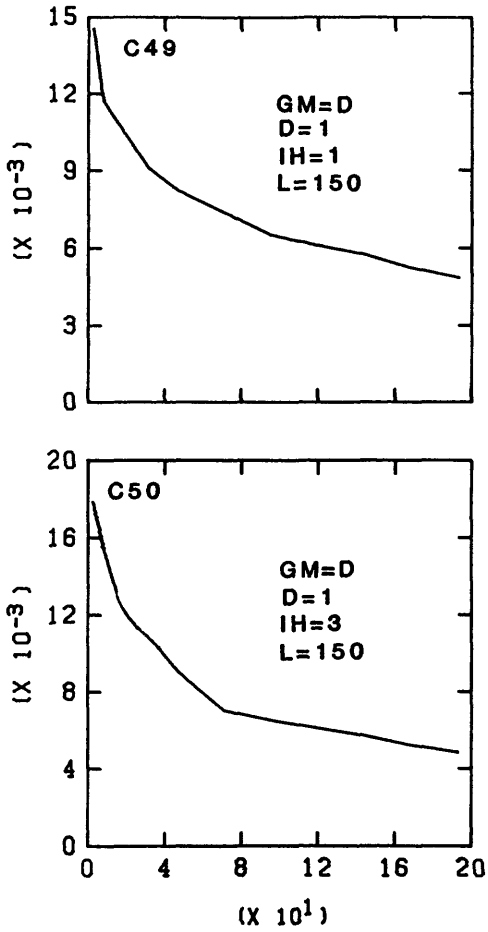
TIME, DIMENSIONLESS

SEEPAGE FLUX, DIMENSIONLESS



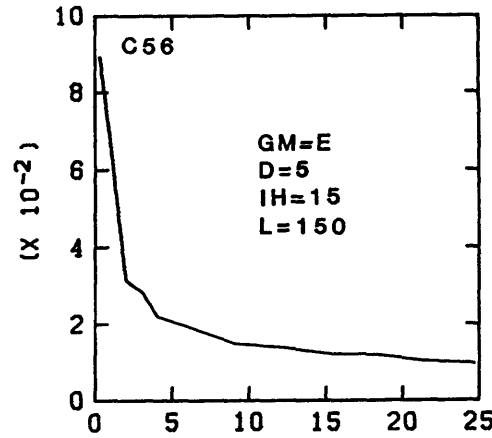
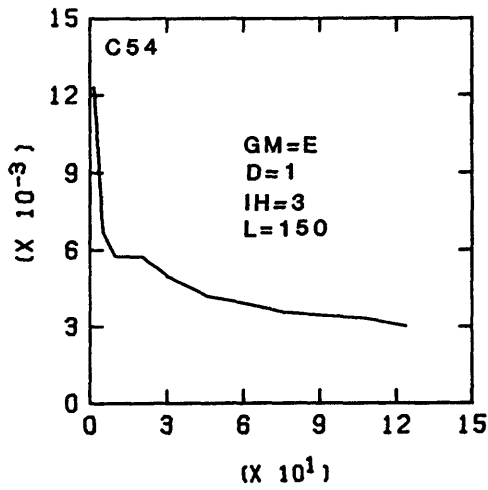
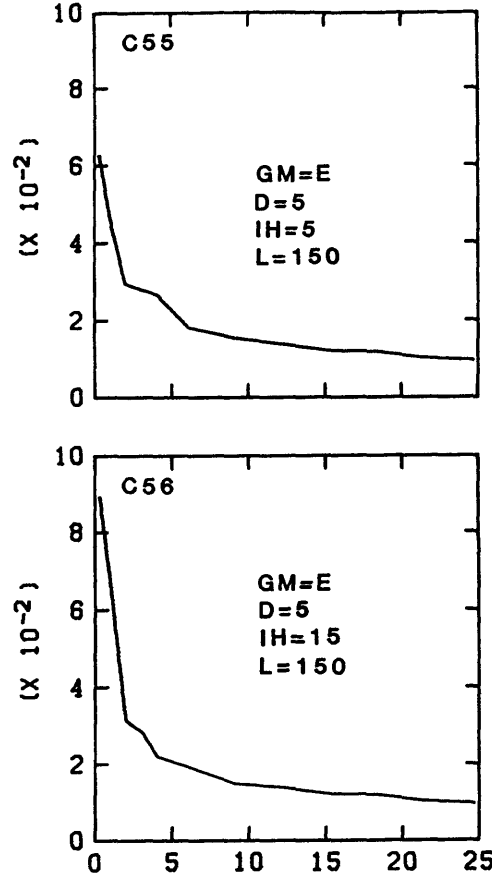
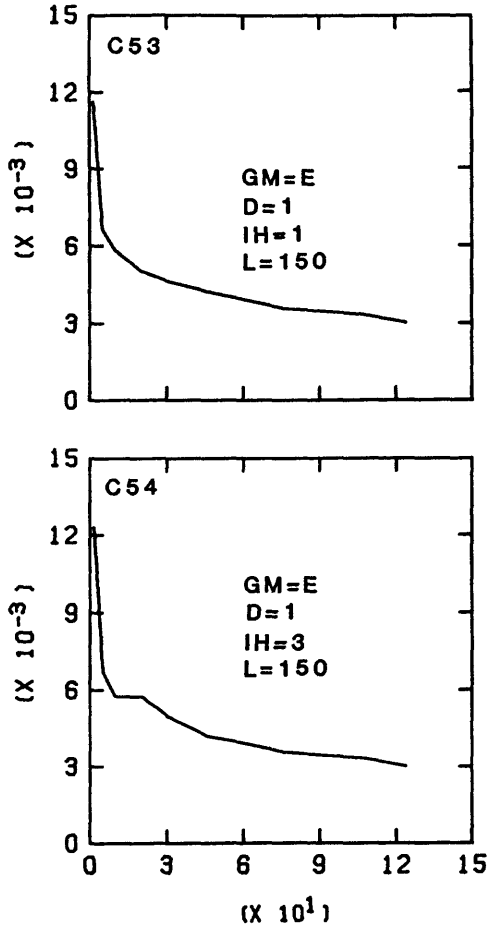
TIME, DIMENSIONLESS

SEEPAGE FLUX, DIMENSIONLESS



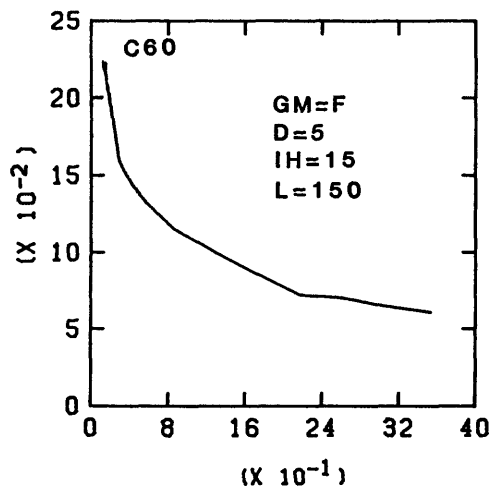
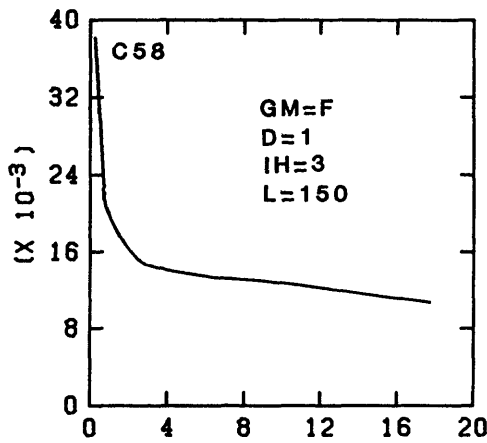
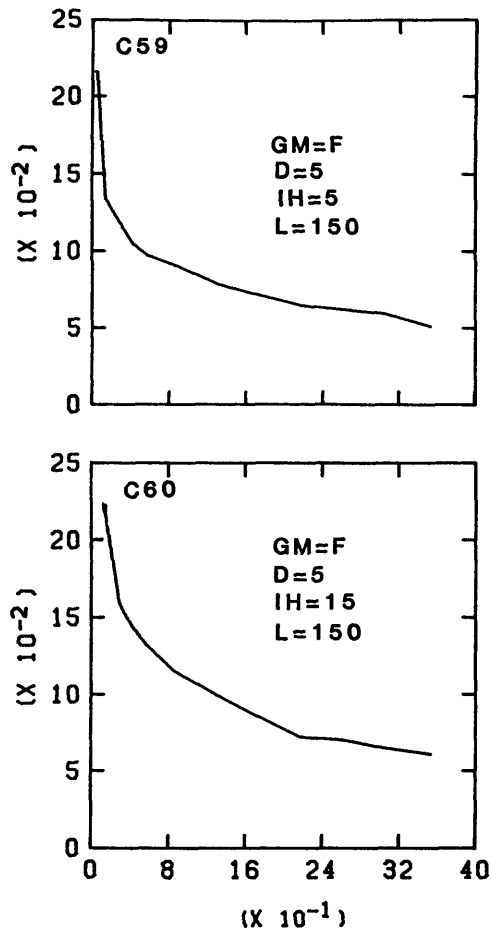
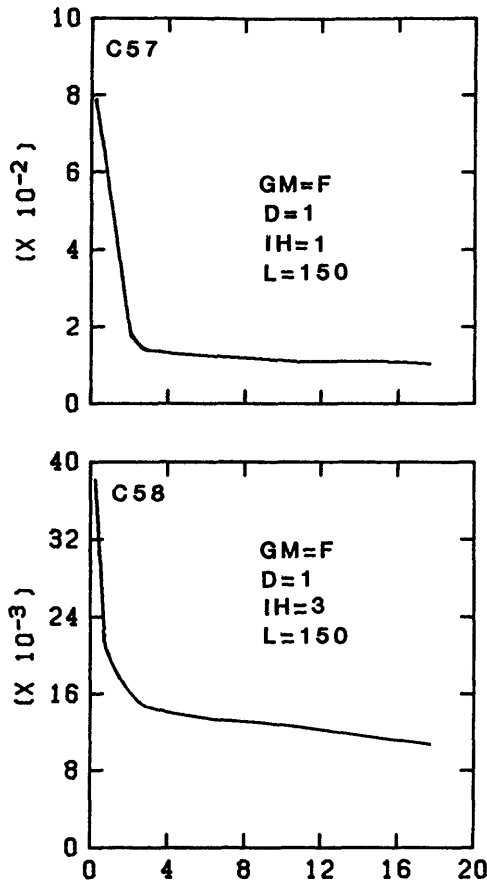
TIME, DIMENSIONLESS

SEEPAGE FLUX, DIMENSIONLESS



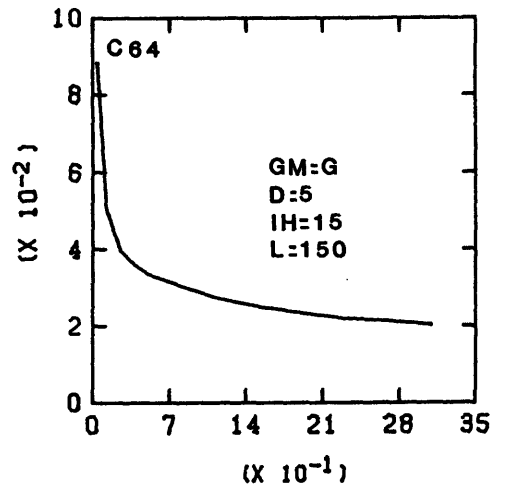
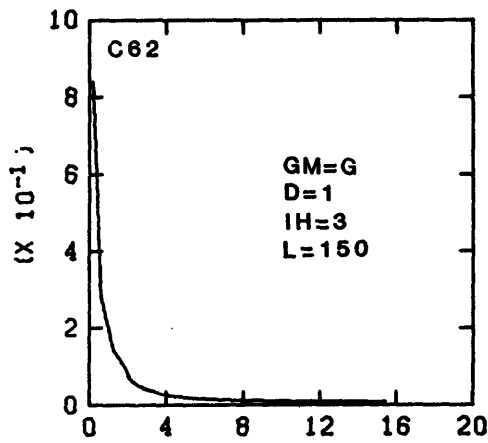
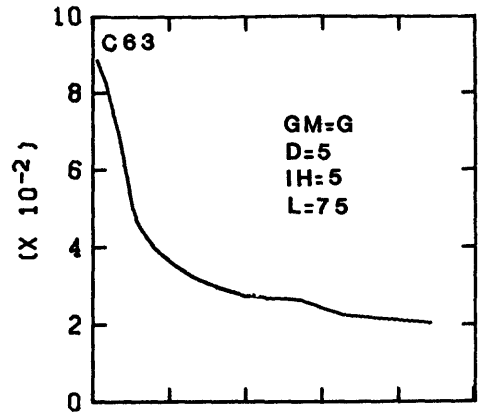
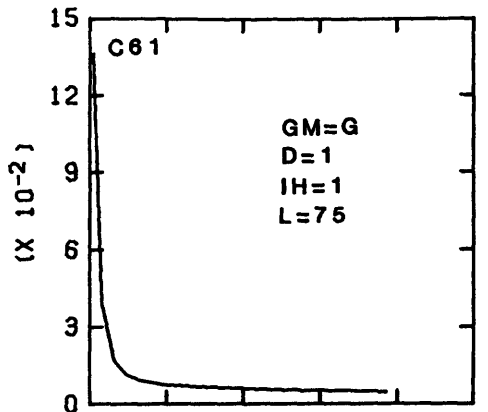
TIME, DIMENSIONLESS

SEEPAGE FLUX, DIMENSIONLESS



TIME, DIMENSIONLESS

SEEPAGE FLUX, DIMENSIONLESS



TIME, DIMENSIONLESS

APPENDIX D

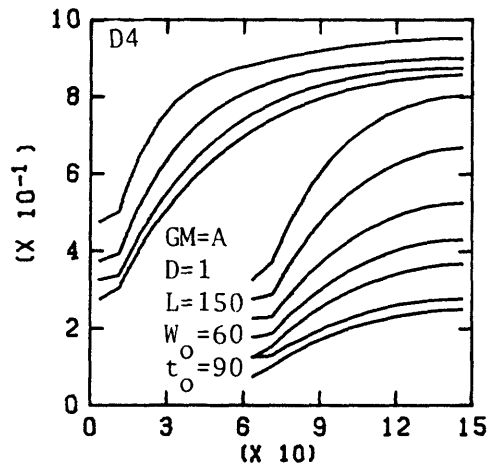
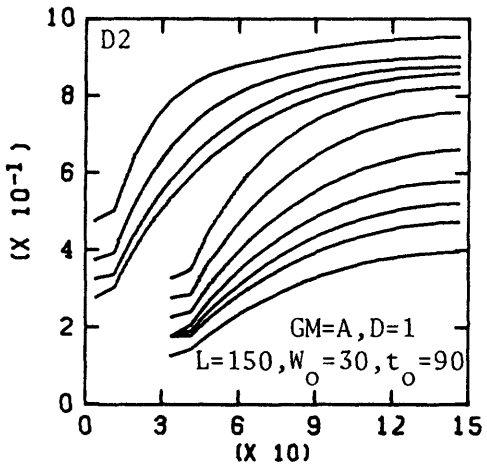
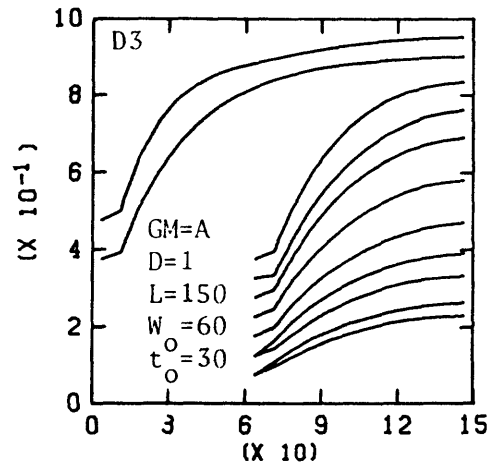
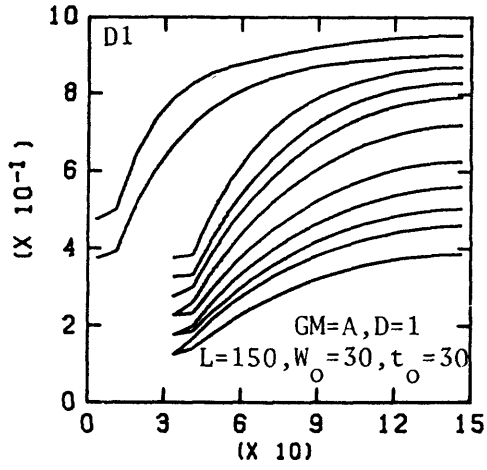
Dimensionless total-head profiles for the hypothetical-aquifer/multiple-cut combinations.

Symbols.--The following symbols appear with graphs D1 through D174 of Appendix D:

<u>Symbol</u>	<u>Explanation</u>
GM	Geologic material (table 1).
D	Initial saturated thickness, in meters.
L	Length, in meters.
w_0	Multiple-cut width, in meters.
t_0	Multiple-cut time, in days.

Note: Maximum head values in many figures coincide with top of graphs.

HEAD, DIMENSIONLESS



DISTANCE, DIMENSIONLESS

Curves numbered from top to bottom.

Graphs D1 and D2

Graphs D3 and D4

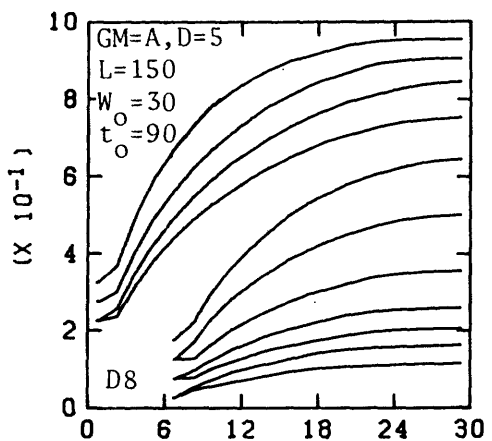
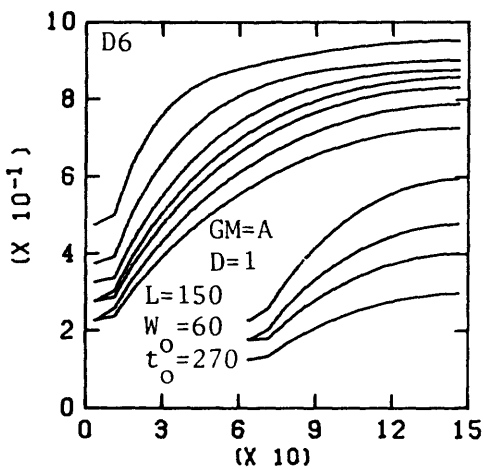
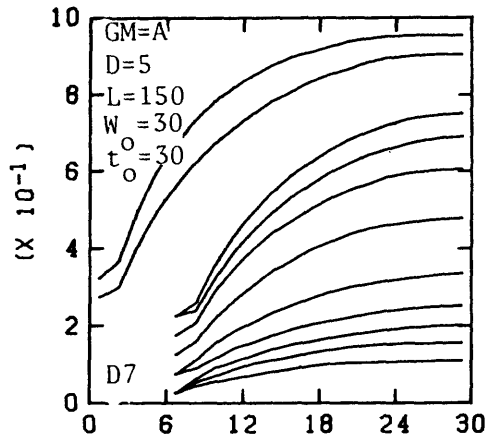
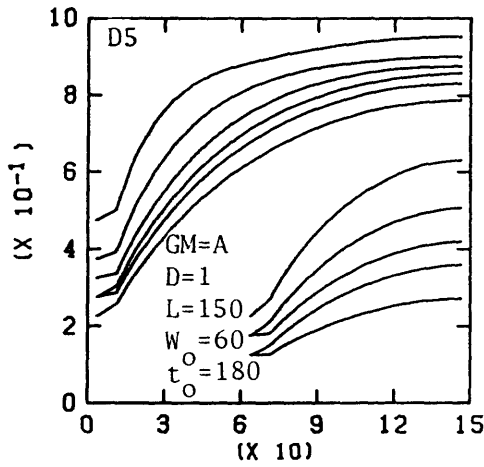
Curve Dimensionless time

Curve Dimensionless time

1	292
2	876
3	1752
4	2628
5	3504
6	5256
7	7884
8	10512
9	13139
10	15767
11	21315

1	292
2	876
3	1752
4	2628
5	3504
6	5256
7	7884
8	10512
9	13139
10	18395
11	21315

HEAD, DIMENSIONLESS



DISTANCE, DIMENSIONLESS

Curves numbered from top to bottom.

Graphs D5 and D6

Graphs D7 and D8

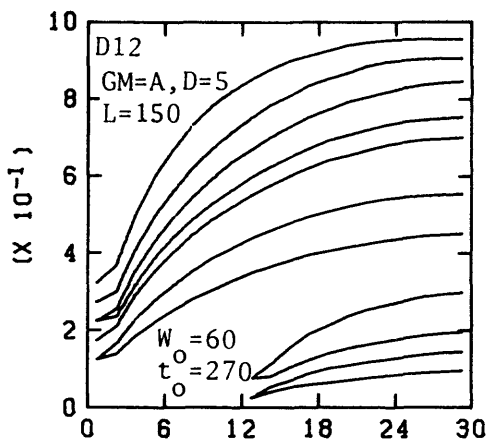
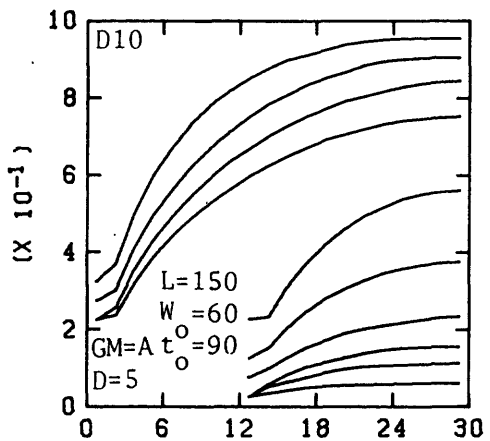
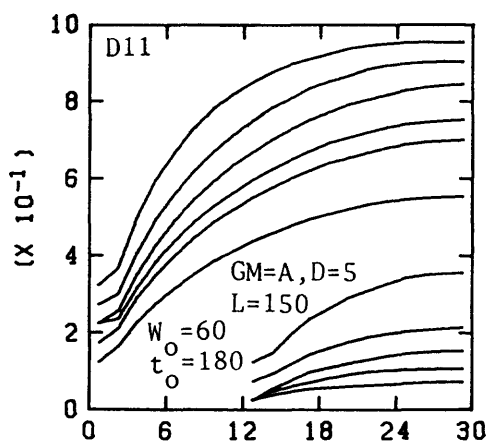
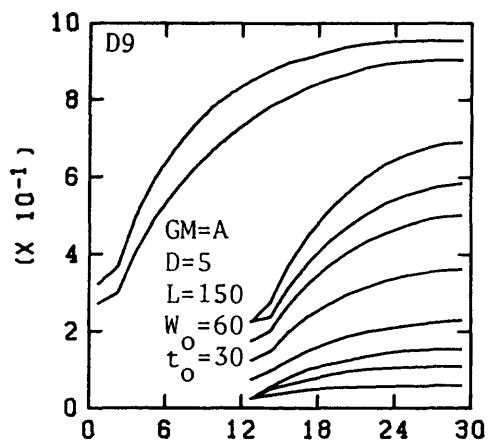
Curve Dimensionless time

Curve Dimensionless time

1	292
2	876
3	1752
4	2628
5	3504
6	5256
7	7884
8	10512
9	13139
10	15767
11	21315

1	58
2	175
3	350
4	526
5	701
6	1051
7	1577
8	2102
9	2628
10	3153
11	4263

HEAD, DIMENSIONLESS



DISTANCE, DIMENSIONLESS

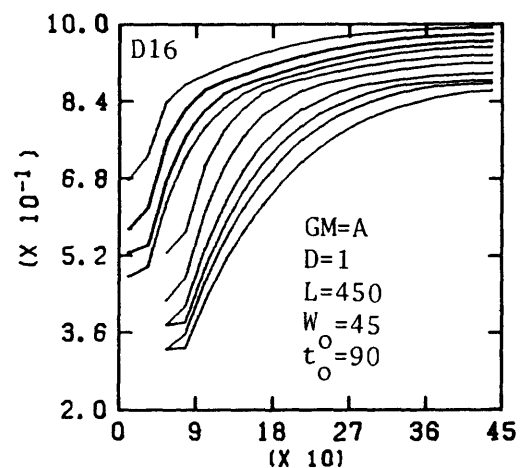
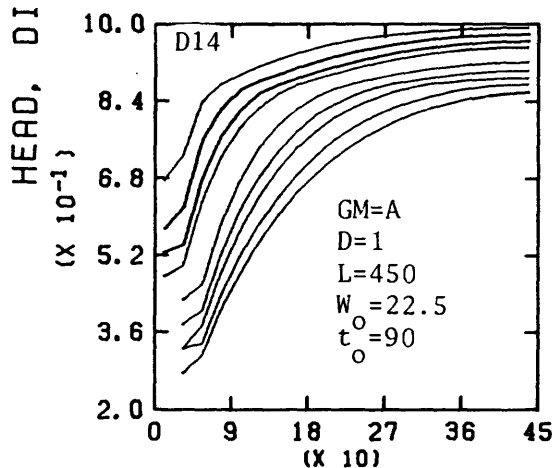
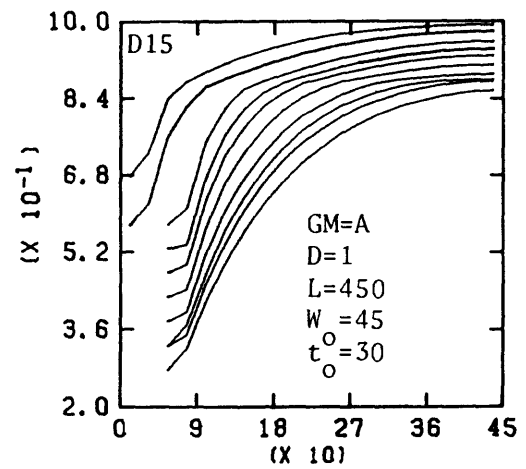
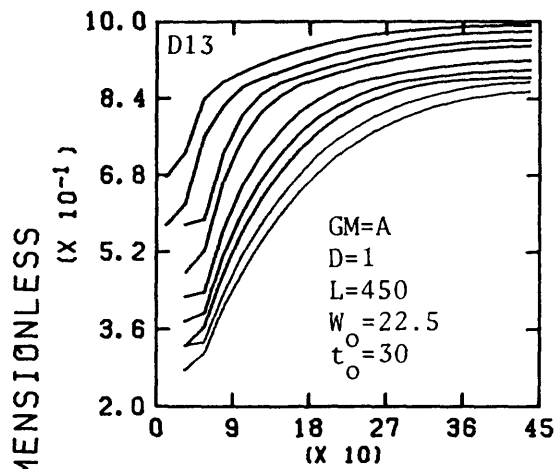
Curves numbered from top to bottom.

Graphs D9 and D10

Graphs D11 and D12

Curve	Dimensionless time
1	58
2	175
3	350
4	526
5	701
6	1051
7	1577
8	2102
9	2628
10	4263

Curve	Dimensionless time
1	58
2	175
3	350
4	526
5	701
6	1051
7	1577
8	2102
9	2628
10	3153
11	4263



DISTANCE, DIMENSIONLESS

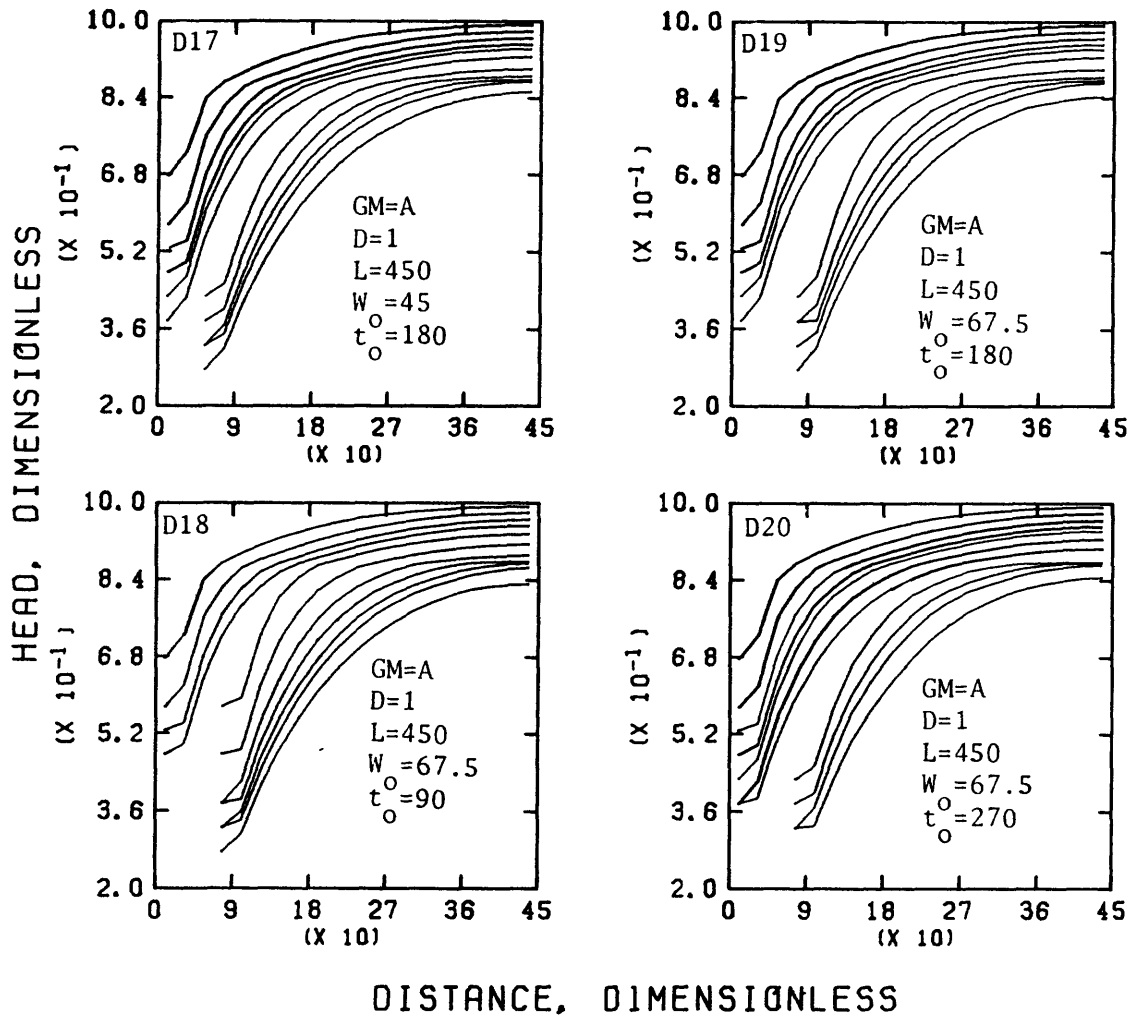
Curves numbered from top to bottom.

Graphs D13 and D14

Graphs D15 and D16

Curve	Dimensionless time
1	292
2	876
3	1752
4	2628
5	5256
6	7884
7	10512
8	15767
9	21315

Curve	Dimensionless time
1	292
2	876
3	1752
4	2628
5	3504
6	5256
7	7884
8	10512
9	13139
10	18395



Curves numbered from top to bottom.

Graphs D17 and D18

Graphs D19 and D20

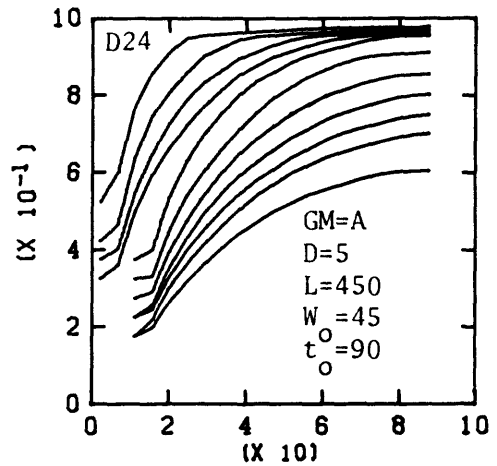
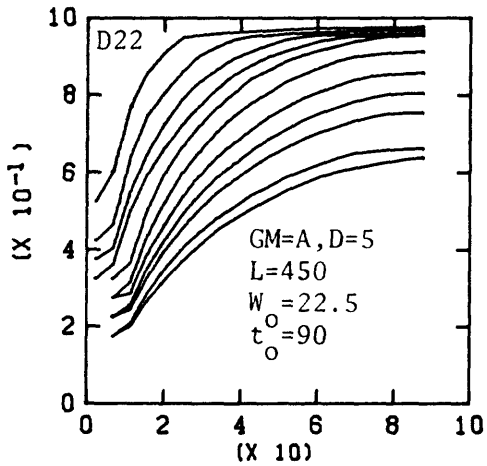
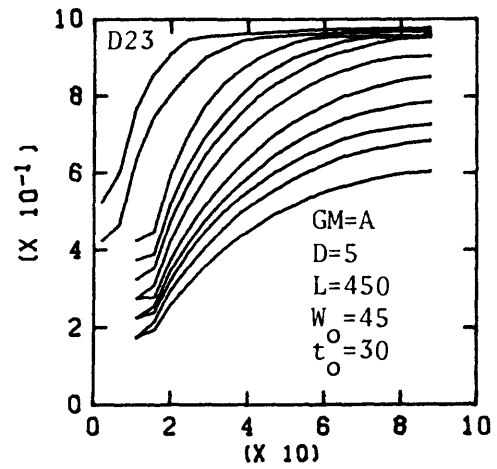
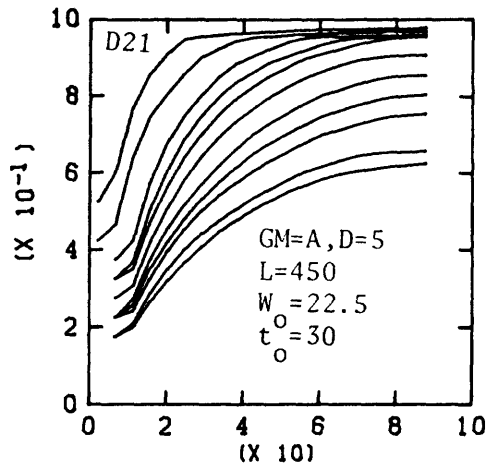
Curve Dimensionless time

1	292
2	876
3	1752
4	2628
5	3504
6	5256
7	7884
8	10512
9	13139
10	15767
11	21315

Curve Dimensionless time

1	292
2	876
3	1752
4	2628
5	3504
6	5256
7	7884
8	10512
9	13139
10	15767
11	21315

HEAD, DIMENSIONLESS
(X 10⁻¹)



DISTANCE, DIMENSIONLESS

Curves numbered from top to bottom.

Graphs D21 and D22

Graphs D23 and D24

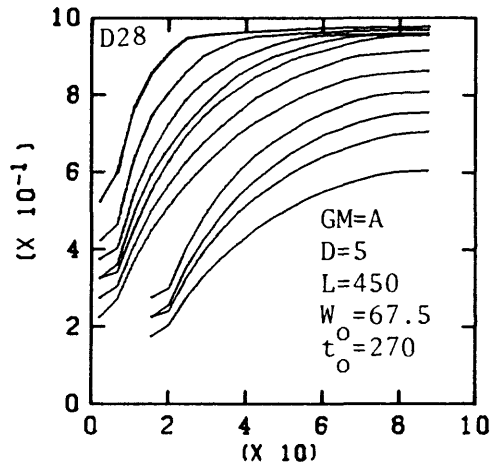
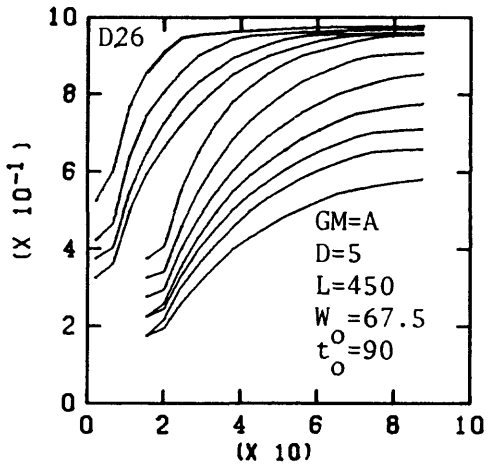
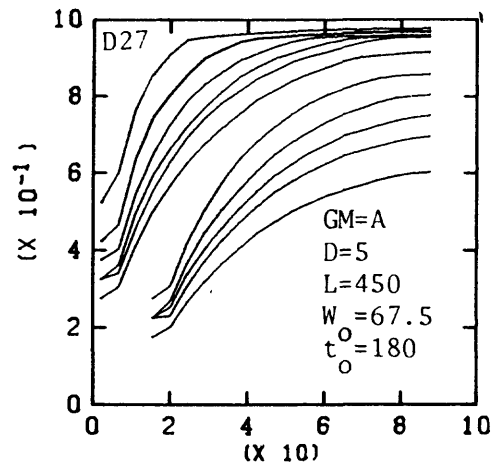
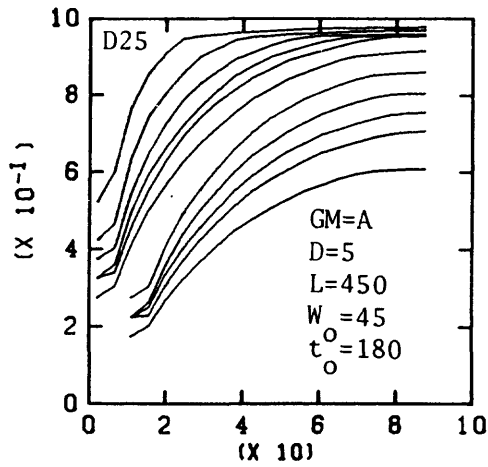
Curve Dimensionless time

1	58
2	175
3	350
4	526
5	701
6	1051
7	1577
8	2102
9	2628
10	3679
11	4263

Curve Dimensionless time

1	58
2	175
3	350
4	526
5	701
6	1051
7	1577
8	2102
9	2628
10	3153
11	4263

HEAD, DIMENSIONLESS
(X 10⁻¹)



DISTANCE, DIMENSIONLESS

Curves numbered from top to bottom.

Graphs D25 and D26

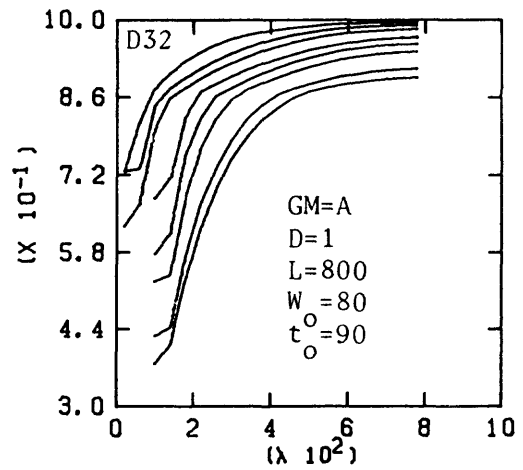
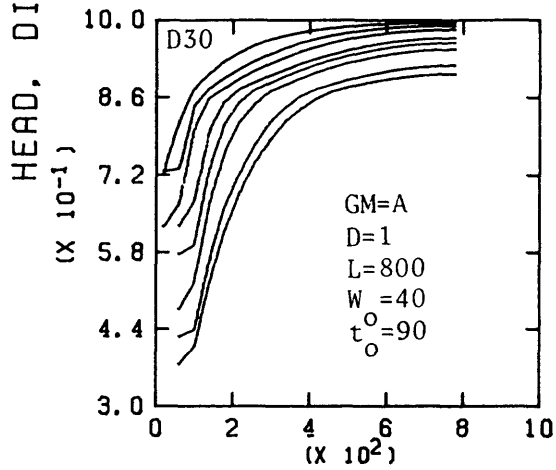
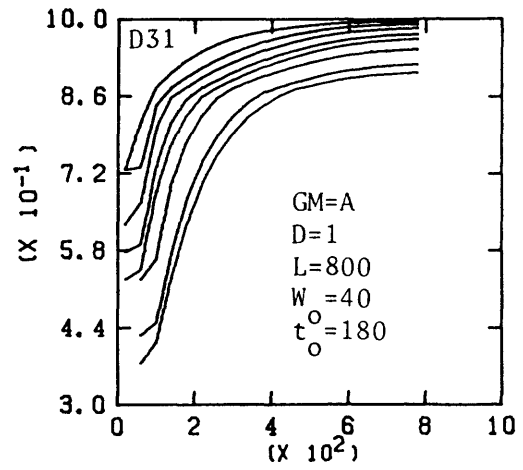
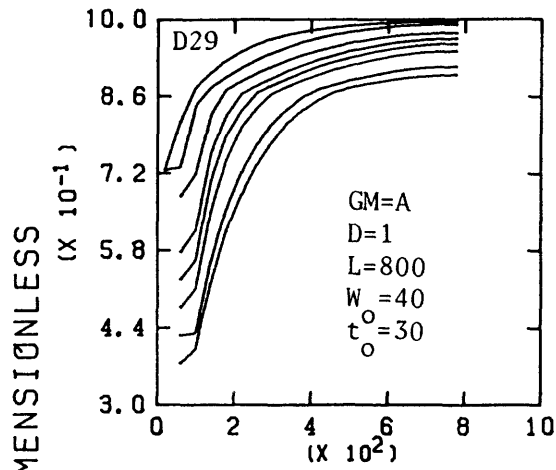
Graphs D27 and D28

Curve Dimensionless time

1	58
2	175
3	350
4	526
5	701
6	1051
7	1577
8	2102
9	2628
10	3153
11	4263

Curve Dimensionless time

1	58
2	175
3	350
4	526
5	701
6	1051
7	1577
8	2102
9	2628
10	3153
11	4263



DISTANCE, DIMENSIONLESS

Curves numbered from top to bottom.

Graphs D29 and D30

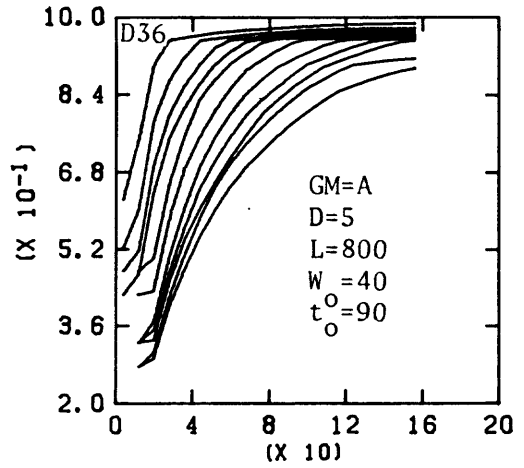
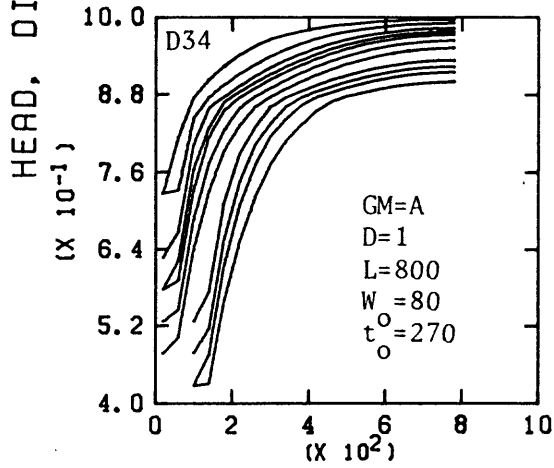
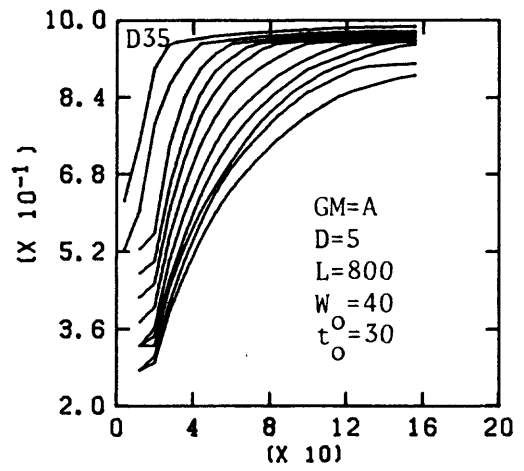
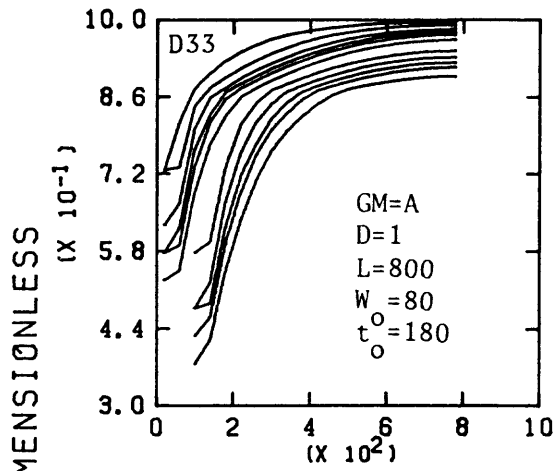
Graphs D31 and D32

Curve Dimensionless time

Curve Dimensionless time

1	292
2	876
3	1752
4	3504
5	5256
6	7884
7	15767
8	21315

1	292
2	876
3	1752
4	3504
5	5256
6	7884
7	15767
8	21315



DISTANCE, DIMENSIONLESS

Curves numbered from top to bottom.

Graphs D33 and D34

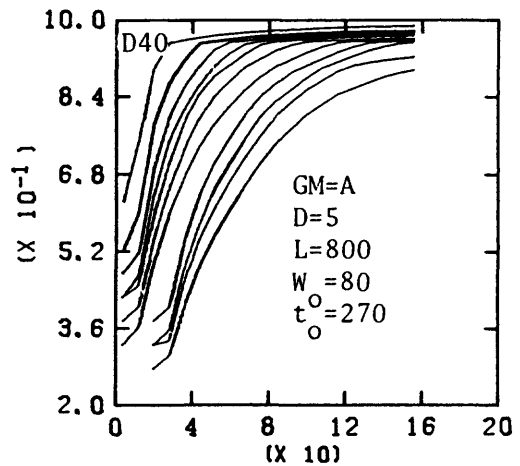
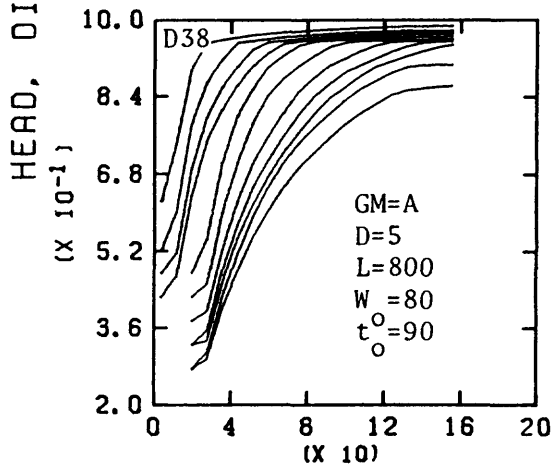
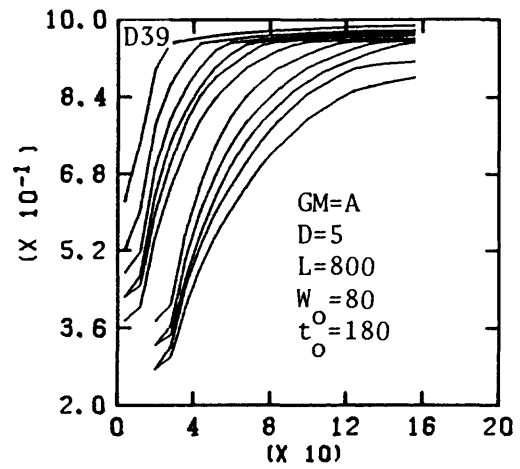
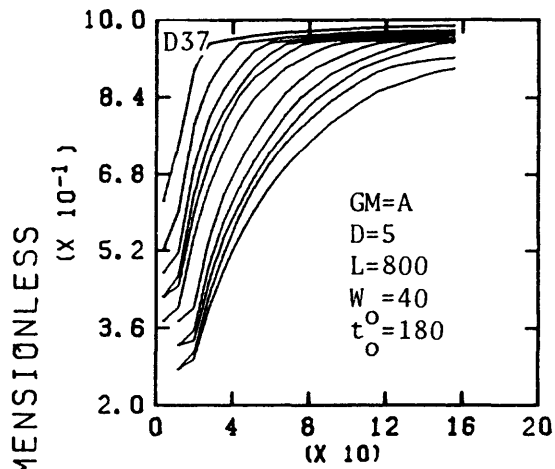
Graphs D35 and D36

Curve Dimensionless time

Curve Dimensionless time

1	292
2	876
3	1752
4	2628
5	3504
6	5256
7	7884
8	10512
9	13139
10	15767
11	21315

1	58
2	175
3	350
4	526
5	701
6	1051
7	1577
8	2102
9	2628
10	3153
11	4263



DISTANCE, DIMENSIONLESS

Curves numbered from top to bottom.

Graphs D37 and D38

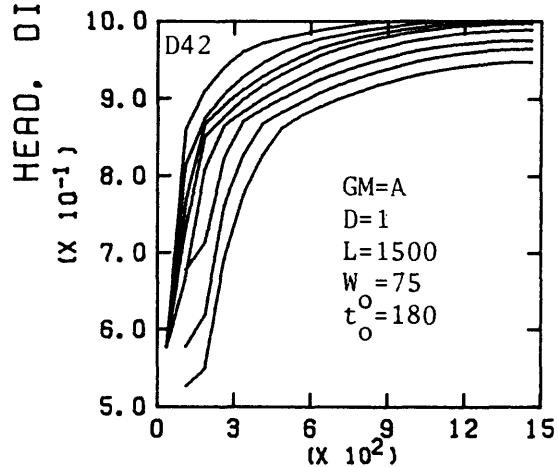
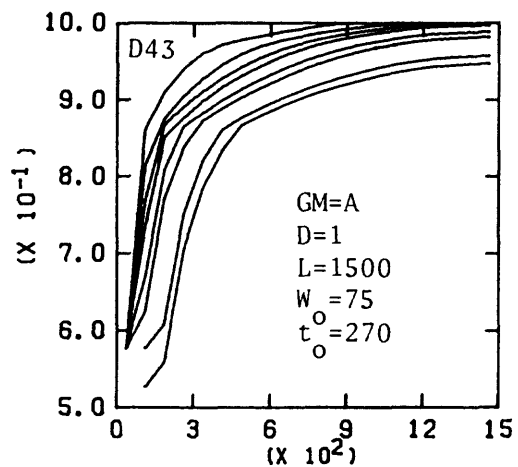
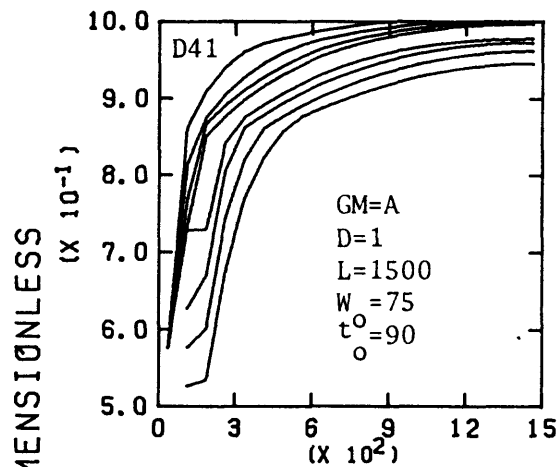
Graphs D39 and D40

Curve Dimensionless time

1	58
2	175
3	350
4	526
5	701
6	1051
7	1577
8	2102
9	2628
10	3153
11	4263

Curve Dimensionless time

1	58
2	175
3	350
4	526
5	701
6	1051
7	1577
8	2102
9	2628
10	3153
11	4263



DISTANCE, DIMENSIONLESS

Curves numbered from top to bottom.

Graphs D41 and D42

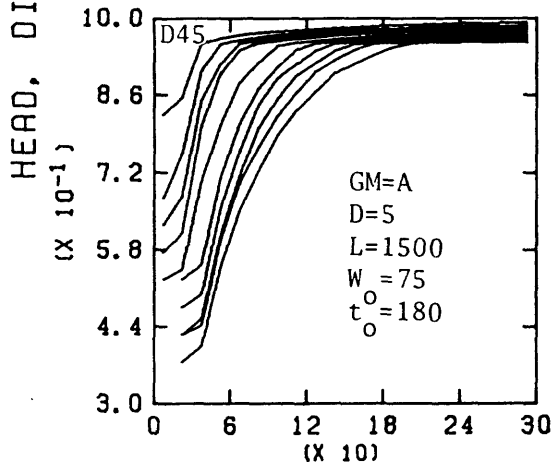
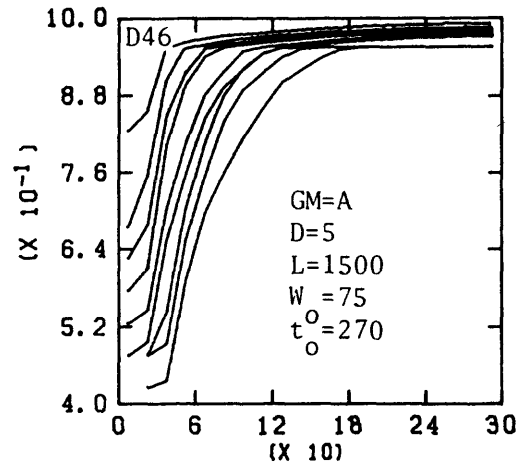
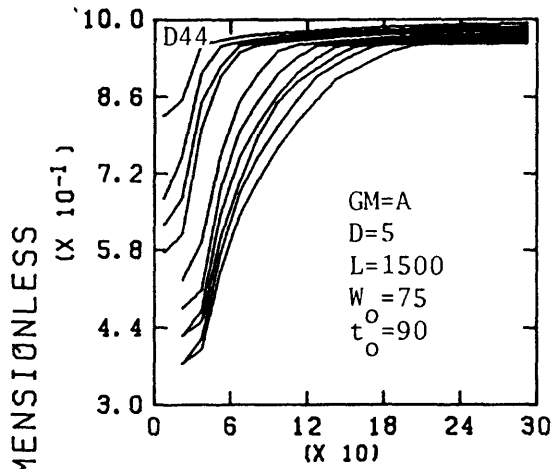
Graph D43

Curve Dimensionless time

1	292
2	876
3	1752
4	2628
5	5256
6	7884
7	13139
8	21315

Curve Dimensionless time

1	292
2	876
3	1752
4	2628
5	5256
6	7884
7	15767
8	21315



DISTANCE, DIMENSIONLESS

Curves numbered from top to bottom.

Graphs D44 and D45

Graph D46

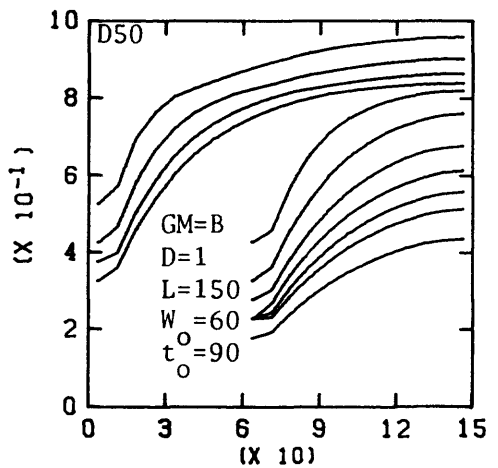
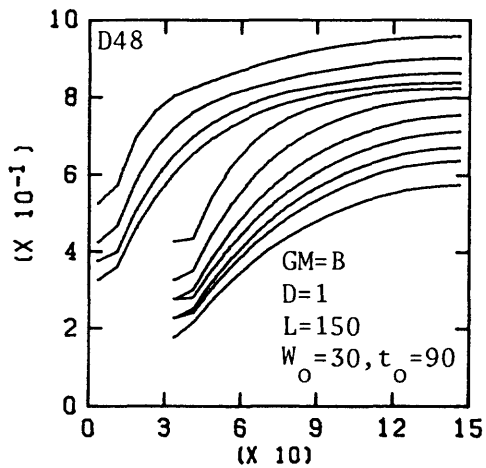
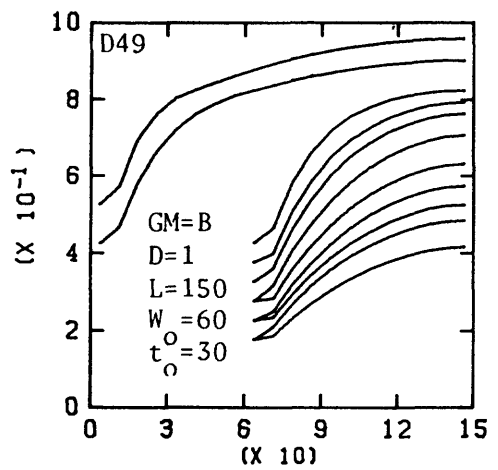
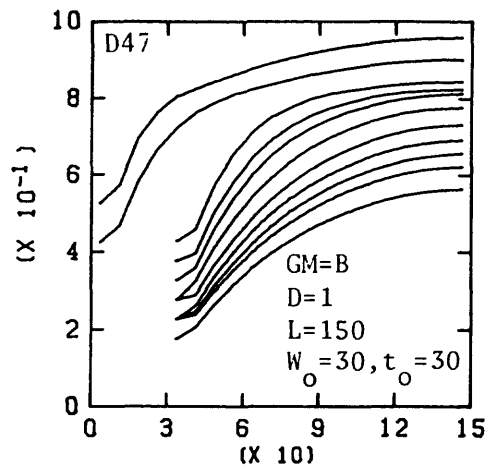
Curve Dimensionless time

Curve Dimensionless time

1	58
2	175
3	350
4	526
5	1051
6	1577
7	2102
8	2628
9	3153
10	4263

1	58
2	175
3	350
4	526
5	1051
6	1577
7	2628
8	3153
9	4263

HEAD, DIMENSIONLESS



DISTANCE, DIMENSIONLESS

Curves numbered from top to bottom.

Graphs D47 and D48

Graphs D49 and D50

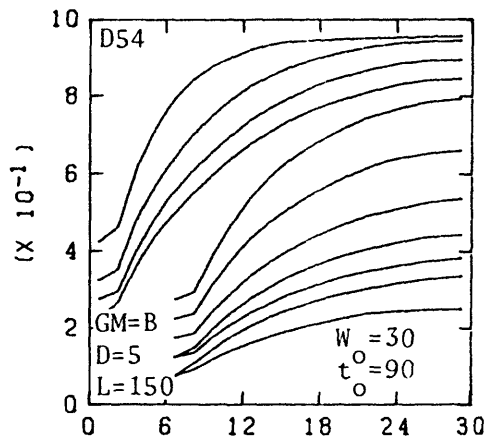
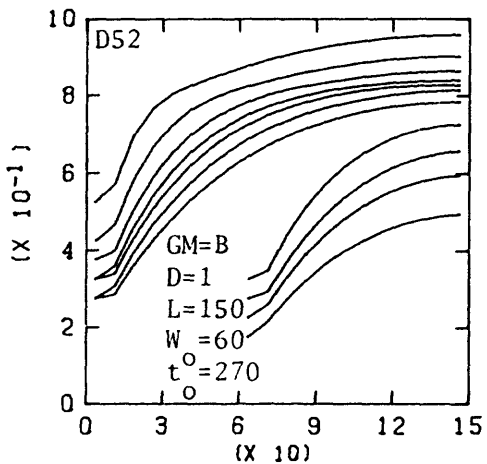
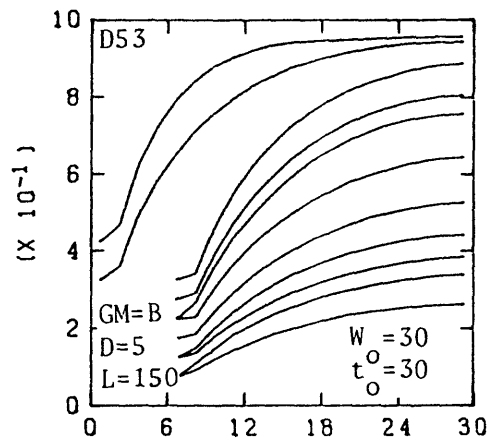
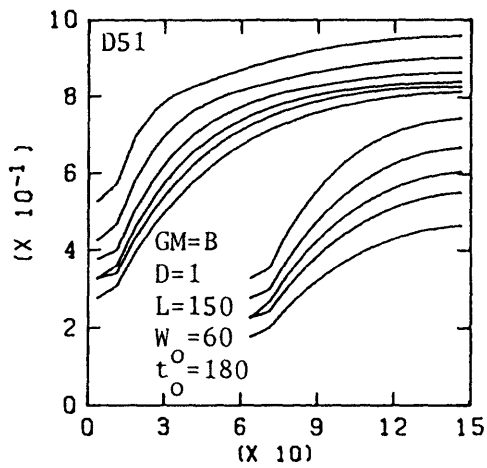
Curve Dimensionless time

Curve Dimensionless time

1	94
2	282
3	565
4	847
5	1129
6	1694
7	2540
8	3387
9	4234
10	5081
11	6868

1	94
2	282
3	565
4	847
5	1129
6	1694
7	2540
8	3387
9	4234
10	5081
11	6868

HEAD, DIMENSIONLESS



DISTANCE, DIMENSIONLESS

Curves numbered from top to bottom.

Graphs D51 and D52

Graphs D53 and D54

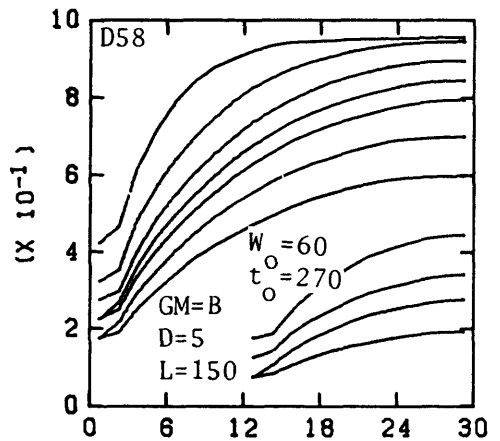
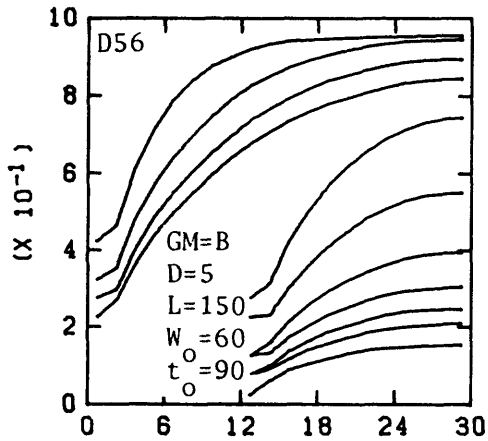
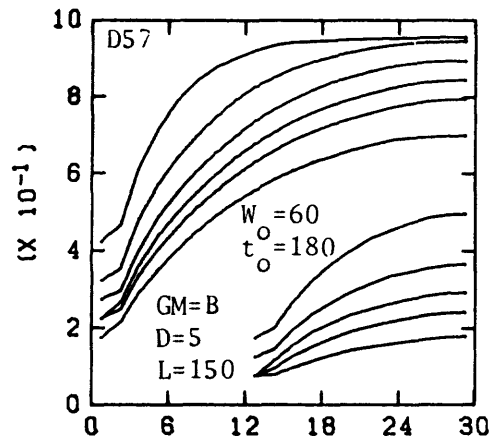
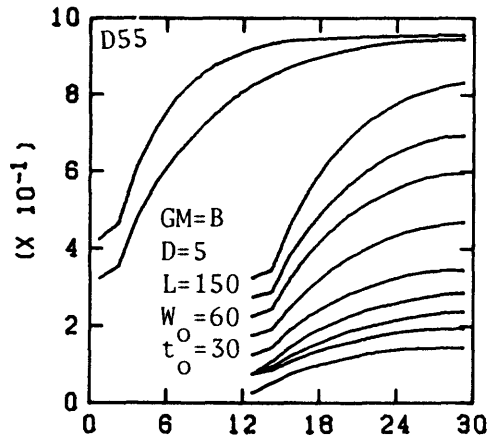
Curve Dimensionless time

1	94
2	282
3	565
4	847
5	1129
6	1694
7	2540
8	3387
9	4234
10	5081
11	6868

Curve Dimensionless time

1	19
2	56
3	113
4	169
5	226
6	339
7	508
8	677
9	847
10	1016
11	1374

HEAD, DIMENSIONLESS
(X 10⁻¹)



DISTANCE, DIMENSIONLESS

Curves numbered from top to bottom.

Graphs D55 and D56

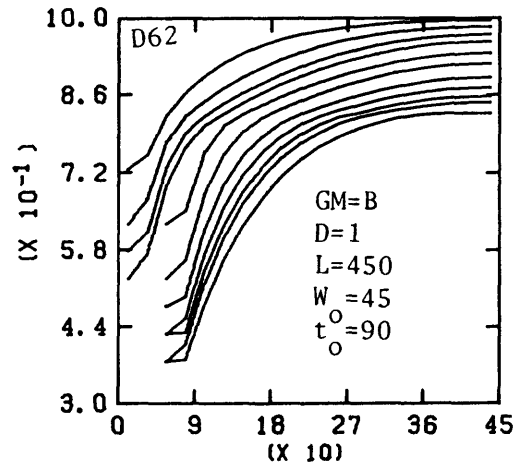
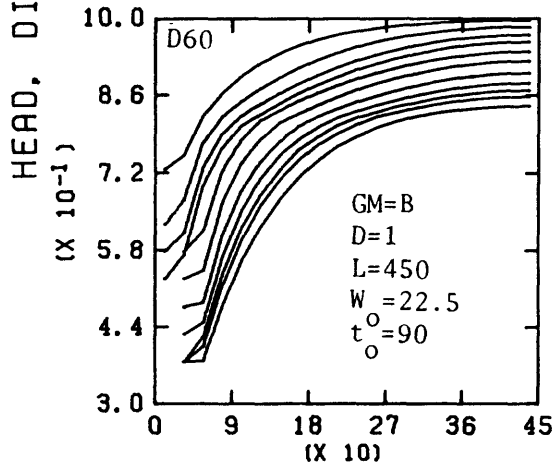
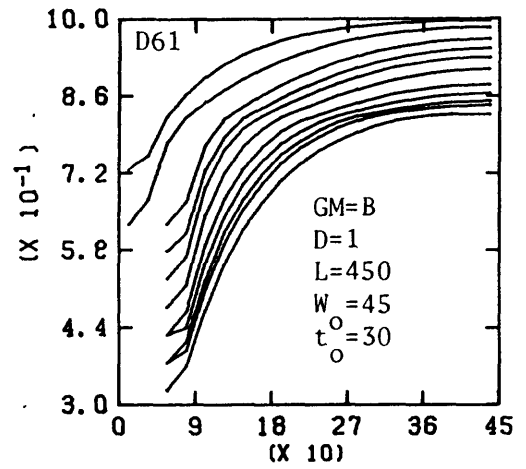
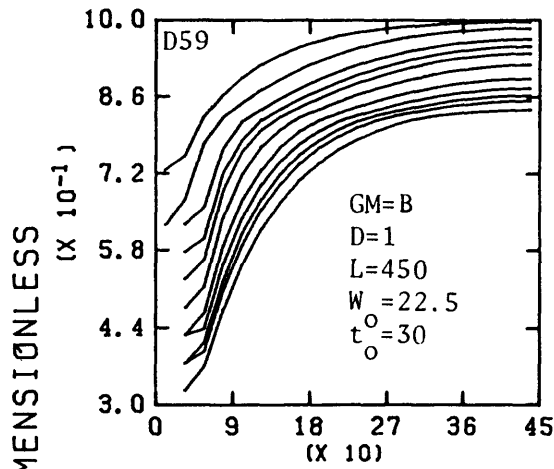
Graphs D57 and D58

Curve Dimensionless time

Curve Dimensionless time

1	19
2	56
3	113
4	169
5	226
6	339
7	508
8	677
9	847
10	1016
11	1374

1	19
2	56
3	113
4	169
5	226
6	339
7	508
8	677
9	847
10	1016
11	1374



DISTANCE, DIMENSIONLESS

Curves numbered from top to bottom.

Graphs D59 and D60

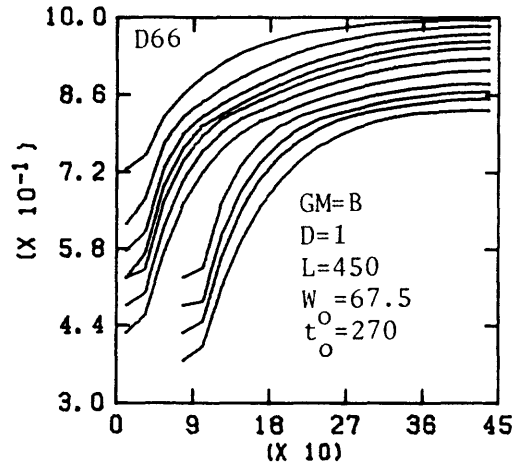
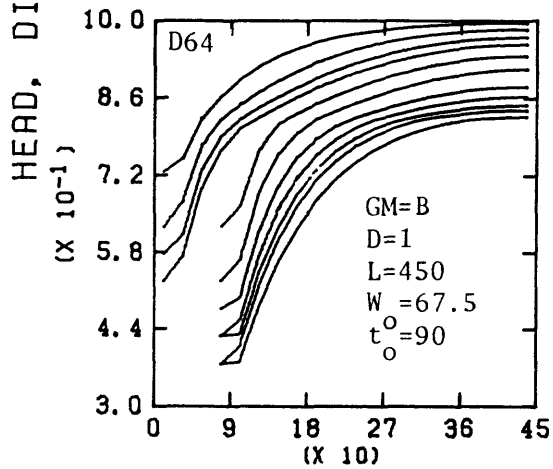
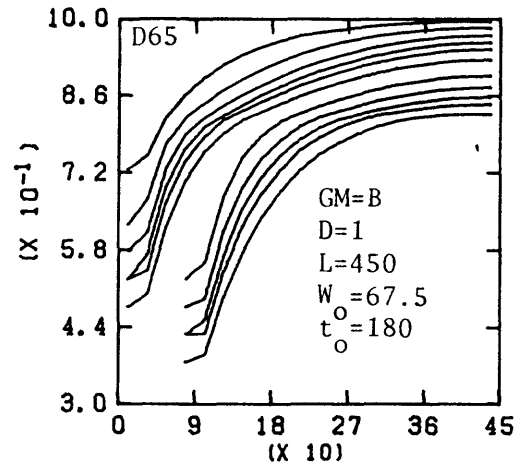
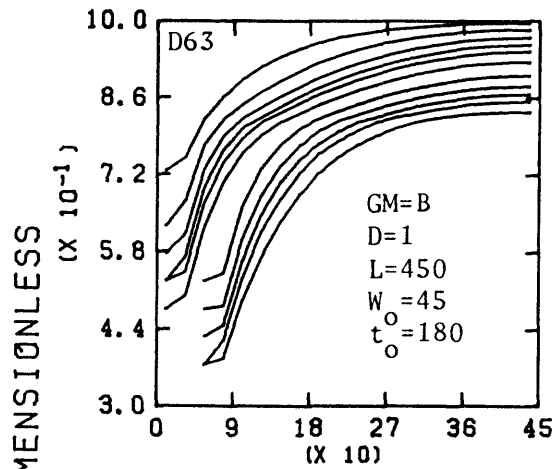
Graphs D61 and D62

Curve Dimensionless time

Curve Dimensionless time

1	94
2	282
3	565
4	847
5	1129
6	1694
7	2540
8	3387
9	4234
10	5081
11	6868

1	94
2	282
3	565
4	847
5	1129
6	1694
7	2540
8	3387
9	4234
10	5081
11	6868



DISTANCE, DIMENSIONLESS

Curves numbered from top to bottom.

Graphs D63 and D64

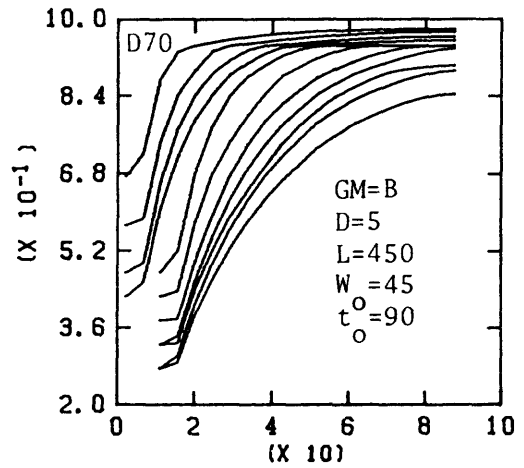
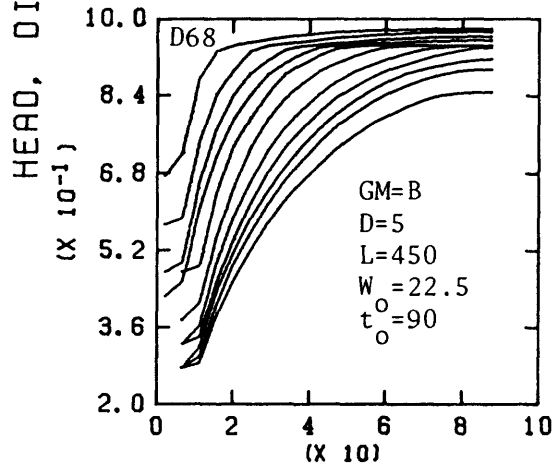
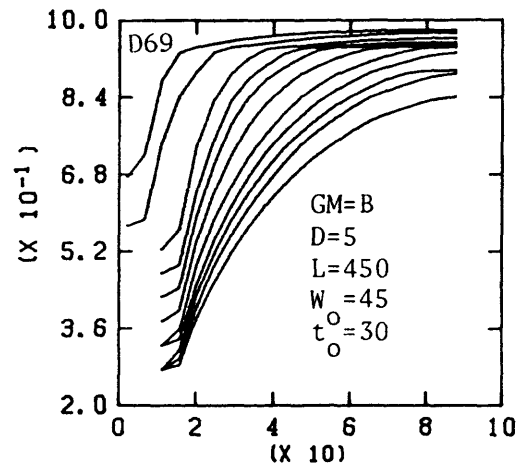
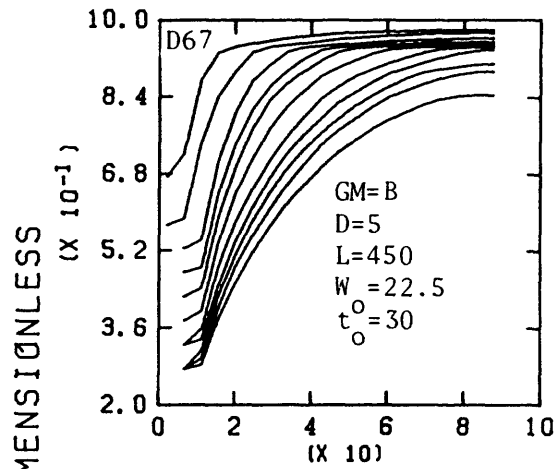
Graphs D65 and D66

Curve Dimensionless time

1	94
2	282
3	565
4	847
5	1129
6	1694
7	2540
8	3387
9	4234
10	5081
11	6868

Curve Dimensionless time

1	94
2	282
3	565
4	847
5	1129
6	1694
7	2540
8	3387
9	4234
10	5081
11	6868



DISTANCE, DIMENSIONLESS

Curves numbered from top to bottom.

Graphs D67 and D68

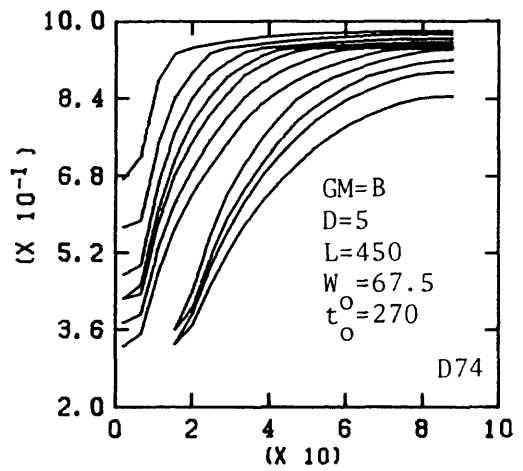
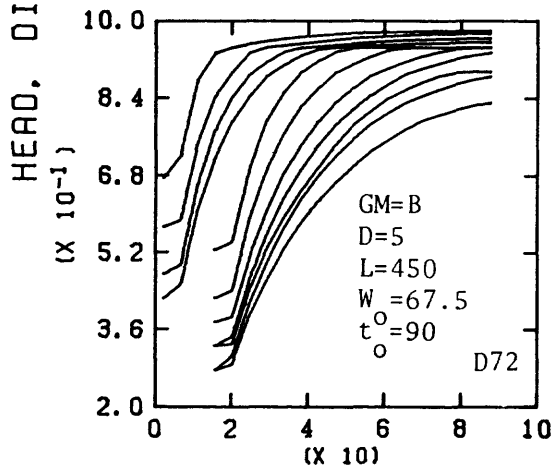
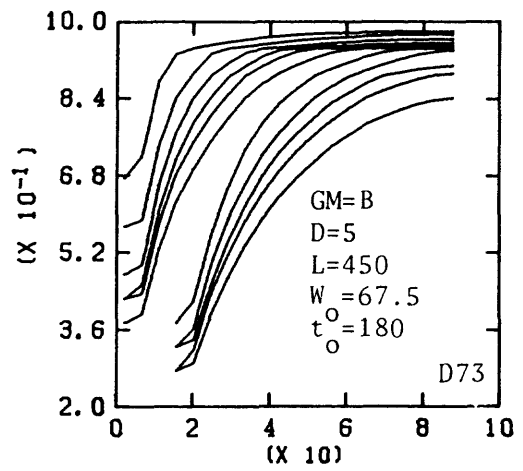
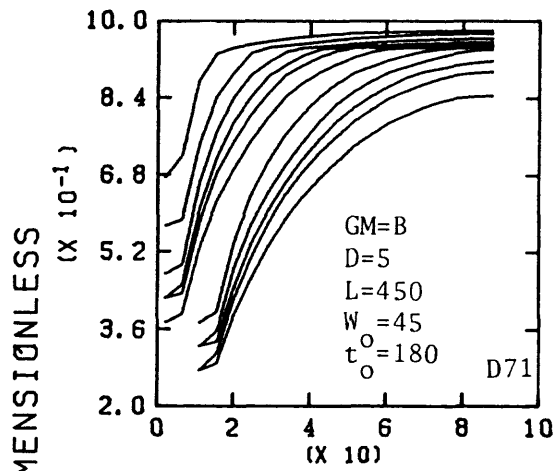
Graphs D69 and D70

Curve Dimensionless time

Curve Dimensionless time

1	19
2	56
3	113
4	169
5	226
6	339
7	508
8	677
9	847
10	1016
11	1374

1	19
2	56
3	113
4	169
5	226
6	339
7	508
8	677
9	847
10	1016
11	1374



DISTANCE, DIMENSIONLESS

Curves numbered from top to bottom.

Graphs D71 and D72

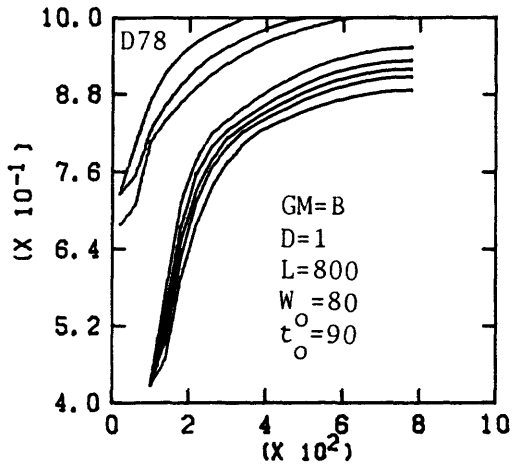
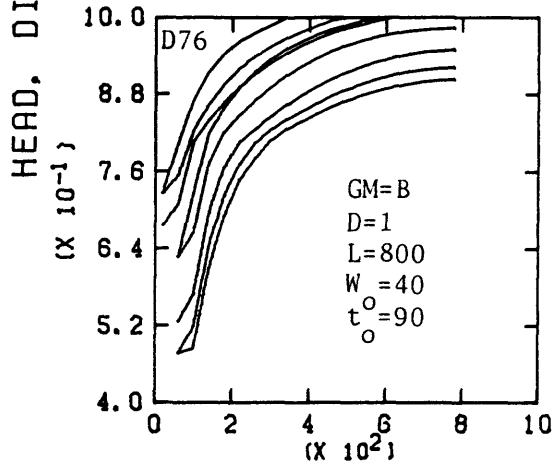
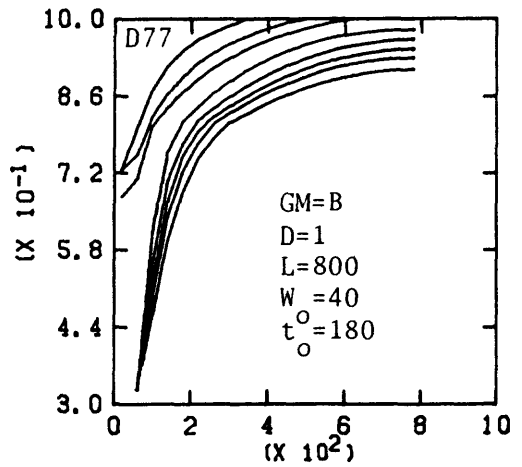
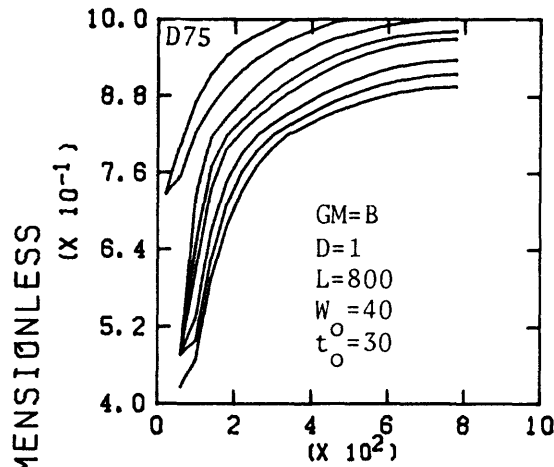
Graphs D73 and D74

Curve Dimensionless time

1	19
2	56
3	113
4	169
5	226
6	339
7	508
8	677
9	847
10	1016
11	1374

Curve Dimensionless time

1	19
2	56
3	113
4	169
5	226
6	339
7	508
8	677
9	847
10	1016
11	1374



DISTANCE, DIMENSIONLESS

Curves numbered from top to bottom.

Graphs D75 and D76

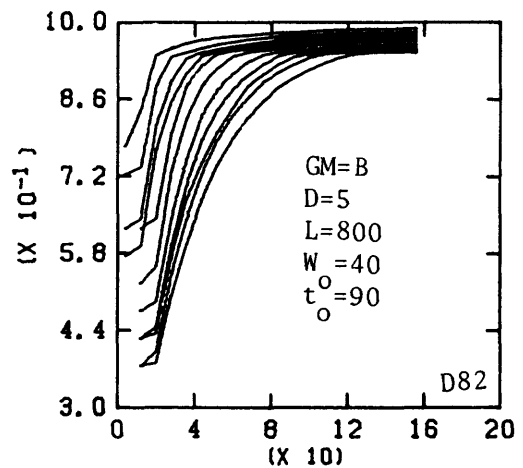
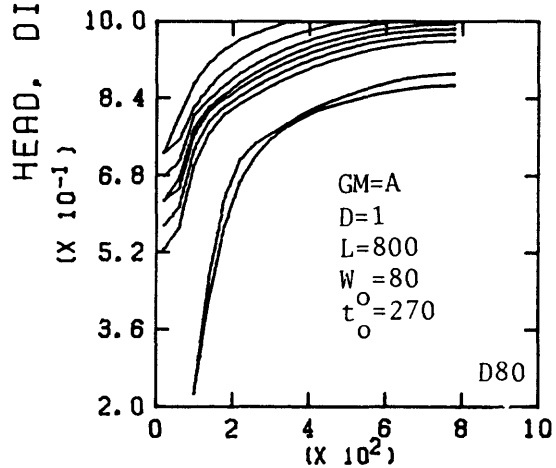
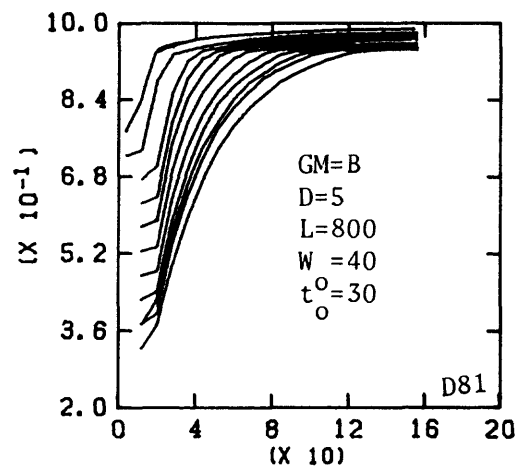
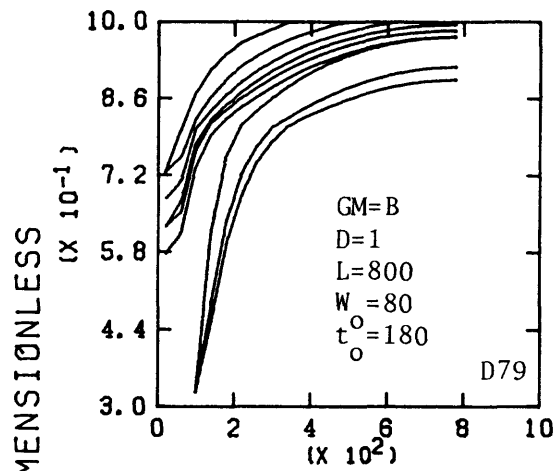
Graphs D77 and D78

Curve Dimensionless time

1	94
2	282
3	565
4	1129
5	1694
6	3387
7	5081
8	6868

Curve Dimensionless time

1	94
2	282
3	565
4	2540
5	3387
6	4234
7	5081
8	6868



DISTANCE, DIMENSIONLESS

Curves numbered from top to bottom.

Graphs D79 and D80

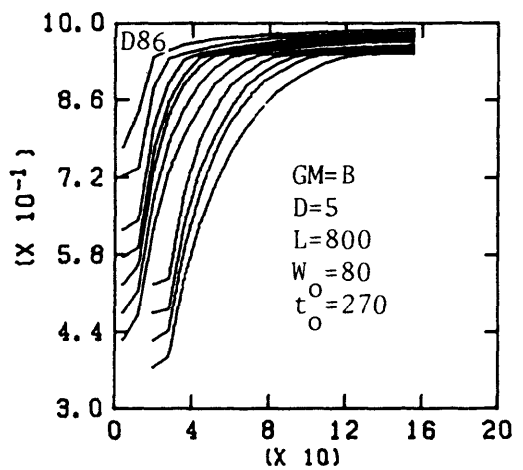
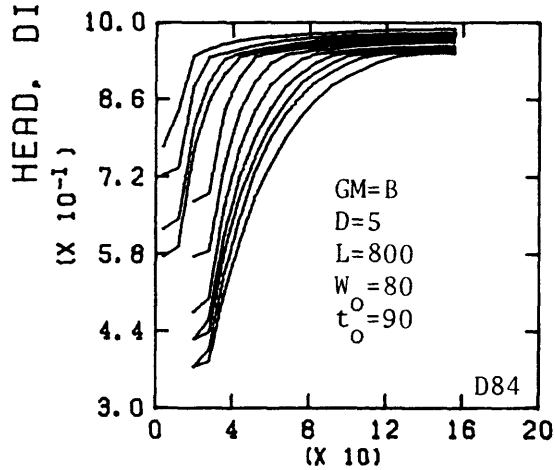
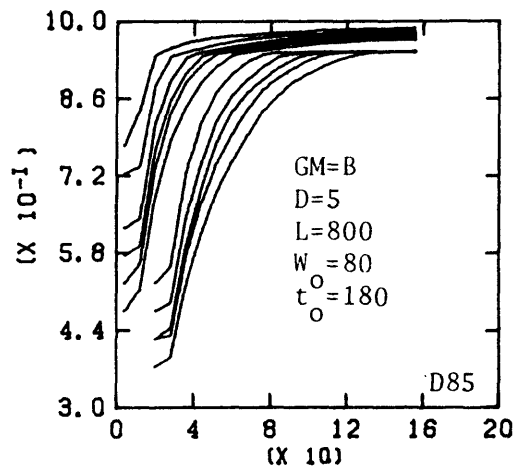
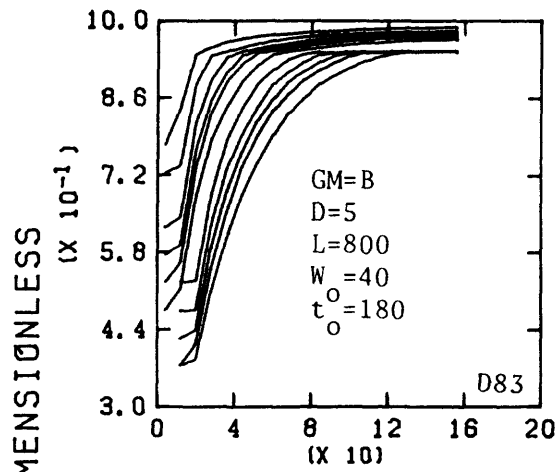
Graphs D81 and D82

Curve Dimensionless time

1	94
2	282
3	565
4	847
5	1129
6	1694
7	2540
8	5081
9	6868

Curve Dimensionless time

1	19
2	56
3	113
4	169
5	226
6	339
7	508
8	677
9	847
10	1016
11	1374



DISTANCE, DIMENSIONLESS

Curves numbered from top to bottom.

Graphs D83 and D84

Graphs D85 and D86

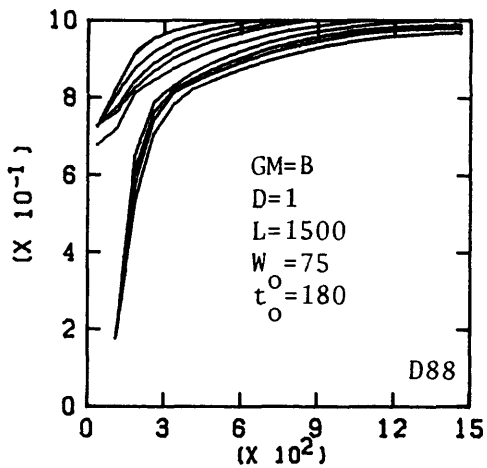
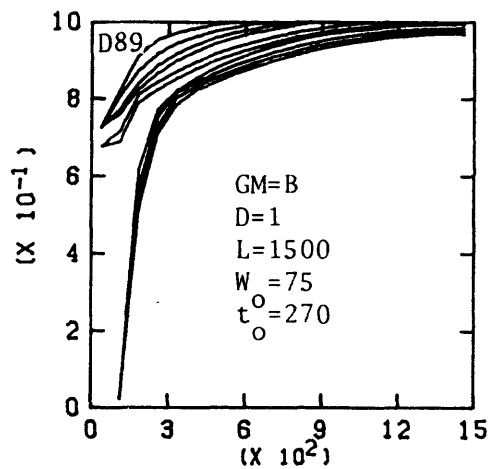
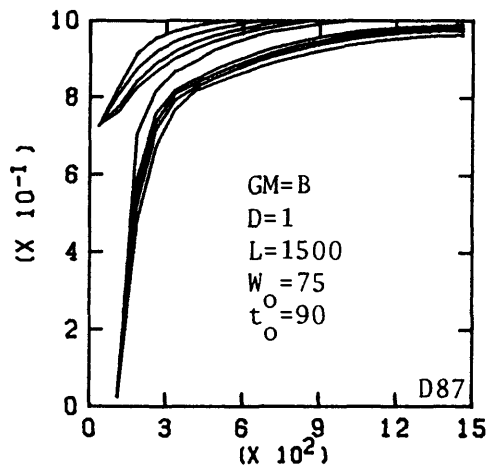
Curve Dimensionless time

Curve Dimensionless time

1	19
2	56
3	113
4	169
5	226
6	339
7	508
8	677
9	847
10	1016
11	1374

1	19
2	56
3	113
4	169
5	226
6	339
7	508
8	677
9	847
10	1016
11	1374

HEAD, DIMENSIONLESS



DISTANCE, DIMENSIONLESS

Curves numbered from top to bottom.

Graphs D87 and D88

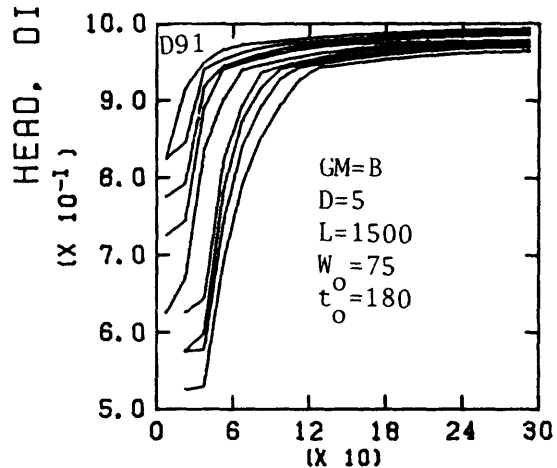
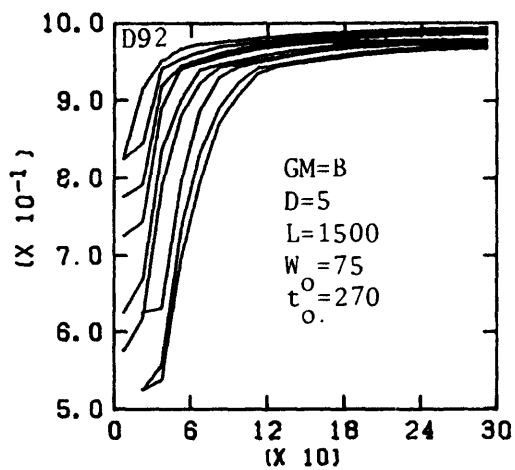
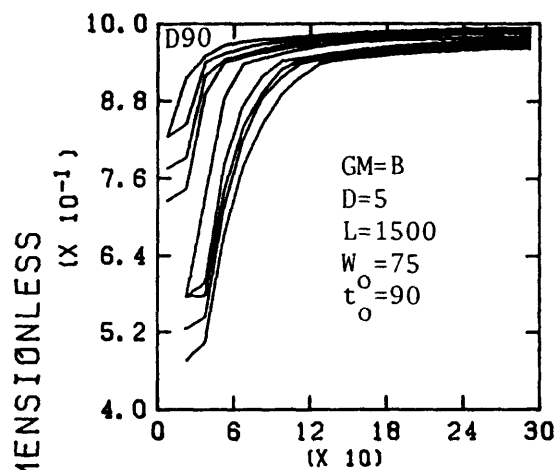
Graph D89

Curve Dimensionless time

1	94
2	282
3	565
4	847
5	1694
6	3387
7	4234
8	5081
9	6868

Curve Dimensionless time

1	94
2	282
3	565
4	847
5	1694
6	2540
7	4234
8	5081
9	5927
10	6868



DISTANCE, DIMENSIONLESS

Curves numbered from top to bottom.

Graphs D90 and D91

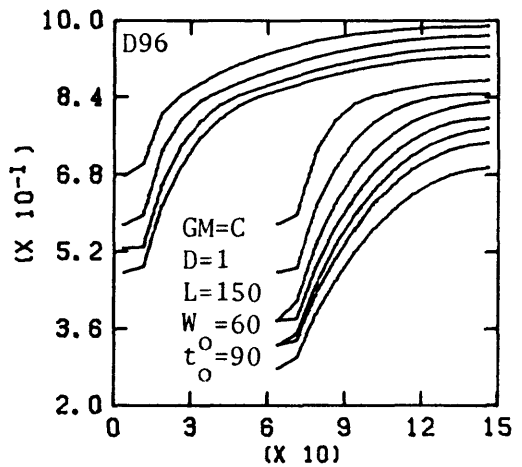
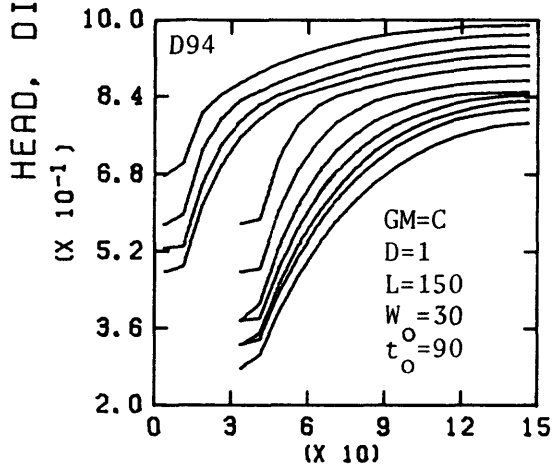
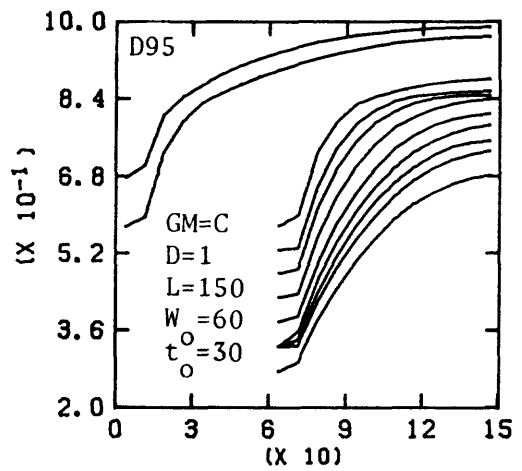
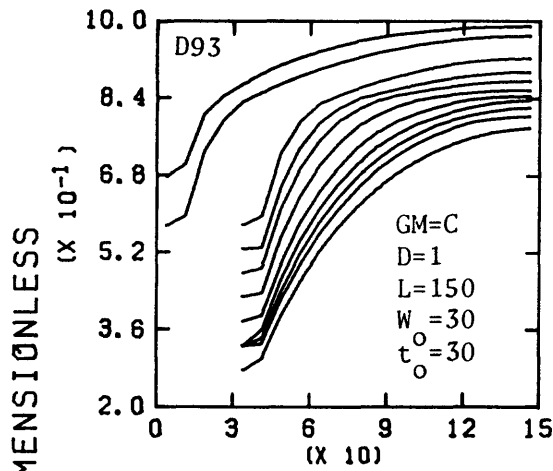
Graph D92

Curve Dimensionless time

Curve Dimensionless time

1	19
2	56
3	113
4	169
5	339
6	677
7	847
8	1016
9	1374

1	19
2	56
3	113
4	169
5	339
6	508
7	847
8	1185
9	1374



DISTANCE, DIMENSIONLESS

Curves numbered from top to bottom.

Graphs D93 and D94

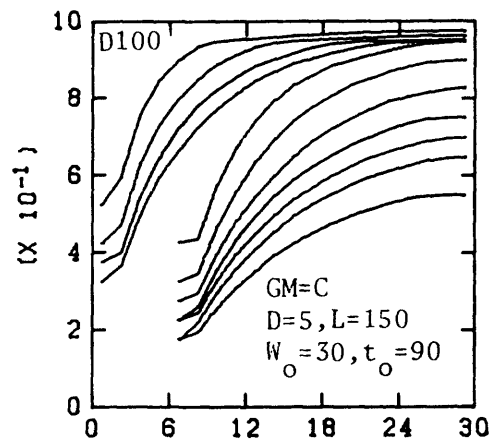
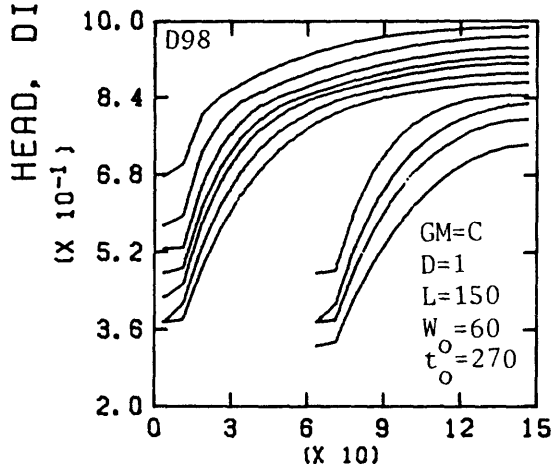
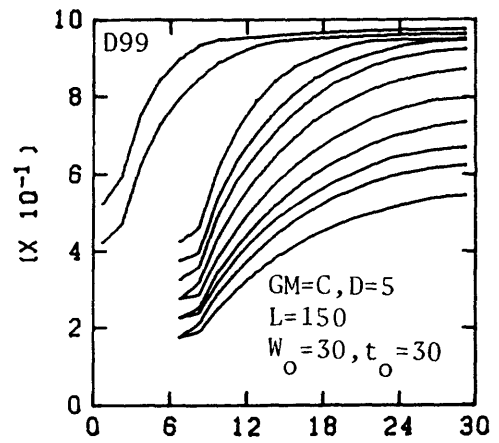
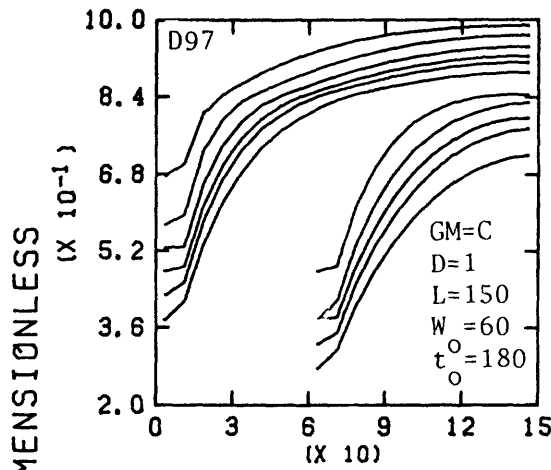
Graphs D95 and D96

Curve Dimensionless time

1	30
2	91
3	181
4	272
5	363
6	544
7	817
8	1089
9	1361
10	1633
11	2208

Curve Dimensionless time

1	30
2	91
3	181
4	272
5	363
6	544
7	817
8	1089
9	1361
10	1633
11	2208



DISTANCE, DIMENSIONLESS

Curves numbered from top to bottom.

Graphs D97 and D98

Graphs D99 and D100

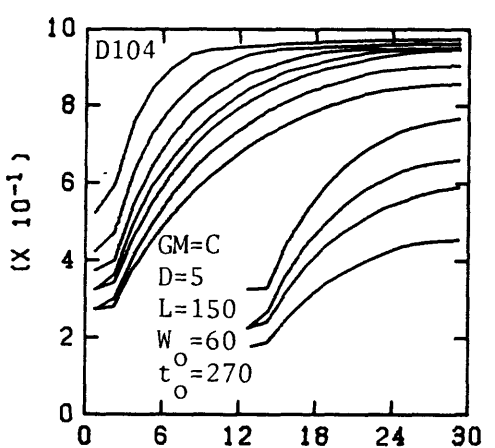
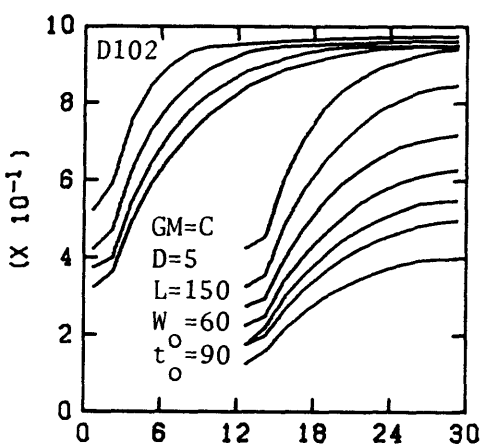
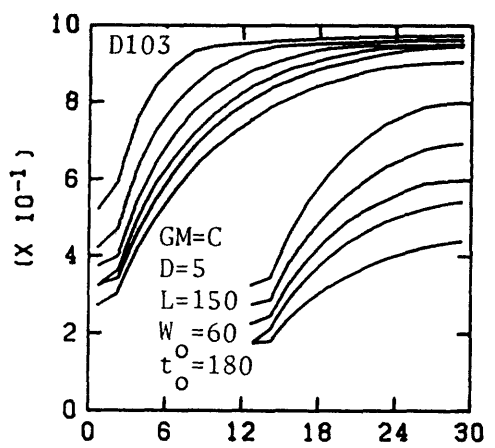
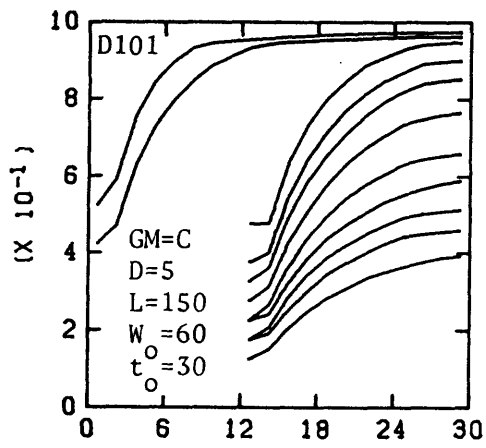
Curve Dimensionless time

Curve Dimensionless time

1	30
2	91
3	181
4	272
5	363
6	544
7	817
8	1089
9	1361
10	1633
11	2208

1	6.0
2	18
3	36
4	54
5	73
6	109
7	163
8	218
9	272
10	327
11	442

HEAD, DIMENSIONLESS



DISTANCE, DIMENSIONLESS

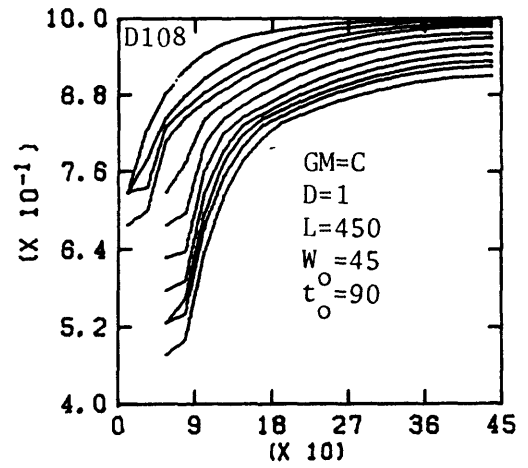
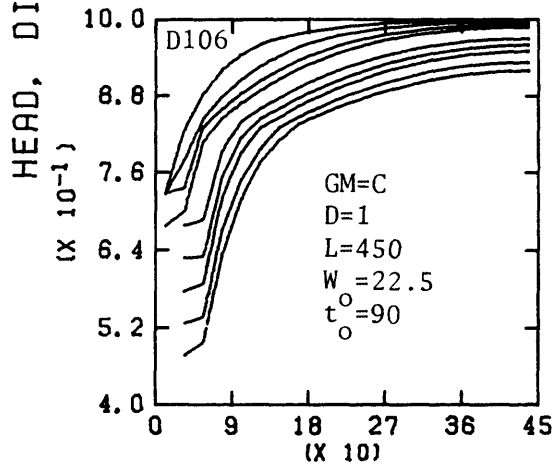
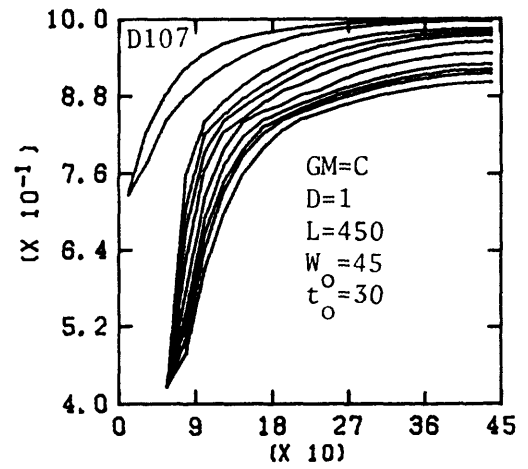
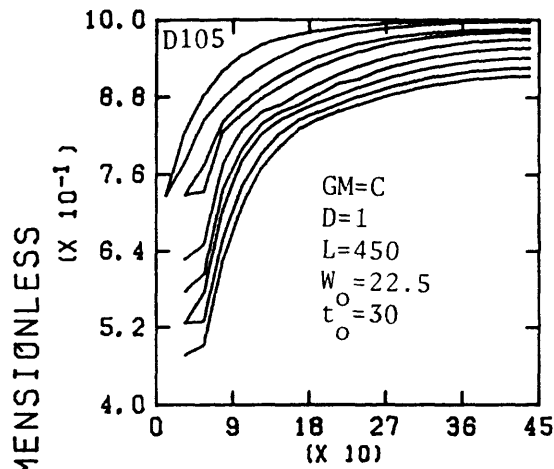
Curves numbered from top to bottom.

Graphs D101 and D102

Graphs D103 and D104

Curve	Dimensionless time
1	6.0
2	18
3	36
4	54
5	73
6	109
7	163
8	218
9	272
10	327
11	442

Curve	Dimensionless time
1	6.0
2	18
3	36
4	54
5	73
6	109
7	163
8	218
9	272
10	327
11	442



DISTANCE, DIMENSIONLESS

Curves numbered from top to bottom.

Graphs D105 and D106

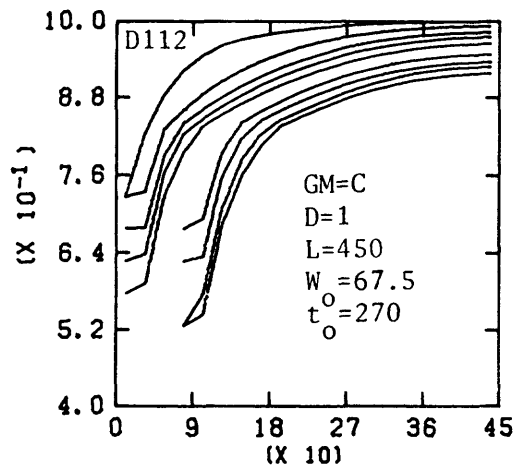
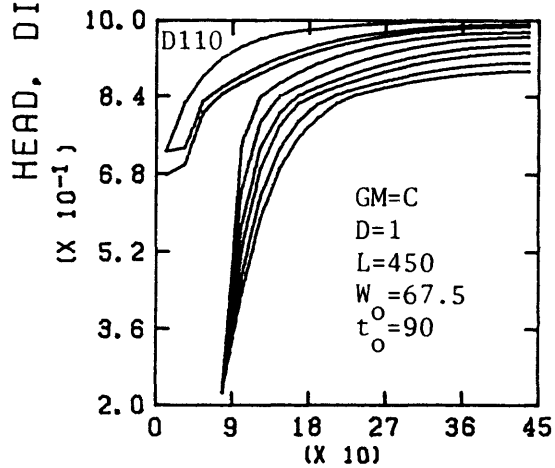
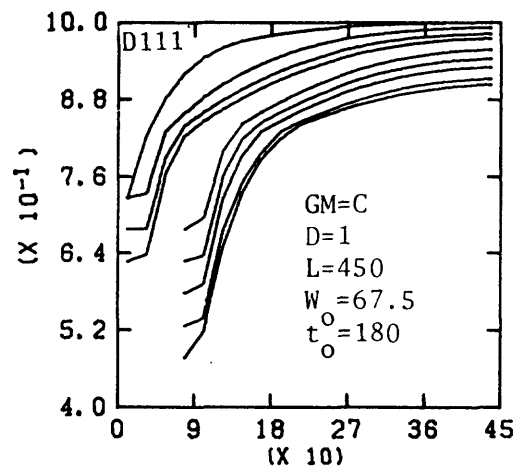
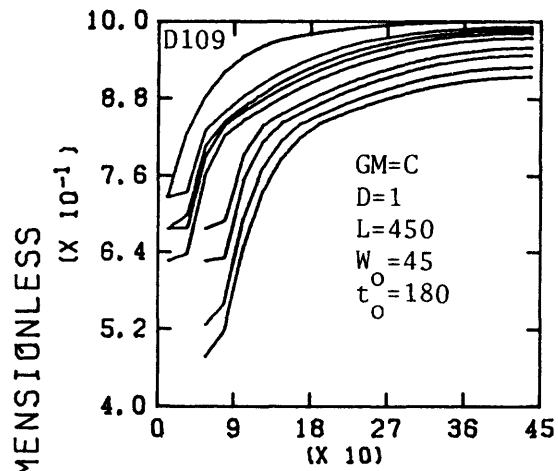
Graphs D107 and D108

Curve Dimensionless time

1	30
2	91
3	181
4	272
5	544
6	817
7	1089
8	1633
9	2208

Curve Dimensionless time

1	30
2	91
3	181
4	272
5	363
6	544
7	817
8	1089
9	1361
10	1633
11	2208



DISTANCE, DIMENSIONLESS

Curves numbered from top to bottom.

Graphs D109 and D110

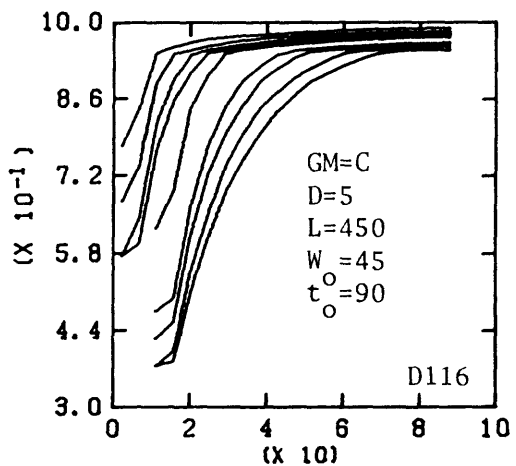
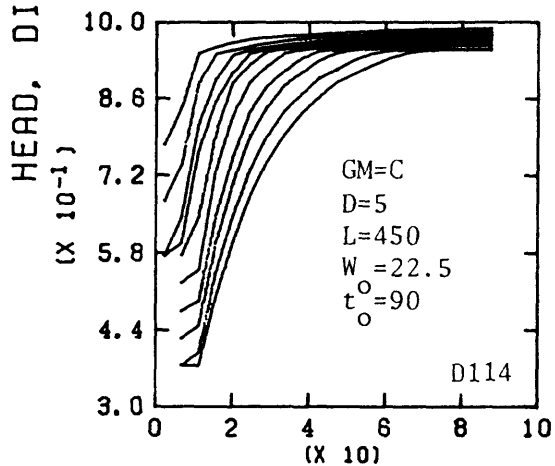
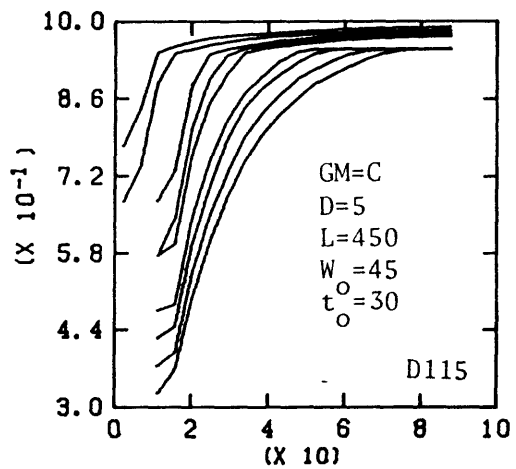
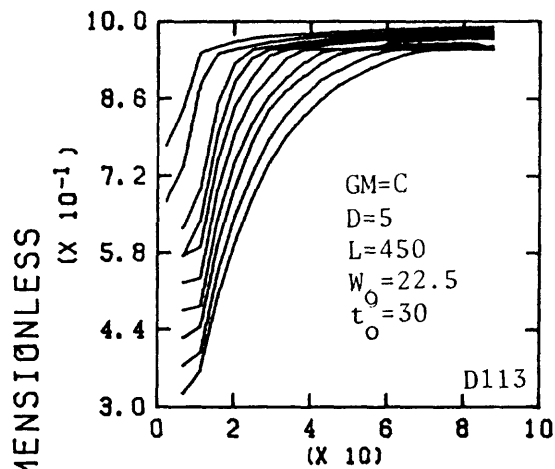
Graphs D111 and D112

Curve Dimensionless time

1	30
2	181
3	272
4	363
5	544
6	817
7	1089
8	1633
9	2208

Curve Dimensionless time

1	30
2	181
3	363
4	544
5	817
6	1089
7	1361
8	1905
9	2208



DISTANCE, DIMENSIONLESS

Curves numbered from top to bottom.

Graphs D113 and D114

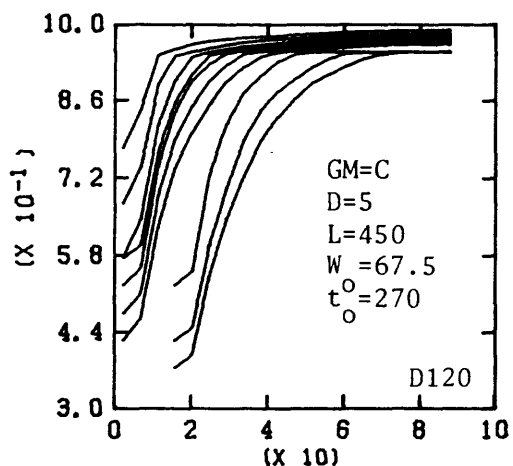
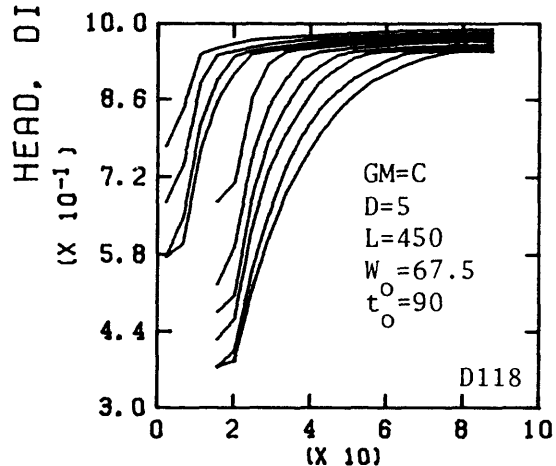
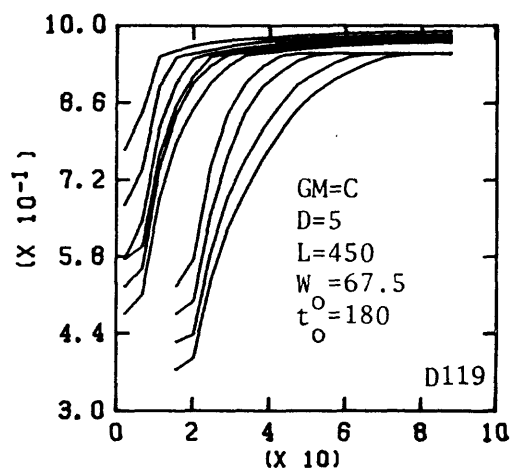
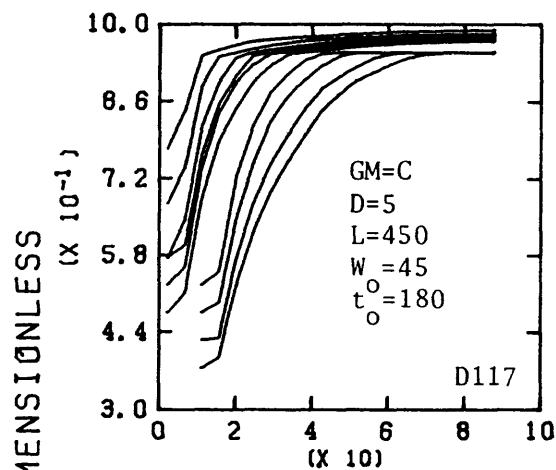
Graphs D115 and D116

Curve Dimensionless time

1	6.0
2	18
3	36
4	54
5	73
6	109
7	163
8	218
9	327
10	442

Curve Dimensionless time

1	6.0
2	18
3	36
4	54
5	73
6	163
7	218
8	327
9	442



DISTANCE, DIMENSIONLESS

Curves numbered from top to bottom.

Graphs D117 and D118

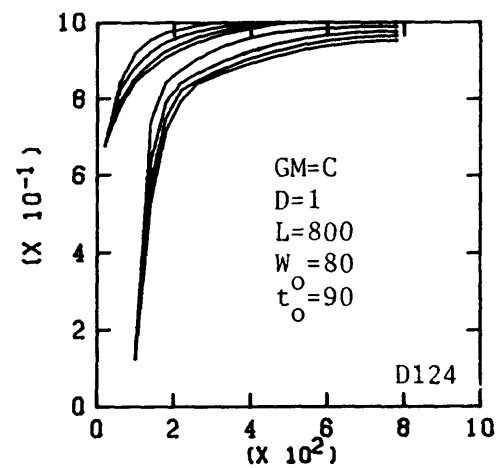
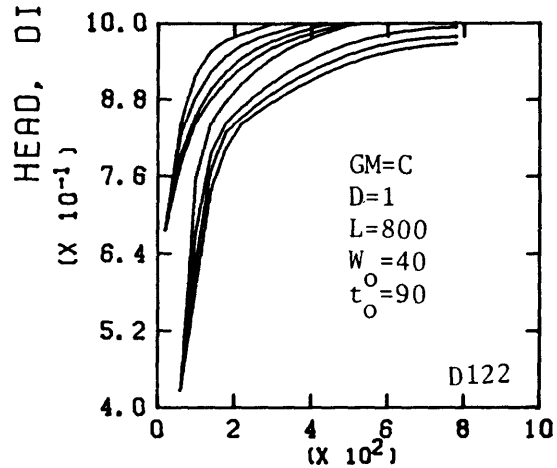
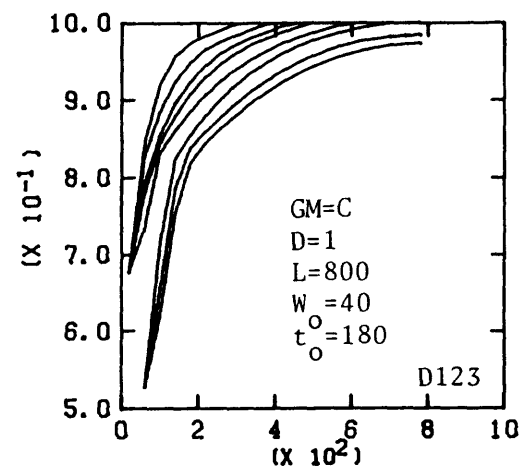
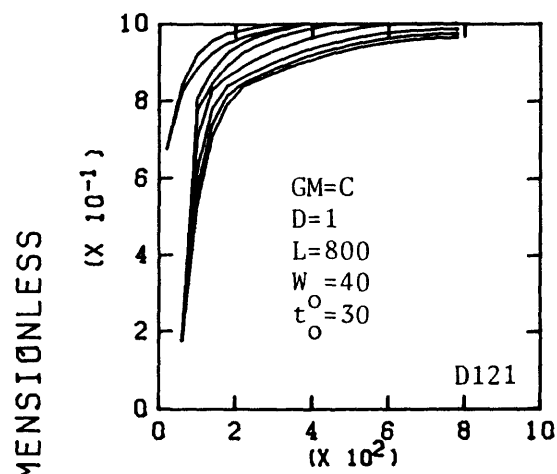
Graphs D119 and D120

Curve Dimensionless time

Curve Dimensionless time

1	6.0
2	18
3	36
4	54
5	73
6	109
7	163
8	218
9	327
10	442

1	6.0
2	18
3	36
4	54
5	73
6	109
7	163
8	218
9	327
10	442



DISTANCE, DIMENSIONLESS

Curves numbered from top to bottom.

Graphs D121 and D122

Graphs D123 and D124

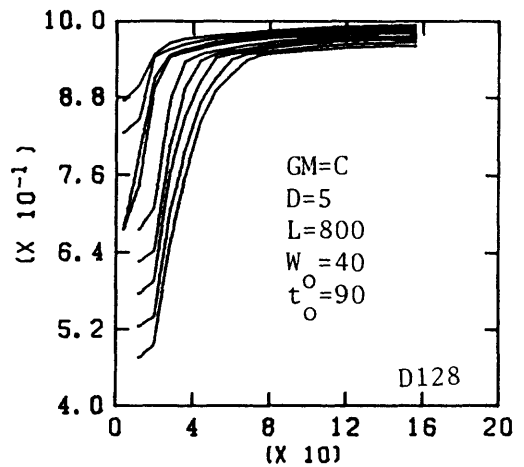
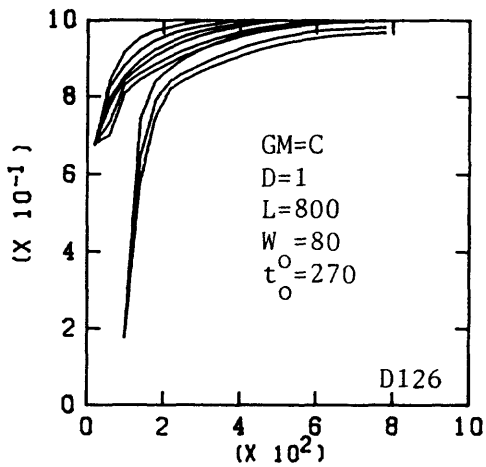
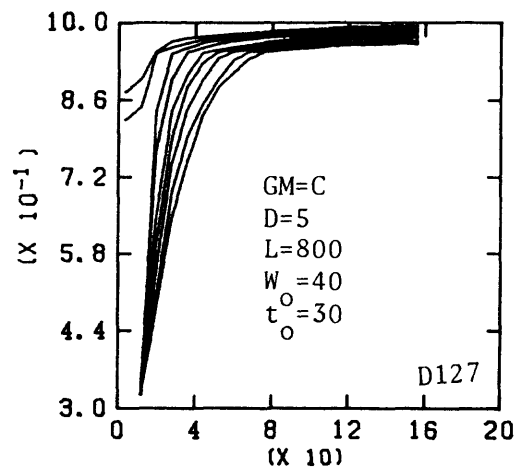
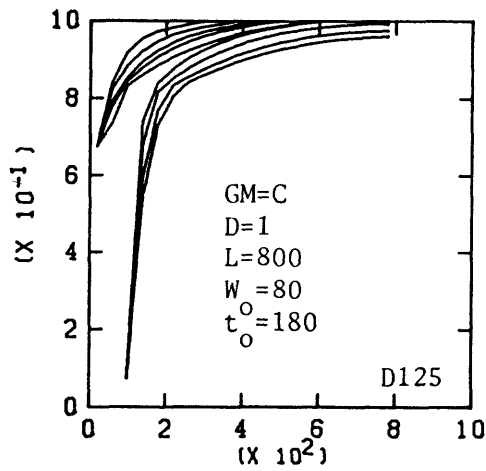
Curve Dimensionless time

Curve Dimensionless time

1	30
2	91
3	181
4	272
5	544
6	1089
7	1633
8	2208

1	30
2	91
3	181
4	272
5	544
6	1089
7	1633
8	2208

HEAD, DIMENSIONLESS



DISTANCE, DIMENSIONLESS

Curves numbered from top to bottom.

Graphs D125 and D126

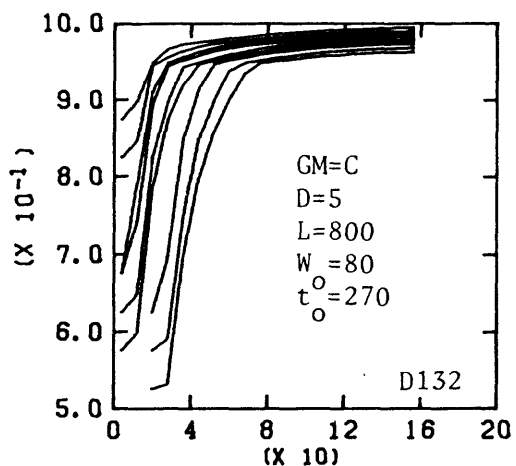
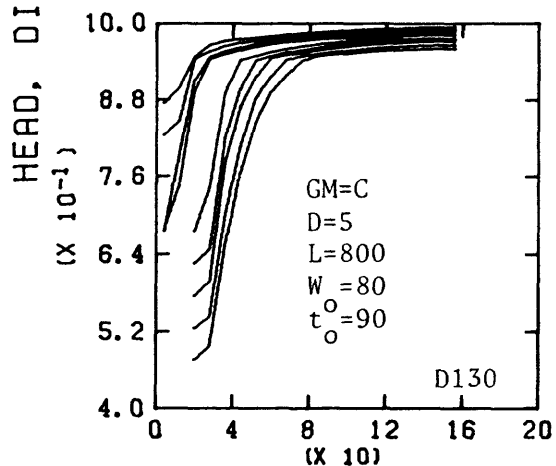
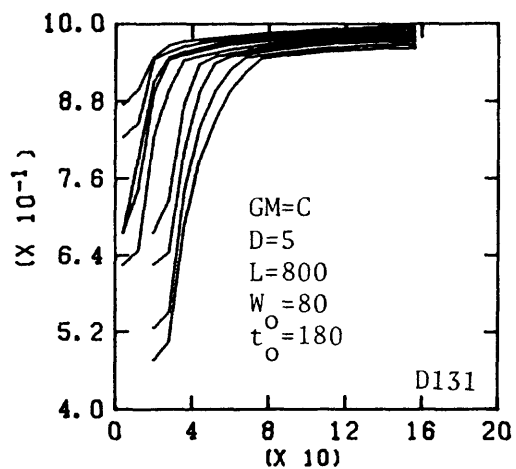
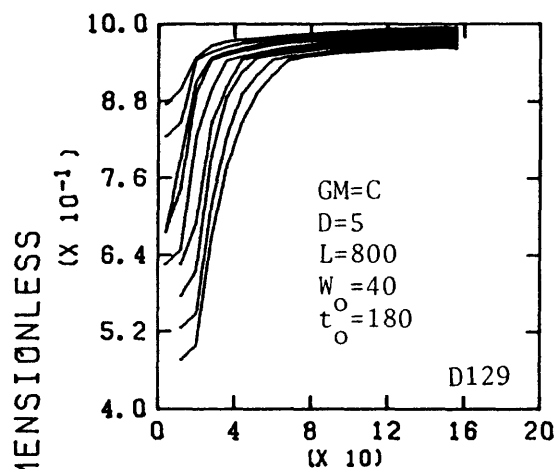
Graphs D127 and D128

Curve Dimensionless time

1	30
2	91
3	181
4	272
5	544
6	817
7	1089
8	1633
9	2208

Curve Dimensionless time

1	6.0
2	18
3	36
4	54
5	109
6	163
7	218
8	327
9	442



DISTANCE, DIMENSIONLESS

Curves numbered from top to bottom.

Graphs D129 and D130

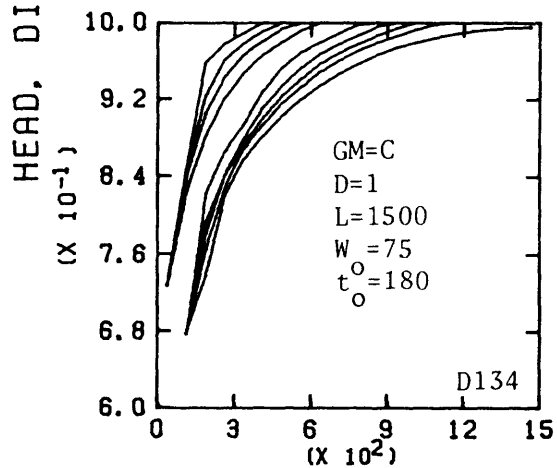
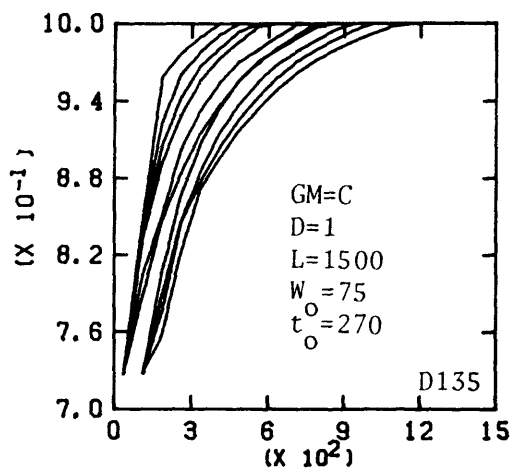
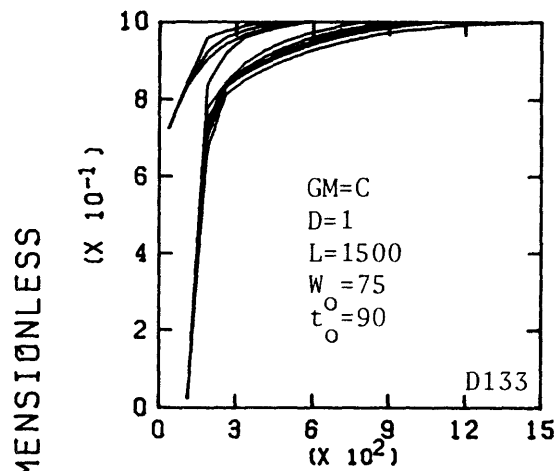
Graphs D131 and D132

Curve Dimensionless time

1	6.0
2	18
3	36
4	54
5	109
6	163
7	218
8	327
9	442

Curve Dimensionless time

1	6.0
2	18
3	36
4	54
5	109
6	163
7	218
8	327
9	442



DISTANCE, DIMENSIONLESS

Curves numbered from top to bottom.

Graphs D133 and D134

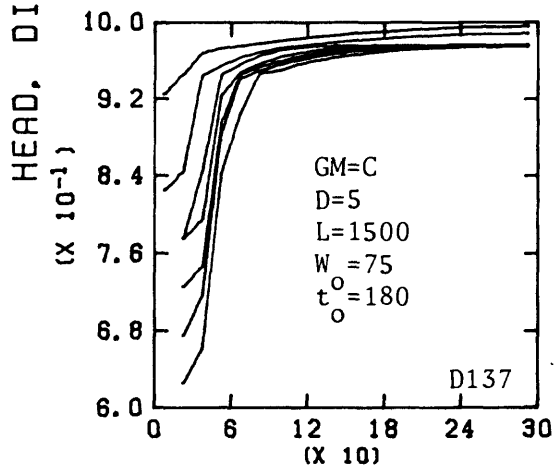
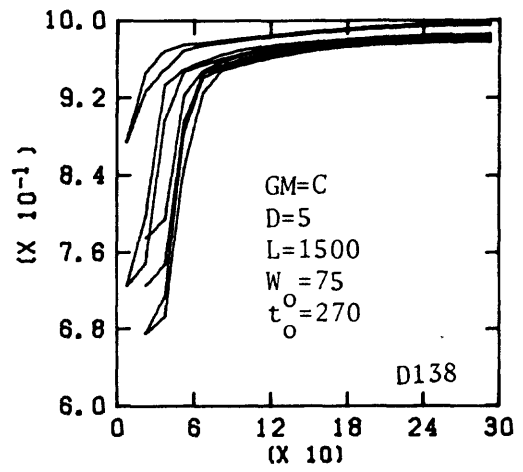
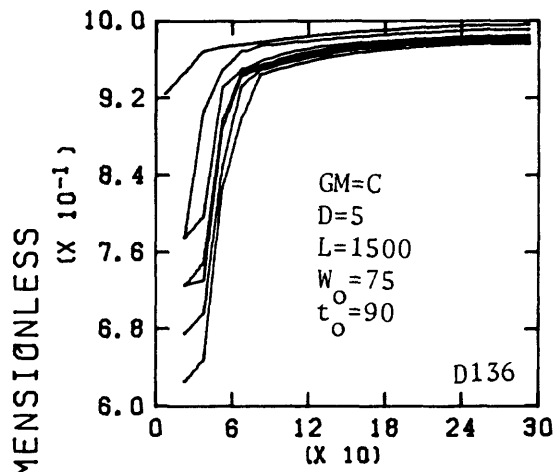
Graphs D135

Curve Dimensionless time

1	30
2	91
3	181
4	363
5	817
6	1089
7	1361
8	1633
9	2208

Curve Dimensionless time

1	30
2	91
3	181
4	272
5	544
6	817
7	1361
8	1633
9	1905
10	2208



DISTANCE, DIMENSIONLESS

Curves numbered from top to bottom.

Graphs D136 and D137

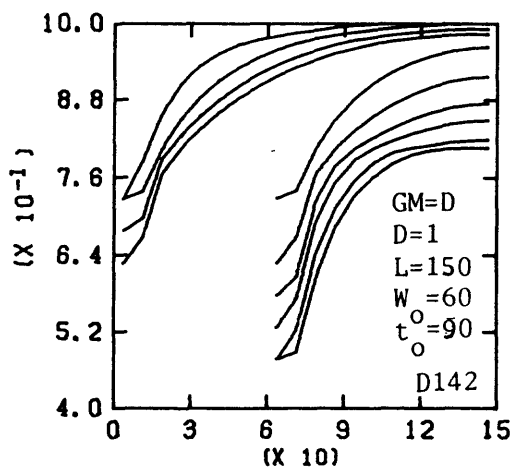
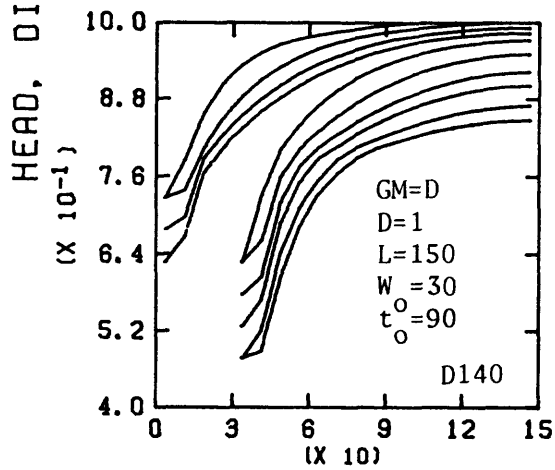
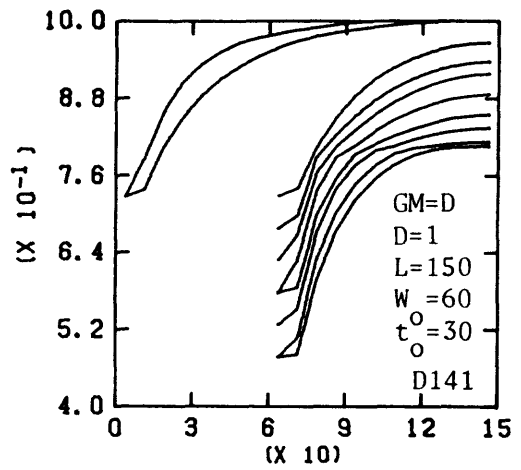
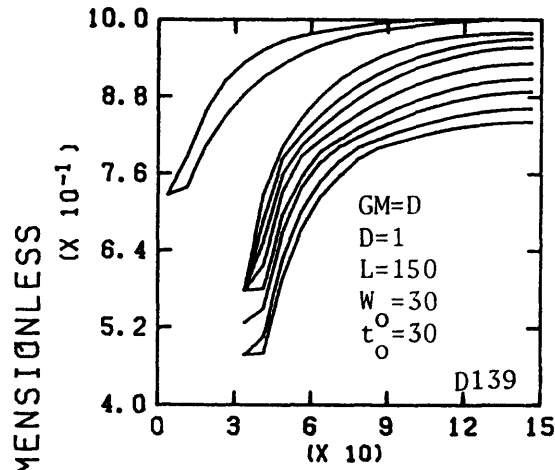
Graphs D138

Curve Dimensionless time

1	6.0
2	73
3	163
4	218
5	272
6	327
7	442

Curve Dimensionless time

1	6.0
2	18
3	109
4	163
5	272
6	327
7	381
8	442



DISTANCE, DIMENSIONLESS

Curves numbered from top to bottom.

Graphs D139 and D140

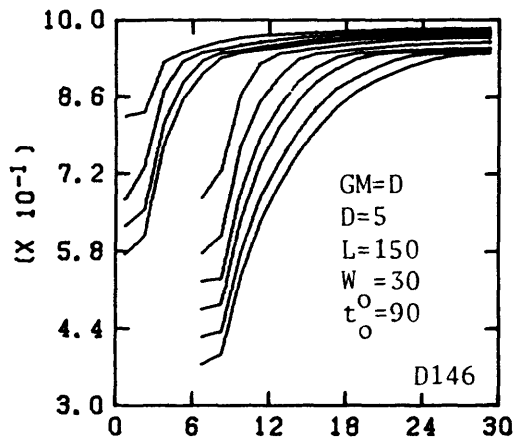
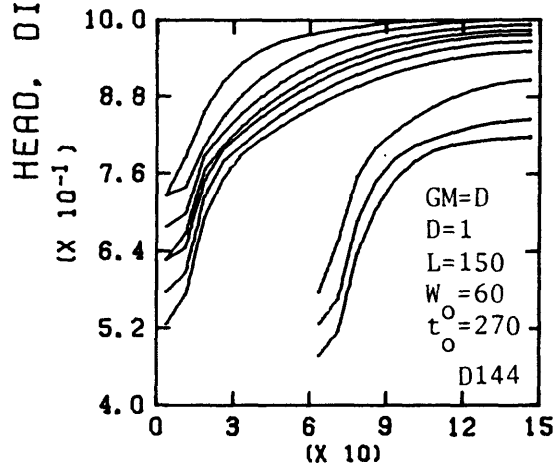
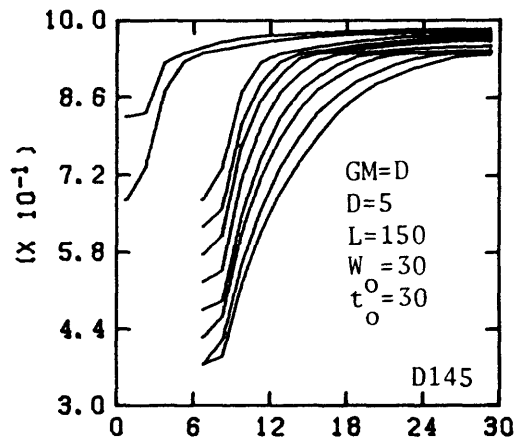
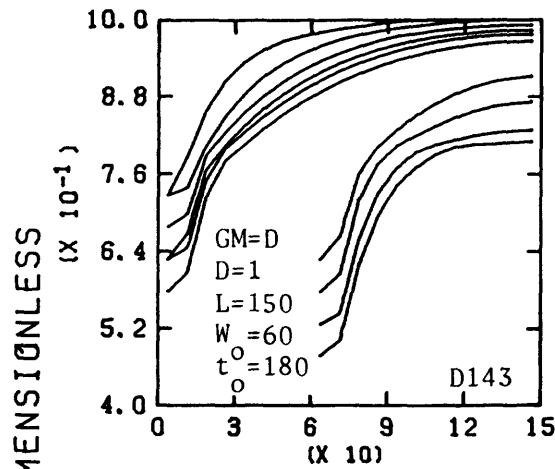
Graphs D141 and D142

Curve Dimensionless time

1	2.6
2	7.9
3	16
4	24
5	32
6	48
7	71
8	95
9	143
10	193

Curve Dimensionless time

1	2.6
2	7.9
3	16
4	24
5	32
6	48
7	71
8	95
9	143
10	193



DISTANCE, DIMENSIONLESS

Curves numbered from top to bottom.

Graphs D143 and D144

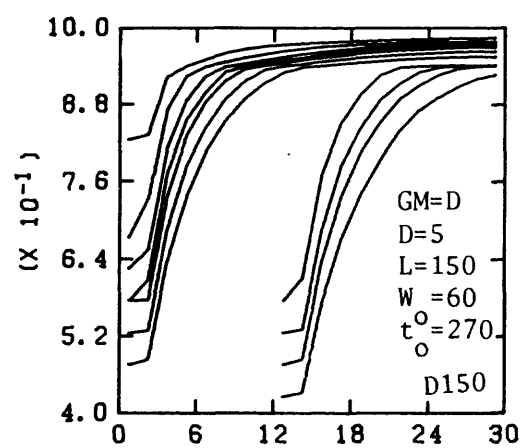
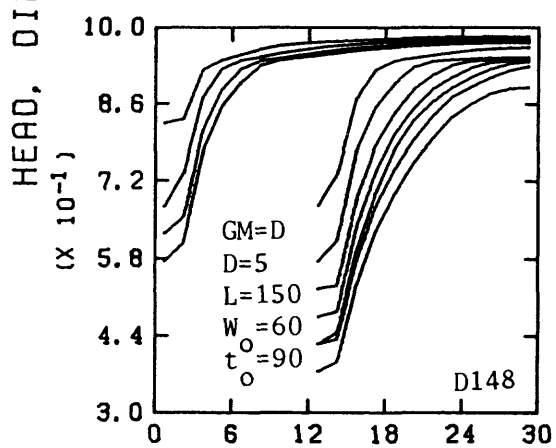
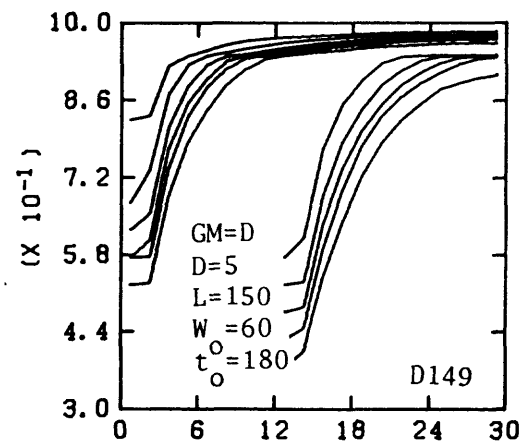
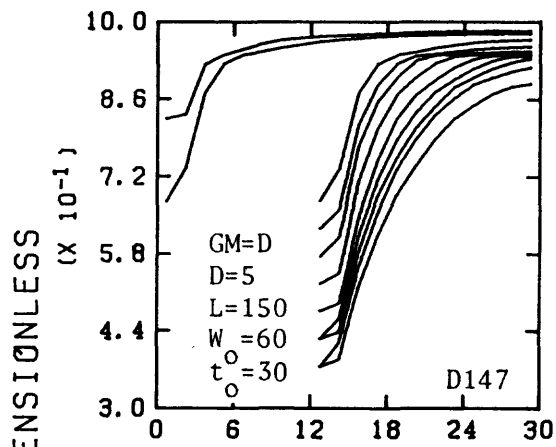
Graphs D145 and D146

Curve Dimensionless time

Curve Dimensionless time

1	2.6
2	7.9
3	16
4	24
5	32
6	48
7	71
8	95
9	143
10	193

1	0.53
2	1.6
3	3.2
4	4.8
5	6.4
6	9.5
7	14
8	19
9	29
10	39



DISTANCE, DIMENSIONLESS

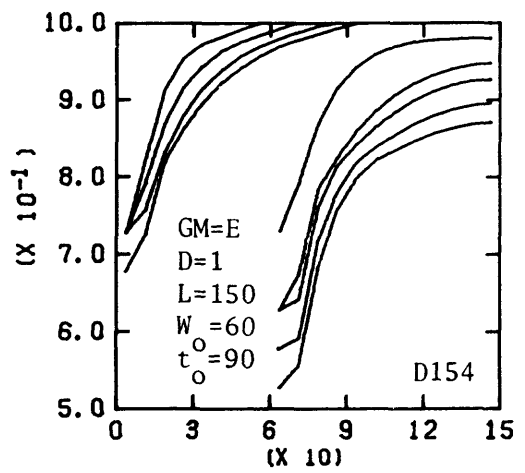
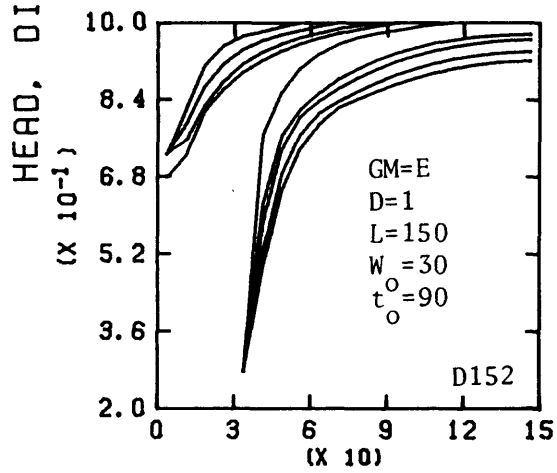
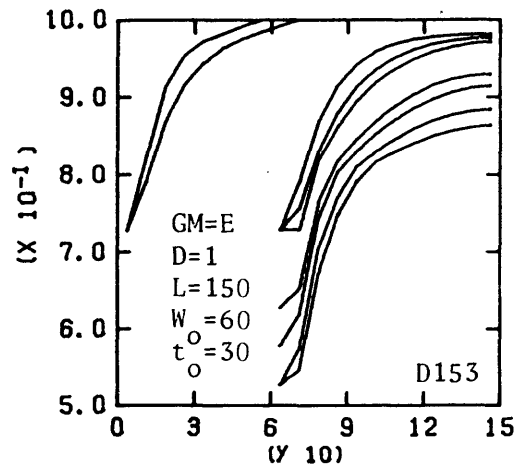
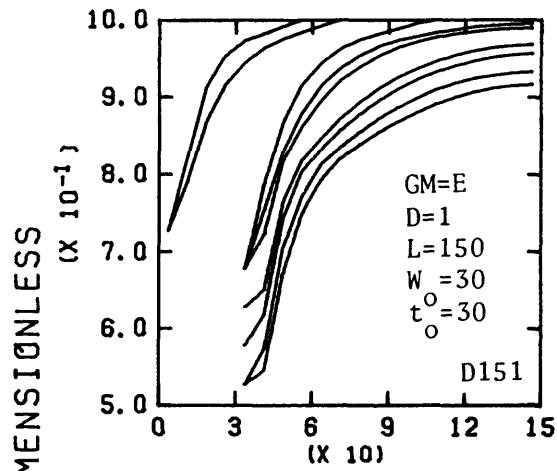
Curves numbered from top to bottom.

Graphs D147 and D148

Graphs D149 and D150

Curve	Dimensionless time
1	0.53
2	1.6
3	3.2
4	4.8
5	6.4
6	9.5
7	14
8	19
9	24
10	29
11	39

Curve	Dimensionless time
1	0.53
2	1.6
3	3.2
4	4.8
5	6.4
6	9.5
7	14
8	19
9	24
10	29
11	39



DISTANCE, DIMENSIONLESS

Curves numbered from top to bottom.

Graphs D151 and D152

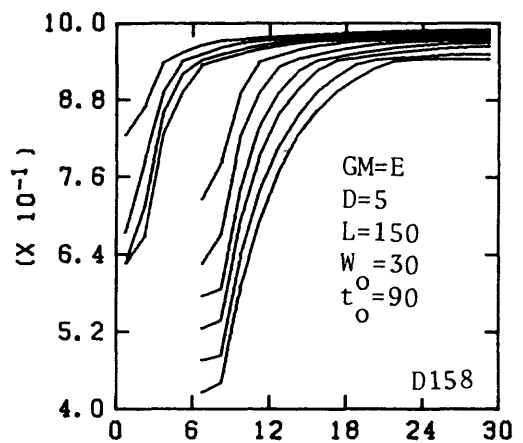
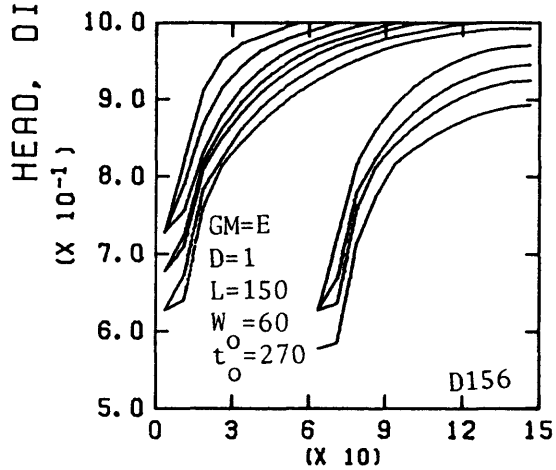
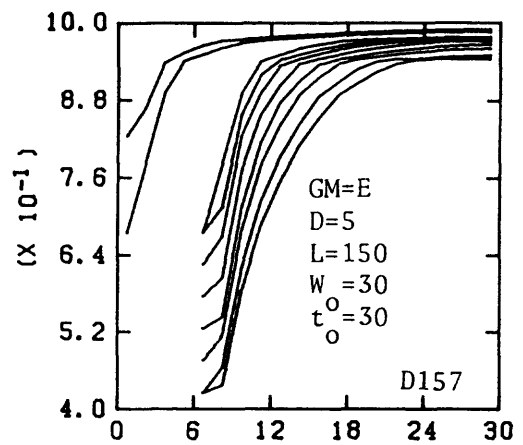
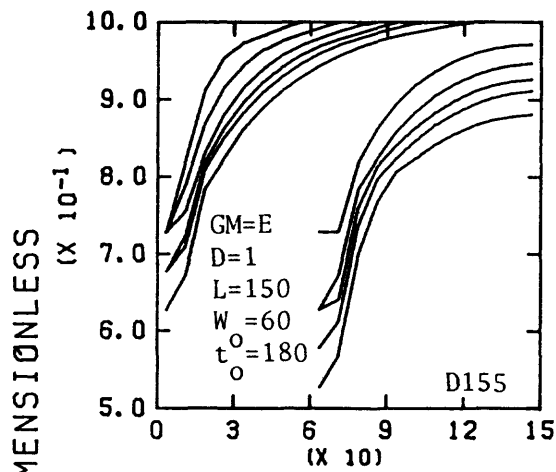
Graphs D153 and D154

Curve Dimensionless time

1	1.7
2	5.1
3	10
4	15
5	20
6	46
7	61
8	91
9	124

Curve Dimensionless time

1	1.7
2	5.1
3	10
4	15
5	20
6	46
7	61
8	91
9	124



DISTANCE, DIMENSIONLESS

Curves numbered from top to bottom.

Graphs D155 and D156

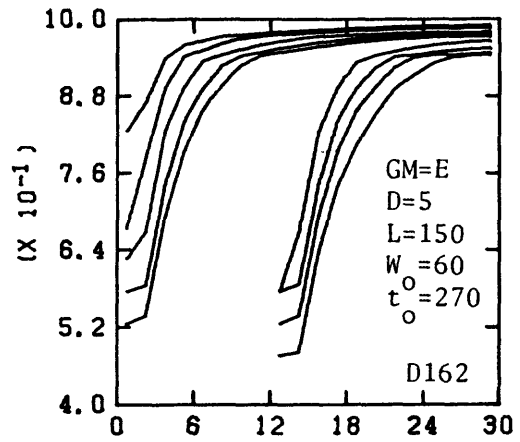
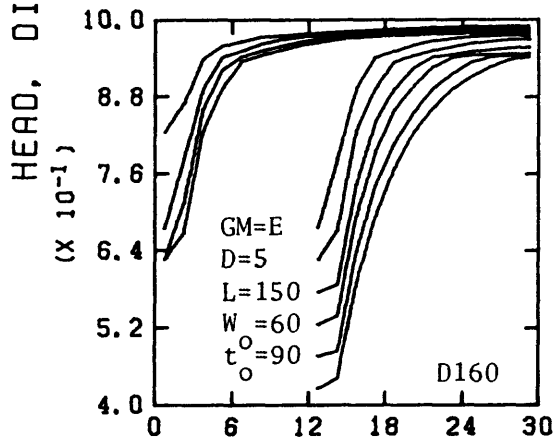
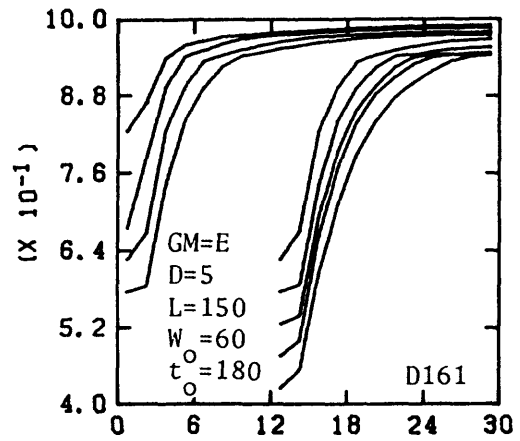
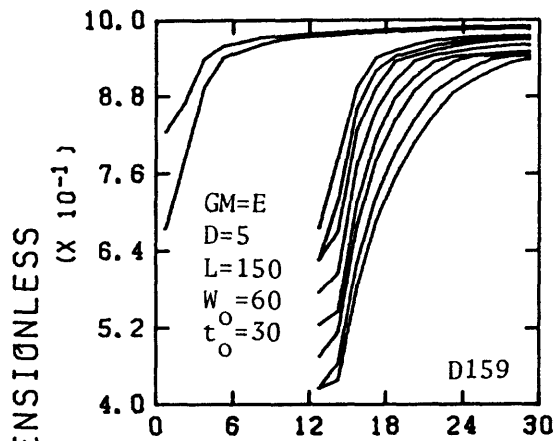
Graphs D157 and D158

Curve Dimensionless time

Curve Dimensionless time

1	1.7
2	5.1
3	10
4	15
5	20
6	30
7	46
8	61
9	76
10	91
11	124

1	0.34
2	1.0
3	2.0
4	3.0
5	4.1
6	6.1
7	9.1
8	12
9	18
10	25



DISTANCE, DIMENSIONLESS

Curves numbered from top to bottom.

Graphs D159 and D160

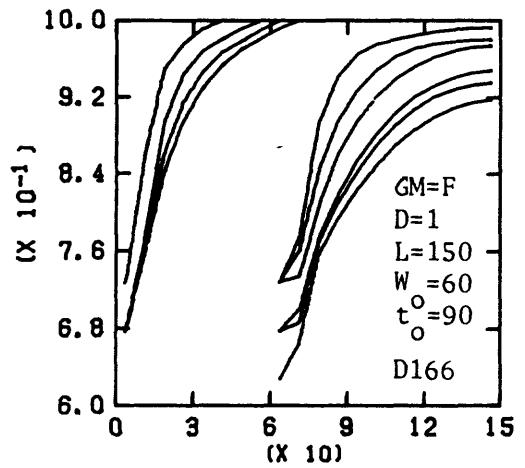
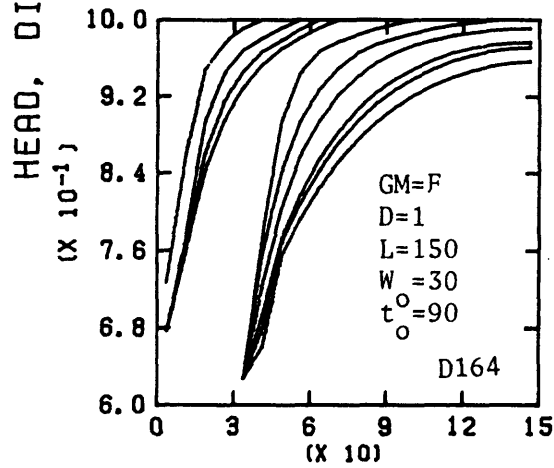
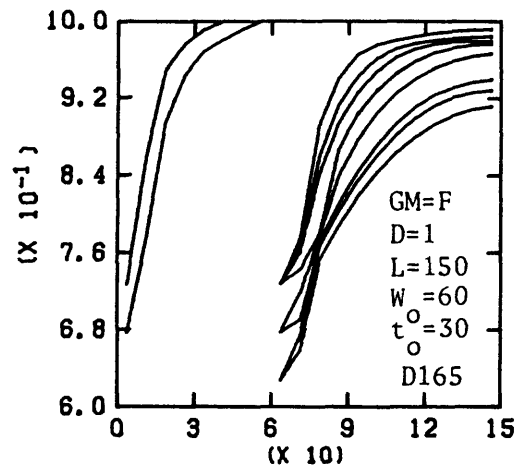
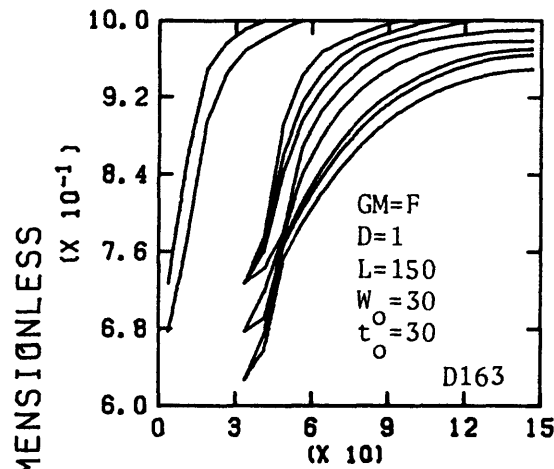
Graphs D161 and D162

Curve Dimensionless time

1	0.34
2	1.0
3	2.0
4	3.0
5	4.1
6	6.1
7	9.1
8	12
9	18
10	25

Curve Dimensionless time

1	0.34
2	1.0
3	3.0
4	6.1
5	9.1
6	12
7	15
8	18
9	25



DISTANCE, DIMENSIONLESS

Curves numbered from top to bottom.

Graphs D163 and D164

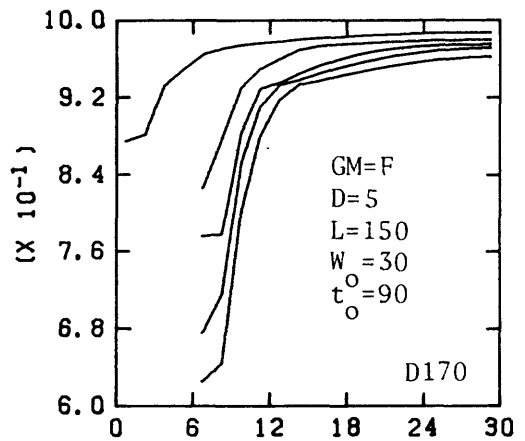
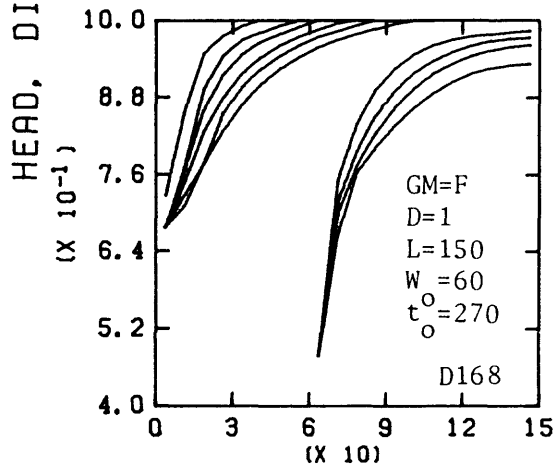
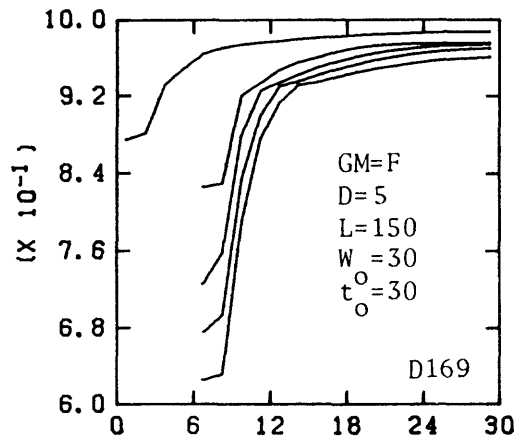
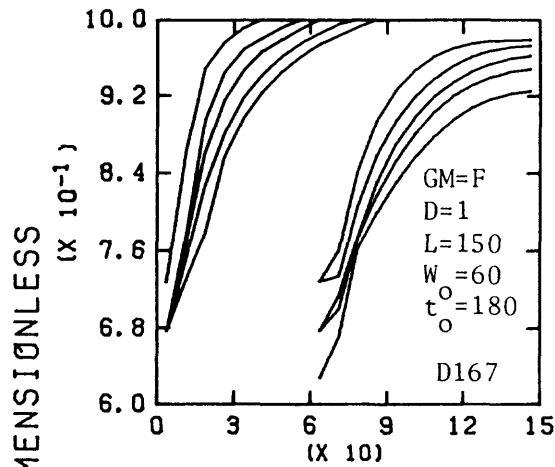
Graphs D165 and D166

Curve Dimensionless time

Curve Dimensionless time

1	0.24
2	0.73
3	1.5
4	2.2
5	2.9
6	4.4
7	6.5
8	11
9	13
10	18

1	0.24
2	0.73
3	1.5
4	2.2
5	2.9
6	4.4
7	6.5
8	11
9	13
10	18



DISTANCE, DIMENSIONLESS

Curves numbered from top to bottom.

Graphs D167 and D168

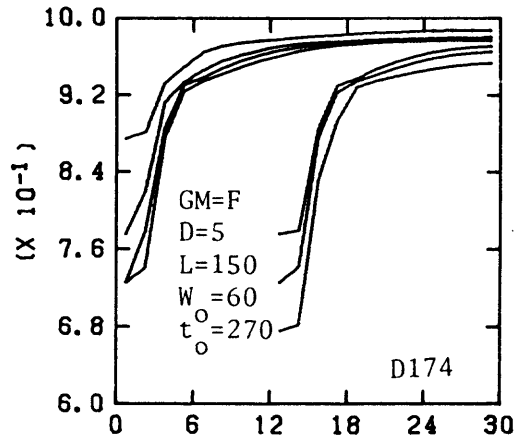
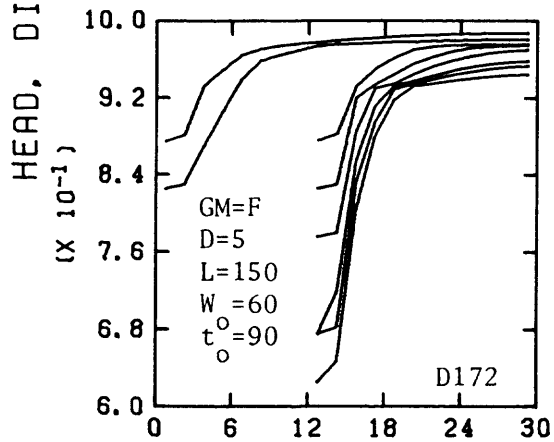
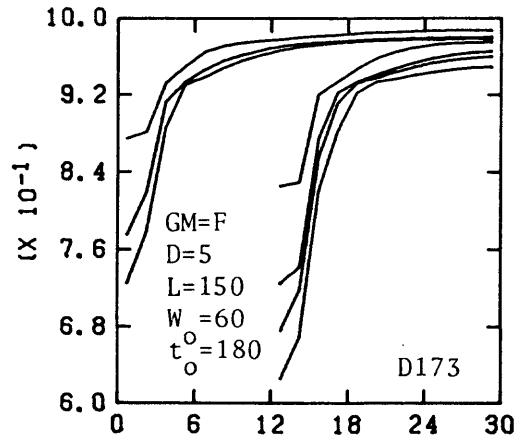
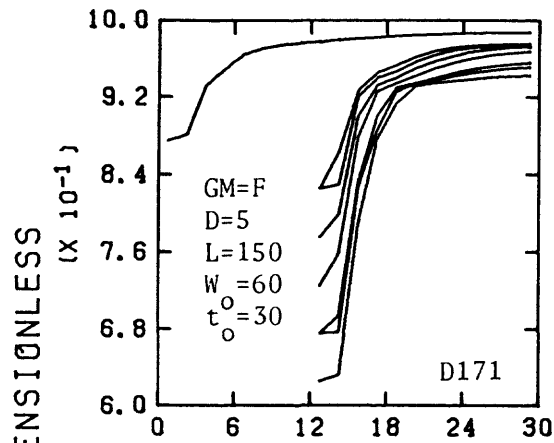
Graphs D169 and D170

Curve Dimensionless time

Curve Dimensionless time

1	0.24
2	0.73
3	1.5
4	2.9
5	4.4
6	6.5
7	8.7
8	11
9	13
10	18

1	0.15
2	0.58
3	1.3
4	2.2
5	3.5



DISTANCE, DIMENSIONLESS

Curves numbered from top to bottom.

Graphs D171 and D172

Graphs D173 and D174

Curve Dimensionless time

Curve Dimensionless time

1	0.15
2	0.44
3	0.58
4	0.87
5	1.3
6	2.2
7	2.6
8	3.5

1	0.15
2	0.58
3	0.87
4	1.3
5	2.2
6	2.6
7	3.5

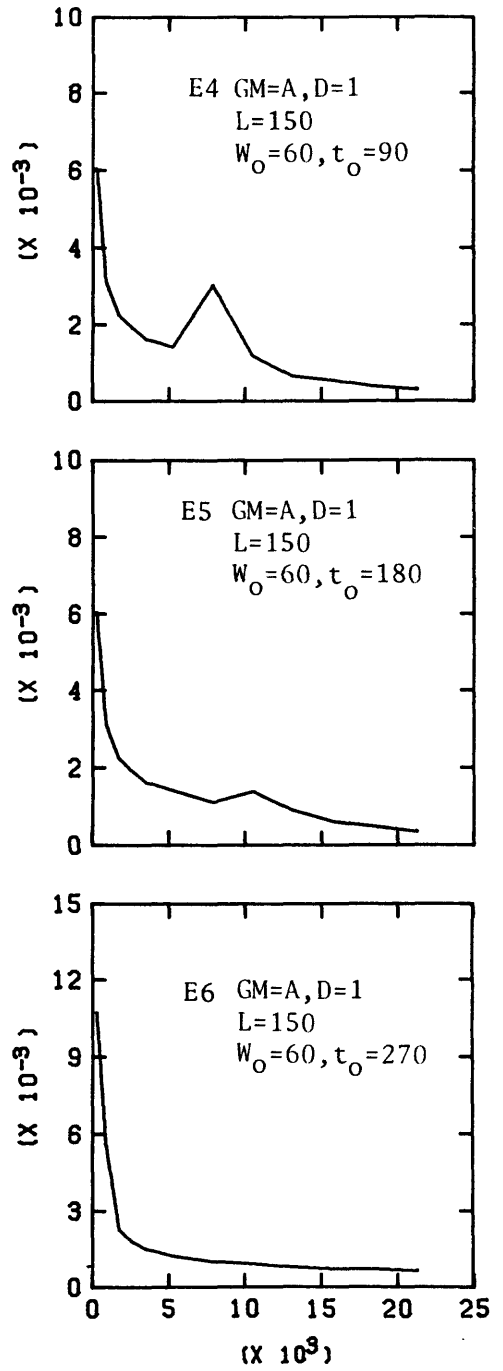
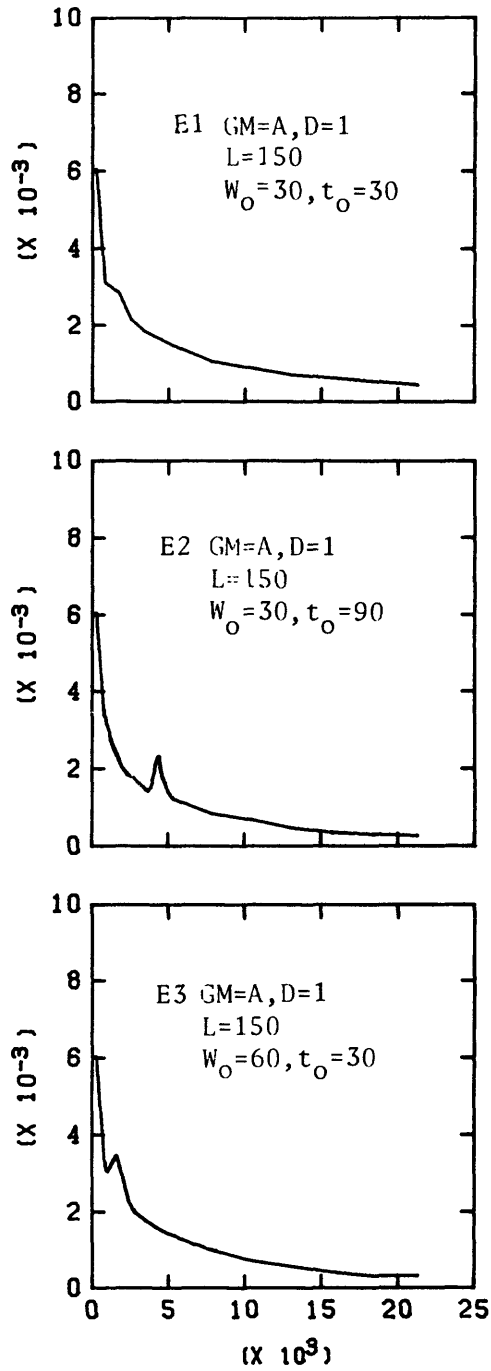
APPENDIX E

Dimensionless seepage-flux profiles for the hypothetical-aquifer/multiple-cut combinations.

Symbols.--The following symbols appear with graphs E1 through E174 of Appendix E:

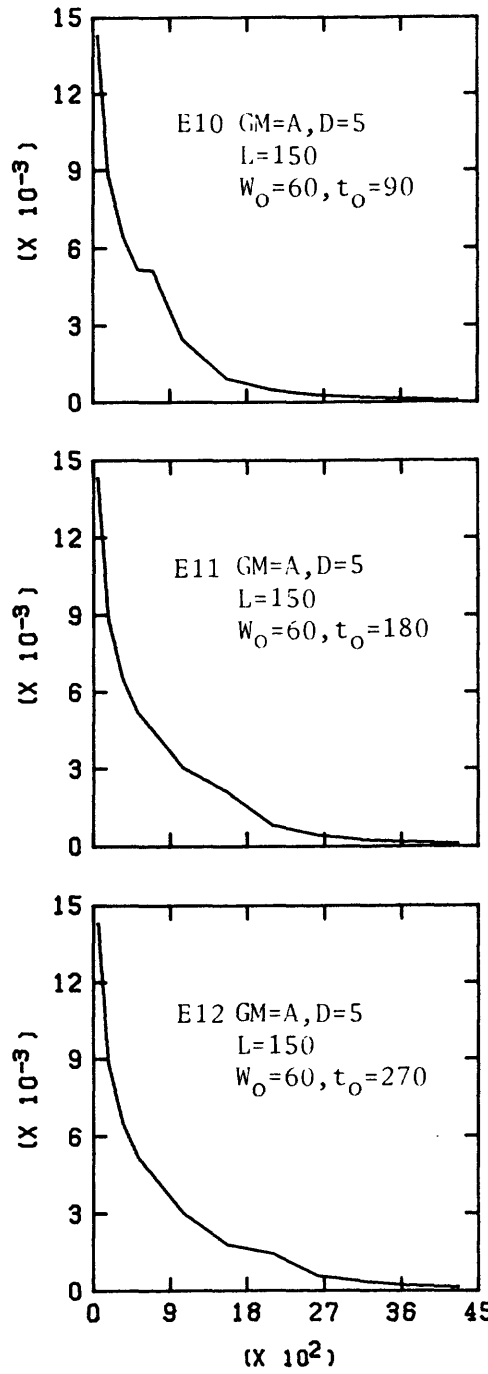
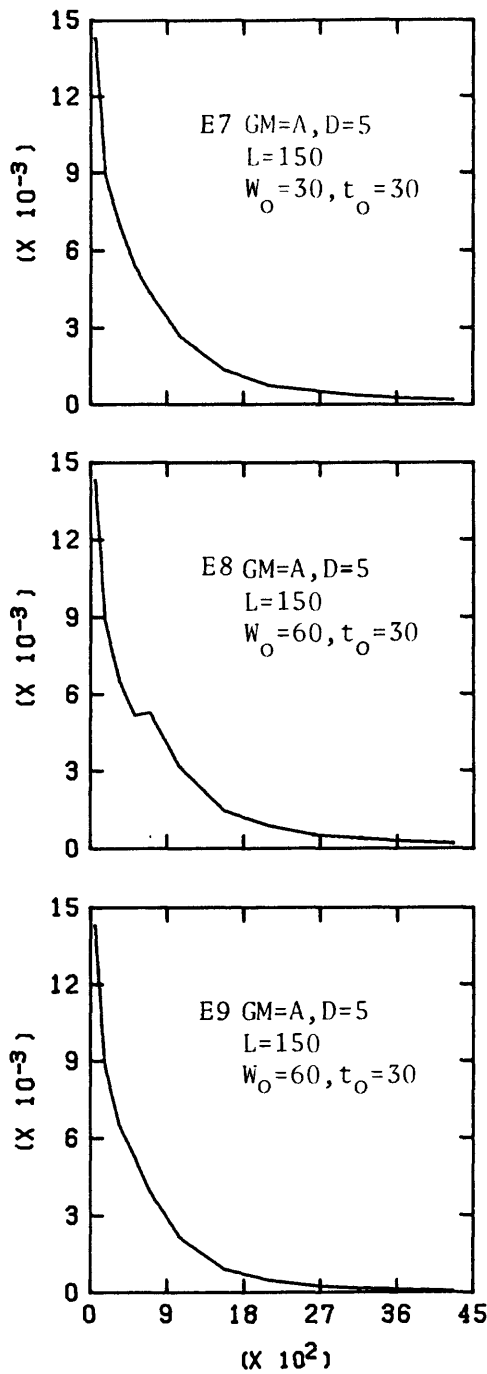
<u>Symbol</u>	<u>Explanation</u>
GM	Geologic material (table 1).
D	Initial saturated thickness, in meters.
L	Length, in meters.
w_0	Multiple-cut width, in meters.
t_0	Multiple-cut time, in days.

SEEPAGE FLUX, DIMENSIONLESS



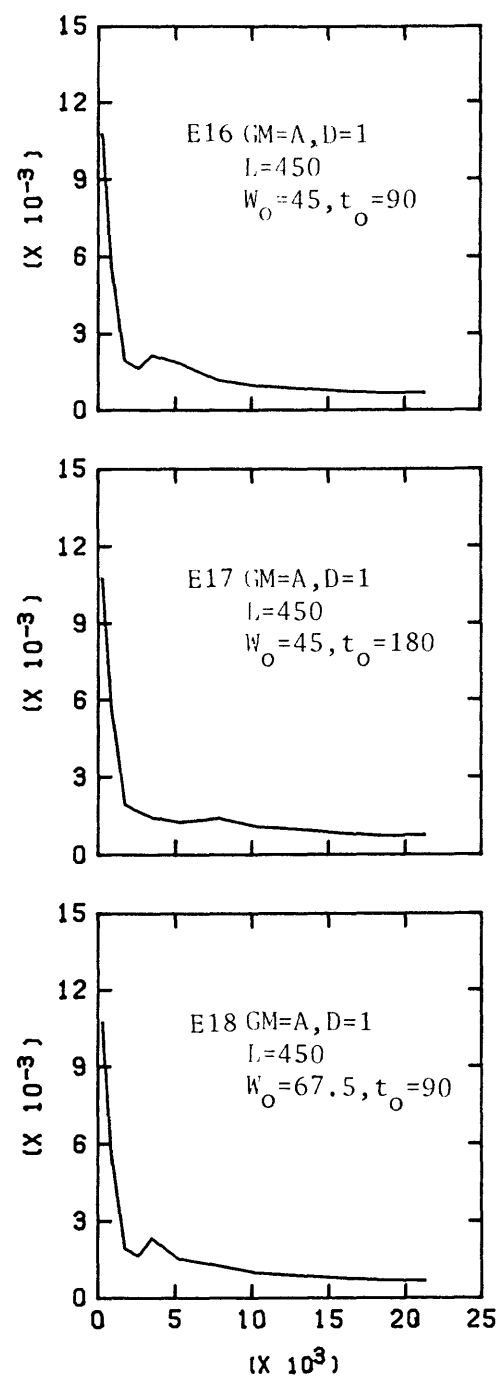
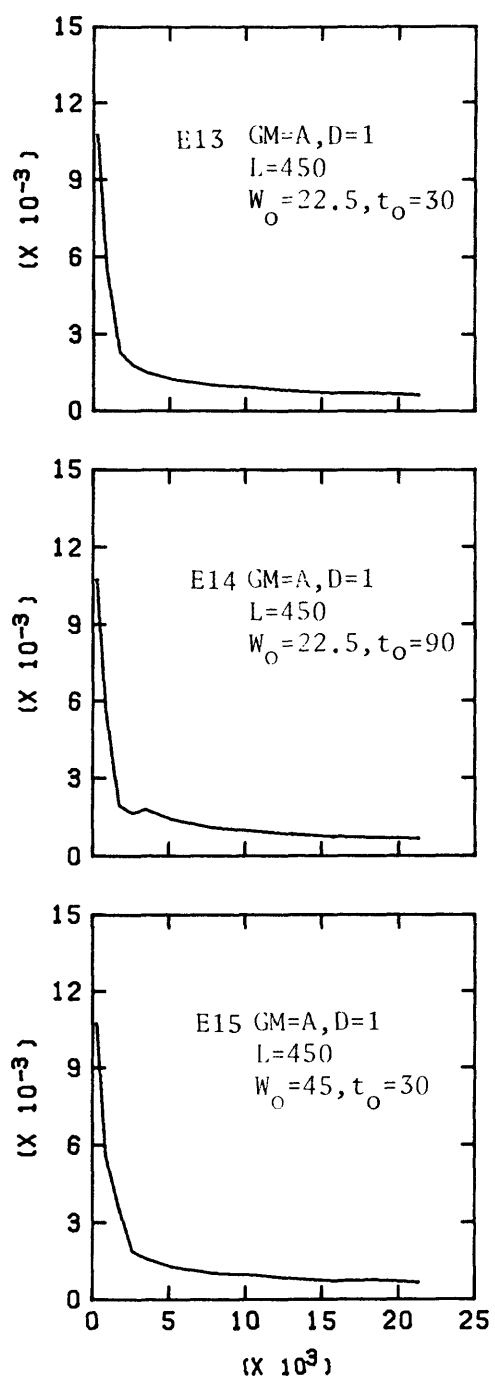
TIME, DIMENSIONLESS

SEEPAGE FLUX, DIMENSIONLESS



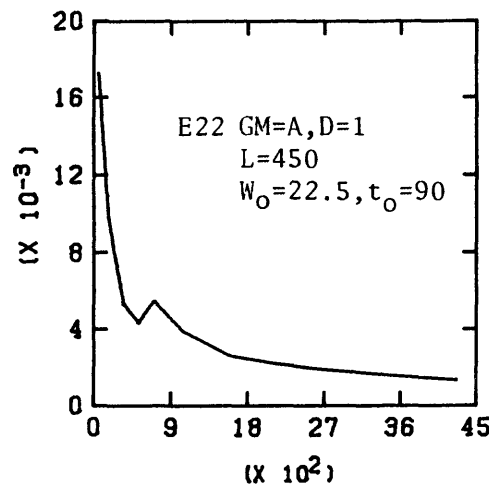
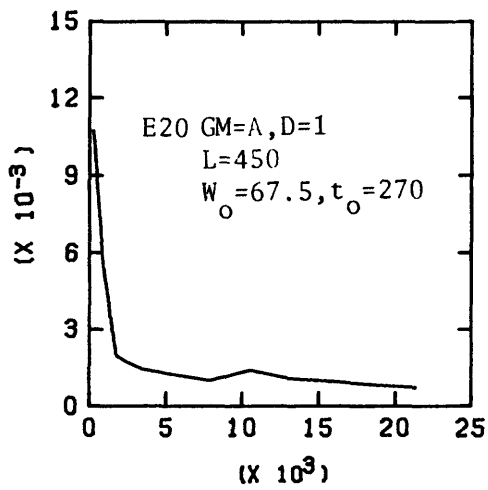
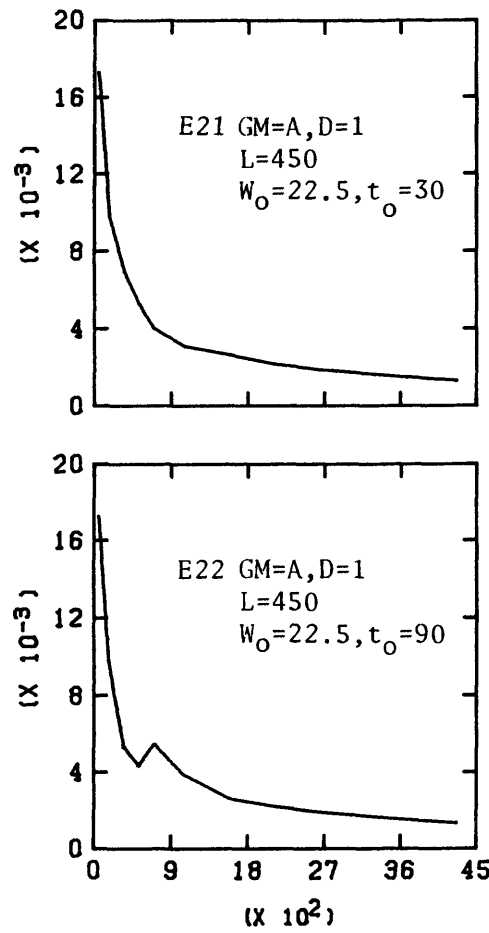
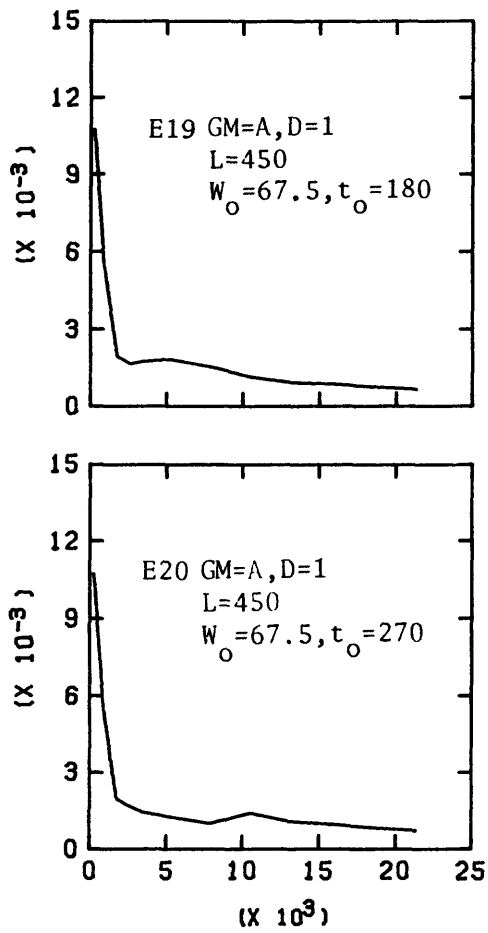
TIME, DIMENSIONLESS

SEEPAGE FLUX, DIMENSIONLESS



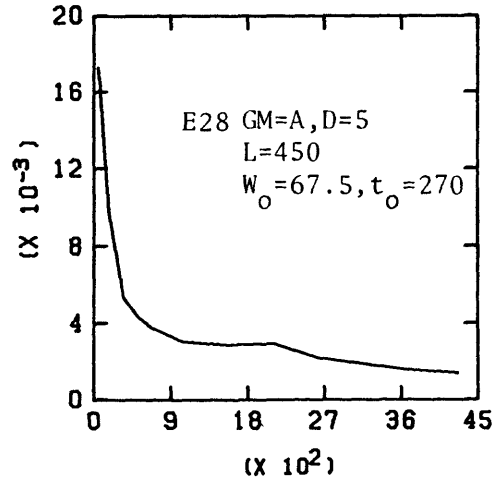
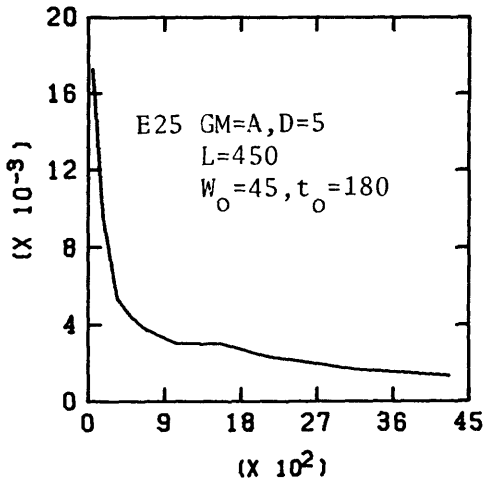
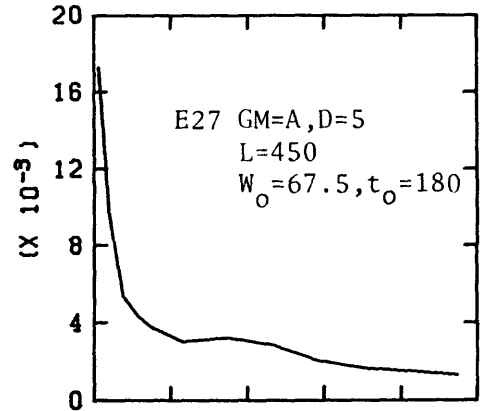
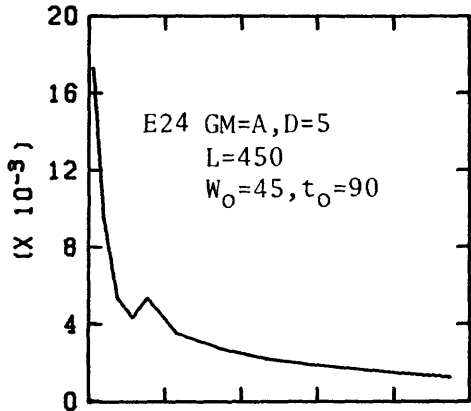
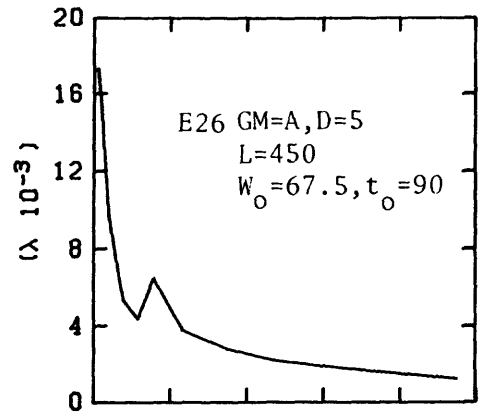
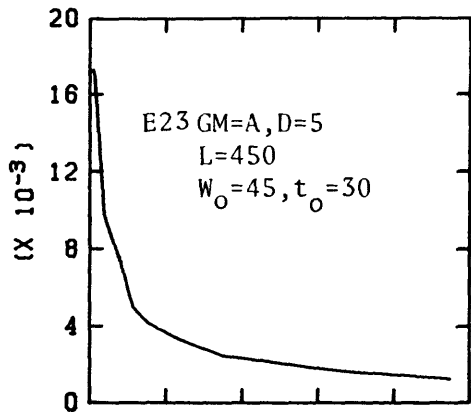
TIME, DIMENSIONLESS

SEEPAGE FLUX, DIMENSIONLESS



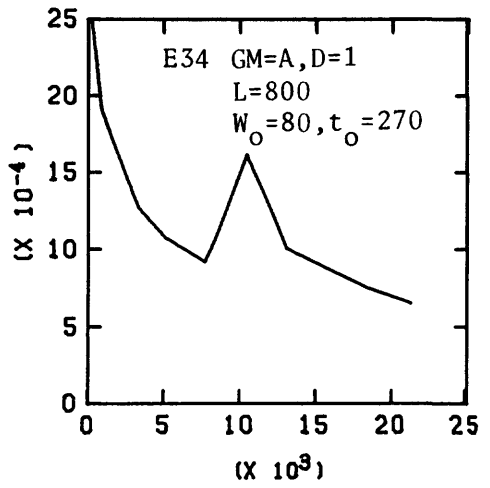
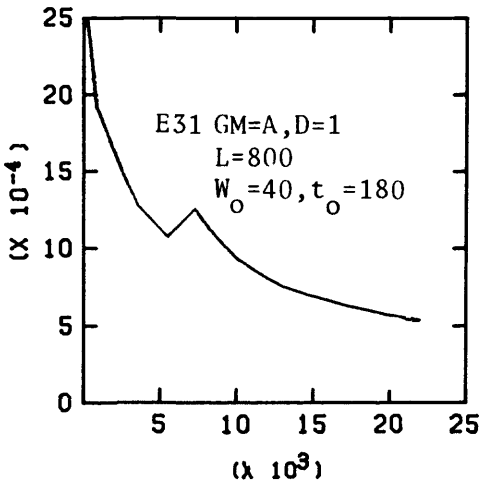
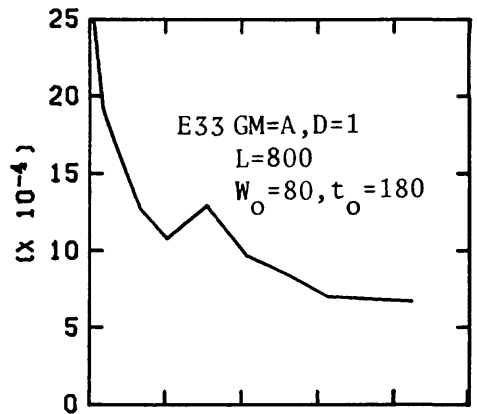
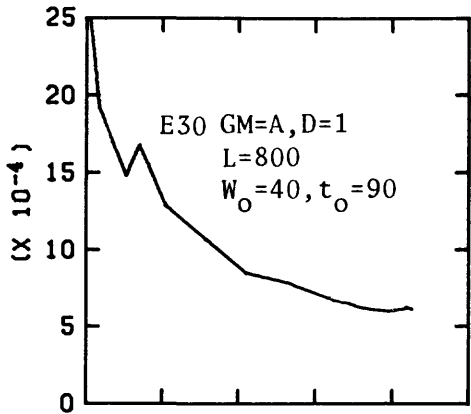
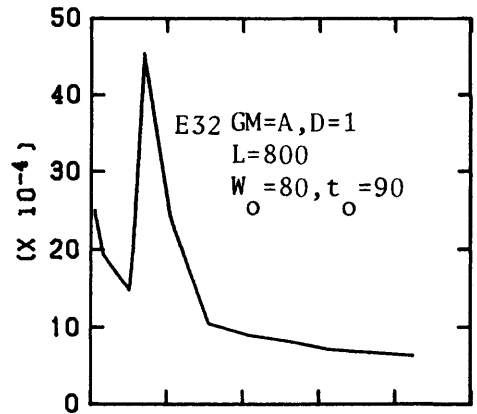
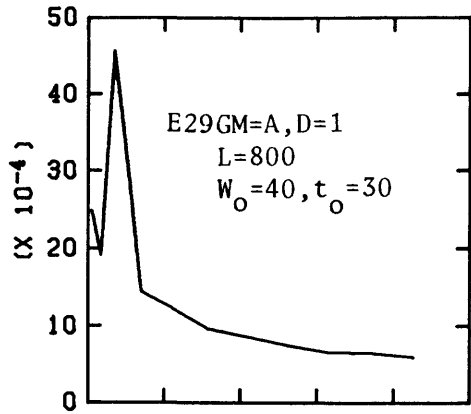
TIME, DIMENSIONLESS

SEEPAGE FLUX, DIMENSIONLESS



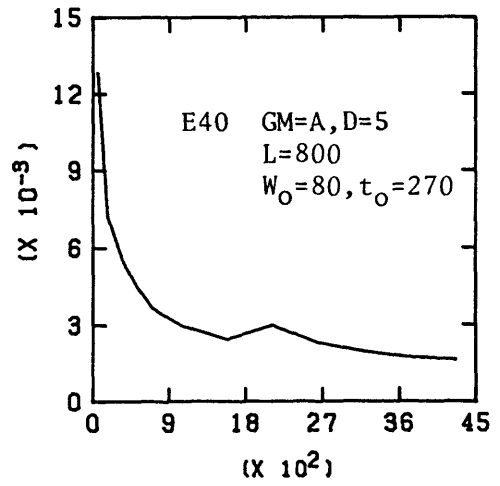
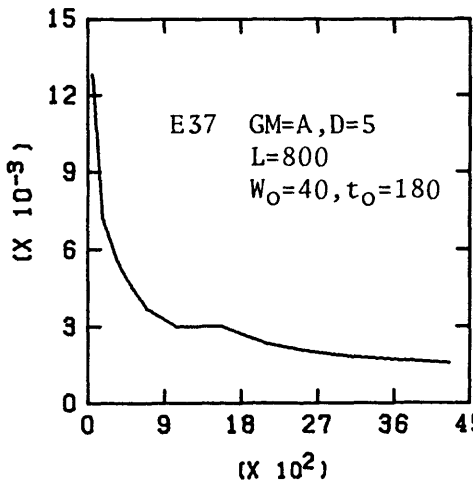
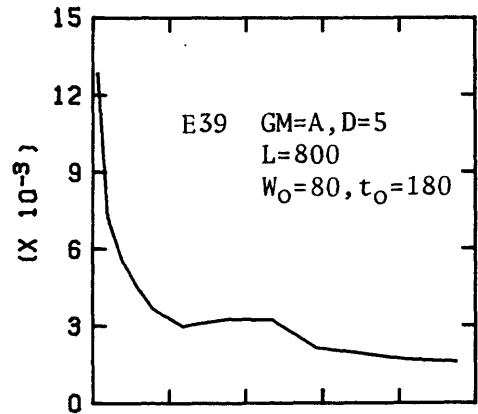
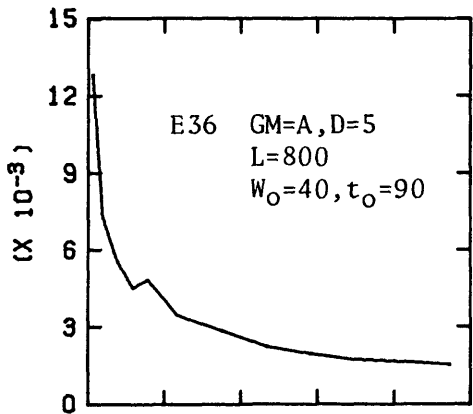
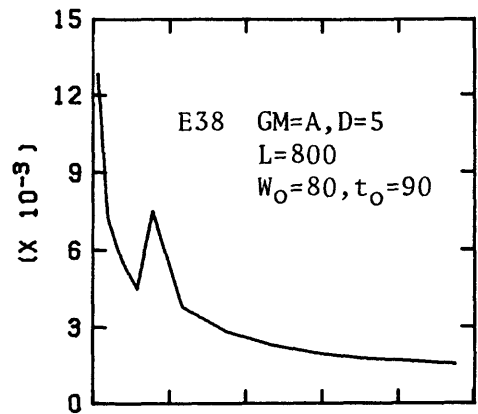
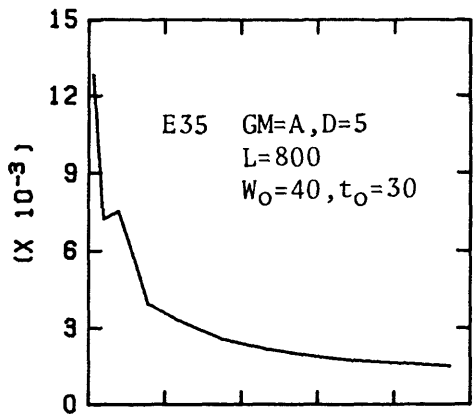
TIME, DIMENSIONLESS

SEEPAGE FLUX, DIMENSIONLESS



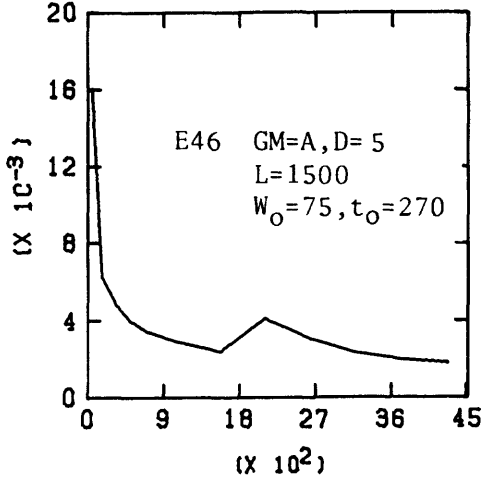
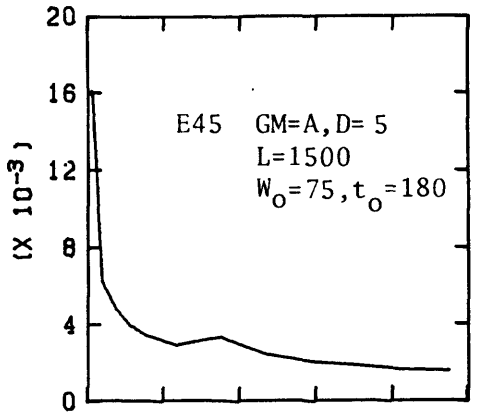
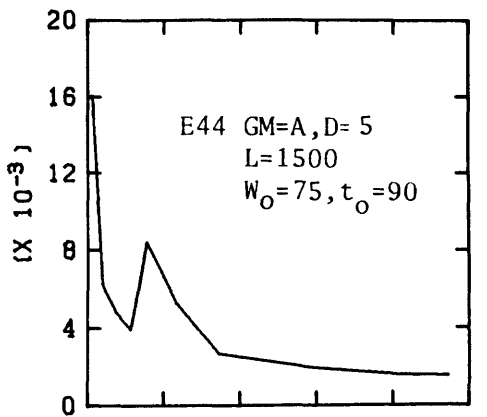
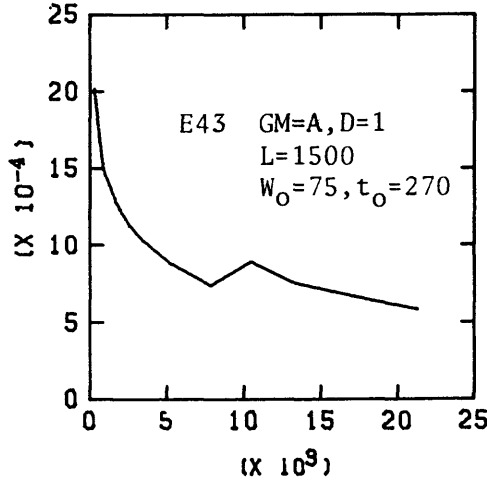
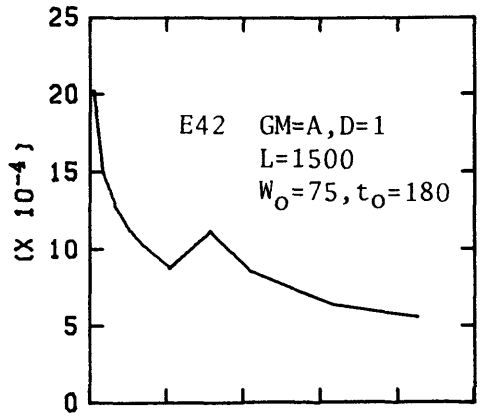
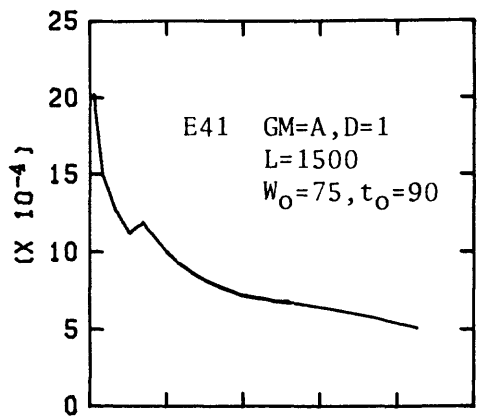
TIME, DIMENSIONLESS

SEEPAGE FLUX, DIMENSIONLESS



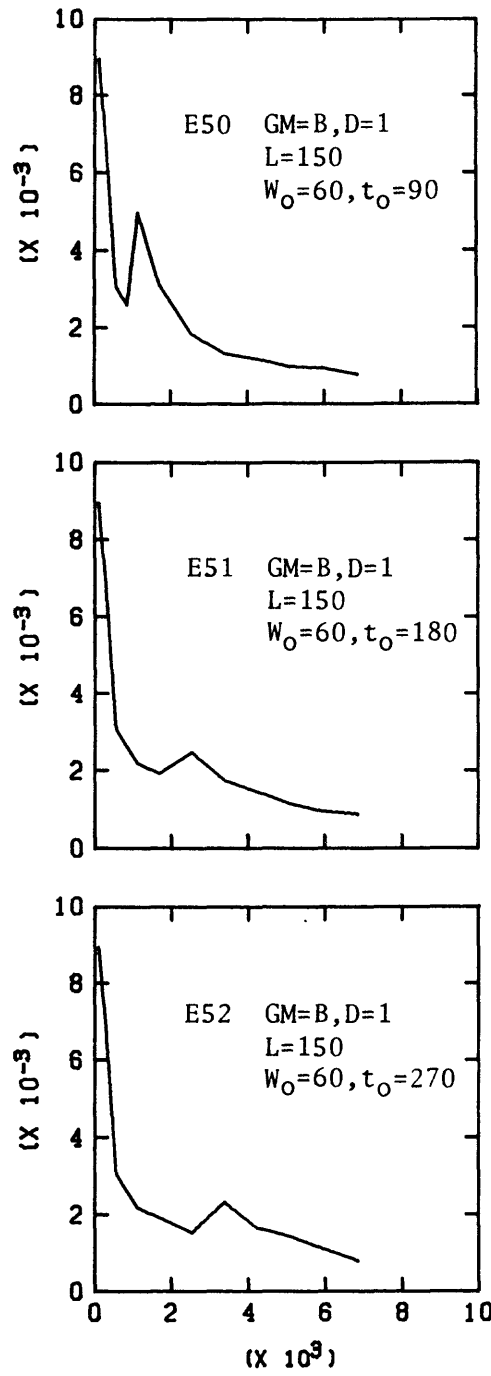
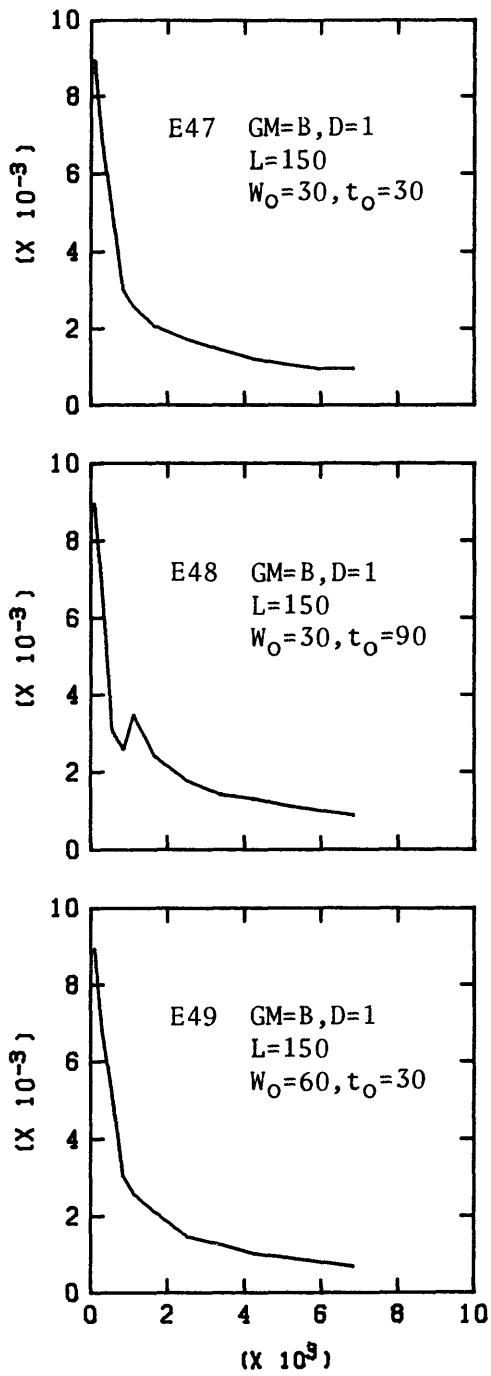
TIME, DIMENSIONLESS

SEEPAGE FLUX, DIMENSIONLESS



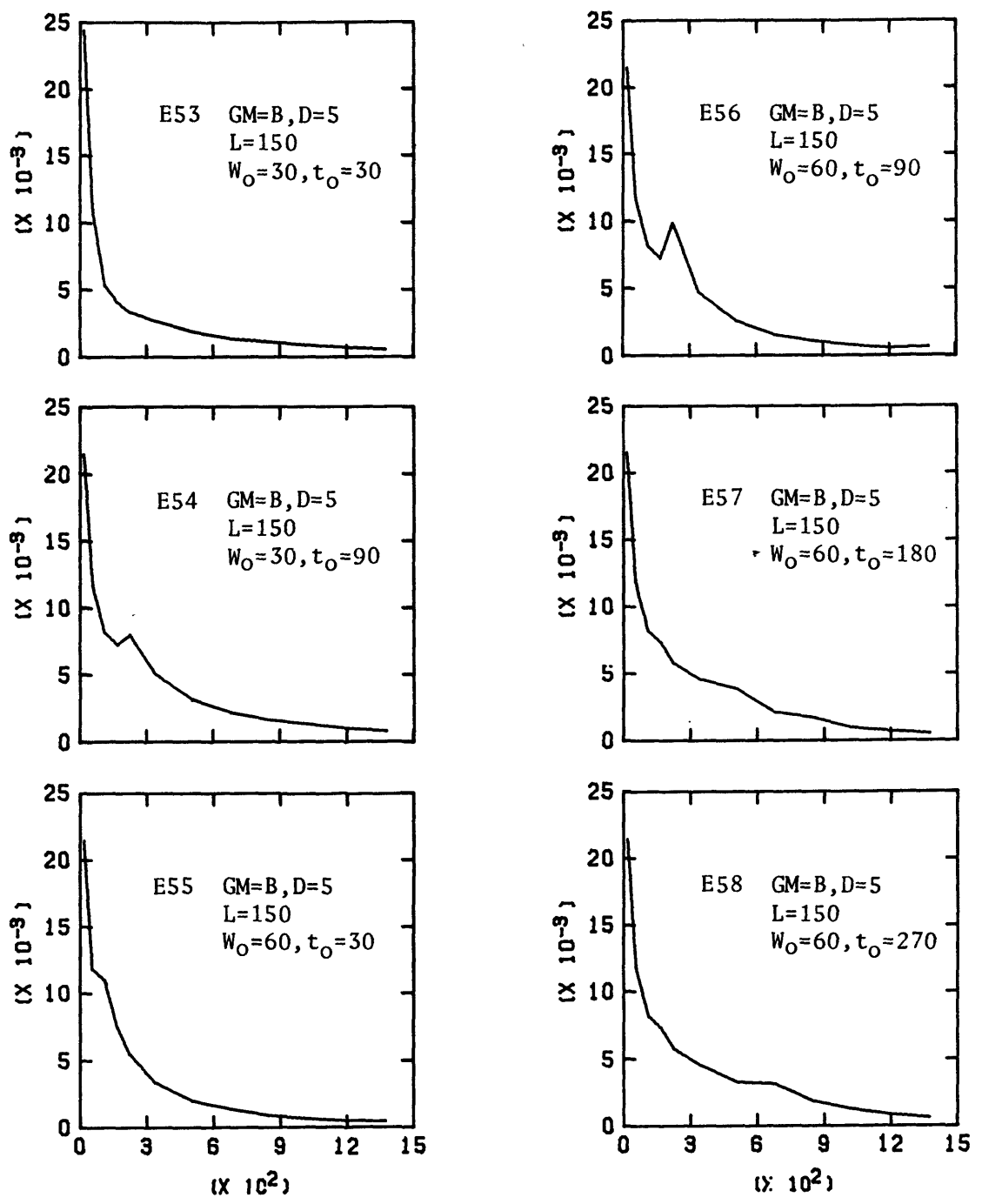
TIME, DIMENSIONLESS

SEEPAGE FLUX, DIMENSIONLESS



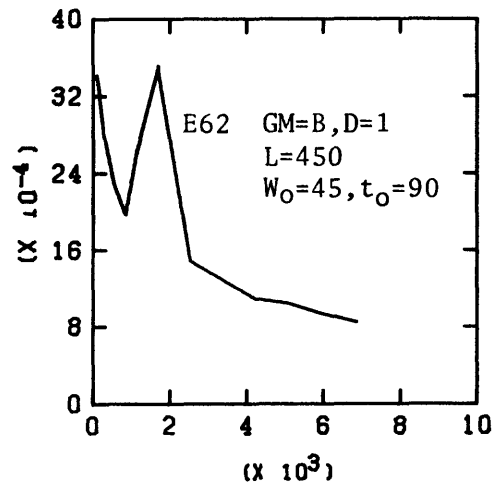
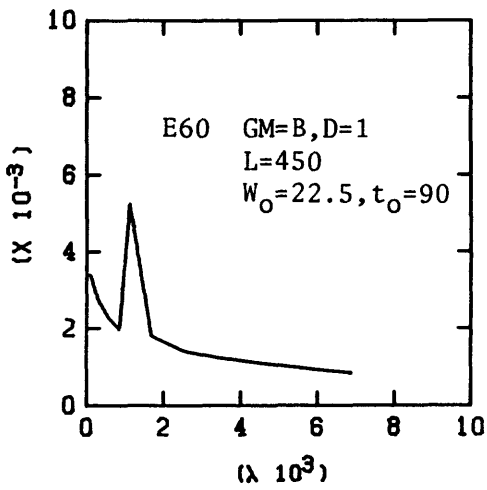
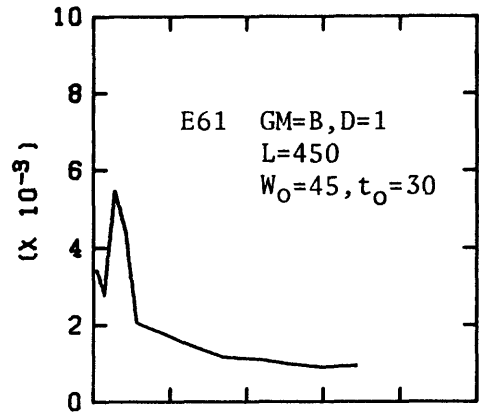
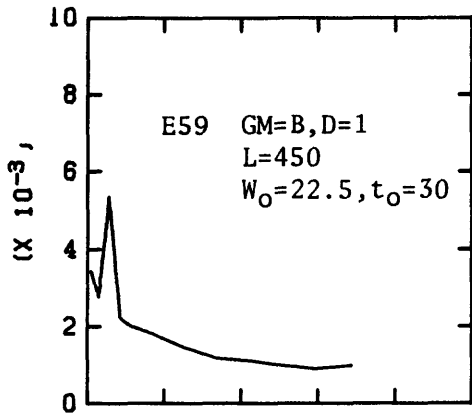
TIME, DIMENSIONLESS

SEEPAGE FLUX, DIMENSIONLESS



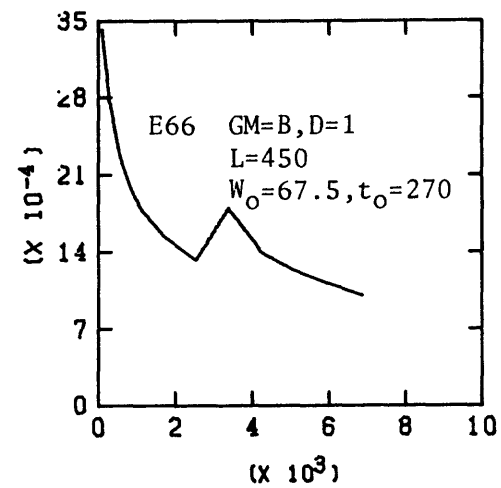
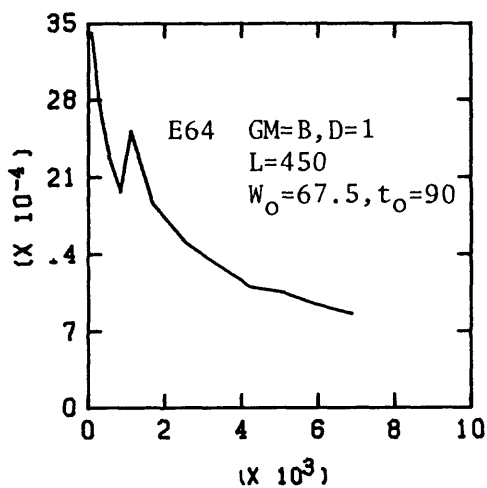
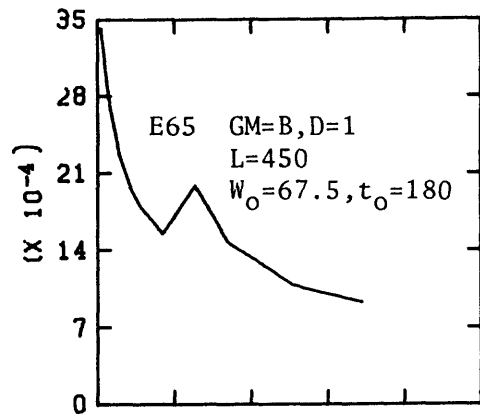
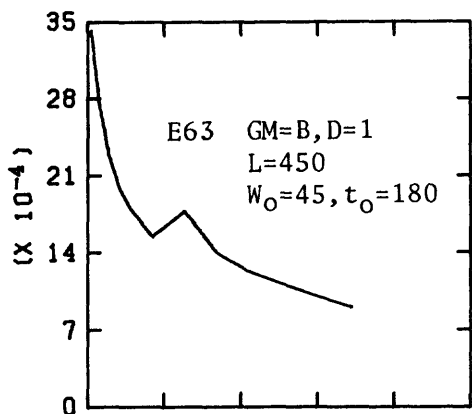
TIME, DIMENSIONLESS

SEEPAGE FLUX, DIMENSIONLESS



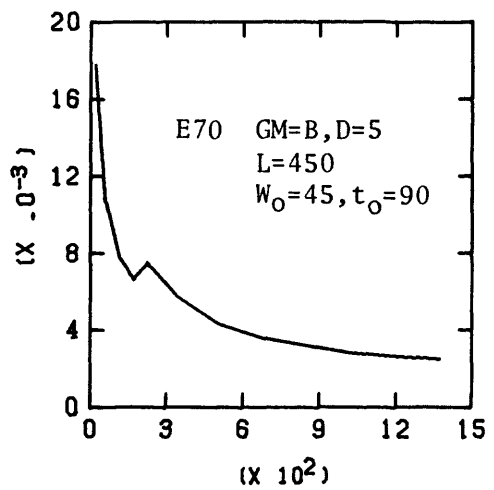
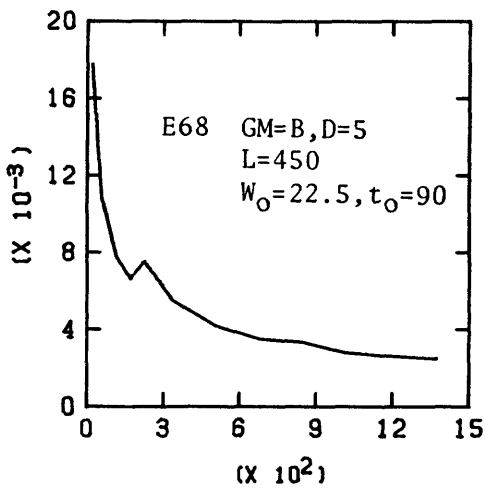
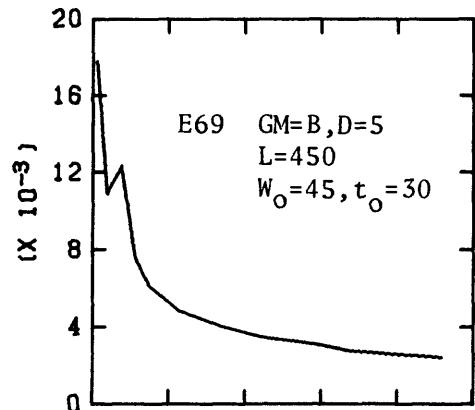
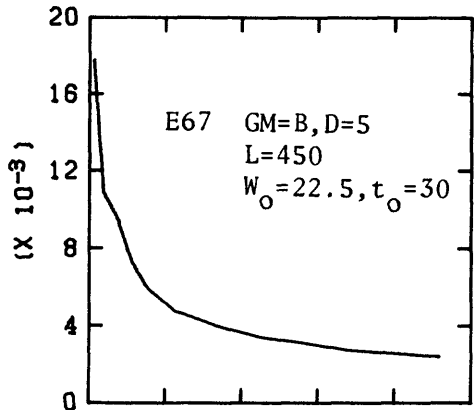
TIME, DIMENSIONLESS

SEEPAGE FLUX, DIMENSIONLESS



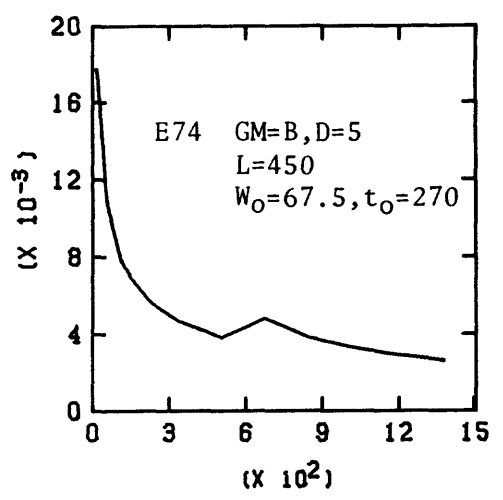
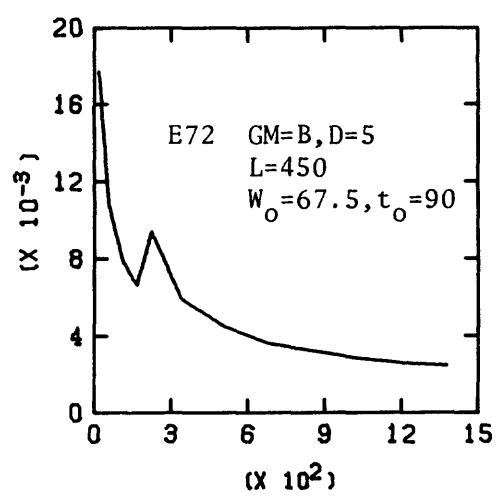
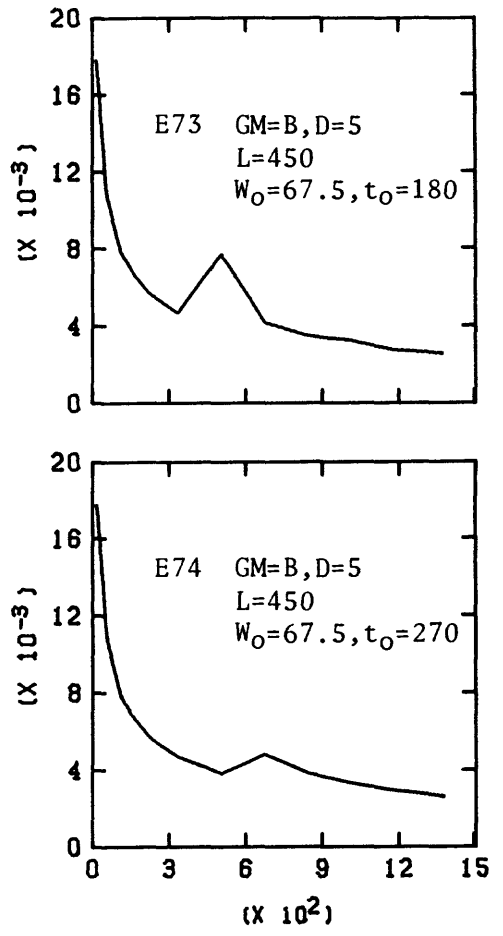
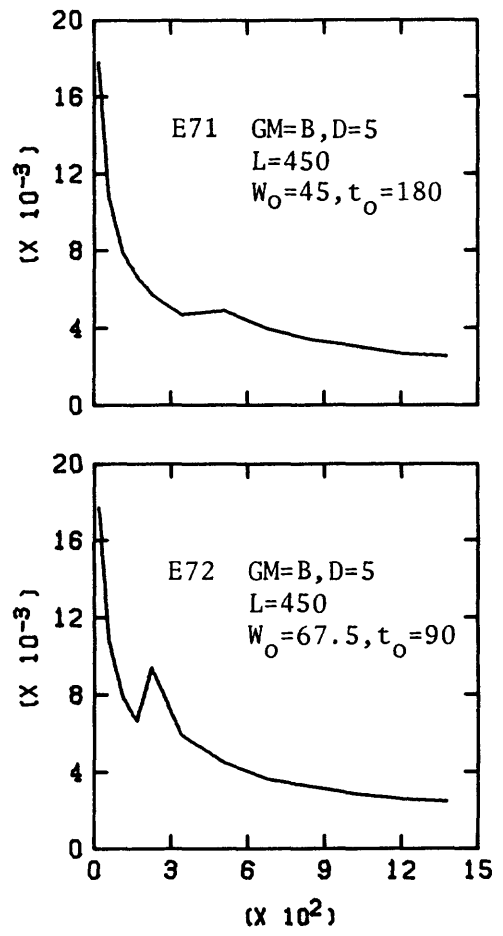
TIME, DIMENSIONLESS

SEEPAGE FLUX, DIMENSIONLESS



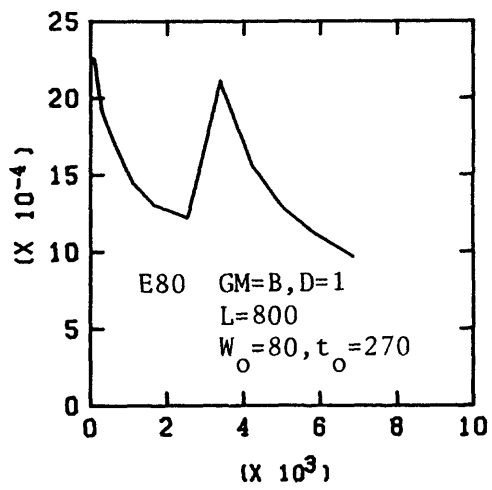
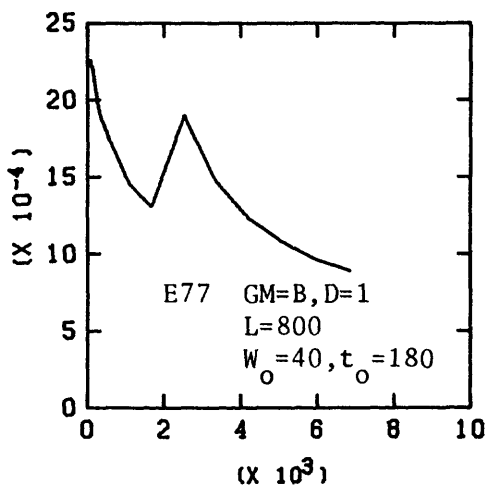
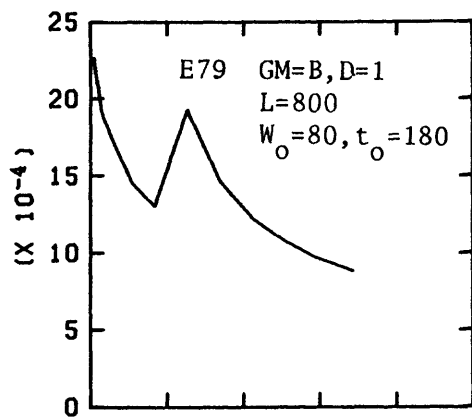
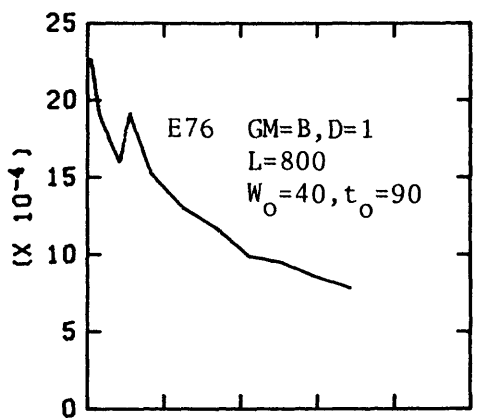
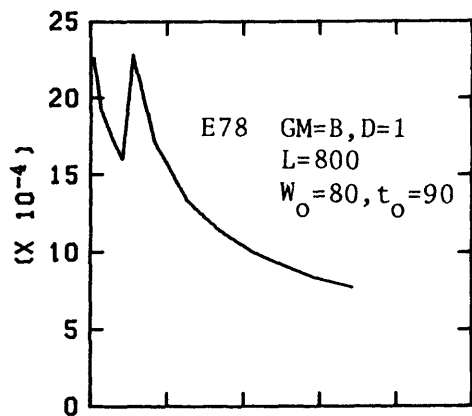
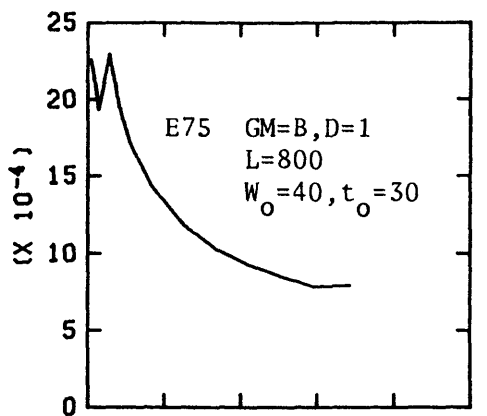
TIME, DIMENSIONLESS

SEEPAGE FLUX, DIMENSIONLESS



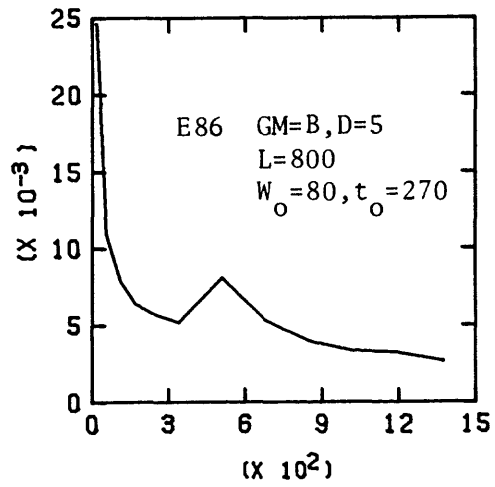
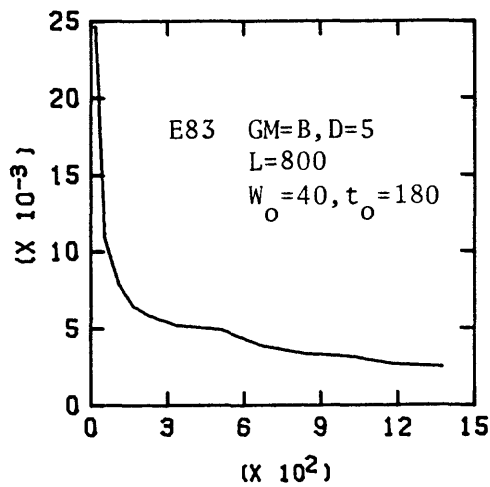
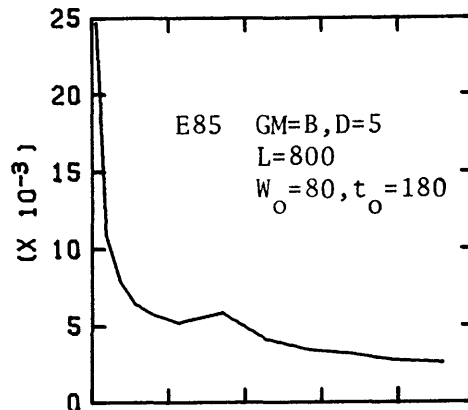
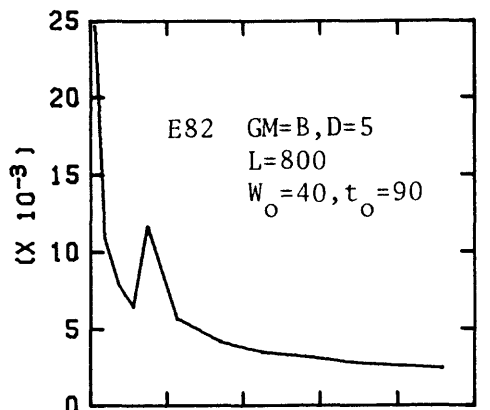
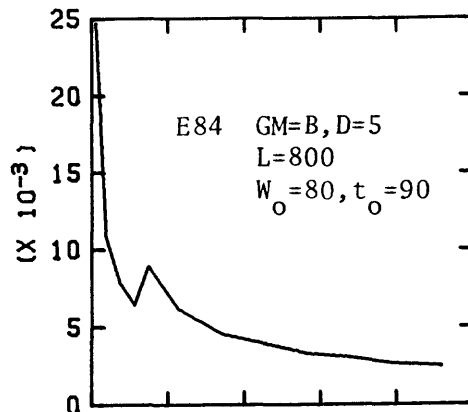
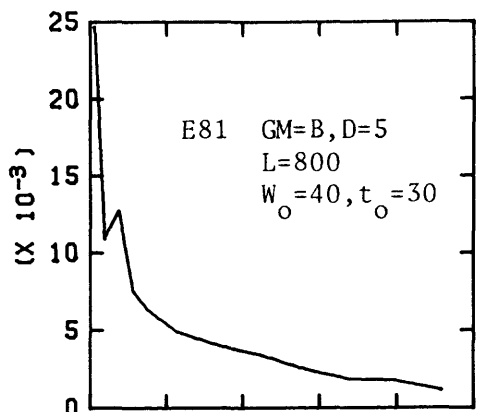
TIME, DIMENSIONLESS

SEEPAGE FLUX, DIMENSIONLESS



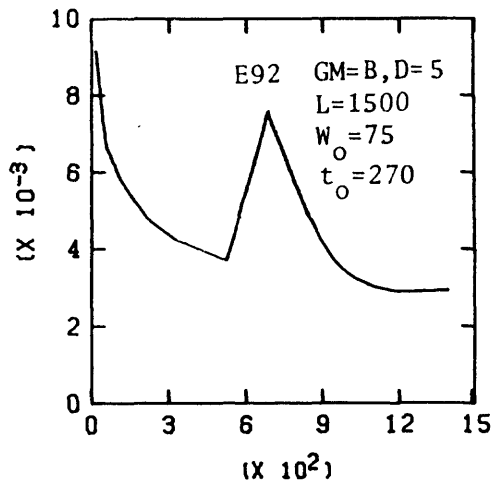
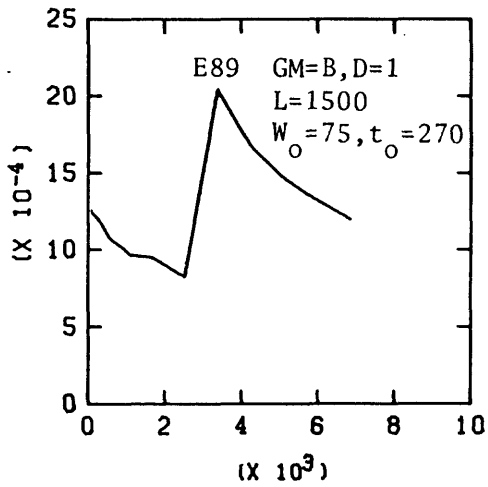
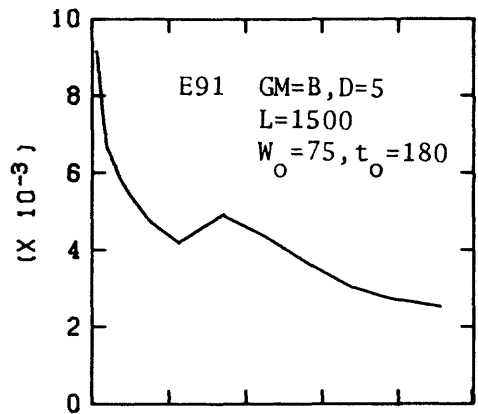
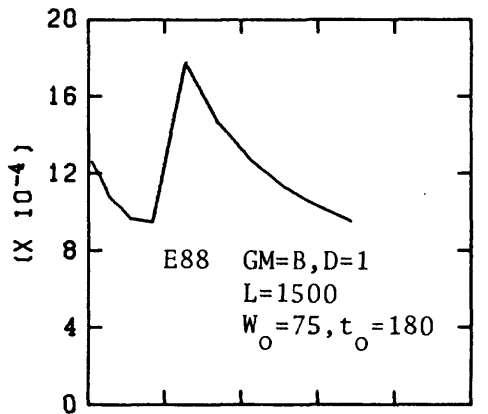
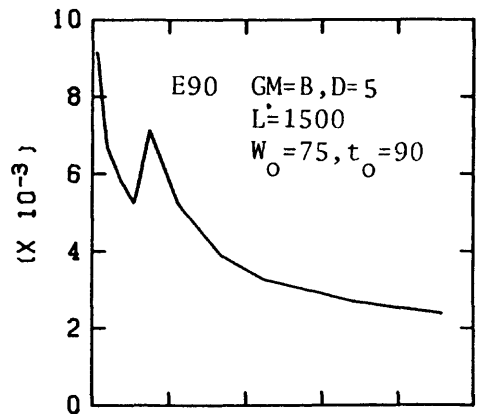
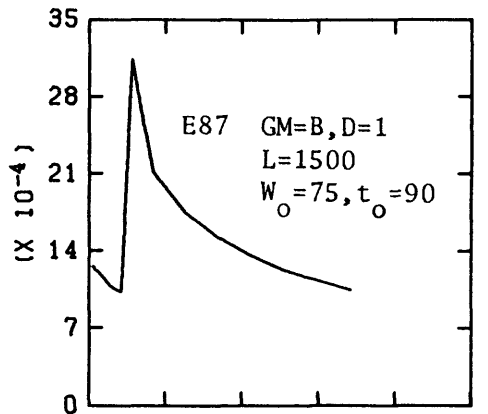
TIME, DIMENSIONLESS

SEEPAGE FLUX, DIMENSIONLESS



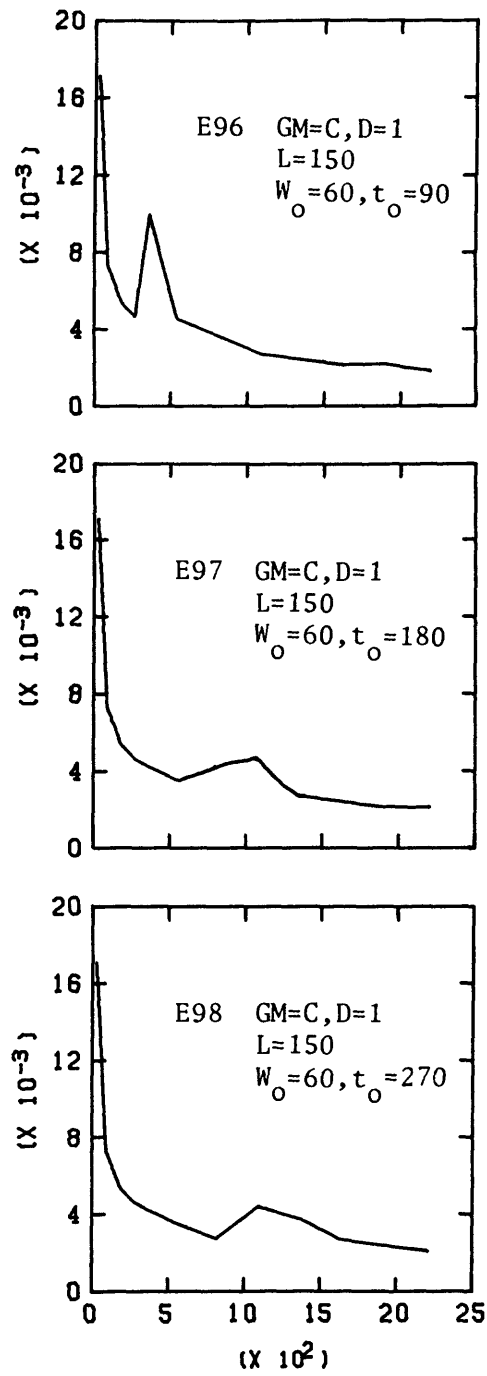
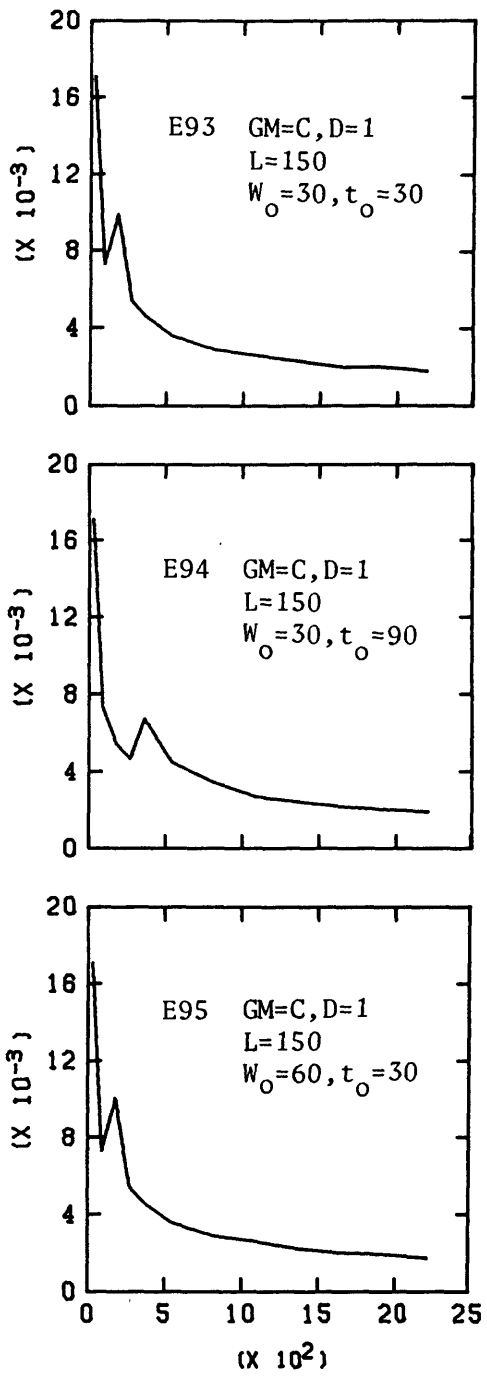
TIME, DIMENSIONLESS

SEEPAGE FLUX, DIMENSIONLESS



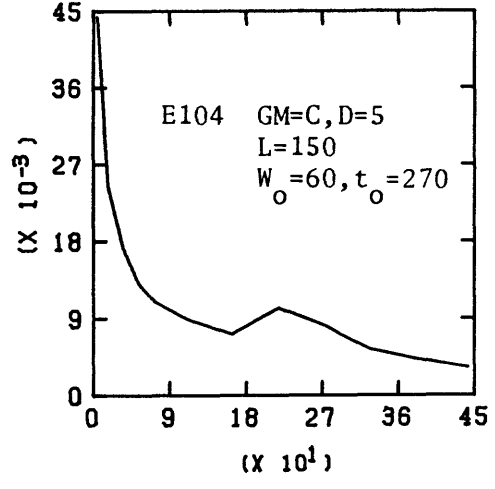
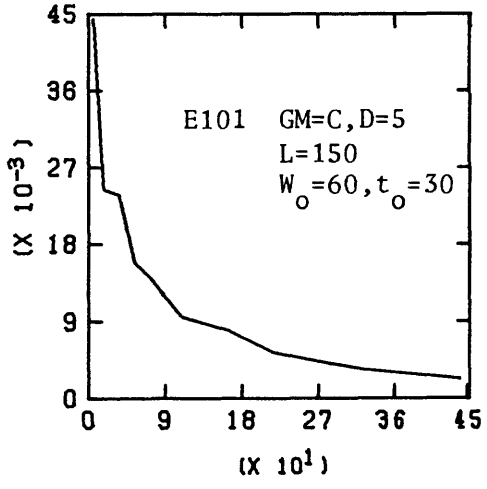
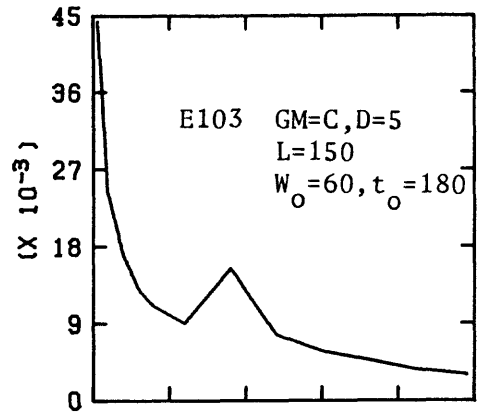
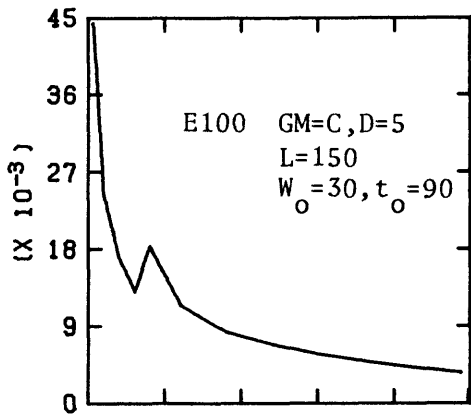
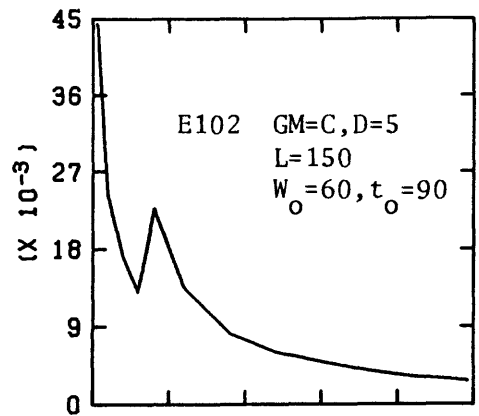
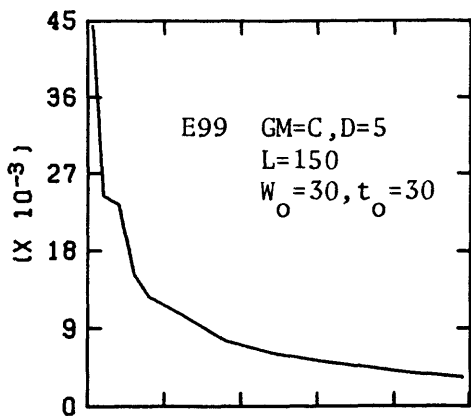
TIME, DIMENSIONLESS

SEEPAGE FLUX, DIMENSIONLESS



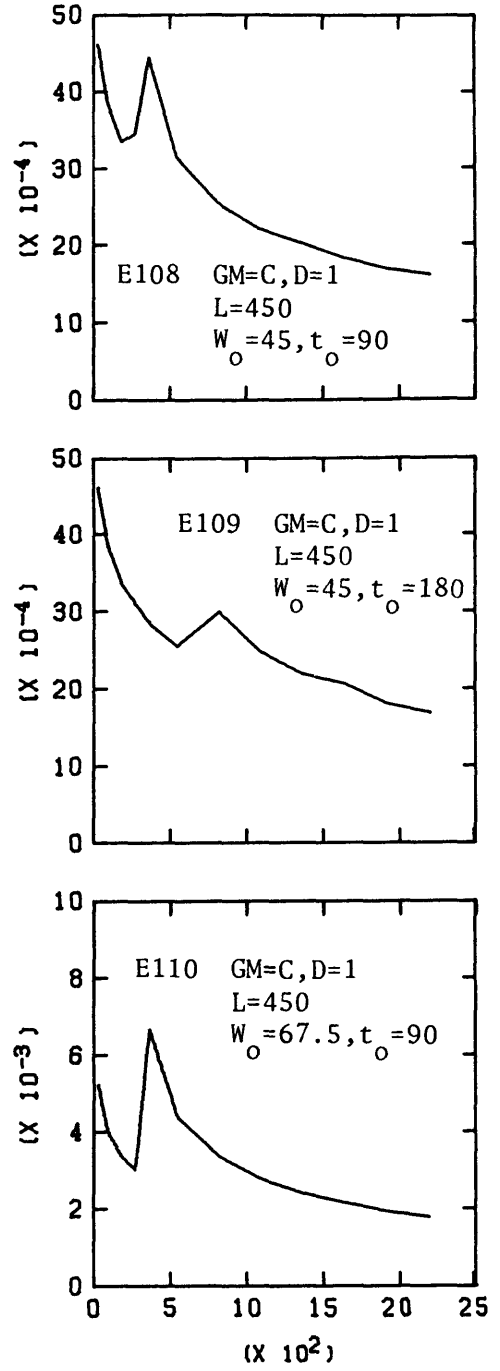
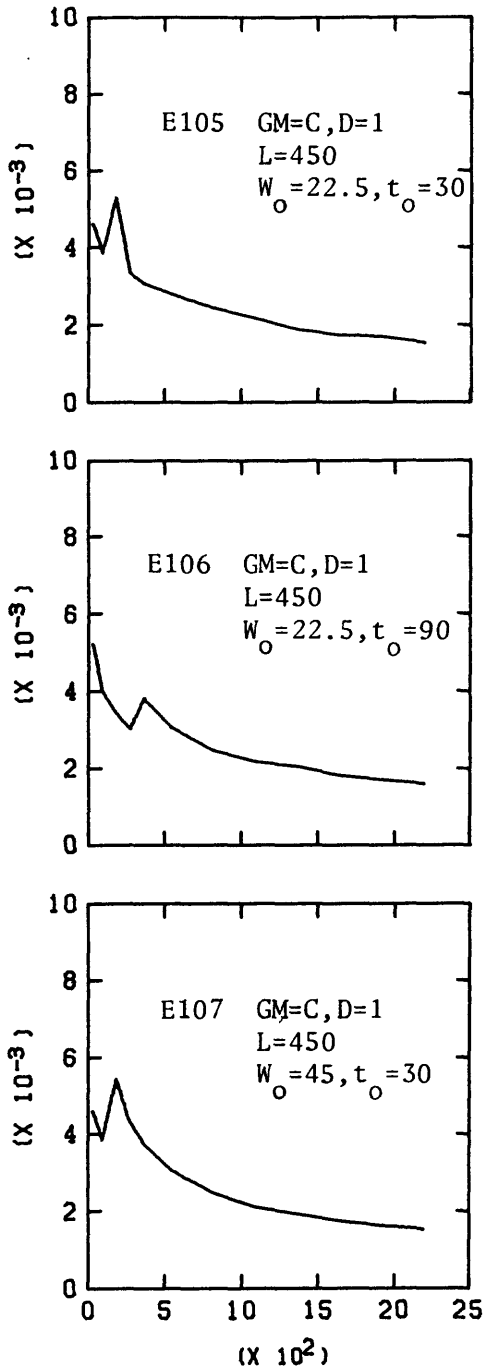
TIME, DIMENSIONLESS

SEEPAGE FLUX, DIMENSIONLESS



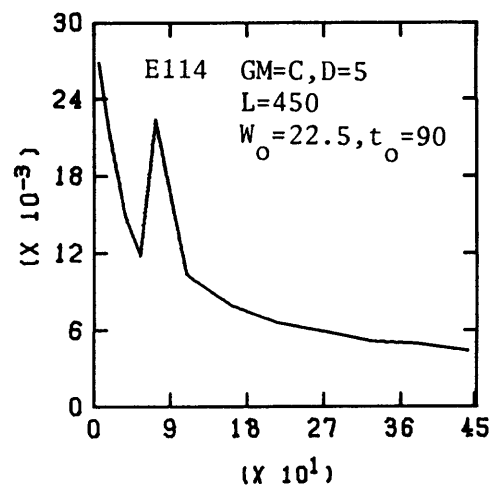
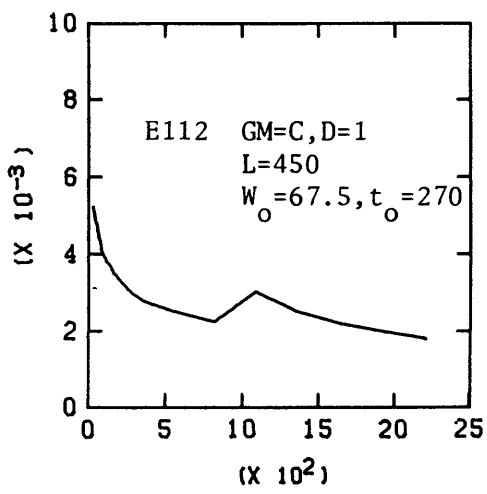
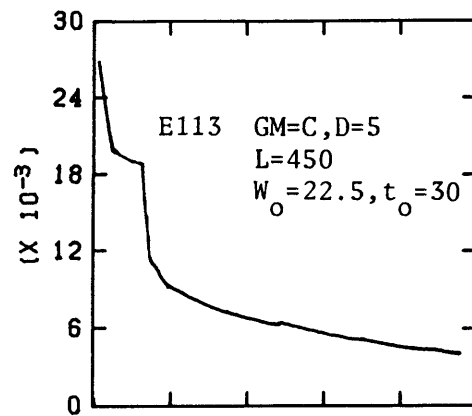
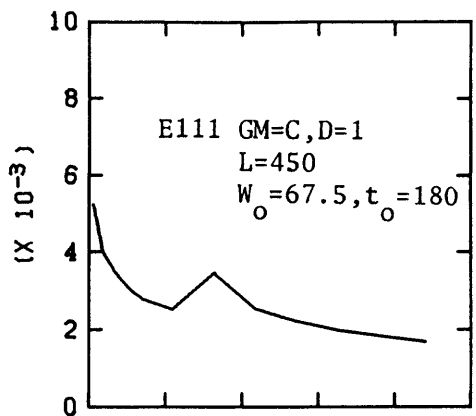
TIME, DIMENSIONLESS

SEEPAGE FLUX, DIMENSIONLESS



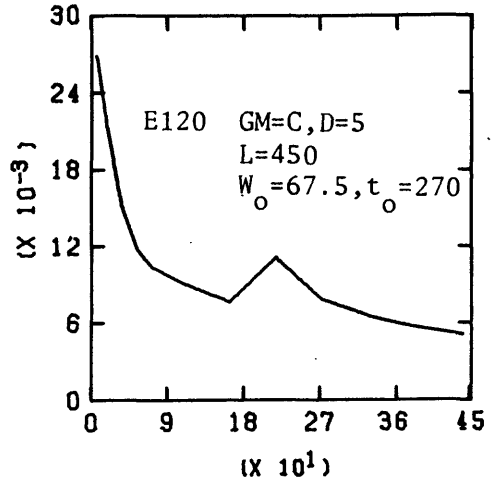
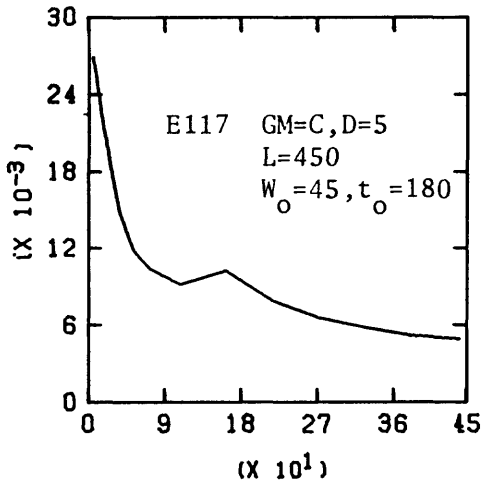
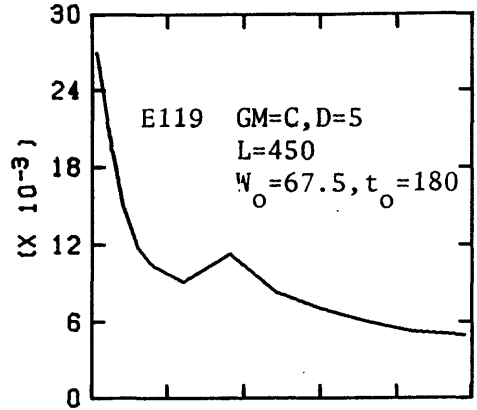
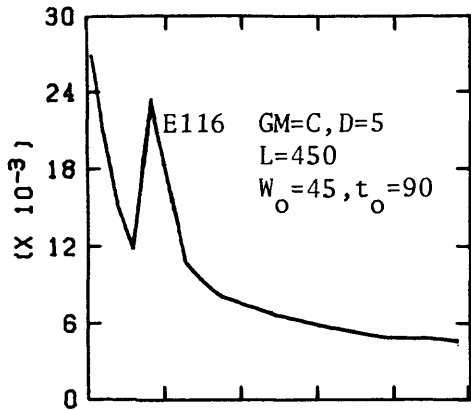
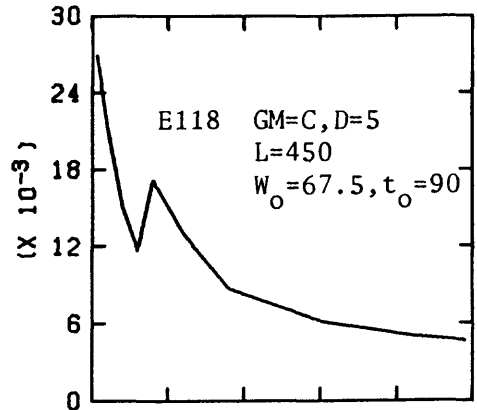
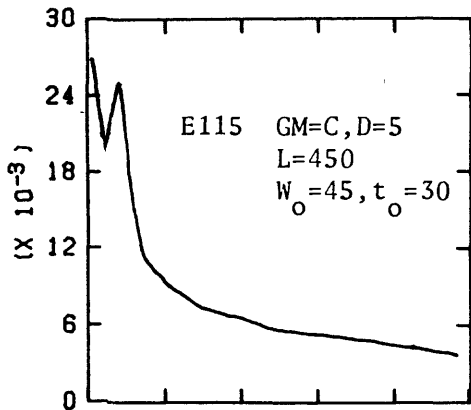
TIME, DIMENSIONLESS

SEEPAGE FLUX, DIMENSIONLESS



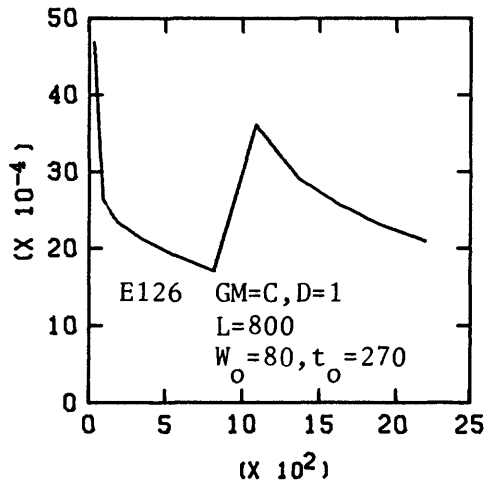
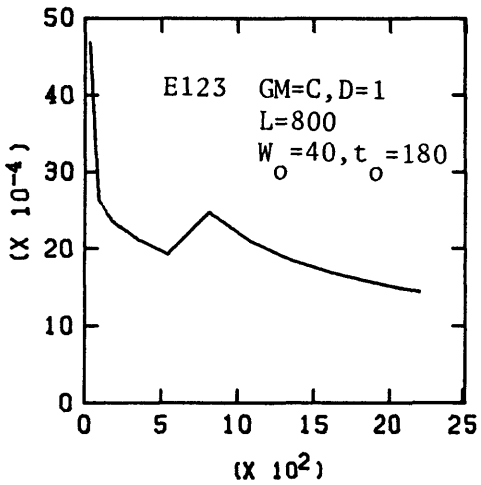
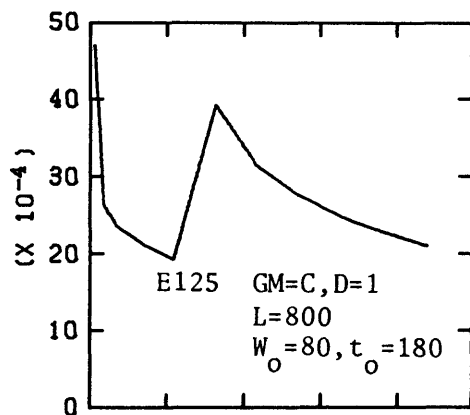
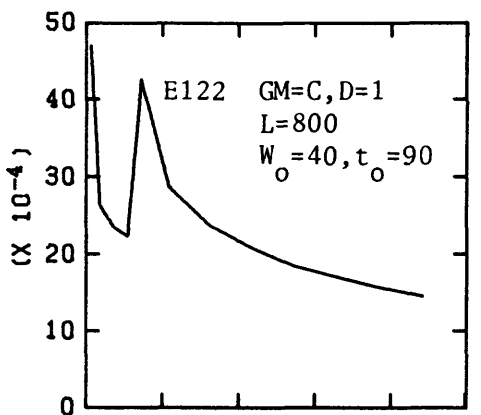
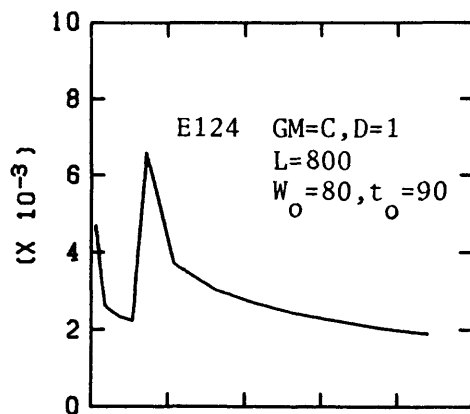
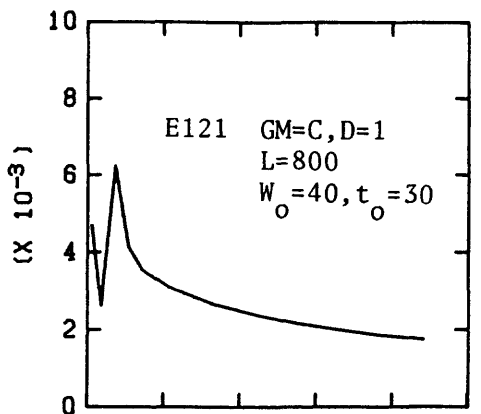
TIME, DIMENSIONLESS

SEEPAGE FLUX, DIMENSIONLESS



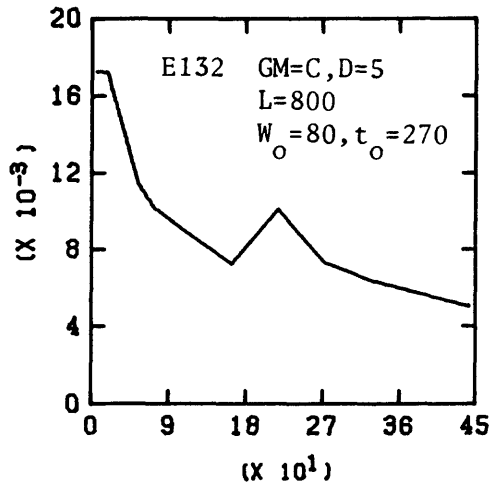
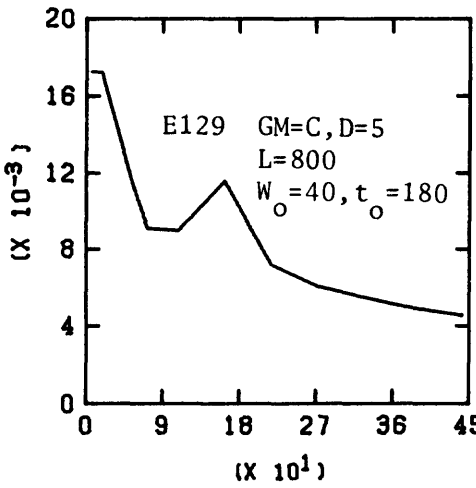
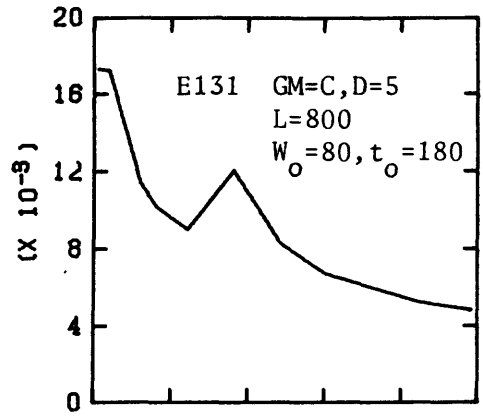
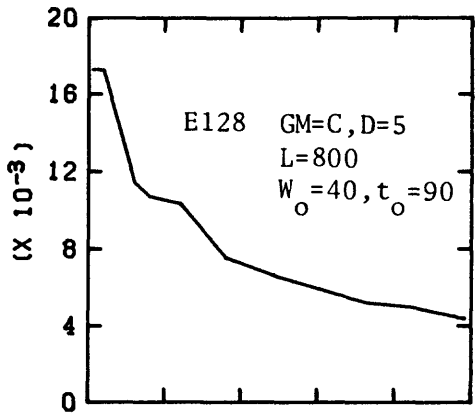
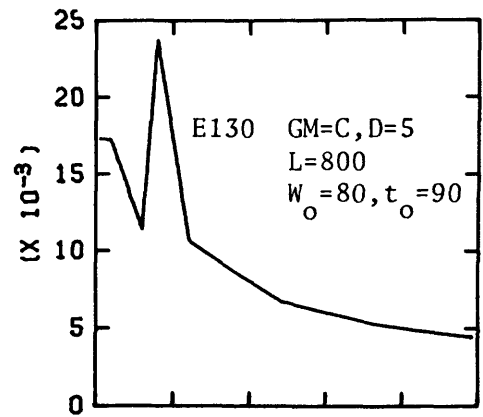
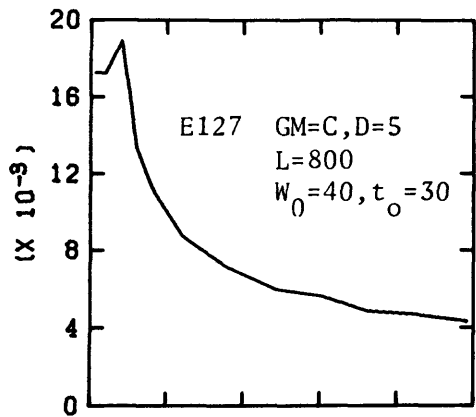
TIME, DIMENSIONLESS

SEEPAGE FLUX, DIMENSIONLESS



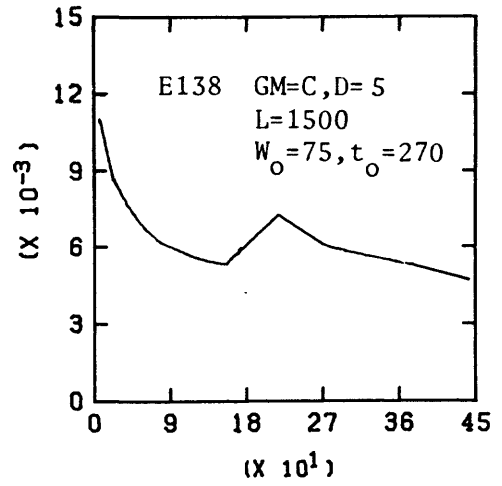
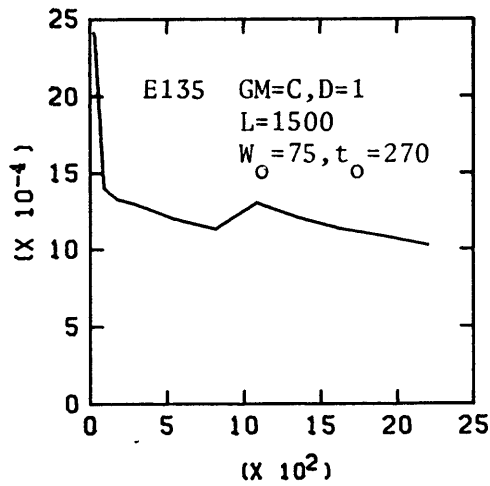
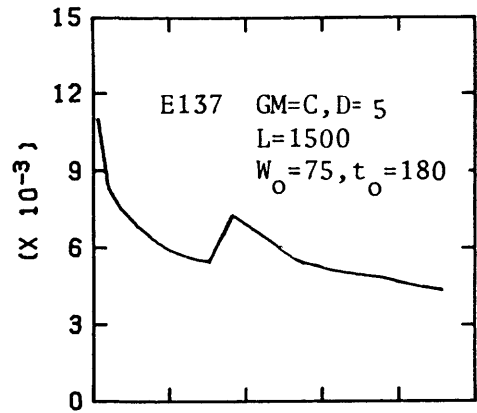
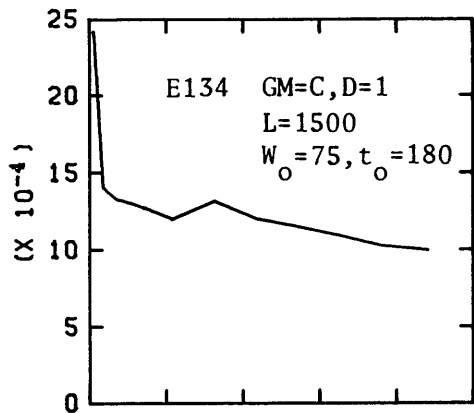
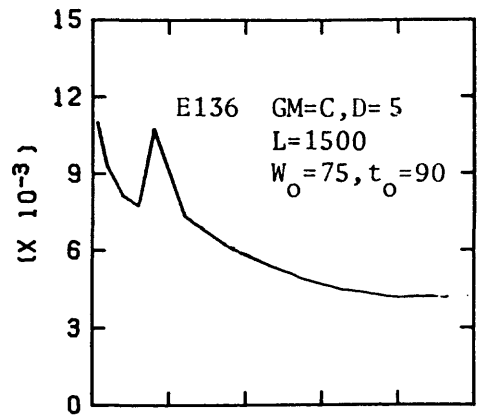
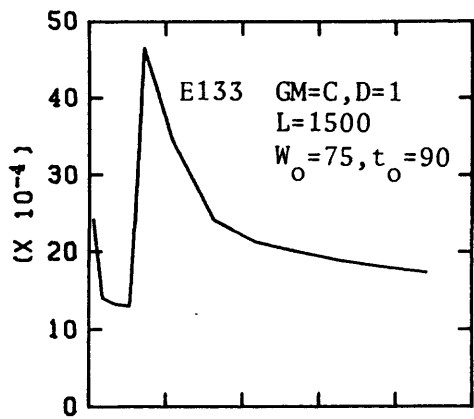
TIME, DIMENSIONLESS

SEEPAGE FLUX, DIMENSIONLESS



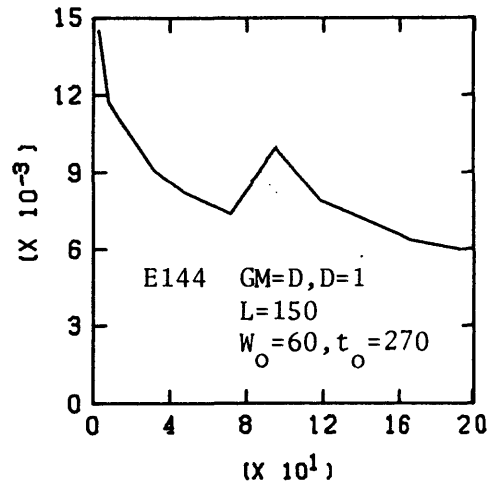
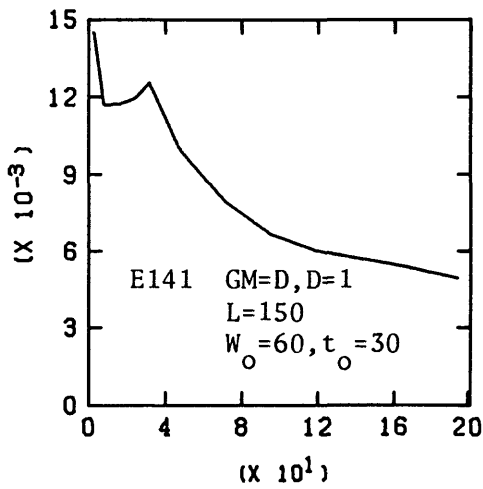
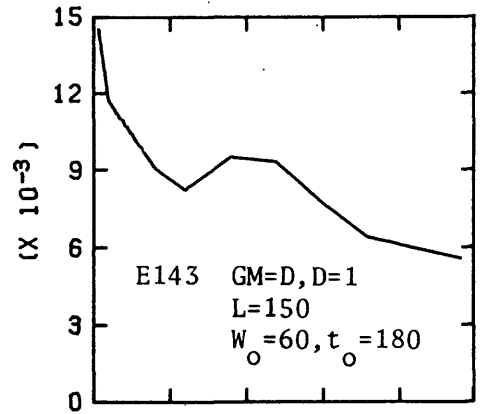
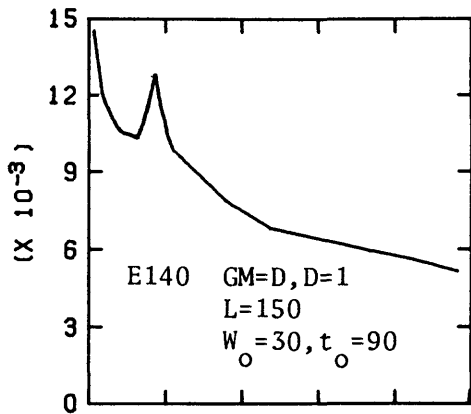
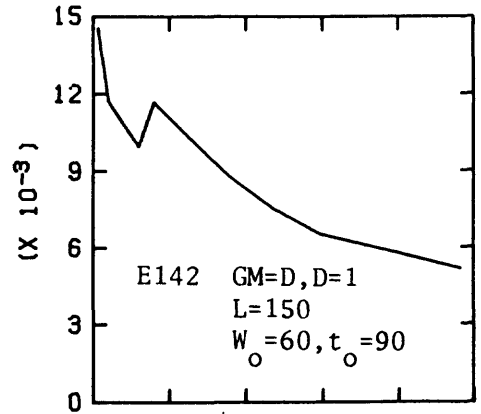
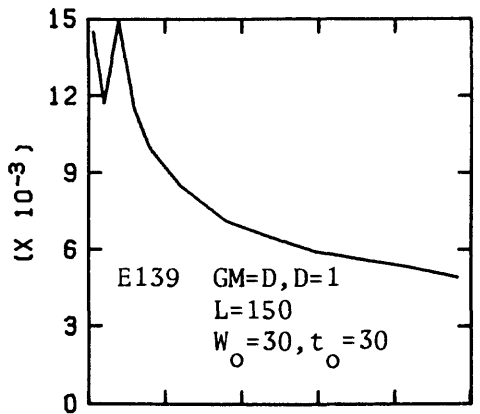
TIME, DIMENSIONLESS

SEEPAGE FLUX, DIMENSIONLESS



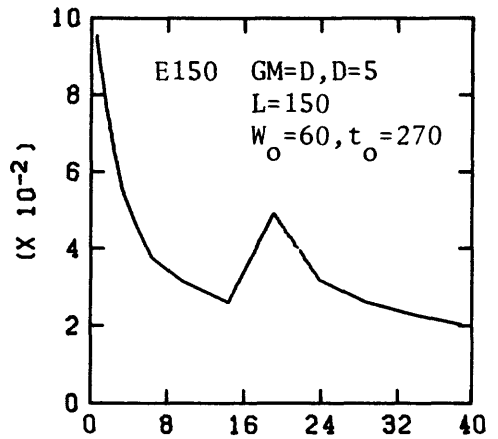
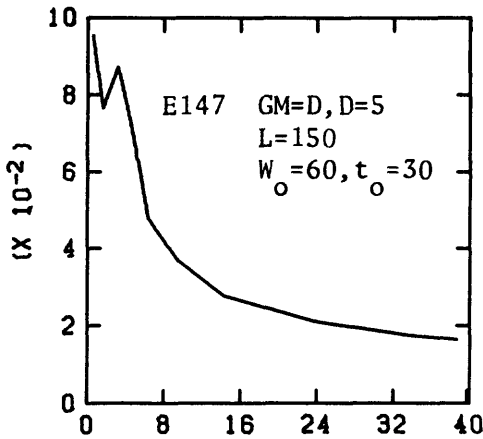
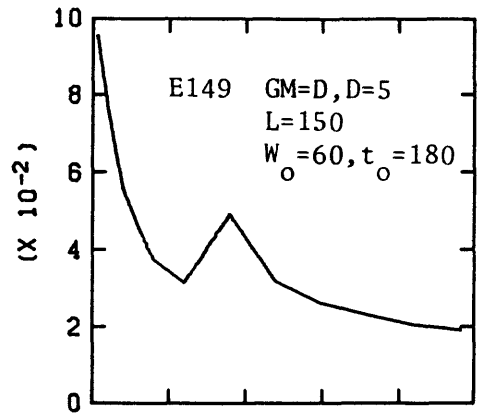
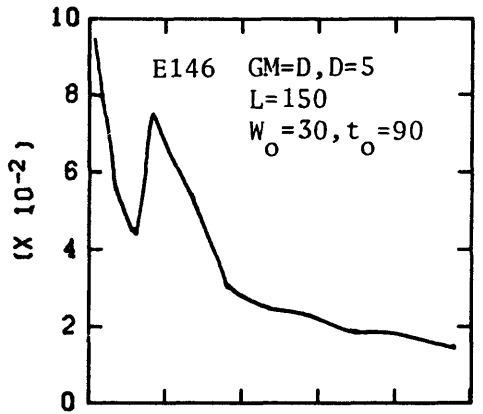
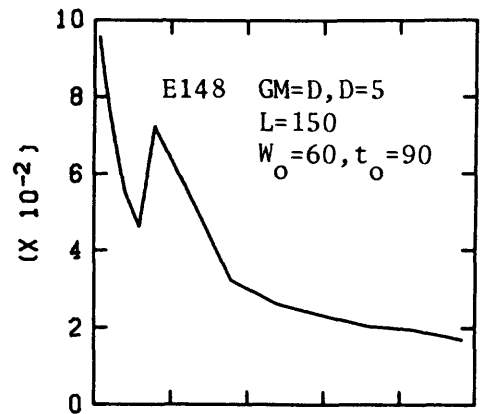
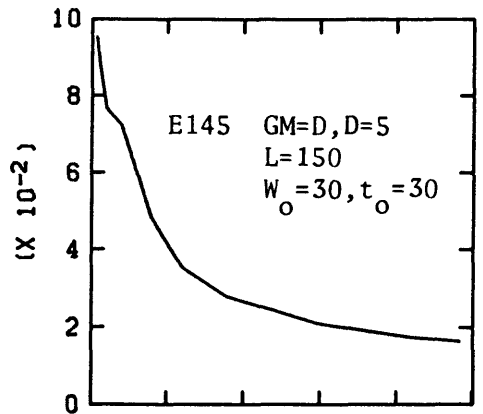
TIME, DIMENSIONLESS

SEEPAGE FLUX, DIMENSIONLESS



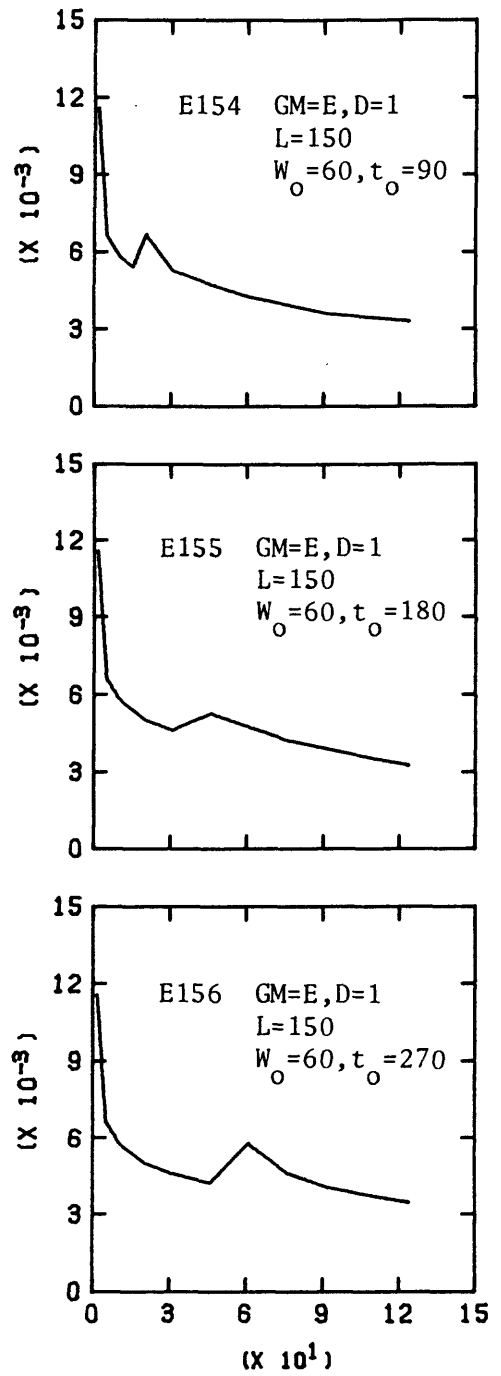
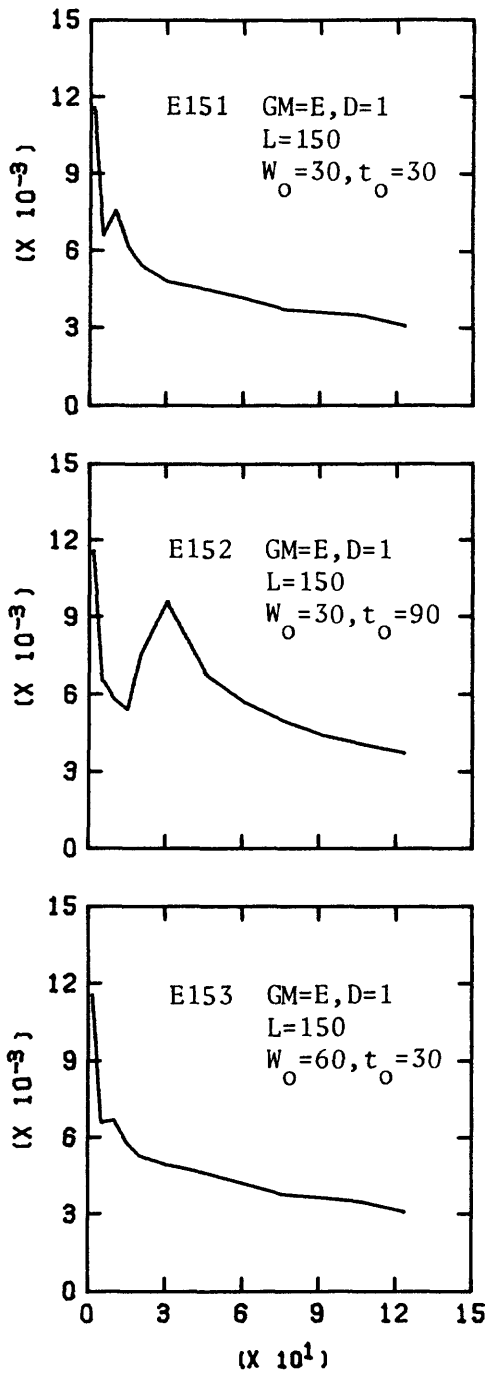
TIME, DIMENSIONLESS

SEEPAGE FLUX, DIMENSIONLESS



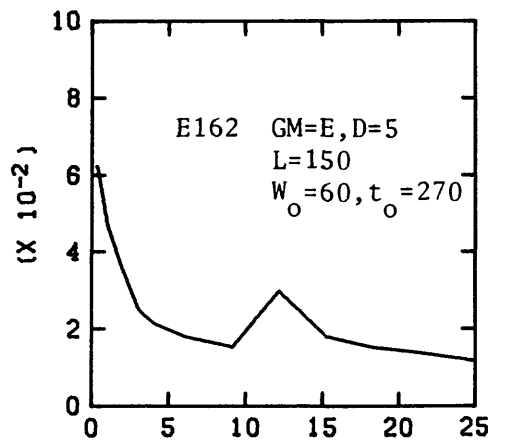
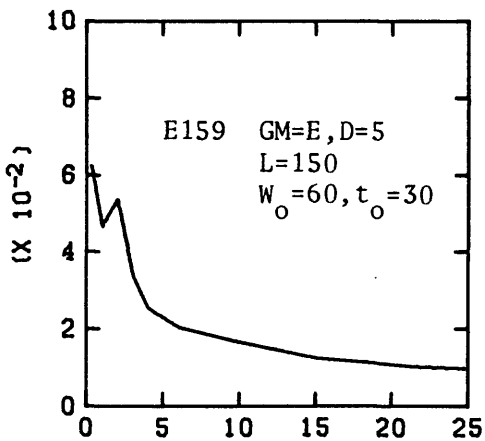
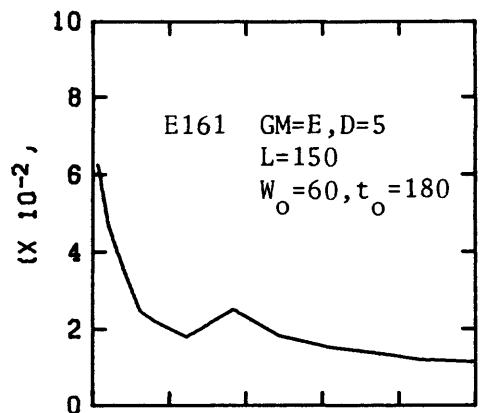
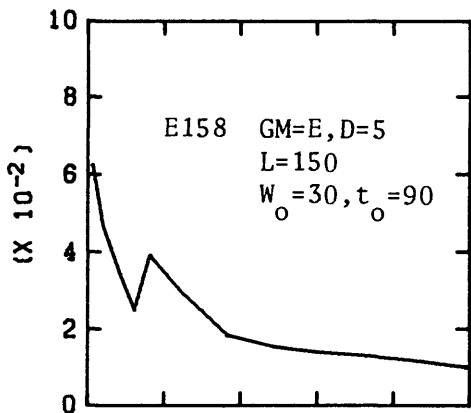
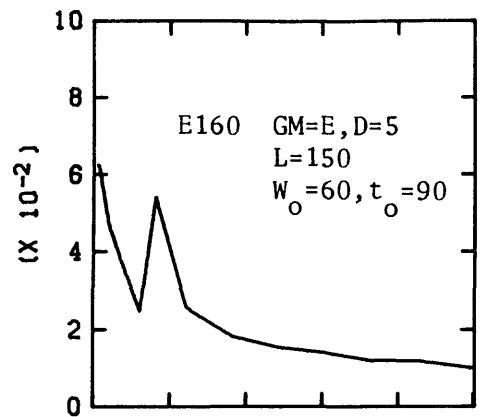
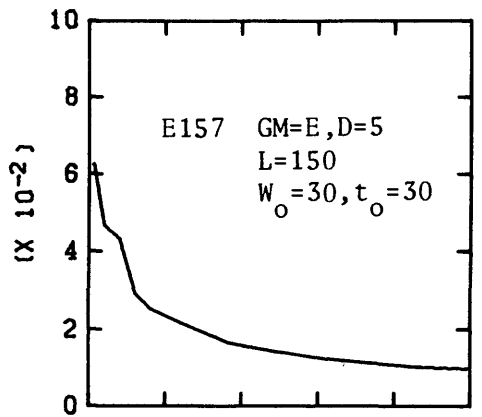
TIME, DIMENSIONLESS

SEEPAGE FLUX, DIMENSIONLESS



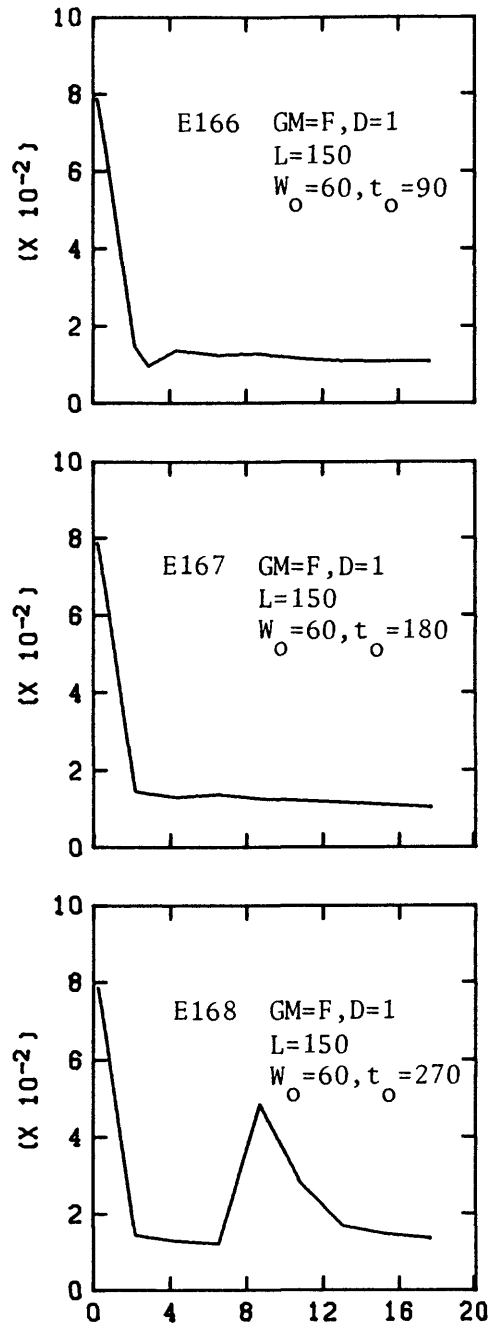
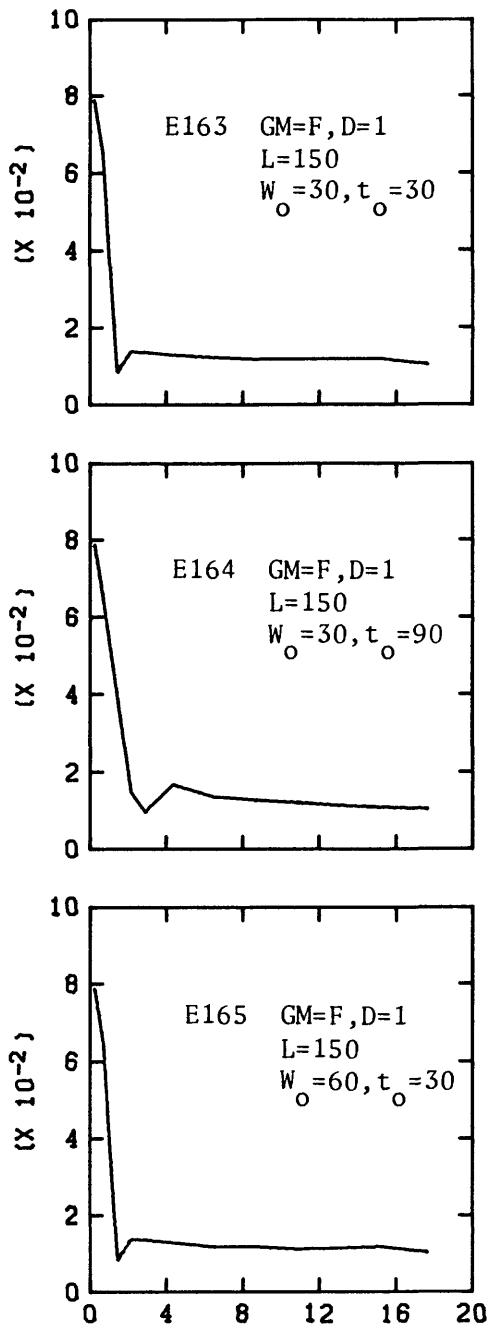
TIME, DIMENSIONLESS

SEEPAGE FLUX, DIMENSIONLESS



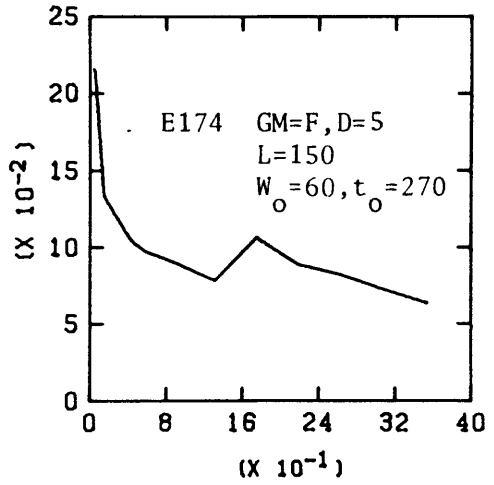
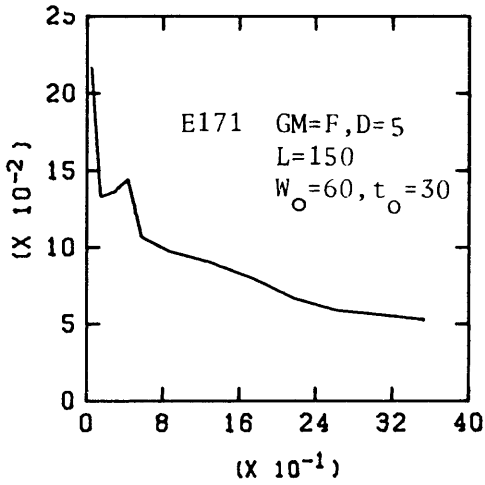
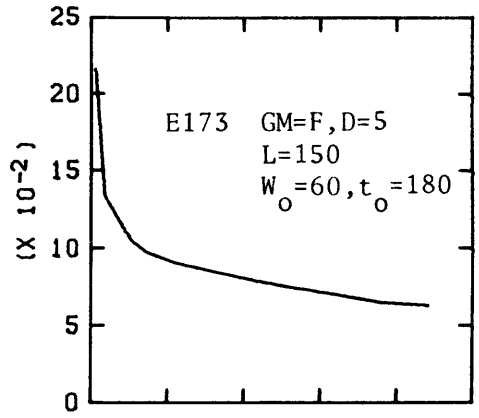
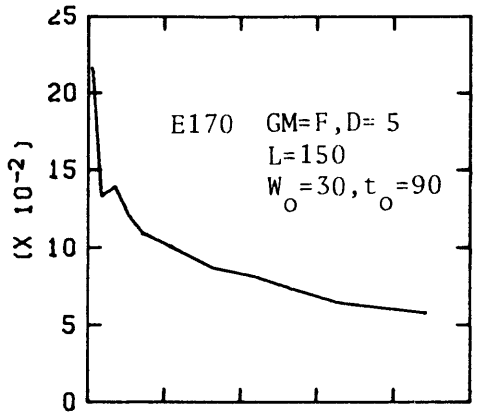
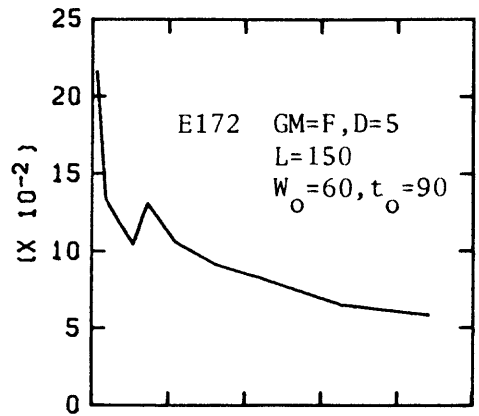
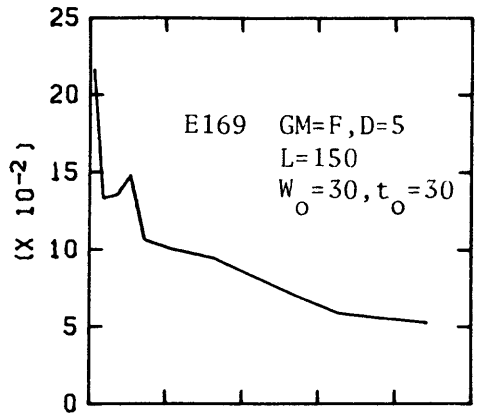
TIME, DIMENSIONLESS

SEEPAGE FLUX, DIMENSIONLESS



TIME, DIMENSIONLESS

SEEPAGE FLUX, DIMENSIONLESS



TIME, DIMENSIONLESS